Changing Arctic zooplankton:

aspects of physiology, food web structures and connectivity

Dissertation
zur Erlangung des Doktorgrades
der Naturwissenschaften
- Dr. rer. nat. -

dem Fachbereich 2 Biologie/Chemie
der Universität Bremen
vorgelegt von

Patricia Kaiser

Bremen, April 2024

'I must say that the charm of the Arctic, its infinite diversity, its aloofness from the rest of the world, made it a field which gives its own reward. Only those who have seen the magnificent sunsets over the ice, who have… been buffeted by storms… can appreciate the spell which always draws us back there.'

Louise Arner Boyd

CONTENTS

Contents

ABBREVIATIONS

ASV	amplicon sequences variant
AW	Atlantic Water
bp	base pairs
CCA	canonical correspondence analysis
CI	carnivory indices
CTD	conductivity temperature depth
DM	dry mass
EG	East Greenland
EGC	East Greenland Current
FA	fatty acid
FAME	fatty acid methyl ester
FATM	fatty acid trophic marker
fn	false negative
fp	false positive
MALDI-TOF	matrix assisted laser desorption ionization - time of flight
MHW	marine heat waves
MIZ	marginal ice zone
MS	mass spectrometry
MSRR	mass-specific respiration rates
MYI	multi-year ice
nMDS	non-metric multidimensional scaling
PCA	principal component analysis
PSW	polar surface water
RF	random forest
rDNA	ribosomal DNA
SI	stable isotope
SNR	signal to noise ratio
stn	station
TAG	triacylglycerols
TFAlc	total fatty acid alcohols
TL	total lipid
tn	true negative
tp	true positive
WS	West Spitsbergen
WSC	West Spitsbergen Current

SUMMARY

The Arctic Ocean and adjacent ice-covered seas are the regions that are most rapidly affected by climate change. Air temperatures are rising four times faster in the Arctic than the global average, leading to a rapid and substantial loss in sea-ice volume. Concurrently, the inflows of warm, saline Atlantic water into the Arctic Basin through Fram Strait and the Barents Sea are increasing, a phenomenon referred to as Atlantification. This Atlantification is not only driving physical changes of the Arctic environment, but also facilitates a northward range shift of boreal taxa. Consequently, polar zooplankton species are confronted with increasing temperatures and changing food web structures whilst at the same time face increasing competition by boreal-Atlantic congeners.

This thesis provides a comprehensive approach investigating the different factors of climate change on Arctic zooplankton species, focusing on the calanoid copepods *Calanus hyperboreus*, *Calanus glacialis*, *Paraeuchata glacialis* and the hyperiid amphipod *Themisto libellula*, as key representatives. Boreal-Atlantic congeners *Calanus finmarchicus*, *Paraeuchaeta norvegica* and *Themisto abyssorum* are considered as expatriates, which are extending their distribution ranges into the Arctic in the course of global warming.

For the assessment of physiological responses of Arctic and boreal zooplankton species to rising temperatures, their respiration rates were measured from 0 to 10 °C. A key finding was the resilience of Arctic species to temperature increases, as evidenced by their wide thermal tolerance and lack of metabolic stress response (low Q_{10} ratios). On the other hand, boreal species exhibited a more pronounced and rapid increase in respiration rates with rising temperatures, suggesting enhanced metabolic activity and overall performance under warmer conditions. Consequently, the temperature threshold at which boreal species outperform their Arctic congeners is likely to be a key determinant of zooplankton dynamics in a warming Arctic, rather than the absolute physiological limits of the species.

Analyses of food webs, utilizing both fatty acid and stable isotope biomarkers, across Arctic and Atlantic-influenced regions in Fram Strait were conducted to explore changes in trophic structures associated with the sea ice decline and increased Atlantification. The results emphasized the importance of (sea ice) diatoms in the Arctic ice-covered regions and shows a shift towards a more flagellate-based food web, with a higher degree of omnivory, in the Atlantic regime. The ability of Arctic *Calanus* species to rely on alternative food sources other than (sea ice) diatoms highlighted their dietary flexibility, which may become increasingly important with the predicted increase in

flagellate production in the future Arctic Ocean. The high relevance of *Calanus* fatty acid trophic markers in higher trophic levels in the Atlantic regime was likely a reflection of high abundances of *C. finmarchicus* in this region, showing its importance to the diet of carnivorous zooplankton as Atlantification progresses. Among Arctic and boreal congeners, an increased dietary overlap was observed between *C. glacialis* and *C. finmarchicus* as well as between *P. glacialis* and *P. norvegica* in areas of co-occurrence.

The evaluation of zooplankton data in context with the physical-oceanographic observations of a submesoscale filament emphasized the significance of such dynamics in shaping the pelagic environment. Strong horizontal and vertical velocities associated with these features play a major role in structuring the pelagic ecosystem, facilitating Atlantification processes and influencing species allocation and biological connectivity.

Additionally, proteomic fingerprinting was demonstrated as a rapid and accurate methodology for identifying climate-relevant but morphologically similar indicator species *C. glacialis* and *C. finmarchicus* to species and even developmental stages level. This technique has thus the potential to significantly enhance species identification in long-term monitoring studies, which is vital for deepening our understanding of ecosystem responses to climate change.

In conclusion, this thesis demonstrates that Arctic zooplankton exhibit a considerable resilience and adaptability to environmental changes, including elevated temperatures and alterations in the food web structures. However, it also emphasizes the challenges posed by the intrusion of boreal species, which, under more boreal-like conditions, may outcompete polar Arctic species. The findings underline that the future of Arctic species in a warming ocean depends not only on their physiological tolerance and ecological adaptability but also on the competitive interactions with boreal congeners.

ZUSAMMENFASSUNG

Der Arktische Ozean und die angrenzenden eisbedeckten Meere sind die Regionen, die am schnellsten vom Klimawandel betroffen sind. Die Lufttemperaturen steigen in der Arktis viermal schneller als im globalen Durchschnitt, was zu einem schnellen und erheblichen Verlust des Meereisvolumens führt. Gleichzeitig verstärkt sich der Zustrom von wärmerem und salzhaltigerem Atlantikwasser in den Arktischen Ozean durch die Framstraße und die Barentssee, ein Phänomen, das als Atlantifizierung bezeichnet wird. Diese Atlantifizierung bewirkt nicht nur physische Veränderungen der arktischen Umwelt, sondern fördert auch eine Ausbreitung borealer Arten nordwärts. Folglich werden einheimische polare Zooplanktonarten mit steigenden Temperaturen und sich verändernden Nahrungsnetzstrukturen konfrontiert, während sie gleichzeitig einem zunehmendem Wettbewerb durch boreal-atlantische Artgenossen gegenüberstehen.

Diese Dissertation bietet einen umfassenden Ansatz zur Untersuchung der verschiedenen Auswirkungen des Klimawandels auf arktisches Zooplankton, wobei der Fokus auf den calanoiden Copepoden *Calanus hyperboreus*, *Calanus glacialis*, *Paraeuchaeta glacialis* und dem hyperiiden Amphipoden *Themisto libellula* als Schlüsselarten liegt. Die boreal-atlantischen Artgenossen *Calanus finmarchicus*, *Paraeuchaeta norvegica* und *Themisto abyssorum* wurden als ‚Expatriaten' betrachtet, die ihre Verbreitungsgebiete im Zuge der globalen Erwärmung in die Arktis ausdehnen.

Um die physiologischen Reaktionen arktischer und borealer Zooplanktonarten auf steigende Temperaturen zu untersuchen, wurden ihre Respirationsraten im Temperaturbereich von 0 bis 10 °C gemessen. Ein zentrales Ergebnis war die bemerkenswerte Widerstandsfähigkeit der arktischen Arten gegenüber Temperaturanstiegen, gekennzeichnet durch eine breite thermische Toleranz und geringe metabolische Stressreaktionen (niedrige Q_{10}-Werte). Im Gegensatz dazu zeigten boreale Arten bei steigenden Temperaturen einen deutlichen und schnellen Anstieg ihrer Respirationsraten, was auf eine erhöhte Stoffwechselaktivität und eine generell verbesserte metabolische Leistung unter wärmeren Bedingungen hindeutet. Folglich ist der Temperaturschwellenwert, bei dem boreale Arten ihre arktischen Artgenossen übertreffen, wahrscheinlich ein entscheidender Faktor für die Dynamik des Zooplanktons in einer sich erwärmenden Arktis, anstatt der absoluten physiologischen Grenzen der Arten.

Analysen von Nahrungsnetzen in arktischen und atlantisch beeinflussten Regionen der Framstraße wurden mithilfe von Fettsäure- und stabile Isotopenbiomarker durchgeführt, um Verän-

derungen in den trophischen Strukturen im Zusammenhang mit dem Rückgang des Meereises und der zunehmenden Atlantifizierung zu untersuchen. Die Ergebnisse heben die Bedeutung von (Meereis-)Diatomeen in den arktischen, von Eis bedeckten Gebieten hervor und zeigen eine Verschiebung hin zu einem mehr auf Flagellaten basierenden Nahrungsnetz mit höherem Grad an Omnivorie im atlantischen Regime. Die Fähigkeit der arktischen *Calanus* Arten, alternative Nahrungsquellen neben (Meereis-)Diatomeen zu nutzen, unterstrich ihre Flexibilität, die mit der prognostizierten Zunahme der Flagellatenproduktion im zukünftigen Arktischen Ozean zunehmend wichtiger werden könnte. Die hohe Relevanz der Fettsäure Marker von *Calanus* für höhere trophische Ebenen im atlantischen Regime, die wahrscheinlich auf *C. finmarchicus* zurückzuführen waren, könnte weiterhin dessen Bedeutung für die Ernährung von karnivorem Zooplankton in einer sich erwärmenden Arktis zeigen. Unter arktischen und borealen Artgenossen wurde eine erhöhte Überschneidung der Ernährungsweise zwischen *C. glacialis* und *C. finmarchicus* sowie zwischen *P. glacialis* und *P. norvegica* in Regionen ihres gemeinsamen Vorkommens beobachtet.

Die Auswertung von Zooplankton-Daten im Zusammenhang mit der physikalisch-ozeanografischen Beobachtung eines submesoskaligen Filaments unterstreicht deren Bedeutung für die Gestaltung des pelagischen Regimes. Starke horizontale und vertikale Fließgeschwindigkeiten, die mit diesen Strukturen verbunden sind, spielen eine wichtige Rolle bei der Strukturierung des pelagischen Ökosystems, fördern Atlantifizierungsprozesse und beeinflussen die Verteilung von Arten sowie deren biologische Vernetzung.

Zusätzlich wurde in dieser Arbeit proteomisches Fingerprinting als eine effiziente und akkurate Methode zur Identifizierung der klimarelevanten, jedoch morphologisch schwer unterscheidbaren Arten *C. glacialis* und *C. finmarchicus* demonstriert. Die Identifizierung der Organismen war sowohl auf der Ebene der Art als auch der Entwicklungsstadien möglich. Diese Technik hat somit das Potenzial, die Artenidentifizierung in Langzeit-Monitoring-Studien erheblich zu verbessern, was für ein tieferes Verständnis der Reaktionen von Ökosystemen auf den Klimawandel von entscheidender Bedeutung ist.

Zusammenfassend zeigt diese Arbeit, dass arktisches Zooplankton eine beträchtliche Resilienz und Anpassungsfähigkeit an Umweltveränderungen, einschließlich erhöhter Temperaturen und Veränderungen in den Nahrungsnetzstrukturen, aufweist. Sie betont jedoch auch die Herausforderungen, die durch das Eindringen borealer Arten entstehen, die unter borealeren Bedingungen die polaren arktischen Arten verdrängen können. Die Ergebnisse unterstreichen, dass die Zukunft der arktischen Arten in einem sich erwärmenden Ozean nicht nur von ihrer physiologischen Toleranz und ökologischen Anpassungsfähigkeit abhängt, sondern auch von den Konkurrenzinteraktionen mit borealen Artgenossen.

GENERAL INTRODUCTION

A brief history of Arctic exploration

The Arctic Ocean has long been a focus of human curiosity and scientific inquiry. Its exploration has a rich history, dating back as early as the 16th century. Expeditions during these early times were focused on and motivated by mapping of uncharted territories, discovering new regions/lands and identifying new maritime routes. A key objective was to find a navigable passage from the Atlantic to the Pacific Ocean via the Arctic, offering a more direct trading route to Asia. Early endeavors to locate the Northeast Passage along the coasts of Norway and Russia were undertaken by Willem Barents between 1594 and 1597. Although his quest for this route was unsuccessful, it led to the discovery of Spitsbergen and Bear Island and contributed significantly to the mapping of the region (Seibold 2003). Similarly, Henry Hudson's attempt to locate the Northwest Passage along North America's northern coast in 1610-1611 did not succeed, but he became the first European to encounter Hudson Bay, which he mistook for the Pacific Ocean (Mills 2003).

The following centuries witnessed numerous expeditions to uncover the passages. Potentially the most tragic attempt was made by Sir John Franklin with the ships *Terror* and *Erebus* in 1845, resulting in the loss of all 129 crew members (Bayliss 2002; Hickey et al. 1993). It was not until roughly three centuries after the first attempts that the Northeast Passage was successfully navigated by Adolf Erik Nordenskiöld between 1878-1880, and a Northwest Passage was traversed by Roald Amundsen's expedition from 1903-1906 (Mills 2003).

Alongside exploration, expeditions increasingly focused on scientific research, with the First International Polar Year 1882-1883 establishing a foundation for systematic scientific exploration of the polar regions (Serreze and Barry 2014). Among the most notable of these early scientific expeditions was Fridtjof Nansen's *Fram* expedition from 1893-1896.

Nansen was the first scientist to explore and study the interior part of the Arctic Ocean. Based on the transpolar drift hypothesis developed by Henrik Mohn, Nansen set his mind on reaching the North Pole by drifting with the ice. For this mission, the ship *Fram* was specifically constructed, designed to withstand the ice pressure by floating atop of it. Although Nansen did not achieve his original goal of reaching the North Pole, the expedition yielded significant scientific discoveries. The expedition validated the transpolar drift theory, discovered that the Arctic Basin is deep and resulted in the first collections of valuable oceanographic data and plankton samples from the

Arctic Basin.

Around 10 years later, both Frederick Cook (1907-1908) and Robert Peary (1908-1909) claimed to be the first to reach the North Pole. Over time, however, skepticism has surrounded the accuracy of these claims. The first verifiable arrival at the North Pole is credited to Roald Amundsen, alongside pilot Umberto Nobile and explorer Lincoln Ellsworth, who reached the Pole in 1926 aboard the airship *Norge*.

The same year, Louise Arner Boyd made history as the first woman to lead a polar expedition, having chartered her own ship and crew (Mills 2003). Her pioneering work, using self-financed scientific equipment, significantly contributed to the mapping of Greenland ice and glaciers. Today, her photographs and topographic maps are used in scientific research as important historical records, contributing to the understanding of Arctic environmental change (Isaksson and Ryall 2023).

These and many more early expeditions laid the groundwork for our understanding of the Arctic's geography, oceanography and environment, paving the way for future scientific research. The names of many Arctic regions, seas, and basins bear testament to those explorers such as the Barents Sea, the Amundsen Basin, the Nansen Basin and Louise Boyd Land, among others.

Today, with the availability of modern research icebreakers, the Arctic has become more accessible and research less perilous, marking a new era of scientific exploration. Scientific research is shaped by long-term monitoring observatories and regular expeditions to the Arctic Basin and adjacent seas. Given the rapid changes occurring in the Arctic environment as a result of climate change, scientific research in these regions has become more crucial than ever.

Study area – Fram Strait

Fram Strait, named after the ship *Fram*, is situated between Greenland and Spitsbergen and an ideal location to study the effects of ongoing climate change on Arctic zooplankton dynamics. As a major gateway and the only deep-water connection between the Atlantic and the Arctic Oceans, it plays a key role in connectivity. The strait spans roughly 300 km at its deep section, with an average depth of around 2500 m (Figure 1). On the western side of Fram Strait, the East Greenland Current (EGC) exports cold, polar water and sea ice out of the Arctic Ocean (de Steur et al. 2009), whereas the West Spitsbergen Current (WSC) carries warm, saline water of Atlantic origin into the Arctic Ocean on the eastern side (Beszczynska-Möller et al. 2012). Part of the Atlantic water, transported by the WSC, turns westward to 'recirculate' underneath the Polar Surface Water of the EGC (Hattermann et al. 2016). The zone in between the WSC and EGC is thus characterized by a highly dynamic and turbulent regime with many (sub-)mesoscale eddies and filaments (Kawasaki and Hasumi 2016; von Appen et al. 2018). The contrast of Atlantic and Arctic water masses in close proximity makes Fram Strait a natural laboratory to study current Arctic conditions on its western flank and potential future ice-free and boreal-like scenarios on the eastern side.
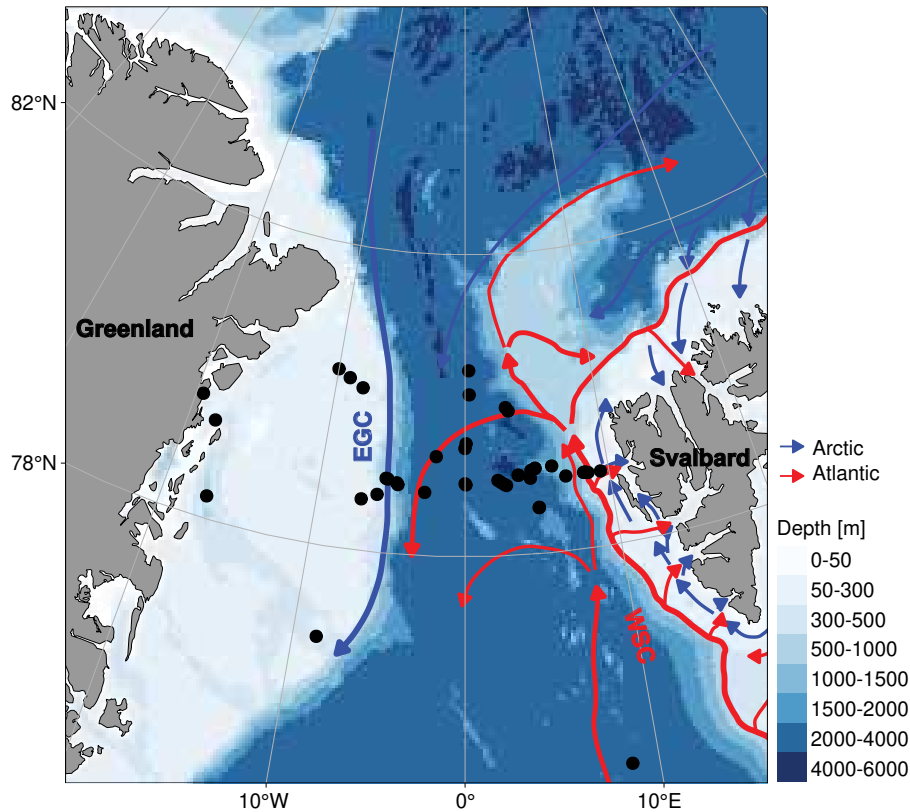
Figure 1: Map of Fram Strait including Arctic- (blue) and Atlantic- (red) currents. Black dots indicate sampling stations included in this thesis. EGC: East Greenland Current, WSC: West Spitsbergen Current. Map generated with ggOceanMaps in R (Vihtakari 2024).

An overview of the Arctic sympagic-pelagic ecosystem

Annual cycle of primary production

The Arctic ecosystem is characterized by its perennially or seasonally ice-covered regions and by prolonged phases of constant light (polar day) and darkness (polar night), resulting in a seasonally light limited system. Yet, even when there is sufficient light available during polar day, the water column can still be light limited due to the extensive ice and snow cover. This high seasonality of the light regime predetermines the available time frame/window for photoautotrophic primary production. Highly specialized algae, commonly referred to as ice algae, have adapted to these conditions, being able to inhabit brine channels in the sea ice and thrive under low light conditions (Arrigo 2017). During winter/polar night, autotrophic ice algal production is generally absent and the sea ice community rather consists of heterotrophic organisms such as (dino-)flagellates (Lund-Hansen et al. 2020). In polar spring, when daylight becomes increasingly available, ice algae, which are usually dominated by pennate diatoms (Arrigo 2014; Leu et al. 2015), rapidly increase in concentration and reach their maximum abundances within the ice. This early primary production, before the onset of the open water phytoplankton bloom, serves as a valuable resource for many sympagic and pelagic organisms (Søreide et al. 2013; Søreide et al. 2010). Although phy-

3

toplankton production usually exceeds that of ice algae in seasonally ice-covered regions, the ice algae bloom is an important early carbon source especially in areas with perennial sea-ice cover, where it can be the only source of primary production (Gosselin et al. 1997). In late spring/summer, when the ice melts, algae, which are released from the ice can either be immediately grazed upon and thus channeled into the pelagic food web (Szymanski and Gradinger 2016) and/or sink to the seafloor, providing a relevant food source for benthic organisms (Boetius et al. 2013; Koch et al. 2023; Søreide et al. 2013).

Typically, the phytoplankton bloom first appears after the melt of sea ice. This timing is partly due to insufficient irradiances beneath the ice, especially when competing with ice algae, whose pigments absorb most of the available light (Mundy et al. 2014). Consequently, only minimal light reaches the water column. During the ice melt, the released freshwater further leads to a strong stratification of the water column, sustaining nutrients and algae in the upper layers and thereby supporting the phytoplankton bloom (Janout et al. 2016). After the sea-ice breakup, the pelagic algal community composition rapidly shifts to one dominated by typical 'summer' centric diatom species and/or (dino-)flagellates, with increasing influence by heterotrophic species later in the season, when inorganic nutrients become depleted (Sergeeva et al. 2010; Sukhanova et al. 2009; von Quillfeldt 2000).

In autumn, as the sea ice begins to re-form, a second ice algal bloom may develop. These blooms are usually short- lived and accumulate lower biomass compared to summer blooms (Garrison et al. 2005; Garrison et al. 2003; Meiners et al. 2003). Autumn phytoplankton blooms are generally absent due to the formation of sea ice and associated limited light availability and vertical mixing (Ardyna et al. 2014).

Zooplankton in the Arctic

'One sees phosphorescence in the water here whenever there is the smallest opening in the ice. There is by no means such a scarcity of animal life as one might expect.'

Fridtjof Nansen in 'Farthest North', 1897

A large part of the biomass produced by the sympagic and pelagic primary producers is consumed by few zooplankton species. This herbivorous feeding habit of key Arctic zooplankton species forms an essential link from ice-associated and pelagic primary producers to higher trophic levels (Berge et al. 2020).

Arctic zooplankton have evolved a variety of adaptations to cope with the highly seasonal Arctic environment (Hagen 1999). Common traits shared among many taxa are their large body size, slow growth, multi-year life cycles and the extensive energy storage in form of lipids (Auel and Werner 2003; Falk-Petersen et al. 2000). Lipids are commonly stored as triacylglycerols (TAG) in many zooplankton species, which are regarded as readily accessible short-term reserves (Lee et al.

2006). In species from higher latitudes, which face prolonged periods of limited food availability, wax esters (WE) are more commonly used as an energy storage (Hagen and Auel 2001). Unlike TAG, WE are long-term stores, providing a crucial survival mechanism in the highly seasonal regimes (Kattner and Hagen 2009; Lee et al. 2006).

Copepods typically dominate the zooplankton community in terms of diversity, abundance and biomass (Kosobokova 2009; Kosobokova and Hopcroft 2010; Kosobokova et al. 2011). Among them, *Calanus* is the most important genus with regard to biomass and importance for food web dynamics in the Arctic (Auel and Hagen 2002; Ehrlich et al. 2021).

Three species of *Calanus* co-occur in Arctic environments, the two polar species, *C. hyperboreus* and *C. glacialis*, and one expatriate from the boreal-Atlantic, *C. finmarchicus* (Wassmann et al. 2015). These species have in common that they accumulate extensive amounts of lipids (up to 70% of their dry mass) to overwinter in diapause at depth, an energy-saving state marked by reduced metabolism and non-feeding (Hirche 1996; Hirche et al. 1997). With this ontogenetic vertical migration, these lipid-rich species transport an substantial amount of carbon to the deep ocean, significantly contributing to carbon sequestration (Jónasdóttir et al. 2015). Beside these similarities, they differ in aspects such as body size, main distribution area, lifespan, overwintering stage and recruitment strategy.

C. hyperboreus, the largest among the three species, has its core distribution associated with deep-water regions like the Greenland Sea and the central Arctic Ocean (Choquet et al. 2017; Hirche 1991). The life cycle of *C. hyperboreus* spans 2 to 5 years (Daase et al. 2021; Falk-Petersen 1999; Hirche et al. 1997) with overwintering possible from copepodite stage C3 onward (Hirche et al. 1997). The medium-sized *C. glacialis* predominately occurs in Arctic shelf and marginal seas, has a lifespan of 1 to 3 years and its first overwintering stage is C4 (Kosobokova 1999). The smallest of the three, the boreal *C. finmarchicus*, has a one-year life cycle and predominately overwinters as C5 at its northern distribution range (Broms et al. 2009; Daase et al. 2021). Originating from core areas such as the Norwegian Sea, this species is advected through currents into the Arctic, where its distribution overlaps with its Arctic congeners in regions where the Arctic and Atlantic water masses meet (Torgersen and Huse 2005). The variation in size among the three *Calanus* species directly correlates with differences in their lipid content. *C. hyperboreus*, being the largest, has the highest individual lipid content, while the smallest *C. finmarchicus* has the least. This variation in lipid content affects the nutritional value and food quality of the species for higher trophic levels.

Beside their longer life cycles, ability to overwinter as younger copepodite stages and larger individual lipid reserves, both Arctic *Calanus* species are able to reproduce independent of food supply. This is most prominent in females of *C. hyperboreus*, which mature and spawn in winter while still in deeper water layers, fueled only by their internal lipid resources (capital breeding) (Hirche 1996). The lipid-rich eggs are buoyant, floating to the surface where the nauplii hatch and develop (Conover and Siferd 1993). By the onset of the ice algal bloom in spring, these

nauplii have matured to their feeding stages (naupliar stage 3 onward), allowing them to take full advantage of the brief productive season for growth and development (Berge et al. 2020). Similarly, *C. glacialis* can start spawning at low rates before the algal bloom by utilizing its internal lipid reserves, but readily takes advantage of the food supply with increased egg production rates (Hirche and Kattner 1993; Niehoff et al. 2002). *C. finmarchicus* in contrast, is generally dependent on food intake for reproduction (income breeding) (Daase et al. 2021). The earlier spawning in Arctic *Calanus* species gives their offspring a head start, increasing their chances to develop into overwintering stages with a sufficient amount of lipids before the end of the short productive season.

Generally, accumulating extensive lipid reserves and entering a state of dormancy are strategies by primarily herbivorous species in polar regimes (Berge et al. 2020). In addition, other strategies include sexual regression and body shrinkage to minimize energetic costs in euphausiids (Huenerlage et al. 2015) or a shift to more opportunistic feeding in *Pseudocalanus minutus* when lipid storages are insufficient for overwintering (Lischka and Hagen 2007).

Besides *Calanus* as a key species in the Arctic ecosystem, other species can be important in terms of abundance and biomass such as the calanoid copepods *Microcalanus* spp., *Paraeuchaeta* spp., the cyclopoid copepod *Oithona* spp., as well as hyperiid amphipods *Themisto* spp. and chaetognaths (Kosobokova and Hopcroft 2010; Kosobokova et al. 2011)). In contrast to the primarily herbivorous *Calanus* spp., these omnivorous and carnivorous species are less dependent on the spring and summer seasons for feeding, due to the year-round availability of their food sources. Consequently, their survival strategies differ from herbivores (Hagen 1999).

Omnivorous species are flexible regarding their diet and are often opportunistic feeders (Hagen 1999). In these organisms, state of dormancy is generally absent. However, to endure the winter period, they may reduce their metabolic activity and exhibit an increased reliance on their energy storage (Berge et al. 2020). Predominantly carnivorous organisms, such as the hyperiid amphipods *Themisto* spp. or chaetognaths, typically maintain a 'business as usual' strategy, but may follow their prey to different depth layers and/or adjust their feeding habits (Berge et al. 2020; Kraft et al. 2013; Kraft et al. 2015). In some carnivorous species, reproduction is synchronized with the spawning period of their prey (Dalpadado 2002), whereas omnivores may spawn throughout the year (Darnis et al. 2012; Hirche and Kosobokova 2011).

Climate change in the Arctic and its implications for sympagic-pelagic processes

Arctic warming

Due to human activity, such as fossil fuel burning and deforestation, atmospheric CO_2 levels are higher than at any phase in our history, with similarly high levels last occurring 3 millions years ago (Rae et al. 2021). This CO_2 increase, which is ten times faster than during any time of the last 66 millions years (Zeebe et al. 2016), is resulting in distinct warming of the globe.

In the Arctic, sea surface temperatures are rising at a rate four times faster than the global average (Rantanen et al. 2022), a phenomenon known as Arctic amplification (England et al. 2021; Previdi et al. 2021). The strong increase in temperature has led to a rapid and substantial loss in sea-ice volume, altering the surface albedo. Unlike sea ice, which reflects much of the solar irradiance, the ice-free, darker ocean absorbs most of it, resulting in an even more pronounced warming (Previdi et al. 2021).

This increase in temperature directly impacts Arctic organisms. Due to species-specific thermal tolerance limits and temperature-dependence of their performance, organisms occupy distinct thermal niches, which play an important role in determining their biogeographical distribution (Schulte et al. 2011).

Over the past decade, several studies investigated the performance response of *Calanus* species on rising temperatures (Grote et al. 2015; Henriksen et al. 2012; Hildebrandt et al. 2014; Hirche and Kosobokova 2007; Jung-Madsen and Nielsen 2015; Kjellerup et al. 2012; Pasternak et al. 2013). Several studies reported restricted physiological performances at temperatures between 5 to 10 °C of Arctic *Calanus* species (Grote et al. 2015; Hildebrandt et al. 2014; Pasternak et al. 2013), whereas others observed no negative effects (Henriksen et al. 2012; Hirche and Kosobokova 2007; Kjellerup et al. 2012; Weydmann et al. 2015).

Many of these studies have been limited to one or two *Calanus* species. To date, there appears to be only one early study that included all three *Calanus* species in experiments involving temperature increases (Hirche 1987). Comparing experimentally determined physiological responses across and within studies can lead to inconsistent conclusions when individuals were sampled at different locations or times due to phenotypic plasticity among individuals and/or varying performances linked to seasonal differences. For instance, Pasternak et al. (2013) detected a decrease in fed *C. glacialis* egg production above 5 °C, whereas *C. finmarchicus'* increased up to experimental temperatures of 10 °C under fed conditions. Since the egg production of *C. glacialis* was only measured in May, females might have taken higher temperatures as an indicator to cease spawning and prepare for dormancy (Kosobokova 1998; Niehoff and Hirche 2005). Further, although egg production rates of *C. glacialis* decreased with increasing temperature, at 10 °C its rate was still at a similar level as *C. finmarchicus*. Concurrently, egg production rates measured by Kjellerup et al. (2012) during pre-bloom (March), bloom (April) and post-bloom (May) conditions show an increase for *C. glacialis* during pre-bloom and bloom conditions up to 7.5 to 10 °C. At post-bloom conditions the rates show a unimodal curve, similar to those of *C. glacialis* measured in May by Pasternak et al. (2013). This emphasizes the importance of considering life history strategies of species for a comprehensive understanding of their responses to warming.

Additionally, there is a noticeable gap in our knowledge regarding the response of other important zooplankton taxa like *Paraeuchaeta* spp. and *Themisto* spp., as most studies have focused on *Calanus* spp. Addressing this gap is essential for a more complete comprehension of the impact of climate change on the Arctic marine ecosystem.

Decline in sea ice

The warming-induced decline in Arctic sea ice is evident in spatial and temporal extent as well as in thickness. There is a consistent downward trend in extent across all months, particularly pronounced in summer and autumn, with a maximum decrease of 13% per decade in September (Figure 2, Serreze and Meier 2019; Stroeve et al. 2012, leading to predictions of an ice-free Arctic summer by 2050 (Notz and Stroeve 2018). Concurrently, the melting season is starting earlier and ending later, thus prolonging the ice-free period in seasonally ice-covered Arctic regions (Serreze et al. 2016; Stroeve and Notz 2018). This change shortens the duration of ice algae blooms, potentially reducing ice algal production (Selz et al. 2018; Tedesco and Vichi 2014). Expansion and duration of open-water areas further promotes phytoplankton growth (Arrigo et al. 2008; Kahru et al. 2016). The phytoplankton bloom may not only occur earlier (Kahru et al. 2011) but also experience an increased likelihood of a second bloom in the autumn, driven by wind-induced upwelling of nutrients in open-water regions (Ardyna et al. 2014; Nishino et al. 2015; Waga and Hirawake 2020).

Sea ice extent in September

1985   **2023**
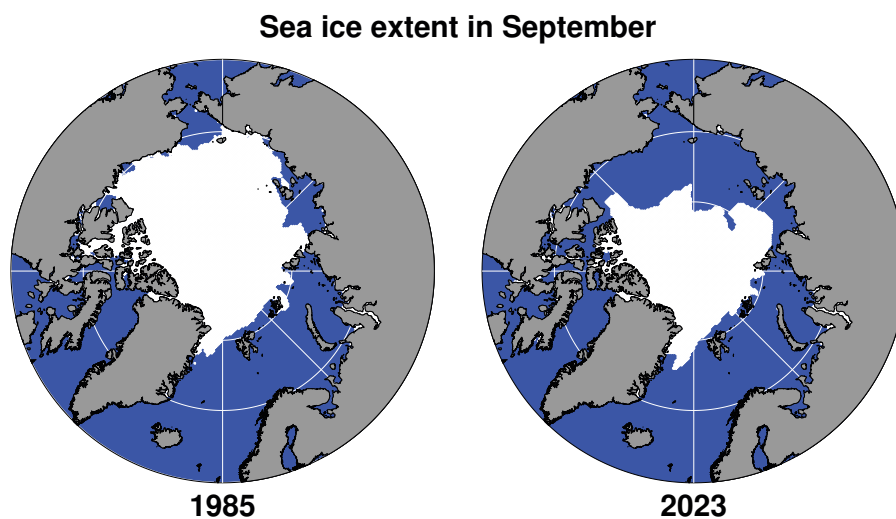
Figure 2: Extent of Arctic sea ice in September 1985 (left) and September 2023 (right). Plot generated with ggOceanMaps in R (Vihtakari 2024) based on data from the National Snow and Ice Data Center.

Additionally, the structure of sea ice is undergoing significant changes, with multi-year ice (MYI), i.e. ice that has survived at least one melting season, increasingly being replaced by younger MYI and first-year ice, i.e. ice that has formed during one growth season (Figure 3). This shift is resulting in a notable decrease in sea ice thickness (Laxon et al. 2013; Serreze and Meier 2019). The impact of this transformation is clearly evident when considering the sea ice volume, which showed a substantial loss of 60% over just 30 years (Lindsay and Schweiger 2015). Thinning sea ice and more prevalent melt ponds may result in more favorable conditions for under-ice phytoplankton blooms (Horvat et al. 2017), suggesting that such blooms might become more abundant with ongoing alterations in sea ice dynamics.

The alteration in timing, location and intensity of sympagic and pelagic primary production could significantly impact Arctic primary consumers, which have efficiently adapted their pehnology and life history traits to these regimes. The shortened duration of ice algal blooms and potential earlier phytoplankton blooms could for instance result in mismatch scenarios of species such as Arctic *Calanus* spp., which time their reproduction so that their offspring can fully exploit primary production (Leu et al. 2011; Søreide et al. 2010).
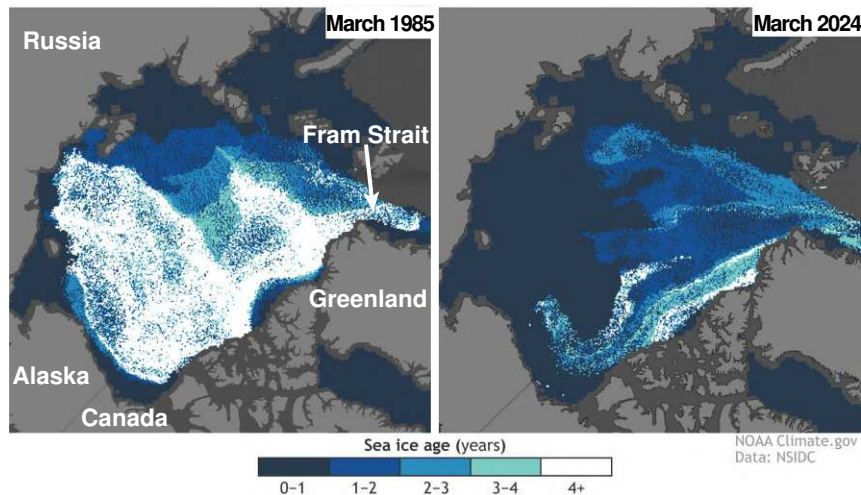
Figure 3: In mid-March 1985 (left), the winter maximum ice pack was dominated by ice at least four years old (white). At the beginning of March 2024 (right), only a small strip of such old ice remained. More than half of the winter ice pack was less than a year old (dark blue). Images by NOAA Climate.gov based on data from the National Snow and Ice Data Center.

Atlantification

An additional factor contributing to the diminishing sea ice in the Eurasian Arctic is the enhanced inflow of warmer, saltier Atlantic water into the Arctic via Fram Strait and the Barents Sea. This process, also referred to as Atlantification (Polyakov et al. 2017; Tesi et al. 2021; Wang et al. 2020), includes Atlantic water extending further poleward, occupying a larger fraction of the water column and/or experiencing a rise in its core water temperature (Asbjørnsen et al. 2020). These changes affect formation of winter sea ice and thereby increasing the area of a more boreal-like ice-free regime in the Arctic environment.

In areas of strong horizontal gradients, such as the upper ocean of the marginal ice zone (MIZ), submesoscale processes can be omnipresent (Gula et al. 2022; von Appen et al. 2018). These features are characterized by small spatial (0.1 to 10 km) and short temporal (hours to weeks) scales and thus have long been assumed to be of minor importance for pelagic processes. However, recent theoretical and empirical studies detected intense vertical and horizontal velocities within such structures (Klein and Lapeyre 2009; von Appen et al. 2018), which may have strong implications for pelagic and Atlantification processes. Yet, the influence of these structures on zooplankton dynamics is still largely unknown, mainly as the *in situ* sampling of such short-lived features is

challenging.

Associated with the inflow of Atlantic water are boreal species, which have recently increasingly extended their biogeographic range northward (Gregory et al. 2009), including bacterial communities (Priest et al. 2023), phytoplankton (Oziel et al. 2020), zooplankton (Mańko et al. 2020; Weydmann et al. 2014) and fishes (Fossheim et al. 2015; Vihtakari et al. 2018). This range shift is emphasized by first evidence of reproduction success among boreal zooplankton species such as the amphipod *Themisto compressa* and the euphausiid *Thysanoessa raschii* in Fram Strait and Kongsfjorden, respectively (Buchholz et al. 2012; Kraft et al. 2015), as well as the reappearance of the blue mussel *Mytilus edulis* along the western coast of Svalbard (Berge et al. 2005; Leopold et al. 2019). These developments signal an increasing invasion and successful colonization of Atlantic-influenced Arctic regions by boreal marine species, resulting in the Atlantification of the Arctic flora and fauna.

The transition from a community dominated by large, lipid-rich zooplankton with multi-year life cycles to populations with smaller, less lipid- rich and shorter-lived species may significantly alter the structure of Arctic food webs and overall ecosystem functioning (Kortsch et al. 2019; Pecuchet et al. 2020). Identifying the primary factors and processes driving and facilitating these regime shifts is crucial to understand and predict future changes in the Arctic marine environment.

Objectives

Arctic species have developed efficient adaptations to cope with and thrive under the extreme conditions of the Arctic environment. However, with ongoing climate change, they increasingly face more boreal-like conditions, including higher temperatures and reduced sea ice, which has physiological and trophodynamic consequences. Their fate in a future Arctic Ocean will partly depend on their capacity to cope with these transformations. Concurrently, the changing environment creates a habitat more and more suitable for boreal species, facilitating their colonization of the Arctic regime. Therefore, investigating ecological interactions, alongside physiological and trophodynamic effects, is essential for a better understanding of the broader implications of global change on this high-latitude ecosystem. The aim of this thesis is to provide a comprehensive understanding of potential impacts of climate change on Arctic zooplankton species by investigating not only physiological and trophodynamic but also oceanographiic processes and potential ecological interactions with boreal congeners.

The first objective of this thesis focuses on physiological responses of Arctic and boreal Atlantic zooplankton species to rising temperatures. Respiration rates of dominant Arctic species, *Calanus hyperboreus*, *Calanus glacialis*, *Paraeuchaeta glacialis* and *Themisto libellula*, and their co-occurring boreal congeners, *Calanus finmarchicus*, *Paraeuchaeta norvegica* and *Themisto abyssorum*, were determined at temperatures from 0 to 10 °C. Evaluating their metabolic reactions will help to assess the sensitivities of these species to ocean warming and to compare the

adaptive responses of polar species with their boreal relatives.

The second objective tackles potential alterations in trophic structures associated with a decline in sea ice and increased Atlantification. Examining the differences in Arctic and Atlantic-influenced food webs across Fram Strait will elucidate prospective future scenarios of a more boreal-like Arctic regime. The approach involves the application of fatty acid and stable isotope biomarker analyses to reveal dietary preferences and trophic levels of key zooplankton species with focus on Arctic and boreal-Atlantic sister species of *Calanus*, *Paraeuchaeta*, and *Themisto*.

The third objective focuses on the influence of small-scale oceanographic features on zooplankton dynamics. These features, characterized by their limited spatial (0.1 – 10 km) and temporal (hours to weeks) scales, present logistic challenges in the *in situ* measurement and thus in the assessment of their impact on biological processes. An *ad hoc* oceanographic and biological sampling campaign was carried out when a submesoscale filament was detected during the PS107 expedition in Fram Strait. By evaluating zooplankton data in context with the physical-oceanographic observations of the filament, this objective aims to shed light on the interactions between submesoscale physical processes and biological dynamics. Based on the results of the first three objectives, the fourth objective is to arrange these findings into a broader context. It aims to create an overall framework that helps us understand and identify the key factors and processes behind potential changes in the Arctic pelagic ecosystem.

Materials and methods

In this section, I introduce a relatively novel methodology for species identification based on their proteome. For other methods utilized in this thesis, which are commonly applied in scientific research, detailed explanations can be found in the respective sections of the manuscripts.

MALDI-TOF Mass Spectrometry proteomic fingerprinting

Monitoring of community composition is necessary to understand if an ecosystem is changing and therefore a precise species identification and quantification of specimens and their developmental stages is essential. The processing of zooplankton samples, however, is often the bottleneck in many monitoring surveys. Morphological analysis is generally the main method for quantitative assessments of zooplankton communities. Yet, morphological identification requires extensive knowledge, is extremely time consuming and prone to bias and human error. Additionally, the absence of distinctive morphological features between congeners, cryptic species or juveniles can further complicate the analysis, making morphological species discrimination challenging or even impossible.

Proteomic fingerprinting using MALDI-TOF MS ('matrix-assisted laser desorption/ionization time-of-flight mass spectrometry') originated in microbiology, where it is now routinely applied in

clinical diagnostics for pathogen identification (Chen et al. 2021; Patel 2015). The identification of organisms is based on the species-specific pattern of peptide- and protein compounds. The advantage over otherwise routinely used morphological or genetic approaches is its time- and cost-efficiency (Kaiser et al. 2018; Rossel et al. 2019).

The preparation of samples and their measurement is straightforward (Laakmann et al. 2013; Rossel et al. 2023): single specimens are placed into a solution which contains a matrix (α– Cyano–4–hydroxycinnamic acid) and a standard solvent consisting of 50% acetonitrile, 47.5% nuclease-free water and 2.5% trifluoroacetic acid. The amount of solution depends on the size of specimens. For different species and developmental stages of *Calanus* $3 - 30\,\mu L$ were used (Rossel et al. 2023). After a 5 min incubation, $1.5\,\mu L$ of the extract is applied to a target plate and allowed to evaporate at room temperature during which the molecules co-crystallize with the matrix. During measurement, short laser pulses cause the desorption and ionization of the sample molecules. These charged molecules are accelerated in an electric field and their time-of-flight is measured in a vacuum flight tube. Depending on this time of flight, the different masses of single molecules are represented as peaks in a mass spectrum between 2 to kDa. The resulting protein mass spectra exhibit a species-specific pattern of peptides and proteins (Kaiser et al. 2018). The entire measurement process for one target plate (96 spots) takes approximately $1.5\,h$. Data processing is conducted in R using the R packages MALDIquantForeign (Gibb 2015) and MALDIquant (Gibb and Strimmer 2012). For detailed description of these steps see Rossel et al. (2023).

The application of MALDI-TOF MS for metazoan identification is relatively novel, but several studies successfully demonstrate the usefulness for the identification of marine invertebrates, including cnidarians (Holst et al. 2019), copepods (Bode et al. 2017; Laakmann et al. 2013; Peters et al. 2023) and molluscs (Wilke et al. 2020), as well as for fish (Rossel et al. 2021).

An example of important, but difficult, accurate species identification in the Arctic ecosystem is the differentiation between congeners of *Calanus*. Both 'true' Arctic species, *C. hyperboreus* and *C. glacialis*, are generally good to distinguish due to morphological differences and the notably larger body size of *C. hyperboreus*. However, differentiating *C. glacialis* from the boreal-Atlantic *C. finmarchicus* is more complex due to the lack of distinct morphological features. A differentiation between both species based on prosome length is commonly used (Hirche and Kosobokova 2011; Kwaśniewski et al. 2003; Unstad and Tande 1991). However, several studies report a considerable overlap in the size ranges of both species (Choquet et al. 2017; Choquet et al. 2018; Parent et al. 2011), which often results in the overestimation of *C. finmarchicus* (Balazy et al. 2023; Gabrielsen et al. 2012). As both species serve as indicators for Arctic and Atlantic water masses, respectively, precise identification is vital for a deeper understanding of the ecosystem's status in relation to climate change and Atlantification.

Therefore, an additional aim of this thesis was to evaluate the applicability of proteomic fingerprinting as a new methodology for the rapid identification of morphologically similar *Calanus* congeners. In Chapter IV we demonstrate that proteomic fingerprinting is a promising method

meeting these requirements. While the approach is semi-quantitative, still necessitating the sorting of specimens from samples, its fast preparation and analytical processing allow for the identification of hundreds of individuals at species and potentially even developmental stage level within a matter of hours. This method could thus substantially facilitate identification of climate-relevant but morphologically similar indicator species such as *C. finmarchicus* and *C. glacialis* in long term monitoring studies, e.g. the Long-Term Ecological Research Observatory HAUSGARTEN of the Alfred Wegener Institute in Fram Strait.

Thesis outline and author contributions

Chapter I – Physiological response to warming

Patricia Kaiser, Wilhelm Hagen, Maya Bode-Dalby, Holger Auel (2022). **Tolerant but facing increased competition: Arctic zooplankton versus Atlantic invaders in a warming ocean**. *Frontiers in Marine Science,* 9: 908638. DOI: 10.3389/fmars.2022.908638

Contributions

Concept and design: 60%

Acquisition of data: 30%

Data analysis: 90%

Preparation of figures and tables: 100%

Drafting of the manuscript: 80%

Chapter II – Arctic versus boreal food web structures

Patricia Kaiser, Wilhelm Hagen, Anna Schukat, Katja Metfies, Sabrina Dorschner, Johanna Biederbick, Holger Auel. **Phytoplankton diversity and zooplankton diets across Fram Strait: Spatial patterns with implications for the future Arctic Ocean**. Manuscript under review in *Progress in Oceanography*

Contributions

Concept and design: 80%

Acquisition of data: 30%

Data analysis: 90%

Preparation of figures and tables: 100%

Drafting of the manuscript: 95%

Chapter III – Role of submesoscale processes

Patricia Kaiser, Wilhelm Hagen, Wilken-Jon von Appen, Barbara Niehoff, Nicole Hildebrandt, Holger Auel (2021). **Effects of a submesoscale oceanographic filament on zooplankton dynamics in the Arctic Marginal Ice Zone**. *Frontiers in Marine Science*, 8: 625395. DOI: 10.3389/fmars.2021.625395

Contributions

Concept and design: 80%

Acquisition of data: 80%

Data analysis: 90%

Preparation of figures and tables: 90%

Drafting of the manuscript: 90%

Chapter IV – Proteomic fingerprinting

Sven Rossel, **Patricia Kaiser**, Maya Bode-Dalby, Jasmin Renz, Silke Laakmann, Holger Auel, Wilhelm Hagen, Pedro Martínez Arbizu, Janna Peters (2022). **Proteomic fingerprinting enables quantitative biodiversity assessments of species and ontogenetic stages in *Calanus* congeners (Copepoda, Crustacea) from the Arctic Ocean**. *Molecular Ecology Resources*, 23: 382-395. DOI: 10.1111/1755-0998.13714

Contributions

Concept and design: 70%
Acquisition of data: 50%
Data analysis: 30%
Preparation of figures and tables: 20%
Drafting of the manuscript: 30%

References

Ardyna, M, Babin, M, Gosselin, M, Devred, E, Rainville, L, and Tremblay, J-É. (2014). Recent Arctic Ocean sea ice loss triggers novel fall phytoplankton blooms. *Geophys Res Lett* 41, 6207–6212.

Arrigo, KR (2014). Sea ice ecosystems. *Annu Rev Mar Sci* 6, 439–467.

Arrigo, KR (2017). Sea ice as a habitat for primary producers. *Sea Ice*. Edited by Thomas, David N. 1st edition. Wiley, 352–369.

Arrigo, KR, Van Dijken, G, and Pabi, S (2008). Impact of a shrinking Arctic ice cover on marine primary production. *Geophys Res Lett* 35, 2008GL035028.

Asbjørnsen, H, Årthun, M, Skagseth, Ø, and Eldevik, T (2020). Mechanisms underlying recent Arctic Atlantification. *Geophys Res Lett* 47, e2020GL088036.

Auel, H and Hagen, W (2002). Mesozooplankton community structure, abundance and biomass in the central Arctic Ocean. *Mar Biol* 140, 1013–1021.

Auel, H and Werner, I (2003). Feeding, respiration and life history of the hyperiid amphipod *Themisto libellula* in the Arctic marginal ice zone of the Greenland Sea. *J Exp Mar Bio Ecol* 296, 183–197.

Balazy, K, Trudnowska, E, Wojczulanis-Jakubas, K, Jakubas, D, Præbel, K, Choquet, M, Brandner, MM, Schultz, M, Bitz-Thorsen, J, Boehnke, R, Szeligowska, M, Descamps, S, Strøm, H, and Błachowiak-Samołyk, K (2023). Molecular tools prove little auks from Svalbard are extremely selective for *Calanus glacialis* even when exposed to Atlantification. *Sci Rep* 13, 13647.

Bayliss, R (2002). Sir John Franklin's last Arctic expedition: a medical disaster. *J R Soc Med* 95, 151–153.

Berge, J, Daase, M, Hobbs, L, Falk-Petersen, S, Darnis, G, and Søreide, JE (2020). Zooplankton in the polar night. *Polar Night Marine Ecology*. Edited by Berge, J, Johnsen, G, and Cohen, JH. Volume 4. Series Title: Advances in Polar Ecology. Cham: Springer International Publishing, 113–159.

Berge, J, Johnsen, G, Nilsen, F, Gulliksen, B, and Slagstad, D (2005). Ocean temperature cscillations enable reappearance of blue mussels *Mytilus edulis* in Svalbard after a 1000 year absence. *Mar Ecol Prog Ser* 303, 167–175.

Beszczynska-Möller, A, Fahrbach, E, Schauer, U, and Hansen, E (2012). Variability in Atlantic water temperature and transport at the entrance to the Arctic Ocean, 1997–2010. *ICES Mar Sci Symp* 69, 852–863.

Bode, M, Laakmann, S, Kaiser, P, Hagen, W, Auel, H, and Cornils, A (2017). Unravelling diversity of deep-sea copepods using integrated morphological and molecular techniques. *J Plankton Res* 39, 600–617.

Boetius, A, Albrecht, S, Bakker, K, Bienhold, C, Felden, J, Fernández-Méndez, M, Hendricks, S, Katlein, C, Lalande, C, Krumpen, T, Nicolaus, M, Peeken, I, Rabe, B, Rogacheva, A, Rybakova, E, Somavilla, R, Wenzhöfer, F, and RV *Polarstern* ARK27-3-Shipboard Science Party (2013). Export of algal biomass from the melting Arctic sea ice. *Sci* 339, 1430–1432.

Broms, C, Melle, W, and Kaartvedt, S (2009). Oceanic distribution and life cycle of *Calanus* species in the Norwegian Sea and adjacent waters. *Deep-Sea Res II* 56, 1910–1921.

Buchholz, F, Werner, T, and Buchholz, C (2012). First observation of krill spawning in the high Arctic Kongsfjorden, west Spitsbergen. *Polar Biol* 35, 1273–1279.

Chen, X-F, Hou, X, Xiao, M, Zhang, L, Cheng, J-W, Zhou, M-L, Huang, J-J, Zhang, J-J, Xu, Y-C, and Hsueh, P-R (2021). Matrix-assisted laser desorption/ionization time of flight mass spectrometry (MALDI-TOF MS) analysis for the identification of pathogenic microorganisms: a review. *Microorganisms* 9, 1536.

Choquet, M, Hatlebakk, M, Dhanasiri, AKS, Kosobokova, K, Smolina, I, Søreide, JE, Svensen, C, Melle, W, Kwaśniewski, S, Eiane, K, Daase, M, Tverberg, V, Skreslet, S, Bucklin, A, and Hoarau, G (2017). Genetics redraws pelagic biogeography of *Calanus*. *Biol Lett* 13, 20170588.

Choquet, M, Kosobokova, K, Kwaśniewski, S, Hatlebakk, M, Dhanasiri, AKS, Melle, W, Daase, M, Svensen, C, Søreide, JE, and Hoarau, G (2018). Can morphology reliably distinguish between the copepods *Calanus finmarchicus* and *C. glacialis*, or is DNA the only way? *Limnol Oceanogr: Methods* 16, 237–252.

Conover, R J and Siferd, Timothy D (1993). Dark-season survival strategies of coastal zone zooplankton in the Canadian Arctic. *Arctic* 46, 303–311.

Daase, M, Berge, J, Søreide, JE, and Falk-Petersen, S (2021). Ecology of Arctic pelagic communities. *Arctic Ecology*. Edited by Thomas, DN, 231–259.

Dalpadado, Padmini (2002). Inter-specific variations in distribution, abundance and possible life-cycle patterns of *Themisto* spp. (Amphipoda) in the Barents Sea. *Polar Biol* 25, 656–666.

Darnis, G, Robert, D, Pomerleau, C, Link, H, Archambault, P, Nelson, RJ, Geoffroy, M, Tremblay, J-É., Lovejoy, C, Ferguson, SH, Hunt, BPV, and Fortier, L (2012). Current state and trends in Canadian Arctic marine ecosystems: II. Heterotrophic food web, pelagic-benthic coupling, and biodiversity. *Clim Change* 115, 179–205.

De Steur, L, Hansen, E, Gerdes, R, Karcher, M, Fahrbach, E, and Holfort, J (2009). Freshwater fluxes in the East Greenland Current: a decade of observations. *Geophys Res Lett* 36, 2009GL041278.

Ehrlich, J, Bluhm, B A, Peeken, I, Massicotte, P, Schaafsma, F L, Castellani, G, Brandt, A, and Flores, H (2021). Sea-ice associated carbon flux in Arctic spring. *Elem Sci Anth* 9, 00169.

England, MR, Eisenman, I, Lutsko, NJ, and Wagner, TJW (2021). The recent emergence of Arctic amplification. *Geophys Res Lett* 48, e2021GL094086.

Falk-Petersen, S (1999). Spatial distribution and life-cycle timing of zooplankton in the Marginal Ice Zone of the Barents Sea during the summer melt season in 1995. *J Plankton Res* 21, 1249–1264.

Falk-Petersen, S, Hagen, W, Kattner, G, Clarke, A, and Sargent, J (2000). Lipids, trophic relationships, and biodiversity in Arctic and Antarctic krill. *Can J Fish Aquat Sci* 57, 178–191.

Fossheim, M, Primicerio, R, Johannesen, E, Ingvaldsen, RB, Aschan, MM, and Dolgov, V (2015). Recent warming leads to rapid borealization of fish communities in the Arctic. *Nat Clim Change* 5, 673–677.

Gabrielsen, TM, Merkel, B, Søreide, JE, Johansson-Karlsson, E, Bailey, A, Vogedes, D, Nyga, H, Varpe, Ø, and Berge, J (2012). Potential misidentifications of two climate indicator species of the marine arctic ecosystem: *Calanus glacialis* and *C. finmarchicus*. *Polar Biol* 35, 1621–1628.

Garrison, Dl, Gibson, A, Coale, Sl, Gowing, Mm, Okolodkov, Yb, Fritsen, Ch, and Jeffries, Mo (2005). Sea-ice microbial communities in the Ross Sea: autumn and summer biota. *Marine Ecology Progress Series* 300, 39–52.

Garrison, DL, Jeffries, MO, Gibson, A, Coale, SL, Neenan, D, Fritsen, C, Okolodkov, YB, and Gowing, MM (2003). Development of sea ice microbial communities during autumn ice formation in the Ross Sea. *Marine Ecology Progress Series* 259, 1–15.

Gibb, S (2015). *MALDIquantForeign: Import/Export routines for MALDIquan. A package for R.*

Gibb, S and Strimmer, K (2012). MALDIquant: a versatile R package for the analysis of mass spectrometry data. *Bioinform* 28, 2270–2271.

Gosselin, M, Levasseur, M, Wheeler, PA, Horner, RA, and Booth, BC (1997). New measurements of phytoplankton and ice algal production in the Arctic Ocean. *Deep-Sea Res II* 44, 1623–1644.

Gregory, B, Christophe, L, and Martin, E (2009). Rapid biogeographical plankton shifts in the North Atlantic Ocean. *Glob Change Biol* 15, 1790–1803.

Grote, U, Pasternak, A, Arashkevich, E, Halvorsen, E, and Nikishina, A (2015). Thermal response of ingestion and egestion rates in the Arctic copepod *Calanus glacialis* and possible metabolic consequences in a warming ocean. *Polar Biol* 38, 1025–1033.

Gula, J, Taylor, J, Shcherbina, A, and Mahadevan, A (2022). Submesoscale processes and mixing. *Ocean Mixing: Drivers, Mechanisms and Impacts*. Edited by Meredith, M and Garabato, AN. Elsevier, 181–214.

Hagen, W (1999). Reproductive strategies and energetic adaptations of polar zooplankton. *Invertebr Reprod Dev* 36, 25–34.

Hagen, W and Auel, H (2001). Seasonal adaptations and the role of lipids in oceanic zooplankton. *Zoology* 104, 313–326.

Hattermann, T, Isachsen, PE, von Appen, W-J, Albretsen, J, and Sundfjord, A (2016). Eddy-driven recirculation of Atlantic Water in Fram Strait. *Geophys Res Lett* 43, 3406–3414.

Henriksen, MV, Jung-Madsen, S, Nielsen, TG, Møller, EF, Henriksen, KV, Markager, S, and Hansen, BW (2012). Effects of temperature and food availability on feeding and egg production of *Calanus hyperboreus* from Disko Bay, western Greenland. *Mar Ecol Prog Ser* 447, 109–126.

Hickey, CG, Savelle, JM, and Hobson, GB (1993). The route of Sir John Franklin's third Arctic expedition: an evaluation and test of an alternative hypothesis. *Arctic* 46, 78–81.

Hildebrandt, N, Niehoff, B, and Sartoris, FJ (2014). Long-term effects of elevated CO_2 and temperature on the Arctic calanoid copepods *Calanus glacialis* and *C. hyperboreus*. *Mar Pollut Bull* 80, 59–70.

Hirche, H-J (1987). Temperature and plankton: II. Effect on respiration and swimming activity in copepods from the Greenland Sea. *Mar Biol* 94, 347–356.

Hirche, H-J (1991). Distribution of dominant calanoid copepod species in the Greenland Sea during late fall. *Polar Biol* 11, 351–362.

Hirche, H-J (1996). Diapause in the marine copepod, *Calanus finmarchicus* — a review. *Ophelia* 44, 129–143.

Hirche, H-J and Kattner, G (1993). Egg production and lipid content of *Calanus glacialis* in spring: indication of a food-dependent and food-independent reproductive mode. *Mar Biol* 117, 615–622.

Hirche, H-J and Kosobokova, K (2007). Distribution of *Calanus finmarchicus* in the northern North Atlantic and Arctic Ocean—expatriation and potential colonization. *Deep-Sea Res II* 54, 2729–2747.

Hirche, H-J and Kosobokova, KN (2011). Winter studies on zooplankton in Arctic seas: the Storfjord (Svalbard) and adjacent ice-covered Barents Sea. *Mar Biol* 158, 2359–2376.

Hirche, H-J, Meyer, U, and Niehoff, B (1997). Egg production of *Calanus finmarchicus*: effect of temperature, food and season. *Mar Biol* 127, 609–620.

Holst, S, Heins, A, and Laakmann, S (2019). Morphological and molecular diagnostic species characters of Staurozoa (Cnidaria) collected on the coast of Helgoland (German Bight, North Sea). *Mar Biodivers* 49, 1775–1797.

Horvat, C, Jones, DR, Iams, S, Schroeder, D, Flocco, D, and Feltham, D (2017). The frequency and extent of sub-ice phytoplankton blooms in the Arctic Ocean. *Sci Adv* 3, e1601191.

Huenerlage, K, Graeve, M, Buchholz, C, and Buchholz, F (2015). The other krill: overwintering physiology of adult *Thysanoessa inermis* (Euphausiacea) from the high-Arctic Kongsfjord. *Aquat Biol* 23, 225–235.

Isaksson, E and Ryall, A (2023). The Queen of the Arctic: Louise Arner Boyd. *Polar Res* 42, 9075.

Janout, Markus A, Hölemann, Jens, Waite, Anya M, Krumpen, Thomas, von Appen, Wilken-Jon, and Martynov, Fedor (2016). Sea-ice retreat controls timing of summer plankton blooms in the Eastern Arctic Ocean. *Geophys Res Lett* 43, 12, 493–12, 501.

Jónasdóttir, SH, Visser, AW, Richardson, K, and Heath, MR (2015). Seasonal copepod lipid pump promotes carbon sequestration in the deep North Atlantic. *Proc Natl Acad Sci USA* 112, 12122–12126.

Jung-Madsen, S and Nielsen, TG (2015). Early development of *Calanus glacialis* and *C. finmarchicus*. *Limnol Oceanogr* 60, 934–946.

Kahru, M, Brotas, V, Manzano-Sarabia, M, and Mitchell, BG (2011). Are phytoplankton blooms occurring earlier in the Arctic? *Glob Change Biol* 17, 1733–1739.

Kahru, M, Lee, Zhongping, Mitchell, BG, and Nevison, CD (2016). Effects of sea ice cover on satellite-detected primary production in the Arctic Ocean. *Biol Lett* 12, 20160223.

Kaiser, P, Bode, M, Cornils, A, Hagen, W, Arbizu, PM, Auel, H, and Laakmann, S (2018). High-resolution community analysis of deep-sea copepods using MALDI-TOF protein fingerprinting. *Deep-Sea Res I* 138, 122–130.

Kattner, G and Hagen, W (2009). Lipids in marine copepods: latitudinal characteristics and perspective to global warming. *Lipids in Aquatic Ecosystems*. Edited by Arts, MT, Brett, M, and Kainz, M. Berlin: Springer, 257–280.

Kawasaki, T and Hasumi, H (2016). The inflow of Atlantic water at the Fram Strait and its inter-annual variability. *J Geophys Res Oceans* 121, 502–519.

Kjellerup, S, Dünweber, M, Swalethorp, R, Nielsen, TG, Møller, EF, Markager, S, and Hansen, BW (2012). Effects of a future warmer ocean on the coexisting copepods *Calanus finmarchicus* and *C. glacialis* in Disko Bay, western Greenland. *Mar Ecol Prog Ser* 447, 87–108.

Klein, P and Lapeyre, G (2009). The oceanic vertical pump induced by mesoscale and subme-soscale turbulence. *Annu Rev Mar Sci* 1, 351–375.

Koch, CW, Brown, TA, Amiraux, R, Ruiz-Gonzalez, C, MacCorquodale, M, Yunda-Guarin, GA, Kohlbach, D, Loseto, LL, Rosenberg, B, Hussey, NE, Ferguson, SH, and Yurkowski, DJ (2023). Year-round utilization of sea ice-associated carbon in Arctic ecosystems. *Nat Commun* 14, 1964.

Kortsch, S, Primicerio, R, Aschan, M, Lind, S, Dolgov, AV, and Planque, B (2019). Food-web structure varies along environmental gradients in a high-latitude marine ecosystem. *Ecography* 42, 295–308.

Kosobokova Kand Hirche, H-J (2009). Biomass of zooplankton in the eastern Arctic Ocean – a base line study. *Prog Oceanogr* 82, 265–280.

Kosobokova, K N (1998). New data on the life cycle of *Calanus glacialis* in the White Sea (Based on seasonal observations of its genital system development). *Oceanologia* 38, 347–355.

Kosobokova, KN (1999). The reproductive cycle and life history of the Arctic Copepod *Calanus glacialis* in the White Sea. *Polar Biol* 22, 254–263.

Kosobokova, KN and Hopcroft, RR (2010). Diversity and vertical distribution of mesozooplankton in the Arctic's Canada Basin. *Deep-Sea Res II* 57, 96–110.

Kosobokova, KN, Hopcroft, RR, and Hirche, H-J (2011). Patterns of zooplankton diversity through the depths of the Arctic's central basins. *Mar Biodiv* 41, 29–50.

Kraft, A, Berge, J, Varpe, Ø, and Falk-Petersen, S (2013). Feeding in Arctic darkness: mid-winter diet of the pelagic amphipods *Themisto abyssorum* and *T libellula*. *Mar Biol* 160, 241–248.

Kraft, A, Graeve, M, Janssen, D, Greenacre, M, and Falk-Petersen, S (2015). Arctic pelagic amphipods: lipid dynamics and life strategy. *J Plankton Res* 37, 790–807.

Kwaśniewski, S, Hop, H, Falk-Petersen, S, and Pedersen, G (2003). Distribution of *Calanus* species in Kongsfjorden, a glacial fjord in Svalbard. *J Plankton Res* 25, 1–20.

Laakmann, S, Gerdts, G, Erler, R, Knebelsberger, T, Mart, P, Arbizu, I, and Raupach, MJ (2013). Comparison of molecular species identification for North Sea calanoid copepods (Crustacea) using proteome fingerprints and DNA sequences. *Mol Ecol Resour* 13, 862–876.

Laxon, SW, Giles, KA, Ridout, AL, Wingham, DJ, Willatt, R, Cullen, R, Kwok, R, Schweiger, A, Zhang, J, Haas, C, Hendricks, S, Krishfield, R, Kurtz, N, Farrell, S, and Davidson, M (2013). CryoSat-2 estimates of Arctic sea ice thickness and volume. *Geophys Res Lett* 40, 732–737.

Lee, RF, Hagen, W, and Kattner, G (2006). Lipid storage in marine zooplankton. *Mar Ecol Prog Ser* 307, 273–306.

Leopold, P, Renaud, PE, Ambrose, WG, and Berge, J (2019). High Arctic *Mytilus* spp.: occurrence, distribution and history of dispersal. *Polar Biol* 42, 237–244.

Leu, E, Mundy, CJ, Assmy, P, Campbell, K, Gabrielsen, TM, Gosselin, M, Juul-Pedersen, T, and Gradinger, R (2015). Arctic spring awakening – Steering principles behind the phenology of vernal ice algal blooms. *Prog Oceanogr* 139, 151–170.

Leu, E, Søreide, JE, Hessen, DO, Falk-Petersen, S, and Berge, J (2011). Consequences of changing sea-ice cover for primary and secondary producers in the European Arctic shelf seas: timing, quantity, and quality. *Prog Oceanogr* 90, 18–32.

Lindsay, R and Schweiger, A (2015). Arctic sea ice thickness loss determined using subsurface, aircraft, and satellite observations. *Cryosphere* 9, 269–283.

Lischka, S and Hagen, W (2007). Seasonal lipid dynamics of the copepods *Pseudocalanus minutus* (Calanoida) and *Oithona similis* (Cyclopoida) in the Arctic Kongsfjorden (Svalbard). *Mar Biol* 150, 443–454.

Lund-Hansen, L C, Søgaard, DH, Sorrell, BK, Gradinger, R, and Meiners, KM (2020). *Arctic Sea Ice Ecology: Seasonal Dynamics in Algal and Bacterial Productivity*. Springer Polar Sciences. Cham: Springer International Publishing, 178 pp.

Mańko, MK, Gluchowska, M, and Weydmann-Zwolicka, A (2020). Footprints of Atlantification in the vertical distribution and diversity of gelatinous zooplankton in the Fram Strait (Arctic Ocean). *Prog Oceanogr* 189, 102414.

Meiners, K, Gradinger, R, Fehling, J, Civitarese, G, and Spindler, M (2003). Vertical distribution of exopolymer particles in sea ice of the Fram Strait (Arctic) during autumn. *Marine Ecology Progress Series* 248, 1–13.

Mills, W J (2003). *Exploring Polar Frontiers: A Historical Encyclopedia*. Santa Barbara, California: ABC-CLIO, 844 pp.

Mundy, CJ, Gosselin, M, Gratton, Y, Brown, K, Galindo, V, Campbell, K, Levasseur, M, Barber, D, Papakyriakou, T, and Bélanger, S (2014). Role of environmental factors on phytoplankton bloom initiation under landfast sea ice in Resolute Passage, Canada. *Mar Ecol Prog Ser* 497, 39–49.

Niehoff, B and Hirche, H-J (2005). Reproduction of *Calanus glacialis* in the Lurefjord (western Norway): indication for temperature-induced female dormancy. *Mar Ecol Prog Ser* 285, 107–115.

Niehoff, B, Madsen, S, Hansen, B, and Nielsen, T (2002). Reproductive cycles of three dominant *Calanus* species in Disko Bay, West Greenland. *Mar Biol* 140, 567–576.

Nishino, S, Kawaguchi, Y, Inoue, J, Hirawake, TU, Fujiwara, A, Futsuki, R, Onodera, J, and Aoyama, M (2015). Nutrient supply and biological response to wind-induced mixing, inertial motion, internal waves, and currents in the northern Chukchi Sea. *J Geophys Res Oceans* 120, 1975–1992.

Notz, D and Stroeve, J (2018). The trajectory towards a seasonally ice-free Arctic Ocean. *Curr Clim Change Rep* 4, 407–416.

Oziel, L, Baudena, A, Ardyna, M, Massicotte, P, Randelhoff, A, Sallée, J-B, Ingvaldsen, RB, Devred, E, and Babin, M (2020). Faster Atlantic currents drive poleward expansion of temperate phytoplankton in the Arctic Ocean. *Nat Commun* 11, 1705.

Parent, GJ, Plourde, S, and Turgeon, J (2011). Overlapping size ranges of *Calanus* spp. off the Canadian Arctic and Atlantic Coasts: impact on species' abundances. *J Plankton Res* 33, 1654–1665.

Pasternak, AF, Arashkevich, EG, Grothe, U, Nikishina, AB, and Solovyev, KA (2013). Different effects of increased water temperature on egg production of *Calanus finmarchicus* and *C. glacialis*. *Oceanol* 53, 547–553.

Patel, R (2015). MALDI-TOF MS for the diagnosis of infectious diseases. *Clin Chem* 61, 100–111.

Pecuchet, L, Blanchet, M-A, Frainer, A, Husson, B, Jørgensen, LL, Kortsch, S, and Primicerio, R (2020). Novel feeding interactions amplify the impact of species redistribution on an Arctic food web. *Glob Change Biol* 26, 4894–4906.

Peters, J, Laakmann, S, Rossel, S, Arbizu, PM, and Renz, J (2023). Perspectives of species identification by MALDI-TOF MS in monitoring—stability of proteomic fingerprints in marine epipelagic copepods. *Mol Ecol Resour* 23, 1077–1091.

Polyakov, IV, Pnyushkov, AV, Alkire, MB, Ashik, I M, Baumann, TM, Carmack, EC, Goszczko, Ilona, Guthrie, John, Ivanov, Vladimir V, Kanzow, T, Krishfield, R, Kwok, R, Sundfjord, A, Morison, J, Rember, R, and Yulin, A (2017). Greater role for Atlantic inflows on sea-ice loss in the Eurasian Basin of the Arctic Ocean. *Sci* 356, 285–291.

Previdi, M, Smith, KL, and Polvani, LM (2021). Arctic amplification of climate change: a review of underlying mechanisms. *Environ Res Lett* 16, 093003.

Priest, T, von Appen, W-J, Oldenburg, E, Popa, O, Torres-Valdés, S, Bienhold, C, Metfies, K, Boulton, W, Mock, T, Fuchs, BM, Amann, R, Boetius, A, and Wietz, M (2023). Atlantic water influx and sea-ice cover drive taxonomic and functional shifts in Arctic marine bacterial communities. *ISME J* 17, 1612–1625.

Rae, JWB, Zhang, YG, Liu, X, Foster, GL, Stoll, HM, and Whiteford, RDM (2021). Atmospheric CO_2 over the past 66 million years from marine archives. *Annu Rev Earth Planet Sci* 49, 609–641.

Rantanen, M, Karpechko, AY, Lipponen, A, Nordling, K, Hyvärinen, O, Ruosteenoja, K, Vihma, T, and Laaksonen, A (2022). The Arctic has warmed nearly four times faster than the globe since 1979. *Commun Earth Environ* 3, 168.

Rossel, S, Barco, A, Kloppmann, M, Arbizu, PM, Huwer, B, and Knebelsberger, T (2021). Rapid species level identification of fish eggs by proteome fingerprinting using MALDI-TOF MS. *J Proteomics* 231, 103993.

Rossel, S, Kaiser, P, Bode-Dalby, M, Renz, J, Laakmann, S, Auel, H, Hagen, W, Arbizu, PM, and Peters, J (2023). Proteomic fingerprinting enables quantitative biodiversity assessments of species and ontogenetic stages in *Calanus* congeners (Copepoda, Crustacea) from the Arctic Ocean. *Mol Ecol Res* 23, 382–395.

Rossel, S, Khodami, S, and Arbizu, PM (2019). Comparison of rapid biodiversity assessment of meiobenthos using MALDI-TOF MS and metabarcoding. *Front Mar Sci* 6, 659.

Schulte, PM, Healy, TM, and Fangue, NA (2011). Thermal performance curves, phenotypic plasticity, and the time scales of temperature exposure. *Integr Comp Biol* 51, 691–702.

Selz, Virginia, Saenz, BT, Van Dijken, G L, and Arrigo, KR (2018). Drivers of ice algal bloom variability between 1980 and 2015 in the Chukchi Sea. *J Geophys Res Oceans* 123, 7037–7052.

Sergeeva, V M, Sukhanova, I N, Flint, M V, Pautova, L A, Grebmeier, J M, and Cooper, L W (2010). Phytoplankton community in the western Arctic in July–August 2003. *Oceanol* 50, 184–197.

Serreze, MC and Barry, RG (2014). *The Arctic climate system*. 2nd edition. Cambridge University Press, 403 pp.

Serreze, MC, Crawford, AD, Stroeve, JC, Barrett, AP, and Woodgate, RA (2016). Variability, trends, and predictability of seasonal sea ice retreat and advance in the Chukchi Sea. *J Geophys Res Oceans* 121, 7308–7325.

Serreze, MC and Meier, WN (2019). The Arctic's sea ice cover: trends, variability, predictability, and comparisons to the Antarctic. *Ann N Y Acad Sci* 1436, 36–53.

Søreide, JE, Carroll, ML, Hop, H, Ambrose, WG, Hegseth, EN, and Falk-Petersen, S (2013). Sympagic-pelagic-benthic coupling in Arctic and Atlantic waters around Svalbard revealed by stable isotopic and fatty acid tracers. *Mar Biol Research* 9, 831–850.

Søreide, JE, Leu, E, Berge, J, Graeve, M, and Falk-Petersen, S (2010). Timing of blooms, algal food quality and *Calanus glacialis* reproduction and growth in a changing Arctic. *Glob Change Biol* 16, 3154–3163.

Stroeve, J and Notz, D (2018). Changing state of Arctic sea ice across all seasons. *Environ Res Lett* 13, 103001.

Stroeve, JC, Kattsov, V, Barrett, A, Serreze, M, Pavlova, T, Holland, M, and Meier, WN (2012). Trends in Arctic sea ice extent from CMIP5, CMIP3 and observations. *Geophy Res Lett* 39, 2012GL052676.

Sukhanova, IN, Flint, MV, Pautova, LA, Stockwell, DA, Grebmeier, JM, and Sergeeva, VM (2009). Phytoplankton of the western Arctic in the spring and summer of 2002: structure and seasonal changes. *Deep-Sea Res II* 56, 1223–1236.

Szymanski, A and Gradinger, R (2016). The diversity, abundance and fate of ice algae and phytoplankton in the Bering Sea. *Polar Biol* 39, 309–325.

Tedesco, L and Vichi, M (2014). Sea ice biogeochemistry: a guide for modellers. *PLoS ONE* 9, e89217.

Tesi, T, Muschitiello, F, Mollenhauer, G, Miserocchi, S, Langone, L, Ceccarelli, C, Panieri, G, Chiggiato, J, Nogarotto, A, Hefter, J, Ingrosso, G, Giglio, F, Giordano, P, and Capotondi, L (2021). Rapid Atlantification along the Fram Strait at the beginning of the 20th century. *Sci Adv* 7, eabj2946.

Torgersen, T and Huse, G (2005). Variability in retention of *Calanus finmarchicus* in the Nordic Seas. *ICES J Mar Sci* 62, 1301–1309.

Unstad, K H and Tande, Kurt S (1991). Depth distribution of *Calanus finmarchicus* and *C. glacialis* in relation to environmental conditions in the Barents Sea. *Polar Res* 10, 409–420.

Vihtakari, M, Welcker, J, Moe, B, Chastel, O, Tartu, S, and Hop, H (2018). Black-legged kittiwakes as messengers of Atlantification in the Arctic. *Sci Rep* 8, 1178.

Vihtakari, Mikko (2024). *ggOceanMaps: Plot Data on Oceanographic Maps using 'ggplot2'*. R package version 2.2.0.

Von Appen, W-J, Wekerle, C, Hehemann, L, Schourup-Kristensen, V, Konrad, C, and Iversen, MH (2018). Observations of a submesoscale cyclonic filament in the Marginal Ice Zone. *Geophys Res Lett* 45, 6141–6149.

Von Quillfeldt, CH (2000). Common diatom species in Arctic spring blooms: their distribution and abundance. *Bot Mar* 43, 499–516.

Waga, H and Hirawake, T (2020). Changing occurrences of fall blooms associated with variations in phytoplankton size structure in the Pacific Arctic. *Front Mar Sci* 7, 209.

Wang, Q, Wekerle, C, Wang, X, Danilov, S, Koldunov, N, Sein, D, Sidorenko, D, von Appen, W-J, and Jung, T (2020). Intensification of the Atlantic water supply to the Arctic Ocean through Fram Strait induced by Arctic sea ice decline. *Geophys Res Lett* 47, e2019GL086682.

Wassmann, P, Kosobokova, KN, Slagstad, D, Drinkwater, KF, Hopcroft, RR, Moore, SE, Ellingsen, I, Nelson, RJ, Carmack, E, Popova, E, and Berge, J (2015). The contiguous domains of Arctic Ocean advection: trails of life and death. *Prog Oceanogr* 139, 42–65.

Weydmann, A, Carstensen, J, I, Goszczko, Dmoch, K, Olszewska, A, and Kwasniewski, S (2014). Shift towards the dominance of boreal species in the Arctic: inter-annual and spatial zooplankton variability in the West Spitsbergen Current. *Mar Ecol Prog Ser* 501, 41–52.

Weydmann, A, Zwolicki, A, Muś, K, and Kwasniewski, S (2015). The effect of temperature on egg development rate and hatching success in *Calanus glacialis* and *C. finmarchicus*. *Polar Res* 34, 23947.

Wilke, T, Renz, J, Hauffe, T, Delicado, D, and Peters, J (2020). Proteomic fingerprinting discriminates cryptic gastropod species. *Malacologia* 63, 131–137.

Zeebe, RE, Ridgwell, A, and Zachos, JC (2016). Anthropogenic carbon release rate unprecedented during the past 66 million years. *Nat Geosci* 9, 325–329.

1

Tolerant but facing increased competition: Arctic zooplankton versus Atlantic invaders in a warming ocean

Patricia Kaiser, Wilhelm Hagen, Maya Bode-Dalby, Holger Auel

Universität Bremen, BreMarE – Bremen Marine Ecology, Marine Zoology, P.O. Box 330440, 28334 Bremen, Germany

Abstract

The Arctic Ocean is rapidly changing. Air temperature is rising two to four times faster in the Arctic than the global average, with dramatic consequences for the ecosystems. Polar zooplankton species have to cope with those increasing temperatures, whilst simultaneously facing increasing competition by boreal-Atlantic sister species advected into the Arctic Ocean via a stronger Atlantic inflow. To assess the sensitivity of Arctic and Atlantic zooplankton to rising temperatures, respiration rates of dominant Arctic species (*Calanus hyperboreus*, *Calanus glacialis*, *Paraeuchaeta glacialis*, *Themisto libellula*) and their co-occurring Atlantic congeners (*Calanus finmarchicus*, *Paraeuchaeta norvegica*, *Themisto abyssorum*) were measured at ambient temperatures and simulated conditions of ocean warming from 0 to 10 °C during three expeditions with RV *Polarstern* to the Arctic Fram Strait. Arctic zooplankton showed only slowly increasing respiration rates with increasing temperatures, also indicated by low Q_{10} ratios. In contrast, boreal-Atlantic representatives responded to higher temperatures by a rapid and steeper increase in their respiration rates (higher Q_{10}), suggesting higher metabolic activity. These results imply that Arctic species are physiologically more tolerant to ocean warming than expected, but might be outcompeted by their Atlantic congeners beyond a certain temperature threshold in areas of strong distribution overlap. Thus, the 'Atlantification' of the Arctic zooplankton community seems to be driven rather by ecological interactions than by physiological limitations. Changes in zooplankton community composition and biodiversity will have major consequences for trophodynamics and energy flux in Arctic ecosystems, since polar species tend to be larger than their southern counterparts and have a higher lipid content, providing more energy-rich food for higher trophic levels.

1.1 Introduction

The Arctic Ocean and adjacent ice-covered seas are the regions that are most rapidly affected by global warming. Air surface temperature is rising two to four times faster in the Arctic than the global average (Bekryaev et al. 2010; Masson-Delmotte et al. 2013; Meredith et al. 2019) and the sea surface and Atlantic Water core temperatures in the Arctic Ocean have been increasing for the last decades (Hartmann et al. 2013; Meredith et al. 2019; Polyakov et al. 2013; Polyakov et al. 2012).

The increasing northward inflow of warm and saline Atlantic waters is referred to as 'Atlantification' or 'Borealization' of the Arctic (Polyakov et al. 2017). Associated with Atlantic water masses are boreal-Atlantic species, which are rapidly expanding their ranges poleward (Beaugrand et al. 2009). For instance, copepods (Beaugrand et al. 2002; Weydmann et al. 2014), gelatinous zooplankton (Mańko et al. 2020) and fishes (Fossheim et al. 2015; Vihtakari et al. 2018) are shifting northward in their biogeographic distribution. This is emphasized by first evidence of repro-

ductive success of boreal zooplankton species, such as the amphipod *Themisto compressa* and the euphausiid *Thysanoessa raschii* near the Svalbard archipelago in Fram Strait and in Kongsfjorden, Svalbard, respectively (Buchholz et al. 2012; Kraft et al. 2013). Thus, the Atlantic-influenced regions of the Arctic Ocean are increasingly invaded and successfully colonized by boreal-Atlantic species, resulting in the Atlantification of the Arctic fauna.

In Fram Strait, the only deep-water connection of the Arctic with the Atlantic Ocean, three species of *Calanus* co-occur, with two 'true polar-Arctic' species, *Calanus hyperboreus* and *C. glacialis*, and one expatriate from the boreal-Atlantic, *C. finmarchicus* (Wassmann et al. 2015). Copepods of the genus *Calanus* are a key component in the Arctic marine food web, as they usually dominate in terms of biomass and represent a crucial link between primary production and higher trophic levels (Auel and Hagen 2002; Kosobokova 2009; Mumm et al. 1998). The three species share similarities considering morphology and life-history traits, however, they differ particularly considering size, life-cycles duration and phenology (Daase et al. 2021; Møller and Nielsen 2020). Both Arctic species are characterized by larger size, higher lipid content and life-cycles exceeding one year (Daase et al. 2021). Reproductive strategies of polar *Calanus* species are highly adapted to the harsh and strongly seasonal Arctic conditions. *C. hyperboreus* is a capital breeder, i.e. using stored lipid resources for reproduction (Daase et al. 2021). Hence, *C. hyperboreus* can reproduce independent of immediate food supply and is able to initiate reproduction prior to the onset of the ice algal bloom. By the time the spring bloom is commencing, nauplii of *C. hyperboreus* have reached their feeding stage (from naupliar stage 3 onward) and are able to utilize the early ice algal bloom for growth and development (Daase et al. 2021; Jung-Madsen et al. 2013). *C. glacialis* is also well adapted due to a high flexibility in its reproductive strategy, being able to fuel reproduction both by lipid reserves and by utilizing the early ice algal bloom (Hirche and Kattner 1993; Wold et al. 2011). *C. finmarchicus*, in contrast, is smaller in size, hence possesses comparably smaller lipid reserves, has a one-year life-cycle and is an income breeder, i.e. reproduction is dependent on direct food intake (Daase et al. 2021).

Shifting from a community dominated by large and lipid-rich copepods with multi-year life cycles to one with smaller, less lipid-rich and shorter-lived species could have consequences for the entire Arctic food web. For instance, the Arctic planktivorous little auk (*Alle alle*) and juvenile polar cod (*Boreogadus saida*) are strongly dependent on the larger Arctic *Calanus* species and, in the case of little auks, even extend their foraging trips to find their preferred prey (Bouchard and Fortier 2020; Karnovsky et al. 2010; Kwaśniewski et al. 2010). It is, thus, crucial to better understand the processes driving transitions in community composition.

As a consequence of species-specific temperature tolerance limits and temperature-dependent effects on performance, organisms occupy distinct thermal niches, which are an important factor in defining their biogeographical distribution (Schulte et al. 2011). Polar marine ectotherms are considered to have a comparably narrow optimum at low temperatures and a limited ability to cope with rising environmental temperatures (Peck 2002). This stenothermy is particularly pronounced

in Antarctic ectotherms (Peck et al. 2010; Pörtner et al. 2007; Sandersfeld et al. 2015), but has also been reported for Arctic invertebrates and fishes (Franklin et al. 2013; Huenerlage and Buchholz 2015).

The concept of oxygen- and capacity-limited thermal tolerance (OCLTT) explains temperature effects on the aerobic scope as a main driver in influencing energy availability for performance and, thus, eventually the biogeographic distribution of species (Pörtner et al. 2017). The aerobic scope is determined by the difference between the standard and maximum metabolic rate and represents excess capacity of aerobic energy available for achieving fitness and supporting biological functions. Beyond a threshold temperature (pejus temperature), a mismatch between oxygen supply capacity and oxygen demand occurs, reducing the aerobic scope and, thus, limiting available energy for essential biological processes such as foraging, growth and reproduction. While temperatures beyond the pejus temperature do not necessarily influence the survival of a species yet, they reduce its performance and, hence, its competitive fitness (Pörtner 2001; Verberk et al. 2016).

To assess the sensitivity of polar-Arctic versus boreal-Atlantic zooplankton to rising temperatures, we conducted respiration measurements as a proxy for metabolic activity at five temperatures ranging from 0 to 10 °C with the three co-existing *Calanus* species in Arctic Fram Strait. In addition, pairs of polar versus boreal-Atlantic congeners of other zooplankton taxa, the predatory copepods *Paraeuchaeta glacialis* and *P. norvegica* and the hyperiid amphipods *Themisto libellula* and *T. abyssorum*, were included in the study. Specifically, we hypothesize that (1) polar species show a stenothermic response, i.e. rapidly increasing metabolic rates at lower temperatures (high Q_{10} value), followed by a narrow optimum and a sharp drop, including increased mortality at higher temperatures; (2) mass-specific respiration rates are generally higher in the smaller boreal-Atlantic species compared to their larger polar congeners; (3) the mechanism behind the Atlantification of the Arctic fauna is mainly driven by physiological limits of Arctic zooplankton to increasing temperatures.

1.2 Materials and methods

1.2.1 Sampling

Sampling was conducted at the end of summer during three cruises with RV *Polarstern* to Arctic Fram Strait in July-September 2016, 2017 and 2019 (PS100, PS107 and PS121, respectively; Figure 1.1).

In situ conditions

In situ temperatures were obtained with a CTD (Conductivity Temperature Depth) profiling system prior to each sampling of zooplankton. *In situ* temperatures did not vary distinctly between years but rather between regions in Fram Strait. The western part of Fram Strait is under strong influence of the East Greenland Current (EGC), exporting cold and fresh Polar Surface Water out
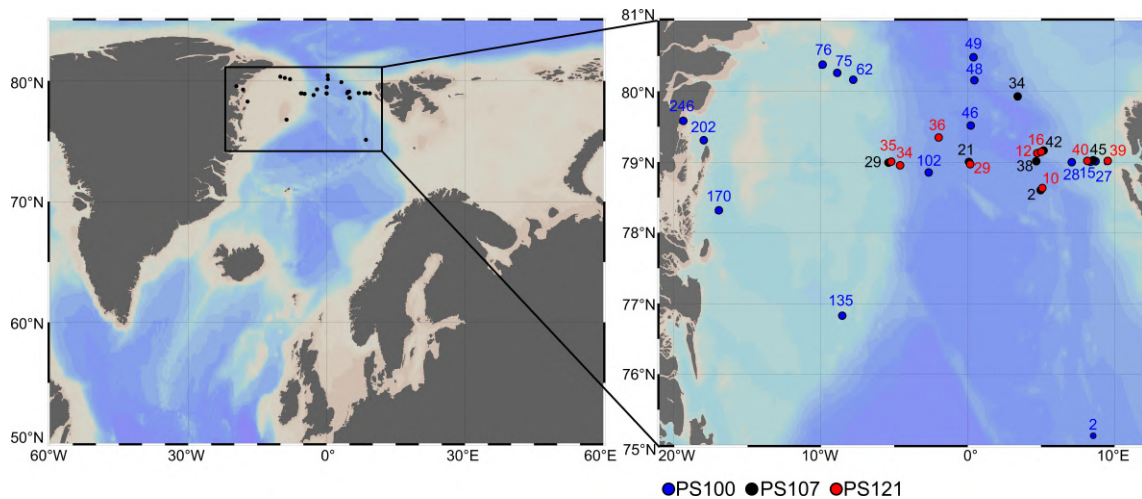
Figure 1.1: Location of stations where zooplankton specimens were collected for respiration experiments during cruises PS100, PS107 and PS121. Numbers above dots indicate respective station number.

of the Arctic Ocean. Temperature profiles of the stations during the three cruises were characterized by temperatures below $0\,^{\circ}\text{C}$ in epipelagic layers (supplement material S1). Between 200 to $300\,\text{m}$ temperatures increased up to a maximum of $3\,^{\circ}\text{C}$ and then decreased again to around $0\,^{\circ}\text{C}$ in $1000\,\text{m}$. In the eastern part of Fram Strait, the West Spitsbergen Current (WSC) flows northward and transports rather warm, saline Atlantic water into the Arctic Ocean. Profiles during the three cruises showed high temperatures of 5 to $9\,^{\circ}\text{C}$ in surface waters. With increasing depth temperatures steadily decreased to $\leq 0\,^{\circ}\text{C}$ below $600\,\text{m}$.

The zone in between the two currents, here referred to as central Fram Strait, is characterized by a highly dynamic and turbulent hydrographic regime (Kawasaki and Hasumi 2016; von Appen et al. 2018). While partly under influence of the EGC, branches of the WSC turn westward to 'recirculate' and subduct below the Polar Surface Water (Hattermann et al. 2016). The variability of central Fram Strait was reflected in the temperature profiles during the three expeditions. Four stations showed similar profiles as the ones under influence of the EGC (PS 100 Stns 48, 49 and PS121 Stns 29, 36), three showed a mix of both characteristics (PS100 Stns 46, 102 and PS107 Stn 21) and one was influenced by the WSC (PS107 Stn 34; Table S1 at https://doi.org/10.3389/fmars.2022.908638).

Zooplankton sampling

Zooplankton sampling was conducted using either a multiple opening and closing net equipped with five nets for stratified vertical hauls (Hydrobios Multinet Midi, mouth opening $0.25\,\text{m}^2$, mesh size $150\,\mu\text{m}$, hauling speed $0.5\,\text{m}^{-1}$) or a bongo net (mesh size: 200 to $500\,\mu\text{m}$, tow speed 1 2 kn) with filtering cod-ends, respectively. Vertical hauls with the Multinet usually sampled the entire water column from the seafloor or a maximum sampling depth of $1500\,\text{m}$ to the surface (Kanzow 2017; Metfies 2020; Schewe 2018). Specimens used for respiration measurements were sorted immediately after the hauls in a temperature-controlled lab container (2 to $4\,^{\circ}\text{C}$). Only apparently

healthy and active individuals were selected and kept at $0\,^\circ\mathrm{C}$. $0\,^\circ\mathrm{C}$ were chosen, as it was within the *in situ* temperature range for all species.

Respiration measurements

Respiration rates of zooplankton organisms were measured on board at different temperatures ($0, 4, 6, 8$ and $10\,^\circ\mathrm{C}$) non-invasively by optode respirometry using a 10-Channel Fiber Optic Oxygen Meter (OXY-10, PreSens, Precision Sensing GmbH, Regensburg, Germany). Each individual was only measured once at one of the experimental temperatures and they were selected randomly for the respective temperatures. Prior to the measurements, specimens were transferred from $0\,^\circ\mathrm{C}$ to the incubator, brought slowly to their respective experimental temperature and acclimated for at least 24 h. For the experiments, individuals were carefully transferred into gas-tight glass bottles containing 13 mL of $0.2\,\mu\mathrm{m}$ GF/F filtered and oxygenated seawater. The number of individuals per bottle depended on size, ontogenetic stage and metabolic activity with a maximum of six specimens per bottle (for *Calanus finmarchicus* copepodite stage C5). Experiments were run in a temperature-controlled incubator in the dark (refrigerator with external precision thermostat) for generally 8 to 24 h with continuous measurements every 15 s. If oxygen levels fell below a critical level (below 60% air saturation), experiments were terminated earlier (usually in case of larger animals such as the amphipods *Themisto* spp.). In each experimental run, two channels of the multi-channel optode respirometer were used for animal-free controls to compensate for potential microbial oxygen consumption or production. After the experiments, the taxonomic identification of species and developmental stages were confirmed under a dissecting microscope (Leica MS5) and amphipods were measured for body length. *Calanus glacialis* and *C. finmarchicus* are two sister species that are morphologically difficult to distinguish. Differentiation based on prosome length is a commonly used method to discriminate between the two congeners (Daase et al. 2018). However, due to an overlap of size distributions in regions of co-occurrence (Choquet et al. 2018; Gabrielsen et al. 2012) and depth-dependent size distributions (Kaiser et al. 2021), this can lead to individuals being misidentified, usually with a bias towards an underestimation of *C. glacialis* (Choquet et al. 2018; Daase et al. 2018). Nevertheless, *C. glacialis* reaches distinctly larger sizes than *C. finmarchicus*. Therefore, to avoid the overlapping size ranges, only larger individuals of the same stage were used for experiments with *C. glacialis* and smaller individuals for *C. finmarchicus*. All individuals were then deep-frozen at $-80\,^\circ\mathrm{C}$ for subsequent dry mass (DM) determination after lyophilization for 48 h, in the home laboratory at the University of Bremen, Germany. Individuals were then weighed using a microbalance (Sartorius MC215).

The first two hours of each measurement (or 20 min when measurements had to be terminated early due to oxygen depletion) were excluded from further analysis to avoid potential bias by handling stress or temperature adjustments at the start of the experiments. Animal-free controls were treated equally. The mean decline in dissolved oxygen concentration in the animal-free controls was subtracted from the respective measurements with animals of the same experimental run. To

compare respiration between different species, mass-specific respiration rates (MSRR) were calculated. Statistical analyses were performed using GraphPad Prism (version 8.0.2). Differences between MSRR during the three years (2016, 2017 and 2019) were tested for significance using Welch-ANOVA as homogeneity of variance was not always met and sample size was highly variable, followed by the Games-Howell's post hoc multiple comparison test. Both analyses were chosen, as they do not assume equal variances and sample sizes. No significant differences were detected in MSRR of the seven species between the three years at each temperature, thus, the experimental results from the different years were pooled.

MSRR were standardized for all species to exclude the factor body mass on respiration. For the standardization, $\log_{10}$ transformed MSRR of all species at $0\,°C$ were plotted against $\log_{10}$ transformed DM to obtain the scaling coefficient $b(-0.25)$ from the linear slope of the regression line. Standardized MSRR were calculated as follows:

$$R_{\mathrm{stand}} = \frac{R_{\mathrm{MSRR}}}{\mathrm{DM}^{(-025)}} * \mathrm{stDM}^{(-0.25)}$$

where R_{MSRR} is the mass-specific respiration rate, DM is the respective dry mass, stDM is the genus- and stage-specific mean DM ($2\,\mathrm{mg}$ for *Calanus* females, $1.2\,\mathrm{mg}$ for *Calanus* C5, $5.6\,\mathrm{mg}$ for *Paraeuchaeta* females, $1.8\,\mathrm{mg}$ for *Paraeuchaeta* C5, $7\,\mathrm{mg}$ for *Themisto*). Genus- and stage-specific DMs were obtained by averaging dry masses of all sampled individuals of the respective genus and stage.

Intraspecific temperature-dependent differences in MSRR were tested for significance using Welch-ANOVA, followed by Games-Howell's post hoc multiple comparisons test. Differences in slopes of linear regression performed on $\log_{10}$ transformed MSRR were tested for significance between species of the same genus to identify significant differences in the species-specific increase of MSRR.

Finally, species- and stage-specific Q_{10} values were calculated based on exponential regression of all MSRR data at the different temperatures. With the obtained exponential function, calculated MSRR rates for $10\,°C$ were divided by rates at $0\,°C$, providing the Q_{10} values, i.e. the factorial increase associated with a $10\,°C$ rise in temperature. To exclude that *Calanus* females and C5 from greater depths had an impact on MSRR, Q_{10} values of specimens from the surface layers (0 to $-100\mathrm{m}$) were compared to Q_{10} values including individuals from deeper layers. Q_{10} values did not distinctly change, whether deeper-dwelling individuals were included in the analysis or not. We therefore assume that these specimens did not yet enter diapause and included all *Calanus* individuals in the analyses.

1.3 Results

In total, 517 measurements of seven different polar (*Calanus hyperboreus, Calanus glacialis, Paraeuchaeta glacialis, Themisto libellula*) and boreal-Atlantic (*Calanus finmarchicus, Paraeuchaeta norvegica, Themisto abyssorum*) zooplankton species were conducted at 0, 4, 6, 8 and 10 °C (Table 1.1, Figure 1.2).

1.3.1 Temperature-dependence of respiration

In general, mass-specific respiration rates (MSRR) increased with temperature for all species and stages (Table 1.1, Figure 1.2). Adult females of polar *Calanus hyperboreus* and *C. glacialis* showed a slow, but steady increase in MSRR (Figure 1.2A, Table 1.1). Respiration rates in these organisms doubled from 0 to 8 °C, which represents a significant increase for *C. hyperboreus* ($p < 0.001$) and *C. glacialis* females ($p < 0.001$; Games-Howell's multiple comparison test). The increase from 0 to 6 °C was also significant in *C. glacialis* ($p = 0.05$). A summary of all statistical analyses can be found in the supplement material S2 at https://doi.org/10.3389/fmars.2022.908638).

In *C. hyperboreus* C5, MSRR remained rather stable between 0 and 6 °C (mean values around 12 nmol O_2 h^{-1} mg^{-1} DM for all three temperatures), but at 8 and 10 °C an increase was noticeable to 20 and 27 nmol O_2 h^{-1} mg^{-1} DM, respectively (0 and 8 °C : $p < 0.001$). In *C. glacialis* C5 no distinct increase in MSRR was observed between 0 and 8 °C ($p > 0.999$; Figure 1.2A, Table 1.1).

Adult females of *C. finmarchicus* showed similar MSRR at 0 °C as their Arctic congeners (Figure 1.2A, Table 1.1). However, in contrast to the slow and steady increase of Arctic *Calanus* species, MSRR of boreal-Atlantic *C. finmarchicus* females showed a much more rapid and steeper increase, with a more than threefold increase in mean MSRR from 0 to 6 °C (i.e. 24 to 90 nmol O_2 h^{-1} mg^{-1} DM, Figure 1.2A, Table 1.1). At 8 °C the distinct rise in MSRR of *C. finmarchicus* females flattened into a plateau. MSRR of *C. finmarchicus* females were significantly different between 0 and 4 °C ($p = 0.04$), 0 and 6 °C ($p < 0.001$) and 4 and 6 °C ($p = 0.02$). The slope of the regression line of $\log_{10}$ transformed MSRR with increasing temperature of *C. finmarchicus* females was significantly higher than the slope of females of *C. hyperboreus* ($p = 0.0089$) and *C. glacialis* ($p = 0.0117$).

Copepodite stages C5 of *C. finmarchicus* also showed a significant increase in MSRR from 0 to 8 °C, with mean values increasing from 15 to 44 nmol O_2 h^{-1} mg^{-1} DM, respectively (0 and 8 °C: $p = 0.02$, 4 and 10 °C: $p = 0.01$). The increase leveled off at 10 °C (Figure 1.2A). The slope of the linear regression of MSRR with increasing temperature was significantly higher in *C. finmarchicus* C5 compared to *C. hyperboreus* C5 ($p = 0.0004$) and *C. glacialis* C5 ($p = 0.0027$).

Adult females of the predatory copepod species *Paraeuchaeta glacialis* and *P. norvegica* showed similar trends among each other with little change in MSRR between 0 and 4 °C and an increase at 8 °C (Figure 1.2B, Table 1.1). At all temperatures, mean MSRR of the Arctic *P. glacialis* females were higher than those of their Atlantic congener *P. norvegica* (Table 1.1). Res-

piration of *P. glacialis* C5 changed only slightly with increasing temperature, with essentially no difference in mean MSRR from 0 to 10 °C (20 and 21 nmol O_2 h^{-1} mg^{-1} DM, respectively). While mean MSRR of *P. norvegica* C5 was similar to *P. glacialis* C5 at 0 °C, a distinct increase of mean values could be observed for *P. norvegica* C5 at temperatures above 4 °C (Figure 1.2B, Table 1.1).

In the amphipods *Themisto libellula* and *T. abyssorum* mean MSRR increased only slightly with temperature for both species. Mean standardized MSRR of the Arctic *T. libellula* were higher than those of the boreal-Atlantic *T. abyssorum* at all temperatures (Table 1.1).
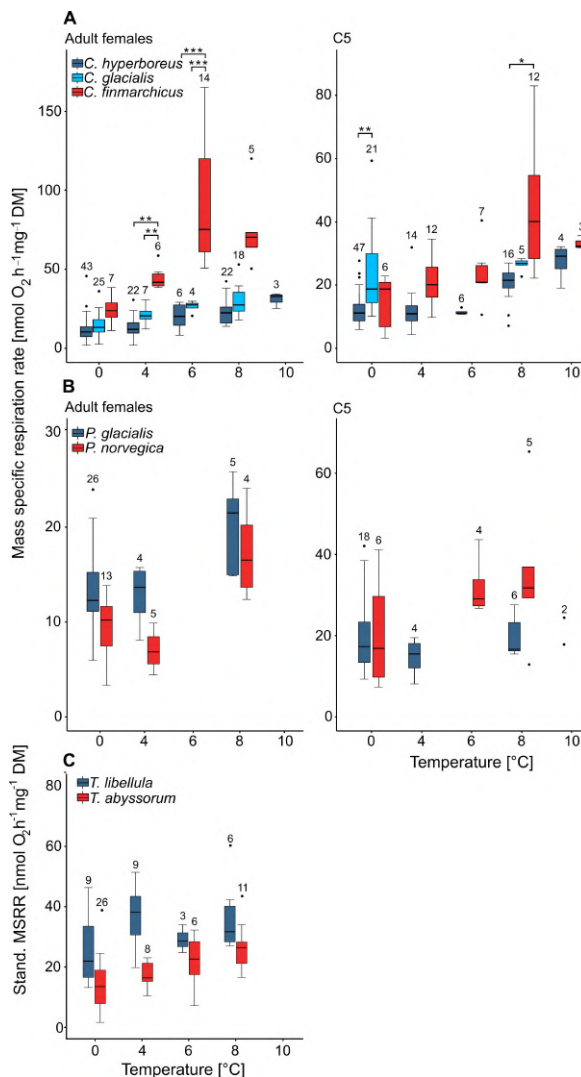
Figure 1.2: Mass-specific (A and B) and standardized mass-specific (C) respiration rates (Stand. MSRR) of polar-Arctic (blue) versus boreal-Atlantic (red) zooplankton species from Fram Strait. Stand. MSRR were used for *Themisto* species, as they had highly variable dry masses. Box represents the interquartile range (lower edge: 25th percentile, the upper edge: 75th percentile, central line: median, whiskers extend to minimum and maximum values within 1.5 times the interquartile range). Dots represent potential outliers that are above or below 1.5 times the interquartile range, respectively. Asterisks show significant differences in standardized respiration rates between species at the respective temperature ($\star p \leq 0.05$, $\star\star p \leq 0.01$, $\star\star\star p \leq 0.001$). Values above the boxplots show number of measurements. (A) *Calanus* spp., (B) *Paraeuchaeta* spp., (C) *Themisto* spp.

Table 1.1: Individual, mass-specific and standardized mass-specific respiration rates of polar-Arctic and boreal-Atlantic zooplankton species measured at different ambient temperatures (Exp.temp.) during three expeditions PS100 (2016), PS107 (2017) and PS121 (2019) with RV *Polarstern* to Arctic Fram Strait in summer (July-September). Data are given as mean values ± standard deviation. f: adult female, C5: copepodite stage C5, DM: dry mass. Exp. temp.: Experimental temperature. Mort.: Mortality.

Species	Stage	Exp. temp. [°C]	Exp. run time [h]	Mort. [%]	*In situ* temp. min/max [°C]	Depth range [m]	Replicates (No. ind.)	Dry mass [mg]	Ind. respiration [nmol O_2 h^{-1} $ind.^{-1}$]	Mass-specific respiration [nmol O_2 h^{-1} mg^{-1} DM]	Stand. mass-specific respiration [nmol O_2 h^{-1} $ind.^{-1}$]
C. hyperboreus	f	0	13.7 ± 5.1	0	-1.8 / 3.5	0-1000	43 (43)	3.92 ± 1.44	46.6 ± 26.4	12.4 ± 7.5	14.3 ± 8.1
		4	16.3 ± 2.3	0	-1.7 / 4.3	0-1500	22 (23)	3.98 ± 1.38	55.4 ± 29.2	13.3 ± 6.4	15.9 ± 7.6
		6	11.9 ± 6.1	0	-1.4 / 9.3	0-50	6 (6)	4.28 ± 1.68	89.6 ± 49.5	20.1 ± 7.8	24.3 ± 10.0
		8	10.9 ± 4.1	0	-1.4 / 2.7	0-1500	22 (22)	4.42 ± 0.90	98.4 ± 26.8	23.2 ± 7.9	25.2 ± 7.8
		10	5.8	0	-1.6 / -1.3	0-50	3 (3)	3.35 ± 0.26	104.1 ± 18.9	30.9 ± 4.0	31.8 ± 4.5
		12	5	100	-1.7 / -1.5	0-50	2 (2)	5.28 ± 0.16	-	-	-
	C5	0	16.2 ± 5.9	0	-1.7 / 3.5	0-350	47 (52)	2.16 ± 0.89	24.6 ± 10.4	12.1 ± 4.6	13.6 ± 4.8
		4	16.0 ± 2.0	0	-1.7 / 2.8	0-1500	14 (14)	2.50 ± 1.00	33.4 ± 24.0	12.4 ± 6.3	14.9 ± 8.5
		6	25.5	0	-	1000-1500	6 (6)	1.80 ± 0.49	20.4 ± 5.0	11.4 ± 0.8	12.5 ± 1.0
		8	13.0 ± 2.6	0	-1.2 / 2.7	0-1500	16 (16)	2.19 ± 0.87	42.5 ± 16.1	20.4 ± 5.3	23.1 ± 5.7
		10	5.8	0	-1.7 / -1.2	0-50	4 (4)	2.52 ± 1.06	63.7 ± 13.9	27.4 ± 5.1	31.7 ± 3.4
		12	5	100	-1.7 / -1	0-50	5 (10)	1.97 ± 0.45	-	-	-
C. glacialis	f	0	16.6 ± 4.8	0	-1.8 / 3.5	0-320	25 (26)	1.50 ± 0.61	20.3 ± 7.7	14.9 ± 7.3	13.4 ± 6.01
		4	17.0 ± 3.9	0	-1.7 / 2.8	0-200	7 (11)	1.26 ± 0.10	27.5 ± 8.4	21.1 ± 5.3	18.9 ± 5.0
		6	18.3 ± 5.4	50	-1.4 / 1.9	0-50	4 (4)	1.37 ± 0.19	36.0 ± 6.4	26.4 ± 3.4	24.0 ± 3.1
		8	12.2 ± 5.1	8	-1.7 / 2.8	0-200	18 (26)	1.34 ± 0.25	40.8 ± 14.2	29.4 ± 8.8	24.1 ± 7.1
	C5	0	16.5 ± 6.1	0	-1.7 / 3.5	0-300	21 (26)	0.73 ± 0.34	13.5 ± 3.5	23.8 ± 12.5	19.3 ± 8.0
		8	9.8 ± 1.7	4	-1.6 / 2.8	0-200	5 (18)	1.13 ± 0.15	30.5 ± 2.4	26.4 ± 2.0	26.1 ± 1.3
		12	5	100	-1.6 / -1	0-50	1 (3)	1.13	-	-	-
C. finmarchicus	f	0	17.5 ± 1.8	5	0 / 6.7	50-100	7 (18)	0.44 ± 0.13	10.5 ± 2.7	24.4 ± 8.5	16.5 ± 5.10
		4	18.3 ± 0.5	0	1.4 / 5.8	0-100	6 (18)	0.38 ± 0.05	16.6 ± 2.6	44.7 ± 7.1	29.3 ± 4.4
		6	12.3 ± 2.3	0	4.6 / 9.3	0-500	14 (22)	0.26 ± 0.08	18.8 ± 5.3	89.7 ± 35.4	50.2 ± 15.9
		8	9.7 ± 0.4	0	4.6 / 7.9	0-500	5 (19)	0.32 ± 0.06	25.7 ± 9.2	75.6 ± 23.6	43.7 ± 13.7
	C5	0	20.9 ± 1.9	0	0 / 6.7	100-770	6 (9)	0.52 ± 0.06	7.5 ± 4.4	14.7 ± 8.2	11.9 ± 6.7
		4	15.5 ± 2.7	2	1.4 / 6.2	0-100	12 (42)	0.42 ± 0.11	7.4 ± 1.7	20.8 ± 7.7	15.2 ± 4.8
		6	8.5 ± 4.3	5	1.5 / 7.5	0-100	7 (21)	0.56 ± 0.13	11.8 ± 3.2	23.7 ± 8.4	18.7 ± 4.8
		8	11.0 ± 2.0	0	1.5 / 7.9	0-50	12 (39)	0.55 ± 0.18	21.8 ± 8.6	44.0 ± 18.8	34.8 ± 13.1
		10	6.8	0	3.4 / 4.2	100-200	3 (14)	0.38 ± 0.04	12.6 ± 1.7	33.3 ± 1.7	24.9 ± 1.7
P. glacialis	f	0	6.9 ± 4.4	8	-1.8 / 3.4	0-400	26 (26)	6.96 ± 1.62	87.8 ± 27.8	13.0 ± 4.1	13.5 ± 3.9
		4	16.0 ± 5.7	0	-1.7 / 1.4	0-1000	4 (4)	5.03 ± 0.63	62.3 ± 9.0	12.8 ± 3.1	11.7 ± 2.7
		8	11.8 ± 1.5	29	-1.5 / 2.8	0-500	5 (5)	4.51 ± 0.79	90.2 ± 22.3	20.0 ± 4.4	18.9 ± 4.2
	C5	0	11.9 ± 5.3	14	-1.8 / 5.3	0-400	18 (19)	1.95 ± 0.74	36.1 ± 14.6	20.2 ± 9.5	19.9 ± 8.6
		4	19.6 ± 3.0	0	-1.7 / -1.5	0-50	4 (4)	1.76 ± 0.45	24.3 ± 7.0	14.6 ± 4.4	14.2 ± 3.7
		8	11.6 ± 1.4	0	-1.2 / 2.8	0-500	6 (6)	2.38 ± 1.00	43.4 ± 12.1	19.6 ± 4.9	20.3 ± 3.4
		10	6.8	50	-1.6 / -1.0	0-50	2 (2)	1.59, 1.68	38.4, 29.4	24.2, 17.5	23.4, 17.2

		0	14.7 ± 6.9	0	-0.6 / 8.8	100-770	13 (13)	4.53 ± 1.17	40.0 ± 10.9	9.5 ± 3.3	8.8 ± 2.8
	f	4	6.8 ± 1.7	0	-0.4 / 2.9	200-1000	5 (5)	5.30 ± 0.53	36.6 ± 7.8	7.1 ± 2.0	6.9 ± 1.8
P. norvegica		8	11.0 ± 2.4	0	0.6 / 3.1	200-850	4 (4)	5.20 ± 0.92	89.2 ± 23.0	17.4 ± 4.6	16.9 ± 4.3
		0	21.3 ± 1.7	0	-1.5 / 9.4	0-320	6 (6)	1.93 ± 1.03	28.2 ± 5.7	20.6 ± 12.5	18.7 ± 9.4
	C5	6	17.4	0	3.2 / 4.4	50-200	4 (4)	1.12 ± 0.39	35.2 ± 10.6	32.1 ± 6.8	28.1 ± 5.7
		8	9.5 ± 3.3	17	1.3 / 4.7	50-500	5 (5)	1.52 ± 0.54	48.8 ± 20.8	35.2 ± 17.0	32.7 ± 15.1
		0	7.6 ± 1.9	36	-1.5 / 8.8	0-600	9 (9)	8.51 ± 8.89	162.4 ± 86.5	28.4 ± 13.5	25.5 ± 10.7
T. libellula		4	2.7 ± 0.5	0	0.9 / 8.8	0-500	9 (9)	15.85 ± 9.37	437.5 ± 184.1	32.5 ± 11.0	36.9 ± 9.4
		6	5.7 ± 2.0	0	0.9 / 2.9	200-500	3 (3)	10.94 ± 4.83	285.5 ± 106.1	26.8 ± 3.2	29.2 ± 3.8
		8	4.3 ± 2.0	0	0.4 / 5.4	0-500	6 (6)	9.65 ± 7.40	309.2 ± 205.8	37.8 ± 12.1	36.9 ± 11.7
		0	13.1 ± 8.0	9	-1.6 / 3.4	0-1500	26 (32)	4.24 ± 5.15	69.3 ± 76.3	20.4 ± 14.2	14.3 ± 8.0
T. abyssorum		4	8.9 ± 3.5	0	-0.4 / 0.9	500-1000	8 (12)	2.91 ± 3.10	77.8 ± 70.9	23.1 ± 5.6	17.5 ± 4.1
		6	16.2	0	1.5 / 7.5	0-500	6 (6)	0.87 ± 0.17	32.6 ± 13.4	36.8 ± 14.1	21.9 ± 8.4
		8	6.3 ± 4.1	0	-1.2 / 2.7	0-1000	11 (13)	7.21 ± 6.85	220.4 ± 201.9	28.2 ± 7.1	26.2 ± 7.2

1.3.2 Q₁₀ values

Q$_{10}$ values were generally higher for boreal-Atlantic congeners than for polar-Arctic species (Figure 1.3). These differences in Q$_{10}$ coefficients were most pronounced in *Calanus* species. Polar-Arctic *C. hyperboreus* and *C. glacialis* had Q$_{10}$ values between 1.3 and 2.7. In contrast, the boreal-Atlantic *C. finmarchicus* had much higher Q$_{10}$ values of 4.2 in C5s and 5.9 in adult females.

Similar, but less pronounced differences in Q$_{10}$ values between polar-Arctic and boreal-Atlantic sister species were determined for *Paraeuchaeta* spp. and *Themisto* spp., with higher values for the Atlantic species (*P. norvegica* C5: 2.3, females: 1.8; *T. abyssorum*: 2.5) compared to the Arctic congeners (*P. glacialis* C5: 1.0, females: 1.7; *T. libellula*: 1.7; Figure 1.3).
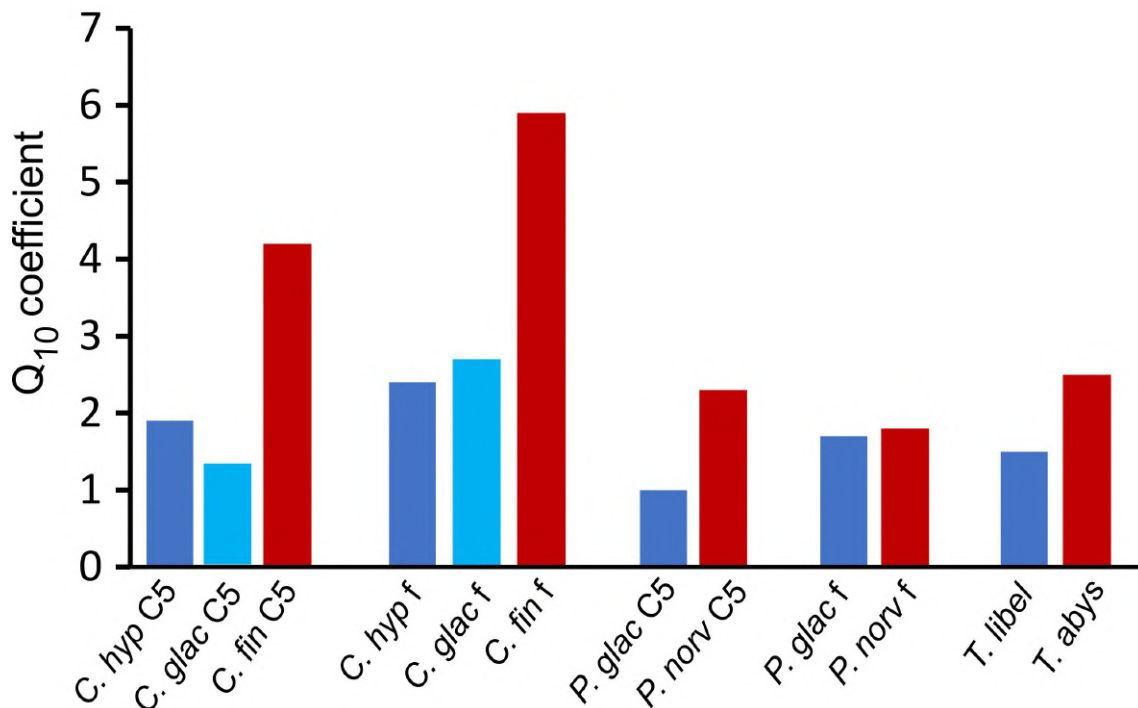
Figure 1.3: Q$_{10}$ values of polar-Arctic (blue) versus boreal-Atlantic (red) zooplankton species based on exponential regression of mass-specific respiration rates at different temperatures (0, 4, 6, 8 and 10 °C). *C. hyp*: *Calanus hyperboreus*, *C. glac*: *Calanus glacialis*, *C. fin*: *Calanus finmarchicus*, *P. glac*: *Paraeuchaeta glacialis*, *P. norv*: *Paraeuchaeta norvegica*, *T. libel*: *Themisto libellula*, *T. abys*: *Themisto abyssorum*. f: adult female, C5: copepodite stage C5.

1.3.3 Mortality

Mortality of the species was generally low (Table 1.1). In *Calanus* species, survival of Arctic *C. hyperboreus* C5 and females was exceptionally high, with 100% at temperatures from 0 to 10 °C (Table 1.1). Survival of the Arctic congener *C. lacialis* was 100% at lower temperatures (0 to 4 °C). At 6 °C mortality of females rose to 50% (mind low number of replicates). At 8 °C mortality was below 10% in females and C5, respectively. During one experimental run at simulated ambient temperatures of 12 °C with *C. hyperboreus* (females, C5) and *C. glacialis* (C5) mortality of both Arctic species was 100%. In contrast, boreal-Atlantic *C. finmarchicus* females and C5 experienced

a low mortality ($\leq 5\%$) at all temperatures. At temperatures $\leq 4\,°C$ (females) and $\leq 8\,°C$ (C5) survival was 100%.

In Arctic *Paraeuchaeta glacialis* the mortality of females and C5s was low ($< 15\%$) at temperatures below 8 and $10\,°C$, respectively. At $8\,°C$ mortality increased to 29% in females and at $10\,°C$ to 50% in C5s (mind low number of replicates). In boreal-Atlantic *P. norvegica* survival rates were high. Mortality was only observed at $8\,°C$ in C5s (17%).

In both *Themisto* species mortalities were only observed at $0\,°C$ with 36% for *T. libellula* and 9% for *T. abyssorum* (Table 1.1).

1.4 Discussion

Between 1982 and 2017 the summer-mixed layer of the seasonally ice-free regions of the Arctic basin have warmed on average by $0.5\,°C$ per decade (Meredith et al. 2019), i.e. by more than $1.5\,°C$ in total. This warming trend is observable throughout various areas of the Arctic Ocean, e.g. in the warming of the Atlantic Water inflow (Beszczynska-Möller et al. 2012), in the northern Barents Sea (Lind et al. 2018) and even in the Deep Water of the Greenland Sea and Eurasian Basin (von Appen et al. 2015). With steadily increasing temperatures, it is expected that the Arctic community composition is shifting towards an Atlantic regime (Chust et al. 2014; Fossheim et al. 2015). As polar zooplankton species are generally bigger and accumulate larger lipid stores (Kattner and Hagen 2009), a shift in species composition towards smaller, less lipid-rich Atlantic congeners negatively affects food quality for higher trophic levels, with consequences for food-web structure and energy flux of the entire Arctic ecosystem (Møller and Nielsen 2020). In the current study we discuss species-specific temperature tolerances and performance ranges of Arctic and co-occurring boreal-Atlantic zooplankton species to elucidate mechanisms causing the ongoing regime shifts.

1.4.1 Evidence against Arctic stenothermy

During our experiments, all Arctic species generally survived up to rather high temperatures of $10\,°C$. Polar zooplankton species showed a slow increase in their metabolic rates, also emphasized by low Q_{10} values, which is contradicting the expected pattern for typical stenotherm species, i.e. a rapid increase of respiration, followed by a narrow optimum and a sharp decline (high Q_{10}, Pörtner et al. 2017). Hence, our first hypothesis of polar stenothermy in these Arctic species has to be rejected. At one experimental run conducted at $12\,°C$, the mortality of *Calanus glacialis* and *C. hyperboreus* was high, suggesting that this temperature is close to their lethal limit. Similar or even higher ($15\,°C$) critical temperatures are reported for both Arctic *Calanus* species by Hirche (1987) for short-term non-feeding experiments with individuals from the Greenland Sea and Hildebrandt et al. (2014) for long-time feeding experiments with specimens from Fram Strait.

The hypothesis of polar stenothermy, i.e. the inability to cope with a broader temperature range in polar species, was mainly based on experiments with invertebrates and fishes from the Southern

Ocean (Peck et al. 2010; Pörtner et al. 2007; Sandersfeld et al. 2015). However, in contrast to the Antarctic, the Arctic Ocean cold-water ecosystem is comparably young and much less isolated (Buchholz et al. 2012) and, thus, Arctic species may be subjected to a much higher variability of temperatures than their southern counterparts (Pörtner et al. 2007). During the present study, *in situ* water temperatures ranged from -1.8 up to $9.3\,^{\circ}\mathrm{C}$ for Arctic zooplankton species (Table 1.1), with higher abundances usually between -1.8 and $3.5\,^{\circ}\mathrm{C}$. Distributional ranges of Arctic *Calanus* species extend from Norwegian fjords and the Gulf of Maine, USA, to the high Arctic. Hence, they cover a wide ambient temperature range from -2 to $8\,^{\circ}\mathrm{C}$ (Hirche and Niehoff 1996; Niehoff and Hirche 2005), suggesting robustness and adaptive mechanisms to cope with such variable temperatures.

1.4.2 Mass-specific respiration

Contradictory to our second hypothesis, larger Arctic *Paraeuchaeta glacialis* and *Themisto libellula* had higher MSRR at each temperature compared to their smaller Atlantic congeners *P. norvegica* and *T. abyssorum*, respectively (except *Paraeuchaeta* C5 at $8\,^{\circ}\mathrm{C}$). For larger specimens the experimental setup may not have been optimal, possibly due to increased stress in the relatively small incubation bottles. Closed-system incubations of larger specimens may also result in rapid depletion of dissolved oxygen concentrations with additional stress. To exclude that stressed large individuals were responsible for higher MSRR, we checked for species-specific correlation between dry mass and MSRR. For *T. libellula*, expected trends were observed, i.e. smaller individuals having higher MSRR than larger ones. Further, smaller sized *T. libellula* with comparable dry mass to *T. abyssorum* generally had higher MSRR. Measured rates of *T. libellula* were within the reported range (Auel and Hagen 2005; Darnis et al. 2017). It is, thus, unlikely that the higher rates were due to handling stress and/or oxygen deficits.

Although further proof is necessary, our results suggest a metabolic adaptation to the cold environment in those polar-Arctic zooplankton species. This is indicated by oxygen consumption and, thus, metabolic activity being generally higher in species of Arctic *Themisto* and *Paraeuchaeta* compared to their Atlantic congeners (see Sandersfeld et al. 2017 for higher metabolic rates in Antarctic fish). The concept of metabolic cold adaptation postulates that polar ectotherms have elevated metabolic rates compared to temperate species, as metabolic costs are higher at low temperatures. It is, however, one of the more controversially discussed hypotheses in polar ecophysiology (Peck and Conway 2000).

1.4.3 Performance of Arctic versus Atlantic zooplankton

Aerobic respiration reflects an organism's current demand of energy (Clarke 2003). At $0\,^{\circ}\mathrm{C}$, Arctic and Atlantic *Calanus* species showed the same ranges of mass-specific respiration rates (MSRR) in the present study, suggesting similar requirements. However, with increasing temperatures, the rise in MSRR differed significantly between Arctic and Atlantic *Calanus* species. While the MSRR of Arctic *C. glacialis* and *C. hyperboreus* showed only a slow increase (Q_{10} between

1.3 and 2.7), the MSRR of boreal-Atlantic *C. finmarchicus* increased much more rapidly (Q_{10} 4.2 and 5.9).

A steep increase in respiration rates could be either stress-related or due to higher metabolic activity (e.g. growth, reproduction, digestion). *C. finmarchicus* usually occurs in highest abundances in temperatures from 0 to 10 °C (Bonnet et al. 2005; Strand et al. 2020), but occurrences in waters < 0 °C and ≥ 15 °C have also been documented (Bonnet et al. 2005; Hirche 1990; Turner et al. 1993). *In situ* temperatures for *C. finmarchicus* (0 to 9 °C) during the present study were within the range of experimental temperatures. Absence of thermal stress is further supported by low mortality rates at high temperatures in the present and similar studies (Hirche et al. 1997). Physiological performances of *C. finmarchicus* at higher temperatures show that this boreal-Atlantic species is thriving with increasing temperatures. For instance, growth, egg production and feeding rates steadily increase with increasing temperatures (measurements from −1.5 to 15 °C; Campbell et al. 2001; Hirche et al. 1997; Pasternak et al. 2013; Smolina et al. 2015, emphasizing a higher energy demand due to higher performance rates. Adaptation to higher temperatures is further supported by gene regulation, as *C. finmarchicus* down-regulates proteins that are associated with thermal stress response at 5 and 10 °C (Smolina et al. 2015), which indicates the absence of stress within this temperature range. In contrast to these performance experiments, specimens were not fed in the present study. Therefore, a stress-related increase in metabolic activity due to starvation cannot be completely ruled out. However, starvation generally did not last longer than a couple of days, suggesting that internal reserves could have been utilized to maintain a high metabolism. Especially C5 individuals had large lipid reserves due to the imminent diapause (mean >40% DM). To exclude that elevated metabolic rates in *C. finmarchicus* were stress related at higher temperatures during starving conditions additional studies are needed.

The weak response in MSRR of Arctic *Calanus* species suggests that they do not experience a distinct increase in their energy demand, neither for metabolic processes nor for a thermal stress response. Apparently, they cannot benefit from higher temperatures with an increase in their performance. The increase in respiration rates in *C. glacialis* and *C. hyperboreus* could solely be due to a passive response (Havird et al. 2020) and, thus, indicates a reduced sensitivity of metabolic processes to temperature. Indeed, our results are supported by a study on the genetic activity of fed *C. glacialis*, which showed no response in up- or down-regulation of protein expression with increasing temperatures from 0 to 10 °C during short and long-term experiments (Smolina et al. 2015).

Our results and the findings by Smolina et al. (2015) on genetic regulation in *C. glacialis* emphasize the absence of a thermal stress response in Arctic *Calanus*. For species inhabiting cold environments, several studies suggest that they accumulate heat shock proteins at a constant level to compensate for the damage associated with protein folding at low temperatures (Buckley et al. 2004; Huenerlage et al. 2016; Place and Hofmann 2005; Place et al. 2004). This adaptation to cold temperatures results in a loss of thermal sensitivity of genes that encode such thermal stress

proteins due to constantly high gene expression (Buckley et al. 2004).

Although respiration rates and genetic activity are not affected by rising temperatures in Arctic *Calanus* species, their physiological performances are reduced at higher temperatures, as has been shown for decreasing assimilation efficiency (experiments with *C. glacialis* up to 10 °C; Grote et al. 2015), declining egg production rates (above 5 °C for *C. glacialis*; Pasternak et al. 2013) and depression of gonad maturation (at 10 °C for *C. hyperboreus*; Hildebrandt et al. 2014). The performance losses observed in Arctic *Calanus* species can be explained by a reduction of available energy associated with a decline in aerobic scope as the pejus temperature is approached.

Hence, with increasing temperatures, Arctic zooplankton species may already reach their pejus temperature, while boreal-Atlantic congeners might still have sufficient energy available for their performance and fitness. High basal metabolic rates, as observed for boreal-Atlantic species in the current study, allow for a greater absolute aerobic scope and, thus, a more active lifestyle (Clarke, 2003). Temperatures around 5 to 6 °C apparently mark a threshold at which *C. finmarchicus* may outcompete its Arctic congeners (Henriksen et al. 2012; Jung-Madsen and Nielsen 2015; Kjellerup et al. 2012). This is in line with our results of a much higher increase in metabolic activity at 4 to 6 °C in *C. finmarchicus* than in the Arctic *Calanus* species. Thus, the Atlantification of Arctic zooplankton communities might be driven rather by ecological interactions, biological fitness and reproductive potential at higher ambient temperatures than by absolute physiological temperature limits, stenothermy and lower resilience against rising temperatures. In conclusion, our third hypothesis, stating that the maindriving force of the Atlantification would be physiological limits of Arctic species owing to increasing temperatures, has to be rejected. Further experiments are necessary to exclude that higher metabolic rates of Atlantic species were a stress response and long-term monitoring of community dynamics in regions of co-occurrence are essential to observe the consequences of different metabolic adaptations.

In the current study, we discussed direct physiological responses of Arctic vs. boreal-Atlantic zooplankton species to rising temperatures, suggesting a higher competitive ability of Atlantic species with increasing temperatures due to higher metabolic activity. Yet, the Arctic Ocean is a harsh environment, which requires efficient adaptation. For instance, Arctic textitCalanus, especially *C. hyperboreus*, are able to start reproducing early in the year before sea-ice break-up and, thus, prior to the onset of a phytoplankton bloom, based on internal energy reserves (Daase et al. 2021). Arctic *Calanus* species therefore have a competitive advantage over boreal *C. finmarchicus* in regions with short-pulsed primary production regimes (Hatlebakk et al. 2022a; Hatlebakk et al. 2022b).

However, due to climate change, environmental conditions in the Arctic Ocean are shifting more and more to boreal regimes. The earlier sea-ice retreat and associated earlier phytoplankton production may result in increasing habitat suitability for boreal species and may further facilitate the successful establishment of boreal-Atlantic zooplankton populations in the Arctic Ocean (Freer et al. 2021). Indeed, Tarling et al. 2022 found first evidence of locally recruiting *C. finmarchicus*

in Fram Strait, indicating that the system is becoming more suitable for boreal species.

At the same time, recent studies show that the shrinking of sea-ice cover results in a northward shift in the core distribution of *C. hyperboreus* and *C. glacialis* (Ershova et al. 2021) and in a mismatch between ice algae production and *Calanus* recruitment (Dezutter et al. 2019), adding to the factors that possibly decrease the competitive ability of Arctic zooplankton species.

A future Arctic ecosystem comprising boreal zooplankton communities with higher Q_{10} values may result in a system of higher metabolic activity and, thus, a shift to a regime with higher turnover rates (Renaud et al. 2018). Individual size and lipid content of zooplankton species may generally become smaller and life-cycles shorter, however, due to the faster growth and higher reproduction rates of boreal species, the future Arctic may be more efficient (Renaud et al. 2018). Yet, in a future Arctic scenario highly prey-selective predators, such as little auks or young polar cods, will have to adapt to smaller and less energy-rich prey, or they will perish.

The present study demonstrates that, besides physiological effects, knowledge about complex ecological interactions are essential for a better understanding of global change implications on marine communities and ecosystems. These interactions should be included in models to develop realistic and reliable predictive capacities. This is especially important in the Arctic, where the Atlantification of the Arctic fauna is accompanied by the strong alternation of the environment. The loss of sea-ice and associated ice algal primary production results in drastic changes in habitat suitability, plankton phenology and overall productivity, affecting the entire Arctic marine ecosystem.

1.5   Funding

1.6   Acknowledgements

1.7   Supplementary material

The   Supplementary   Material   for   this   article   can   be   found   online   at: 10.3389/fmars.2022.908638

References

Auel, H and Hagen, W (2002). Mesozooplankton community structure, abundance and biomass in the central Arctic Ocean. *Mar Biol* 140, 1013–1021.

Auel, H and Hagen, W (2005). Body mass and lipid dynamics of Arctic and Antarctic deep-sea copepods (Calanoida, *Paraeuchaeta*): ontogenetic and seasonal trends. *Deep-Sea Res I* 52, 1272–1283.

Beaugrand, G, Luczak, C, and Edwards, M (2009). Rapid biogeographic plankton shifts in the North Atlantic Ocean. *Glob Change Biol* 15, 1790–1803.

Beaugrand, G, Reid, PC, Ibañez, F, Lindley, JA, and Edwards, M (2002). Reorganization of North Atlantic marine copepod biodiversity and climate. *Sci* 296, 1692–1694.

Bekryaev, RV, Polyakov, IV, and Alexeev, VA (2010). Role of polar amplification in long-term surface air temperature variations and modern Arctic warming. *J Clim* 23, 3888–3906.

Beszczynska-Möller, A, Fahrbach, E, Schauer, U, and Hansen, E (2012). Variability in Atlantic water temperature and transport at the entrance to the Arctic Ocean, 1997–2010. *ICES Mar Sci Symp* 69, 852–863.

Bonnet, D, Richardson, A, Harris, R, Hirst, A, Beaugrand, G, and Edwards, M (2005). An overview of *Calanus helgolandicus* ecology in European waters. *Prog Oceanogr* 65, 1–53.

Bouchard, C and Fortier, L (2020). The importance of *Calanus glacialis* for the feeding success of young polar cod: a circumpolar synthesis. *Polar Biol* 43, 1095–1107.

Buchholz, F, Werner, T, and Buchholz, C (2012). First observation of krill spawning in the high Arctic Kongsfjorden, west Spitsbergen. *Polar Biol* 35, 1273–1279.

Buckley, BA, Place, SP, and Hofmann, GE (2004). Regulation of heat shock genes in isolated hepatocytes from an Antarctic fish, *Trematomus bernacchii*. *J Exp Biol* 207, 3649–3656.

Campbell, RG, Wagner, MM, Teegarden, GJ, Boudreau, CA, and Durbin, EG (2001). Growth and development rates of the copepod *Calanus finmarchicus* reared in the laboratory. *Mar Ecol Prog Ser* 221, 161–183.

Choquet, M, Kosobokova, K, Kwaśniewski, S, Hatlebakk, M, Dhanasiri, AKS, Melle, W, Daase, M, Svensen, C, Søreide, JE, and Hoarau, G (2018). Can morphology reliably distinguish between the copepods *Calanus finmarchicus* and *C. glacialis*, or is DNA the only way? *Limnol Oceanogr: Methods* 16, 237–252.

Chust, G, Castellani, C, Licandro, P, Ibaibarriaga, L, Sagarminaga, Y, and Irigoien, X (2014). Are *Calanus* spp. shifting poleward in the North Atlantic? A habitat modelling approach. *ICES J Mar Sci* 71, 241–253.

Clarke, A (2003). Costs and consequences of evolutionary temperature adaptation. *Trends Ecol Evol* 18, 573–581.

Daase, M, Berge, J, Søreide, JE, and Falk-Petersen, S (2021). Ecology of Arctic pelagic communities. *Arctic Ecology*. Edited by Thomas, DN, 231–259.

Daase, M, Kosobokova, K, Last, KS, Cohen, JH, Choquet, M, Hatlebakk, M, and Søreide, JE (2018). New insights into the biology of *Calanus* spp. (Copepoda) males in the Arctic. *Mar Ecol Prog Ser* 607, 53–69.

Darnis, G, Hobbs, L, Geoffroy, M, Grenvald, JC, Renaud, PE, and Berge, J (2017). From polar night to midnight sun: Diel vertical migration, metabolism and biogeochemical role of zooplankton in a high Arctic fjord (Kongsfjorden, Svalbard. *Limnol Oceanogr* 62, 1586–1605.

Dezutter, T, Lalande, C, Dufresne, C, Darnis, G, and Fortier, L (2019). Mismatch between microalgae and herbivorous copepods due to the record sea ice minimum extent of 2012 and the late sea ice break-up of 2013 in the Beaufort Sea. *Prog Oceanogr* 173, 66–77.

Ershova, EA, Kosobokova, KN, Banas, NS, Ellingsen, I, Niehoff, B, Hildebrandt, N, and Hirche, H-J (2021). Sea ice decline drives biogeographical shifts of key *Calanus* species in the central Arctic Ocean. *Glob Change Biol* 27, 2128–2143.

Fossheim, M, Primicerio, R, Johannesen, E, Ingvaldsen, RB, Aschan, MM, and Dolgov, V (2015). Recent warming leads to rapid borealization of fish communities in the Arctic. *Nat Clim Change* 5, 673–677.

Franklin, CE, Farrell, AP, Altimiras, J, and M, Axelsson (2013). Thermal dependence of cardiac function in arctic fish: implications of a warming world. *J Exp Biol* 216, 4251–4255.

Freer, JJ, Daase, M, and Tarling, GA (2021). Modelling the biogeographic boundary shift of *Calanus finmarchicus* reveals drivers of Arctic Atlantification by subarctic zooplankton. *Glob Change Biol* 28, 429–440.

Gabrielsen, TM, Merkel, B, Søreide, JE, Johansson-Karlsson, E, Bailey, A, Vogedes, D, Nyga, H, Varpe, Ø, and Berge, J (2012). Potential misidentifications of two climate indicator species of the marine arctic ecosystem: *Calanus glacialis* and *C. finmarchicus*. *Polar Biol* 35, 1621–1628.

Grote, U, Pasternak, A, Arashkevich, E, Halvorsen, E, and Nikishina, A (2015). Thermal response of ingestion and egestion rates in the Arctic copepod *Calanus glacialis* and possible metabolic consequences in a warming ocean. *Polar Biol* 38, 1025–1033.

Hartmann, DL, Klein Tank, AMG, Rusticucci, M, Alexander, LV, Brönnimann, S, and Charabi, Y (2013). Observations: Atmosphere and surface. *Climate change 2013: The physical science basiS Contribution of Working Group I to the Fifth Assessment Report of the Intergovernmental Panel on Climate Change*. Cambridge, United Kingdom and New York, NY, USA: Cambridge University Press, 96 pp.

Hatlebakk, M, Kosobokova, K, Daase, M, and Søreide, JE (2022a). Contrasting life traits of sympatric *Calanus glacialis* and *C finmarchicus* in a warming Arctic revealed by a year-round study in Isfjorden, Svalbard. *Front Mar Sci* 9, 877910.

Hatlebakk, M, Niehoff, B, Choquet, M, Hop, H, Wold, A, Hoarau, G, and Søreide, JE (2022b). Seasonal enzyme activities of sympatric *Calanus glacialis* and *C. finmarchicus* in the High-Arctic. *Front Mar Sci* 9, 877904.

Hattermann, T, Isachsen, PE, von Appen, W-J, Albretsen, J, and Sundfjord, A (2016). Eddy-driven recirculation of Atlantic Water in Fram Strait. *Geophys Res Lett* 43, 3406–3414.

Havird, JC, Neuwald, JL, Shah, AA, Mauro, A, Marshall, CA, and Ghalambor, CK (2020). Distinguishing between active plasticity due to thermal acclimation and passive plasticity due to Q_{10} effects: why methodology matters. *Funct Ecol* 34, 1015–1028.

Henriksen, MV, Jung-Madsen, S, Nielsen, TG, Møller, EF, Henriksen, KV, Markager, S, and Hansen, BW (2012). Effects of temperature and food availability on feeding and egg production of *Calanus hyperboreus* from Disko Bay, western Greenland. *Mar Ecol Prog Ser* 447, 109–126.

Hildebrandt, N, Niehoff, B, and Sartoris, FJ (2014). Long-term effects of elevated CO_2 and temperature on the Arctic calanoid copepods *Calanus glacialis* and *C. hyperboreus*. *Mar Pollut Bull* 80, 59–70.

Hirche, H-J (1987). Temperature and plankton: II. Effect on respiration and swimming activity in copepods from the Greenland Sea. *Mar Biol* 94, 347–356.

Hirche, H-J (1990). Egg production of *Calanus finmarchicus* at low temperature. *Mar Biol* 106, 53–58.

Hirche, H-J and Kattner, G (1993). Egg production and lipid content of *Calanus glacialis* in spring: indication of a food-dependent and food-independent reproductive mode. *Mar Biol* 117, 615–622.

Hirche, H-J, Meyer, U, and Niehoff, B (1997). Egg production of *Calanus finmarchicus*: effect of temperature, food and season. *Mar Biol* 127, 609–620.

Hirche, H-J and Niehoff, B (1996). Reproduction of the Arctic copepod *Calanus hyperboreus* in the Greenland Sea - field and laboratory observations. *Polar Biol* 16, 209–219.

Huenerlage, K and Buchholz, F (2015). Thermal limits of krill species from the high-Arctic Kongsfjord (Spitsbergen). *Mar Ecol Prog Ser* 535, 89–98.

Huenerlage, K, Cascella, K, Corre, E, Toomey, L, Lee, CY, Buchholz, F, and Toullec, JY (2016). Responses of the arcto-boreal krill species *Thysanoessa inermis* to variations in water temperature: coupling Hsp70 isoform expressions with metabolism. *Cell Stress Chaperon* 21, 969–981.

Jung-Madsen, S and Nielsen, TG (2015). Early development of *Calanus glacialis* and *C. finmarchicus*. *Limnol Oceanogr* 60, 934–946.

Jung-Madsen, S, Nielsen, TG, Grønkjær, P, Hansen, BW, and Møller, EF (2013). Early development of *Calanus hyperboreus* nauplii: response to a changing ocean. *Limnol Oceanogr* 58, 2109–2121.

Kaiser, P, Hagen, W, von Appen, W-J, Niehoff, N, Hildebrandt, N, and Auel, H (2021). Effects of a submesoscale oceanographic filament on zooplankton dynamics in the Arctic marginal ice zone. *Front Mar Sci* 8, 625395.

Kanzow, T (2017). The expedition PS100 of the research vessel *Polarstern* to the Fram Strait in 2016. *Reports on Polar and Marine Research, Alfred Wegener Institute for Polar and Marine Research* 705, 175 pp.

Karnovsky, N, Harding, A, Walkusz, W, Kwaśniewski, S, Goszczko, I, and Wiktor, J (2010). Foraging distributions of little auks *Alle alle* across the Greenland Sea: implications of present and future Arctic climate change. *Mar Ecol Prog Ser* 415, 283–293.

Kattner, G and Hagen, W (2009). Lipids in marine copepods: latitudinal characteristics and perspective to global warming. *Lipids in Aquatic Ecosystems*. Edited by Arts, MT, Brett, M, and Kainz, M. Berlin: Springer, 257–280.

Kawasaki, T and Hasumi, H (2016). The inflow of Atlantic water at the Fram Strait and its interannual variability. *J Geophys Res Oceans* 121, 502–519.

Kjellerup, S, Dünweber, M, Swalethorp, R, Nielsen, TG, Møller, EF, Markager, S, and Hansen, BW (2012). Effects of a future warmer ocean on the coexisting copepods *Calanus finmarchicus* and *C. glacialis* in Disko Bay, western Greenland. *Mar Ecol Prog Ser* 447, 87–108.

Kosobokova Kand Hirche, H-J (2009). Biomass of zooplankton in the eastern Arctic Ocean – a base line study. *Prog Oceanogr* 82, 265–280.

Kraft, A, Nöthig, EM, Bauerfeind, E, Wildish, DJ, Pohle, GW, and Bathmann, UV (2013). First evidence of reproductive success in a southern invader indicates possible community shifts among Arctic zooplankton. *Mar Ecol Prog Ser* 493, 291–296.

Kwaśniewski, S, Gluchowska, M, Jakubas, D, Wojczulanis-Jakubas, K, Walkusz, W, and Karnovsky, N (2010). The impact of different hydrographic conditions and zooplankton communities on provisioning little auks along the west coast of Spitsbergen. *Prog Oceanogr* 87, 72–82.

Lind, S, Ingvaldsen, RB, and Furevik, T (2018). Arctic warming hotspot in the northern Barents Sea linked to declining sea-ice import. *Nat Clim Change* 8, 634–639.

Mańko, MK, Gluchowska, M, and Weydmann-Zwolicka, A (2020). Footprints of Atlantification in the vertical distribution and diversity of gelatinous zooplankton in the Fram Strait (Arctic Ocean). *Prog Oceanogr* 189, 102414.

Masson-Delmotte, V, Schulz, M, Abe-Ouchi, A, Beer, J, Ganopolski, A, and González Rouco, JF (2013). Information from paleoclimate archives. *Climate change 2013: The physical science basis. Contribution of Working Group I to the Fifth Assessment Report of the Intergovernmental Panel on Climate Change*. Cambridge, United Kingdom and New York, NY, USA: Cambridge University Press, 383–464.

Meredith, M, Sommerkorn, M, Cassotta, S, Derksen, C, Ekaykin, A, and Hollowed, A et al. (2019). Polar Regions. *IPCC Special Reports on the Ocean and Cryosphere in a Changing Climate*. Edited by Pörtner, H-O, Roberts, DC, Masson-Delmotte, V, Zhai, P, Tignor, M, Poloczanska, E, Mintenbeck, K, Alegría, A, Nicolai, M, Okem, A, Petzold, J, Rama, B, and Weyer, NM. Geneva: IPCC, Intergovernmental Panel on Climate Change, 203–320.

Metfies, K (2020). The expedition PS121 of the research vessel *Polarstern* to the Fram Strait in 2019. *Reports on Polar and Marine Research, Alfred Wegener Institute for Polar and Marine Research* 738, 95 pp.

Møller, EF and Nielsen, TG (2020). Borealization of Arctic zooplankton – smaller and less fat zooplankton species in Disko Bay, western Greenland. *Limnol Oceanogr* 65, 1175–1188.

Mumm, N, Auel, H, Hanssen, H, Hagen, W, Richter, C, and Hirche, H-J (1998). Breaking the ice: large-scale distribution of mesozooplankton after a decade of Arctic and transpolar cruises. *Polar Biol* 20, 189–197.

Niehoff, B and Hirche, H-J (2005). Reproduction of *Calanus glacialis* in the Lurefjord (western Norway): indication for temperature-induced female dormancy. *Mar Ecol Prog Ser* 285, 107–115.

Pasternak, AF, Arashkevich, EG, Grothe, U, Nikishina, AB, and Solovyev, KA (2013). Different effects of increased water temperature on egg production of *Calanus finmarchicus* and *C. glacialis*. *Oceanol* 53, 547–553.

Peck, LS (2002). Ecophysiology of Antarctic marine ectotherms: limits to life. *Polar Biol* 25, 31–40.

Peck, LS and Conway, LZ (2000). The myth of metabolic cold adaptation: oxygen consumption in stenothermal Antarctic bivalves. *Geol Soc Spec Pub* 177, 441–450.

Peck, LS, Morley, SA, and Clark, MS (2010). Poor acclimation capacities in Antarctic marine ectotherms. *Mar Biol* 157, 2051–2059.

Place, SP and Hofmann, GE (2005). Constitutive expression of a stress-inducible heat shock protein gene, hsp70, in phylogenetically distant Antarctic fish. *Polar Biol* 28, 261–267.

Place, SP, Zippay, ML, and Hofmann, GE (2004). Constitutive roles for inducible genes: evidence for the alteration in expression of the inducible hsp70 gene in Antarctic notothenioid fishes. *Am J Physiol Regul Integr Comp Physiol* 287, 249–436.

Polyakov, IV, Bhatt, US, Walsh, JE, Abrahamsen, EP, Pnyushkov, AV, and Wassmann, PF (2013). Recent oceanic changes in the Arctic in the context of long-term observations. *Ecol Appl* 23, 1745–1764.

Polyakov, IV, Pnyushkov, AV, Alkire, MB, Ashik, I M, Baumann, TM, Carmack, EC, Goszczko, Ilona, Guthrie, John, Ivanov, Vladimir V, Kanzow, T, Krishfield, R, Kwok, R, Sundfjord, A, Morison, J, Rember, R, and Yulin, A (2017). Greater role for Atlantic inflows on sea-ice loss in the Eurasian Basin of the Arctic Ocean. *Sci* 356, 285–291.

Polyakov, IV, Pnyushkov, AV, and Timokhov, LA (2012). Warming of the Intermediate Atlantic Water of the Arctic Ocean in the 2000s. *J Clim* 25, 8362–8370.

Pörtner, H-O (2001). Climate change and temperature-dependent biogeography: oxygen limitation of thermal tolerance in animals. *Naturwissenschaften* 88, 137–146.

Pörtner, H-O, Bock, C, and Mark, FC (2017). Oxygen- and capacity-limited thermal tolerance: bridging ecology and physiology. *J Exp Biol* 220, 2685–2696.

Pörtner, H-O, Peck, L, and Somero, G (2007). Thermal limits and adaptation in marine Antarctic ectotherms: an integrative view. *Phil Trans Soc B* 362, 2233–2258.

Renaud, PE, Daase, M, Banas, NS, Gabrielsen, TM, Søreide, JE, and Varpe, Ø (2018). Pelagic food-webs in a changing Arctic: a trait-based perspective suggests a mode of resilience. *ICES J Mar Sci* 75, 1871–1881.

Sandersfeld, T, Davison, W, Lamare, MD, Knust, R, and Richter, C (2015). Elevated temperature causes metabolic trade-offs at the whole-organism level in the Antarctic fish *Trematomus bernacchii*. *J Exp Biol* 218, 2373–2381.

Sandersfeld, T, Mark, FC, and Knust, R (2017). Temperature-dependent metabolism in Antarctic fish: do habitat temperature conditions affect thermal tolerance ranges? *Polar Biol* 40, 141–149.

Schewe, I (2018). The expedition PS107 of the research vessel *Polarstern* to the Fram Strait and the AWI-HAUSGARTEN in 2017. *Reports on Polar and Marine Research, Alfred Wegener Institute for Polar and Marine Research* 717, 120 pp.

Schulte, PM, Healy, TM, and Fangue, NA (2011). Thermal performance curves, phenotypic plasticity, and the time scales of temperature exposure. *Integr Comp Biol* 51, 691–702.

Smolina, I, Kollias, S, Møller, EF, Lindeque, P, AYM, Sundaram, JMO, Fernandes, and Hoarau, G (2015). Contrasting transcriptome response to thermal stress in two key zooplankton species, *Calanus finmarchicus* and *C. glacialis*. *Mar Ecol Prog Ser* 534, 79–93.

Strand, E, Bagøien, E, Edwards, M, Broms, C, and Klevjer, T (2020). Spatial distributions and seasonality of four *Calanus* species in the Northeast Atlantic. *Prog Oceanogr* 185, 102344.

Tarling, GA, Freer, JJ, Banas, NS, Belcher, A, Blackwell, M, Castellani, C, Cook, KB, Cottier, Finlo R, Daase, M, Johnson, ML, Last, KS, Lindeque, PK, Mayor, DJ, Mitchell, E, Parry, HE, Speirs, DC, Stowasser, G, and Wootton, M (2022). Can a key boreal *Calanus* copepod species now complete its life-cycle in the Arctic? Evidence and implications for Arctic food-webs. *Ambio* 51, 333–344.

Turner, JT, Tester, PA, and Strickler, JR (1993). Zooplankton feeding ecology: a cinematographic study of animal-to-animal variability in the feeding behavior of *Calanus finmarchicus*. *Limnol Oceanogr* 38, 255–264.

Verberk, WCEP, Overgaard, J, Ern, R, Bayley, M, Wang, T, Boardman, L, and Terblanche, JS (2016). Does oxygen limit thermal tolerance in arthropods? A critical review of current evidence. *Comp Biochem Physiol Part A* 192, 64–78.

Vihtakari, M, Welcker, J, Moe, B, Chastel, O, Tartu, S, and Hop, H (2018). Black-legged kittiwakes as messengers of Atlantification in the Arctic. *Sci Rep* 8, 1178.

Von Appen, W-J, Schauer, U, Somavilla, R, Bauerfeind, E, and Beszczynska-Möller, A (2015). Exchange of warming deep waters across Fram Strait. *Deep-Sea Res* I 103, 86–100.

Von Appen, W-J, Wekerle, C, Hehemann, L, Schourup-Kristensen, V, Konrad, C, and Iversen, MH (2018). Observations of a submesoscale cyclonic filament in the Marginal Ice Zone. *Geophys Res Lett* 45, 6141–6149.

Wassmann, P, Kosobokova, KN, Slagstad, D, Drinkwater, KF, Hopcroft, RR, Moore, SE, Ellingsen, I, Nelson, RJ, Carmack, E, Popova, E, and Berge, J (2015). The contiguous domains of Arctic Ocean advection: trails of life and death. *Prog Oceanogr* 139, 42–65.

Weydmann, A, Carstensen, J, I, Goszczko, Dmoch, K, Olszewska, A, and Kwasniewski, S (2014). Shift towards the dominance of boreal species in the Arctic: inter-annual and spatial zooplankton variability in the West Spitsbergen Current. *Mar Ecol Prog Ser* 501, 41–52.

Wold, A, Darnis, G, Søreide, JE, Leu, E, Philippe, B, and Fortier, L (2011). Life strategy and diet of *Calanus glacialis* during the winter-spring transition in Amundsen Gulf, south-eastern Beaufort Sea. *Polar Biol* 34.

2

Phytoplankton diversity and zooplankton diets across Fram Strait: Spatial patterns with implications for the future Arctic Ocean

Patricia Kaiser[1], Wilhelm Hagen[1], Anna Schukat[1], Katja Metfies[2], Johanna Biederbick[1,3], Sabrina Dorschner[1], Holger Auel[1]

[1]Universität Bremen, BreMarE - Bremen Marine Ecology, Marine Zoology, P.O. Box 330440, 28334 Bremen, Germany

[2]Alfred Wegener Institute Helmholtz Center for Polar and Marine Research, Am Handelshafen 12, 27570 Bremerhaven, Germany

[3]Universität Hamburg, Institute of Marine Ecosystem and Fishery Science (IMF), Olbersweg 24, 22767 Hamburg, Germany

Abstract

The rapid transformations in the Arctic Ocean, characterized by a pronounced increase in Atlantic water inflow and a decline in sea ice, are reshaping the trophic structures within this ecosystem. This study investigates the effects of such environmental changes on the planktonic food web dynamics in Fram Strait, focusing on the comparison between Arctic and Atlantic influenced regions. Utilizing a combination of fatty acid and stable isotope biomarker analyses, we analyze the dietary composition and trophic levels of key zooplankton species, including Arctic and boreal-Atlantic sister species of *Calanus*, *Paraeuchaeta* and *Themisto*. The findings reveal significant differences in the food web structures between the different areas in Fram Strait. In the Arctic region, the food web is primarily influenced by diatoms, as indicated by the dominance of diatom-specific fatty acid trophic markers in all zooplankton species. Conversely, the Atlantic region exhibits a different dietary pattern, pointing to a reduced influence of diatoms and increased importance of (dino-)flagellates for *Calanus*, as well as a higher degree of carnivory in higher tropic levels. Moreover, the comparison of sister species unveils a distinct overlap in ecological niches between congeners of *Calanus* and *Paraeuchatea*, highlighting the increasing potential for competitive interactions as Atlantification progresses. These results underscore the complex relationships within Arctic food webs and the profound impact of environmental changes on trophodynamics. They also emphasize the importance of considering physiological adaptability, life history traits and ecological interactions in predicting the future of Arctic marine ecosystems amidst ongoing climate change.
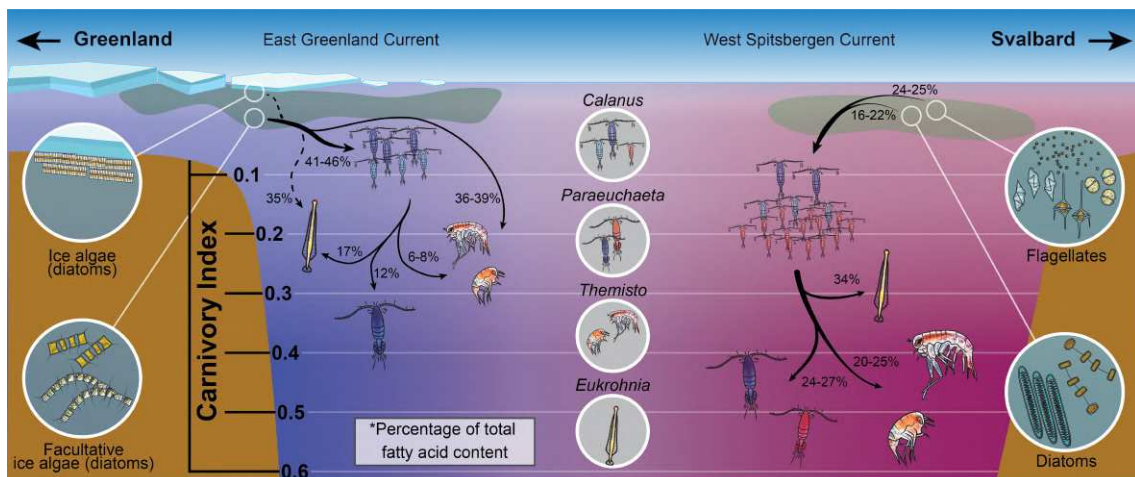
2.1 Introduction

Over the last decades, the Arctic has warmed nearly four times faster than the global average (Rantanen et al. 2022), a phenomenon known as Arctic or polar amplification (England et al. 2021; Serreze and Barry 2011). The strong increase in temperature has led to a rapid and substantial loss in sea-ice volume, which further intensified warming due to feedback processes, such as reduced albedo (Previdi et al. 2021). The reduction in sea ice has profound impacts on ice algae, which grow within or under the ice. Ice algae are crucial to the Arctic ecosystem, serving as an important food source for sympagic, pelagic and benthic organisms (Koch et al. 2023; Kohlbach et al. 2016). The observed shift from multi- to first-year ice may initially expand the habitat available to ice algae (Lim et al. 2022), but the overall consequences are complex, influencing the timing of (ice) algal blooms, the productivity in different regions and the resilience of the ecosystem.

Concurrently, the inflows of warm, saline Atlantic water into the Arctic Basin through Fram Strait and the Barents Sea are increasing, a process known as Atlantification (Polyakov et al. 2017; Tesi et al. 2021; Wang et al. 2020). Atlantification not only induces physical changes of the Arctic system, but also facilitates a northward range shift of boreal taxa, including bacterial communities (Priest et al. 2023), phytoplankton (Oziel et al. 2020), zooplankton (Mańko et al. 2020; Weydmann et al. 2014) and fishes (Vihtakari et al. 2018), potentially reshaping Arctic food-web structures and overall ecosystem functioning (Kortsch et al. 2019; Pecuchet et al. 2020). Hence, it is crucial to assess the effects of these changes on trophic interactions in Arctic ecosystems.

Fram Strait, located between Greenland and Svalbard, is the only deep-water gateway connecting the Arctic with the Atlantic Ocean and is strongly influenced by two major currents, the East Greenland Current (EGC) and the West Spitsbergen Current (WSC). While the EGC transports cold, less saline polar surface water and sea ice southward out of the Arctic on the western side of Fram Strait (de Steur et al. 2009), the WSC carries warm, saline Atlantic water into the Arctic on its eastern side (Beszczynska-Möller et al. 2012). Thus, Fram Strait is characterized by physical and biological properties of both Arctic and Atlantic origin in close proximity and therefore an ideal region to analyze the impact of Atlantification processes on high latitude food webs.

Phytoplankton communities across Fram Strait are typically dominated by diatoms during spring bloom conditions (Richardson et al. 2005; Spies 1987), although (dino-)flagellates can also be common (Rey et al. 2000; Smith et al. 1991). Later in the season, these communities usually shift to being dominated by summer centric diatom species, such as *Chaetoceros* spp., *Nitzschia* spp. and *Thalassiosira* spp., and/or by (dino-)flagellates (Metfies et al. 2016; Richardson et al. 2005; von Quillfeldt 2000). During a warm-water anomaly from 2004 to 2008 the dominance of diatoms in eastern Fram Strait was replaced first by coccolithophores in 2004 and then by *Phaeocystis* (Nöthig et al. 2015; Soltwedel et al. 2016). It is uncertain whether the shift towards flagellate-dominated production is a result of anthropogenic climate change or natural variability (Soltwedel et al. 2016). While large blooms of *Phaeocystis* have been historically observed in the

Arctic (Smith et al. 1991), a recent study suggests an increase in their frequency and expansion with Atlantification/warming (Orkney et al. 2020). The impact of these shifts on pelagic food webs is unclear.

Trophic biomarkers provide valuable information for identifying food-web structures and determining trophic levels (Auel et al. 2002). Fatty acids (FA) serve as indicators of dietary sources and trophic preferences following the fatty acid trophic marker (FATMs) concept. This concept is based on differences in FA composition between algal taxonomic groups and the unmodified transfer of those taxon-specific markers from primary producer to consumers (Dalsgaard et al. 2003 for review). Specifically, diatoms biosynthesize elevated levels of 16:1(n-7), 20:5(n-3) and C16 PUFAs, whereas (dino-)flagellates exhibit particularly high levels of 18:4(n-3) and 22:6(n-3). Other commonly used FATMs are 18:1(n-9), which serves as an indicator for carnivory, and C20 and C22 monounsaturated fatty acids and alcohols, which are only synthesized *de novo* by *Calanus* and *Calanoides* species and can thus be used as an indicator of predation on these calanids by higher trophic levels (Dalsgaard et al. 2003; Hagen and Auel 2001; Kattner and Hagen 1995).

Stable isotope analysis can complement fatty acid data by providing important information on the source of carbon, since the same FATM signal can originate from both phytoplankton (pelagic) or ice algae (sympagic). Ice algae generally exhibit higher enrichment in $\delta^{13}C$ than pelagic algae (Hobson et al. 1995). Given that $\delta^{13}C$ enrichment from the source to the consumer is low ($< 1‰$), this enables effective tracing of the carbon source from primary producers up the food chain (Søreide et al. 2006). Additionally, the stable isotope $\delta^{15}N$ provides insights into the trophic position of organisms within a food web (Post 2002).

With ongoing climate change, Arctic species will be increasingly subjected to boreal conditions and potentially face competition by Atlantic invaders (Kaiser et al. 2022). To better understand the impact of these changes on trophic dynamics, the current study aims to shed new light on differences in Arctic and Atlantic influenced food webs, offering insights into prospective scenarios of a future Arctic. Therefore, we provide information on phytoplankton communities and analyzed the fatty acid composition and stable isotope profiles of key zooplankton species across different regions in Fram Strait. Further, the diets and trophic positions of Arctic and boreal-Atlantic sister species of the copepod genera *Calanus* and *Paraeuchaeta* as well as the amphipod genus *Themisto* are compared in each region. We hypothesize that (1) Arctic and Atlantic influenced regions in Fram Strait show significant differences in their food web structures and that (2) the Arctic food web is strongly dependent on ice algae, indicated by elevated amounts of diatom FATMs in combination with high $\delta^{13}C$ ratios in zooplankton consumers. We further hypothesize that (3) Arctic and boreal-Atlantic zooplankton sister species occupy different ecological niches, expressed by differences in dietary composition and trophic position.

2.2 Materials and methods

2.2.1 Sampling

Sampling of phyto- and zooplankton was conducted at the end of summer during three cruises with RV *Polarstern* to Arctic Fram Strait in July-September 2016, 2017 and 2019 (2016: PS99 for phytoplankton, PS100 for zooplankton, 2017: PS107 and 2019: PS121, Figure 2.1). Phytoplankton samples were collected using a rosette water sampler equipped with 24 Niskin bottles (12 L per bottle). Sampling was carried out during the up-casts at 10, 20-30, 50, and 100 m depth. Subsamples of 2 L were transferred from the Niskin into PVC bottles. Particulate organic matter was collected by sequential filtration of each water sample through three mesh sizes (10 μm, 3 μm, 0.4 μm) on 45 mm diameter Isopore Membrane Filters at 200 mbar using a Millipore Sterifil filtration system (Millipore, USA). After filtration, particulates were stored at $-80\,°C$ until further processing in the laboratory.

Zooplankton was sampled using either a multiple opening and closing net equipped with five nets for stratified vertical hauls (Hydrobios Multinet Midi, mouth opening $0.25\,m^2$, mesh size 150 μm, hauling speed $0.5\,ms^{-1}$) or a bongo net (mesh size: 200 to 500 μm, towing speed 1 to 2 kn), respectively. Vertical hauls with the Multinet usually sampled the entire water column from above the seafloor or a maximum sampling depth of 1500 m to the surface (Kanzow 2017; Metfies 2020; Schewe 2018). Immediately after the haul, individuals were sorted, identified and stored separately in Eppendorf cups at $-80\,°C$.

In situ conditions

In situ profiles were obtained with a CTD (Conductivity Temperature Depth) profiling system prior to each sampling of plankton. Stations in the western part of Fram Strait (Stns 75, 95, 96, 135, EG1, EG2) were under strong influence of the East Greenland Current (EGC), exporting cold and fresh Polar Surface Water with sea ice out of the Arctic Ocean. Temperatures and salinity in the epipelagic layers were generally below $0\,°C$ and 35 psu, respectively. In this study, stations in this area are summarized as the EG region.

Stations which were located in the eastern part of Fram Strait (Stns 15, 27, 28, HG1, HG2, HG3, S3, SV2, SV3) were highly influenced by the West Spitsbergen Current (WSC), which transports rather warm, saline Atlantic water into the Arctic Ocean. Profiles during the different cruises showed high temperatures of 5 to 9 °C to 9 °C in surface waters, which decreased with depth, but stayed above 3 °C in the upper 100 m. Salinity was around 35 psu in the upper 100 m. Stations in this area are referred to as the WS region.

The central Fram Strait, the zone between the EGC and WSC, is characterized by a highly dynamic and turbulent regime, depicting influences of both currents. Stations within this zone are summarized as the central region (Stns 10, 12, 14, 31, 46, 48, 0°, 2°W, HG5, N5).
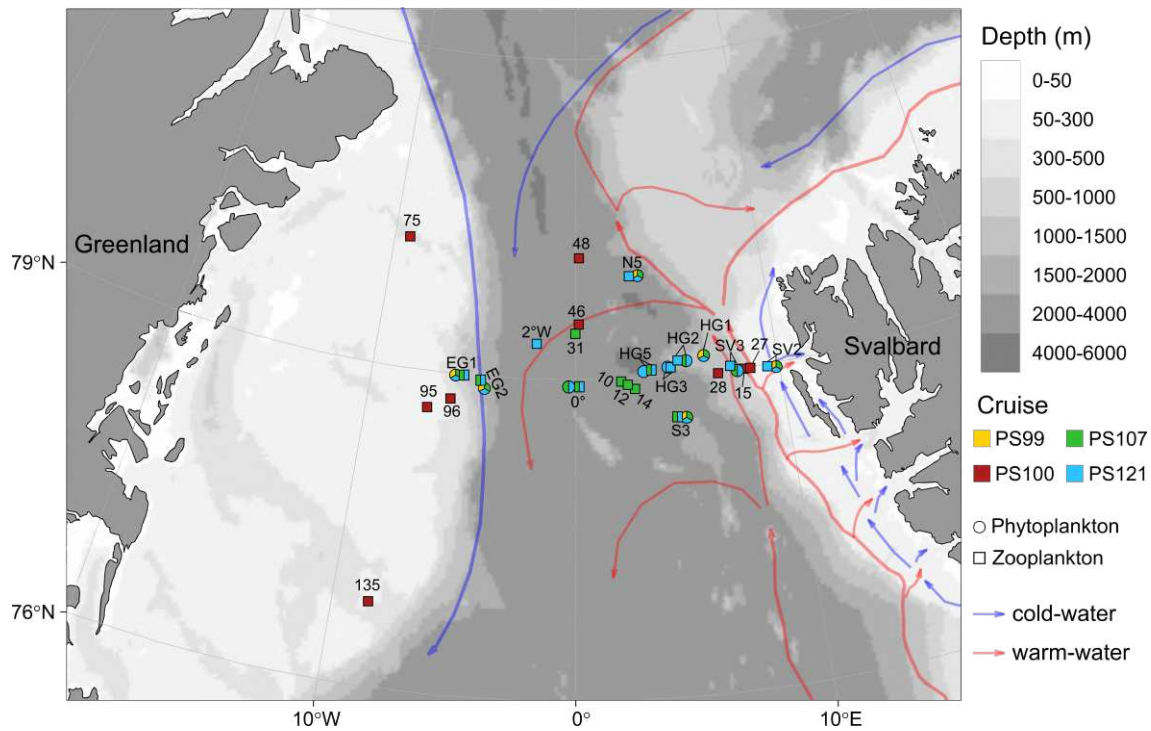
Figure 2.1: Location of stations where phyto- (circles) and zooplankton (squares) samples were collected for metabarcoding, fatty acid and stable isotope analyses during cruises PS99 (yellow), PS100 (red), PS107 (green) and PS121 (blue). Numbers near symbols indicate the respective station number. Arrows represent cold-water (blue) and warm-water (red) currents. Gray shading indicates bathymetry, with lighter gray indicating more shallow and darker gray deeper regions.

Phytoplankton analysis

Genomic DNA extraction from field samples was carried out using the NucleoSpin Plant Kit (Machery-Nagel, Germany) following the manufacturer's protocol. Processing of samples occurred one to two weeks after sampling. DNA extracts were stored at $-20\,°C$.

For Illumina-Sequencing, amplification of a fragment of the 18S rDNA containing the hypervariable V4 region was conducted using the primer set 528iF(GCGGTAATTCCAGCTCC) and 964iR(ACTTTCGTTCTTGATYRR; Metfies et al. 2020). PCR reactions, with a final volume of $50\,µL$, contained $0.02\,U$ Phusion Polymerase (Thermo Fisher, Germany), the 10-fold polymerase buffer per manufacturer's specifications, $0.8\,mM$ (each) dNTP (Eppendorf, Germany), $0.2\,µM$ of each Primer, and $1\,µL$ of template DNA. Amplification was performed with a thermal cycler (Eppendorf, Germany), involving the protocol: initial denaturation ($94\,°C$, $2\,min$) followed by 35 cycles of denaturation ($94\,°C$, $20\,s$), annealing ($85\,°C$, $30\,s$), and extension ($68\,°C$, $30\,s$) with a single final extension ($68\,°C$, $10\,min$). PCR products were purified using the NucleoSpin Gel Kit (Machery-Nagel, Germany) and Minelute PCR Purification kit (Qiagen, Germany) after agarose gel (1% [w/v]) electrophoresis. After the purification, DNA concentration of the samples was determined using a Quantus Fluorometer (Promega, USA). Prior to library preparation, which was based on the 16S metagenomic protocol of Illumina (Illumina, USA), DNA fragments were di-

56

luted with TE-buffer to a concentration of 0.2 ng μL^{-1}. Sequencing of the DNA-fragments was performed using a MiSeq-Sequencer (Illumina, USA). Raw sequences, which had an approximate length of 200 bp, have been deposited in the European Nucleotide Archive (ENA) via GfBio with accession number PRJEB66268.

Further bioinformatic processing of the raw sequences was conducted with the dada2 package v.1.18 in R v.4.0 (Callahan et al. 2016). Sequence realignment and removal of primers were done using Cutadapt v.3.4 (Martin 2011). Low-quality 3' ends were trimmed based on a visual review of the quality plots. Filtering sequences based on expected error ensured a minimum quality for sequence pairs. Remaining sequencing errors were identified using the error profile and rectified by dada2 (Callahan et al. 2016). Sequence pairs were then merged into amplicon sequence variants (ASVs) when having an overlap of at least 25 bp without a mismatch (Callahan et al. 2016). ASVs were taxonomically classified using the Protist Ribosomal Reference database (PR2, Guillou et al. 2012), with the removal of potential chimeras caused by the polymerase chain reaction.

Zooplankton analysis

Lipid analyses

Body dry mass of the deep-frozen specimens was determined after lyophilisation for 48 h. To obtain sufficient biomass, small individuals of identical species, stage (C5 and C6 females for copepods), station and depth were pooled. Lipids were extracted with dichloromethane:methanol (2:1,v:v) followed by a purification step by adding a 0.88% aqueous KCl solution (Folch et al. 1957). Total lipid contents were determined gravimetrically and expressed as percentages of dry mass (Hagen 2000). Percentages of wax esters were calculated from total fatty alcohols. Fatty acids were converted to their fatty acid methyl ester (FAME) derivatives by transesterification in methanol containing 3% concentrated sulphuric acid (Kattner and Fricke 1986; Peters et al. 2007) and were analyzed simultaneously with the fatty alcohols using a gas chromatograph (Agilent Technologies 7890A) equipped with a DB-FFAP column (30 m length, 0.25 mm diameter) and a programmable temperature vaporizer injector using helium as carrier gas. Compounds were identified by comparing the retention times with those of a natural standard (generated from lipids of *Calanus hyperboreus*) with a known fatty acid composition and a synthetic standard (Supelco 37 Component FAME Mix, Sigma-Aldrich).

Based on the fatty acid profiles, carnivory indices (CI) were calculated according to Bode et al. (2015) using the following equation:

$$CI = \frac{18:1(n-9)}{(16:1(n-7)+16:4(n-1)+18:1(n-7)+18:4(n-3)+18:1(n-9))}$$

This index serves as a measure to assess the proportion of carnivorous versus herbivorous feeding within an organism. When the CI is close to zero, the organism is mainly herbivorous,

while a CI approaching 1 signifies a primarily carnivorous diet. Intermediate values reflect various degrees of omnivory.

ANOSIM and SIMPER analyses based on Bray-Curtis similarity of fatty acid profiles between species and regions were conducted to find significant differences and identify key FA contributors to the separations of groups using Primer6 (version 6.1.6; Clarke and Gorley 2006) and in R, using the 'vegan' package (version 2.6-4; Oksanen et al. 2022). Principal component analysis (PCA) and fuzzy clustering were conducted in R, using the prcomp() function and the 'fclust' package (Ferraro et al. 2019), respectively. Samples of the same species collected from the same stations across different years generally showed similar clustering patterns. Thus, the variation from year-to-year had only a minimal effect on the fatty acid patterns and samples from different years were therefore pooled.

Stable isotopes

After lyophilization for 48 h, dried samples were transferred into tin capsules. Depending on individual dry mass, entire animals, pools of individuals with identical parameters or subsamples were used to obtain 0.5 to 5 mg dry mass. Stable isotope analysis was conducted by Agroisolab GmbH in Jülich, Germany, using a mass spectrometer (EA NA1500 Series 2, Carlo Erba Instruments) and helium as carrier gas. Stable isotope ratios of carbon ($^{13}C/^{12}C$) and nitrogen ($^{15}N/^{14}N$) were determined using the standards IAEA-VPDB (IAEA-C1) and atmospheric air (IAEA-N1), respectively. Isotopic ratios are expressed as $\delta^{13}C$ and $\delta^{15}N$ in ‰, referring to the equation established by Hobson et al. (2002). $\delta^{13}C$ values were lipid-corrected considering the molar C/N ratios and applying a model, which normalizes ratios to a constant lipid content and is suitable for C:N ratios of 4.0 (Mintenbeck et al. 2008; Smyntek et al. 2007). Lipid-corrected values are presented as $\delta^{13}C'$.

2.3   Results

2.3.1   Phytoplankton composition

Dinoflagellates dominated in terms of ASV reads at almost all stations (except for Stn EG1, N5 and SV2 in 2019, where diatoms prevailed), with a minimum of 36,700 reads at Stn S3 in 2016 and a maximum of 130 000 reads at Stn EG1 in 2017. The mean number of total reads was highest at stations in the East Greenland Current (EG) region (104 000), followed by the central region (95 000) and the West Spitsbergen Current (WS) region (80 000).

Between the years, small variations were observed, but the trend was generally the same, both across and within taxa (Figure 2.2). The total contribution (mean of percentage contribution for each region, Figure 2.2A) of dinoflagellates and diatoms (Bacillariophyta) was constant (~50% for inoflagellates, ~20% for diatoms) between the regions from EG to WS, while Haptophyta slightly increased (10 to 16%) and Chlorophyta slightly decreased (13 to 8%) from West to East.
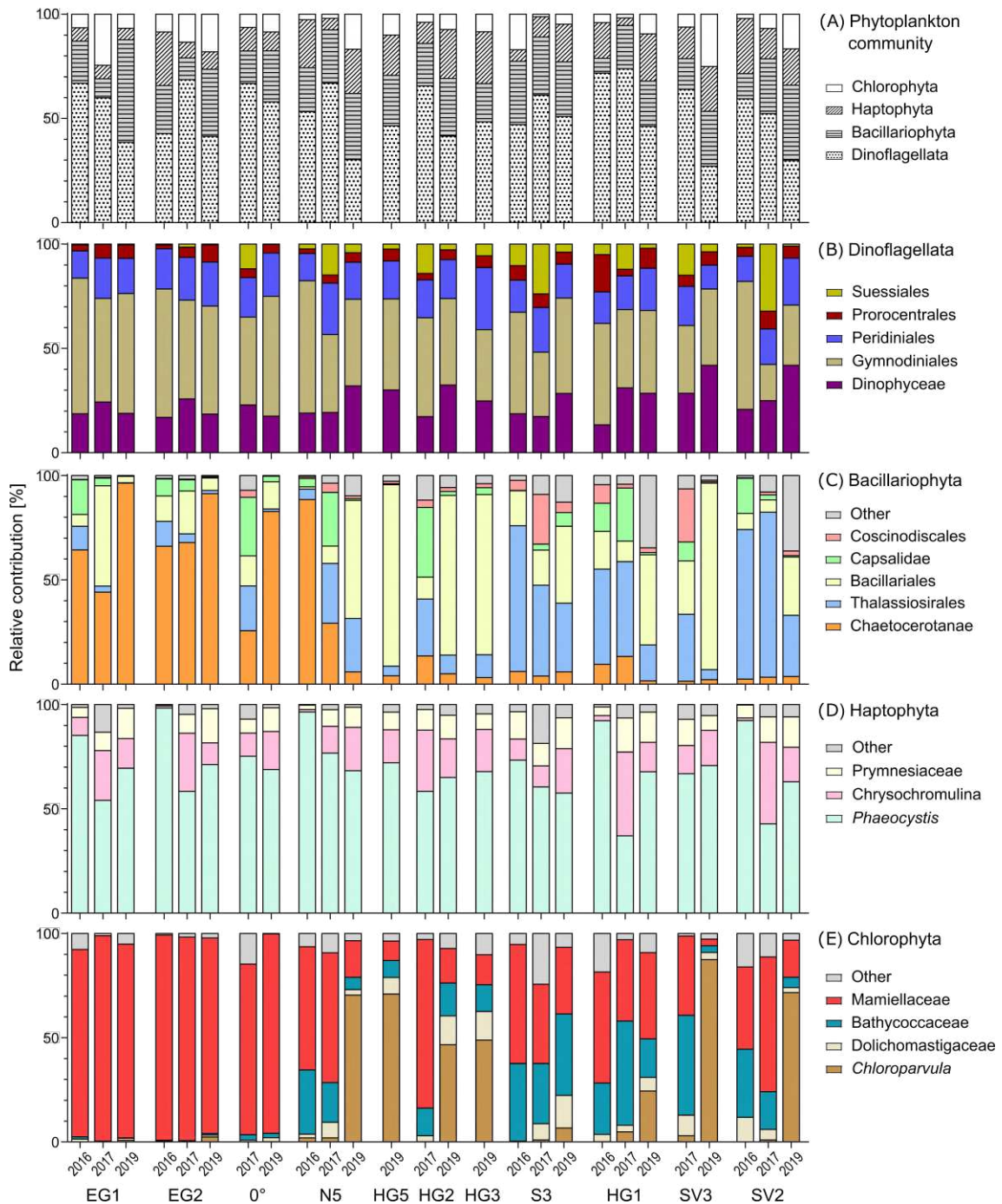
Figure 2.2: Relative phytoplankton community composition (%) across Fram Strait from west (left) to east (right). (A) Overview of phytoplankton taxa. Detailed composition of (B) Dinoflagellata, (C) Bacillariophyta (diatoms), (D) Haptophyta and (E) Chlorophyta.

Within the dinoflagellate community, Gymnodiniales generally dominated in all three regions, but their contribution decreased from EG to WS (mean 56 to 39%, Figure 2.2B). Suessiales were not present in the EG region but occurred in the central and WS regions. Peridiniales and Proro-centrales showed only little regional variation. Syndiniales were excluded from the data as they are mostly parasitic (Groisillier et al. 2006; Guillou et al. 2008).

Chaetocerotanae contributed substantially to the diatom community in the EG region (44 to 96%), but decreased to a mean of 39% in the central and 5% in the WS region (Figure 2.2C). After Chaetocerotanae, Bacillariales overall showed second highest numbers in the EG. Dominating species of the two groups were *Chaetoceros gelidus*, *Chaetoceros neogracilis* (Chaetocerotanae) and *Fragilariopsis cylindrus* (Bacillariales). Conversely, Coscinodiscales and Thalassiosirales showed low numbers in the EG (mean 0 and 5%, resp.), which increased towards the central (2 and 15%) and WS regions (6 and 37). Thalassiosirales and Bacillariales showed altering dominance between stations within the central and WS regions. Species contribution of Bacillariales shifted to a dominance *of Fragilariopsis sublineata* in the WS region. High contributors of Thalassiosirales in the WS were *Thalassiosira* spp. and *Skeletonema* spp.

The Haptophyta community was generally dominated by *Phaeocystis* spp. at all stations with >50% of all Haptophyta (Figure 2.2D), with the exception of HG1 and SV2 in 2017. Chrysochromulina generally showed the second highest number of reads, followed by Prymnesiaceae. Proportions of different Haptophyta remained relatively stable across Fram Strait.

Within the Chlorophyta, Mamiellaceae dominated the community with over 90% in the EG regions and at the EG influenced 0° station (Figure 2.2E). The extremely high contribution of Mamiellaceae decreased towards the central and WS regions but remained among the highest contributors. Among this family, a shift in species dominance occurred from EG to WS. While *Micromonas polaris* dominated in the EG and at the EG influenced 0° station, *M. commoda* generally dominated in the WS. In the central and WS regions, *Chloroparvula* spp. and Bathycoccaceae were other abundant Chlorophyta.

2.3.2 Zooplankton

In total, 363 fatty acid and 292 stable isotope measurements of 19 different species were conducted. The analysis focused on abundant key species, which generally occurred and were sampled in all three regions across Fram Strait, i.e. the calanoid copepods *Calanus hyperboreus*, *Calanus glacialis*, *Calanus finmarchicus*, *Paraeuchaeta glacialis, Paraeuchaeta norvegica* and *Paraeuchaeta barbata*, the hyperiid amphipods *Themisto libellula* and *Themisto abyssorum* , the euphausiid *Thysanoessa longicaudata* and the chaetognath *Eukrohnia* sp. Mean values ± standard deviation of fatty acid percentages and stable isotope ratios of these zooplankton species are shown in Table 2.1. Additional species or taxa include the calanoid copepods *Aetideopsis rostrata*, *Gaetanus brevispinus*, the amphipods *Apherusa glacialis*, *Cyclocaris* sp., the euphausiid *Thysanoessa inermis*, the decapod *Hymenodora glacialis*, as well as Ostracoda, the scyphozoan *Atolla* sp. and the pteropod *Clione limacina*, which are shown in Table S2.1 (fatty acid and SI data) and Figure S2.1 (overview of SI ratios at each region) in the supplementary materials.

Table 2.1: Overview of total lipids, mean fatty acid and wax ester percentages, stable isotope ratios and carnivory indices ($\pm$ standard deviation) for abundant zooplankton taxa across Fram Strait. EG: East Greenland Current region; WS: West Spitsbergen Current region; DM: dry mass; TL: total lipid; WE: wax ester; TFA: total fatty acids; TFAlc: total fatty alcohols. Measurements of different years (2016, 2017, 2019) and developmental stages (C5 and C6 females) are pooled.

	Calanus finmarchicus		*Calanus glacialis*			*Calanus hyperboreus*		
	central	**WS**	**EG**	**central**	**WS**	**EG**	**central**	**WS**
DM [mg ind^{-1}]	0.6 $\pm$ 0.1	0.4 $\pm$ 0.1	2.6 $\pm$ 1.3	1.5 $\pm$ 0.6	2.4 $\pm$ 0.7	3.8 $\pm$ 1.4	4.0 $\pm$ 1.5	3.7 $\pm$ 1.9
TL [% DM]	44.8 $\pm$ 7.4	41.2 $\pm$ 15.0	46.9 $\pm$ 4.6	43.5 $\pm$ 6.3	42.9 $\pm$ 3.8	47.3 $\pm$ 6.0	46.1 $\pm$ 5.2	44.9 $\pm$ 8.2
WE [% TL]	81.4 $\pm$ 2.1	75.1 $\pm$ 12.7	93.8 $\pm$ 9.2	85.1 $\pm$ 5.5	64.1 $\pm$ 17.4	79.9 $\pm$ 12.2	87.2 $\pm$ 5.0	88.3 $\pm$ 6.0
n	4	23	12	11	3	20	25	29
Fatty acids [% TFA]								
14:0	14.4 $\pm$ 1.4	11.1 $\pm$ 3.6	7.3 $\pm$ 1.3	8.1 $\pm$ 1.4	4.9 $\pm$ 3.3	2.4 $\pm$ 0.6	2.7 $\pm$ 0.4	3.2 $\pm$ 0.5
16:0	9.6 $\pm$ 0.2	11.2 $\pm$ 1.6	5.4 $\pm$ 0.8	6.1 $\pm$ 0.5	4.5 $\pm$ 2.4	3.3 $\pm$ 0.5	3.3 $\pm$ 0.6	3.6 $\pm$ 0.7
iso 17:0	0.1 $\pm$ 0.2	0.1 $\pm$ 0.2	0.1 $\pm$ 0.1	0.1 $\pm$ 0.1	0.6 $\pm$ 0.3	0.3 $\pm$ 0.3	0.2 $\pm$ 0.2	0.4 $\pm$ 0.2
18:0	0.7 $\pm$ 0.1	1.0 $\pm$ 0.3	0.2 $\pm$ 0.1	0.2 $\pm$ 0.1	0.4 $\pm$ 0.1	0.2 $\pm$ 0.2	0.2 $\pm$ 0.2	0.5 $\pm$ 0.2
20:0	-	0.1 $\pm$ 0.2	0.4 $\pm$ 0.1	0.5 $\pm$ 0.2	0.5 $\pm$ 0.0	0.5 $\pm$ 0.2	0.4 $\pm$ 0.2	0.3 $\pm$ 0.2
16:1(n-7)	3.8 $\pm$ 0.8	4.5 $\pm$ 1.4	27.2 $\pm$ 6.4	30.0 $\pm$ 5.6	7.8 $\pm$ 2.4	17.4 $\pm$ 3.8	10.9 $\pm$ 4.2	5.1 $\pm$ 2.0
16:3(n-4)	0.2 $\pm$ 0.3	0.4 $\pm$ 0.3	0.5 $\pm$ 0.4	0.2 $\pm$ 0.3	0.9 $\pm$ 0.0	0.8 $\pm$ 0.3	0.5 $\pm$ 0.3	0.1 $\pm$ 0.2
16:4(n-1)	0.6 $\pm$ 0.4	0.6 $\pm$ 0.4	1.7 $\pm$ 1.0	0.9 $\pm$ 0.8	1.1 $\pm$ 0.4	3.0 $\pm$ 1.3	2.2 $\pm$ 1.1	0.7 $\pm$ 0.5
18:1(n-5)	0.2 $\pm$ 0.3	0.5 $\pm$ 0.3	0.9 $\pm$ 0.7	0.7 $\pm$ 0.5	0.4 $\pm$ 0.1	1.0 $\pm$ 1.6	0.6 $\pm$ 0.1	0.7 $\pm$ 0.2
18:1(n-7)	0.4 $\pm$ 0.1	0.4 $\pm$ 0.2	1.1 $\pm$ 0.2	1.1 $\pm$ 0.1	0.6 $\pm$ 0.1	1.3 $\pm$ 0.3	1.0 $\pm$ 0.3	1.0 $\pm$ 0.3
18:1(n-9)	3.8 $\pm$ 0.5	4.0 $\pm$ 1.2	2.9 $\pm$ 0.7	3.5 $\pm$ 0.7	14.2 $\pm$ 13.1	2.3 $\pm$ 1.4	2.2 $\pm$ 0.7	2.9 $\pm$ 1.0
18:2(n-6)	1.3 $\pm$ 0.1	1.4 $\pm$ 0.4	0.6 $\pm$ 0.2	0.8 $\pm$ 0.2	1.6 $\pm$ 0.4	1.1 $\pm$ 0.6	1.6 $\pm$ 0.6	1.8 $\pm$ 0.7
18:3(n-3)	1.6 $\pm$ 0.2	1.1 $\pm$ 0.6	0.3 $\pm$ 0.3	0.3 $\pm$ 0.2	0.9 $\pm$ 0.7	0.8 $\pm$ 0.5	0.9 $\pm$ 0.5	1.4 $\pm$ 0.6
18:4(n-3)	14.7 $\pm$ 5.3	10.4 $\pm$ 3.7	2.0 $\pm$ 1.2	1.8 $\pm$ 1.1	13.3 $\pm$ 7.4	5.6 $\pm$ 3.9	12.6 $\pm$ 8.6	14.1 $\pm$ 6.5
20:1(n-7)	0.9 $\pm$ 0.1	1.1 $\pm$ 0.4	0.9 $\pm$ 0.2	0.9 $\pm$ 0.1	0.6 $\pm$ 0.3	1.8 $\pm$ 0.5	1.5 $\pm$ 0.5	1.1 $\pm$ 0.3
20:1(n-9)	8.7 $\pm$ 0.9	7.3 $\pm$ 2.9	12.2 $\pm$ 3.6	13.8 $\pm$ 3.1	8.5 $\pm$ 5.1	9.3 $\pm$ 1.8	11.1 $\pm$ 1.5	15.6 $\pm$ 4.7
20:1(n-11)	0.7 $\pm$ 0.2	0.6 $\pm$ 0.2	0.2 $\pm$ 0.1	0.1 $\pm$ 0.1	0.6 $\pm$ 0.1	0.7 $\pm$ 0.1	0.9 $\pm$ 0.3	1.2 $\pm$ 0.3
20:4(n-3)	1.4 $\pm$ 0.1	1.2 $\pm$ 0.2	0.5 $\pm$ 0.3	0.4 $\pm$ 0.3	1.3 $\pm$ 0.2	1.0 $\pm$ 0.3	1.4 $\pm$ 0.5	1.1 $\pm$ 0.3
20:5(n-3)	11.0 $\pm$ 2.2	14.4 $\pm$ 3.2	19.0 $\pm$ 5.7	14.0 $\pm$ 5.9	14.1 $\pm$ 1.2	24.0 $\pm$ 5.5	19.6 $\pm$ 7.7	10.8 $\pm$ 3.4
22:1(n-9)	0.9 $\pm$ 0	0.7 $\pm$ 0.3	1.5 $\pm$ 0.4	1.4 $\pm$ 0.4	0.6 $\pm$ 0.4	2.7 $\pm$ 0.8	3.3 $\pm$ 0.9	4.2 $\pm$ 1.5
22:1(n-11)	10.8 $\pm$ 0.3	8.1 $\pm$ 2.7	4.9 $\pm$ 1.3	5.4 $\pm$ 1.5	6.1 $\pm$ 2.4	7.7 $\pm$ 1.7	9.6 $\pm$ 2.2	13.3 $\pm$ 3.9
24:1(n-9)	1.0 $\pm$ 0.4	1.2 $\pm$ 0.7	0.7 $\pm$ 0.3	0.7 $\pm$ 0.4	0.8 $\pm$ 0.1	0.3 $\pm$ 0.2	0.4 $\pm$ 0.3	0.7 $\pm$ 0.3
22:6(n-3)	10.4 $\pm$ 1.2	13.5 $\pm$ 8.3	5.8 $\pm$ 0.9	6.1 $\pm$ 2.1	11.6 $\pm$ 3.2	7.3 $\pm$ 1.1	9.5 $\pm$ 3.1	10.5 $\pm$ 4.2
Carnivory Index (CI)	0.18 $\pm$ 0.07	0.21 $\pm$ 0.07	0.08 $\pm$ 0.03	0.10 $\pm$ 0.02	0.17 $\pm$ 0.04	0.07 $\pm$ 0.03	0.08 $\pm$ 0.03	0.12 $\pm$ 0.06
Fatty alcohols [% TFAlc]								
14:0	1.1 $\pm$ 0.6	1.6 $\pm$ 0.7	1.2 $\pm$ 2.1	2.0 $\pm$ 1.4	2.4 $\pm$ 3.2	4.1 $\pm$ 2.5	3.5 $\pm$ 1.8	3.0 $\pm$ 1.9
16:0	6.2 $\pm$ 0.4	8.5 $\pm$ 3.0	10.4 $\pm$ 2.2	10.1 $\pm$ 1.4	30.1 $\pm$ 25.8	11.1 $\pm$ 7.1	7.0 $\pm$ 2.2	6.5 $\pm$ 3.5
16:1	1.2 $\pm$ 0.3	1.8 $\pm$ 0.5	8.1 $\pm$ 2.1	6.6 $\pm$ 1.9	2.1 $\pm$ 0.1	3.4 $\pm$ 2.0	1.4 $\pm$ 1.0	0.5 $\pm$ 0.6
18:0	0.9 $\pm$ 0.4	1.1 $\pm$ 0.4	1.8 $\pm$ 0.5	1.6 $\pm$ 1.1	2.7 $\pm$ 0.5	1.0 $\pm$ 0.6	0.8 $\pm$ 0.3	1.0 $\pm$ 0.4
18:1(n-7)	0.9 $\pm$ 0.2	1.1 $\pm$ 0.4	3.1 $\pm$ 0.7	2.5 $\pm$ 1.2	1.6 $\pm$ 1.2	1.6 $\pm$ 2.2	0.6 $\pm$ 0.3	0.3 $\pm$ 0.4
20:1(n-7)	-	0.1 $\pm$ 0.4	1.8 $\pm$ 0.7	1.5 $\pm$ 0.7	0.4 $\pm$ 0.6	3.8 $\pm$ 1.5	2.9 $\pm$ 1.2	1.7 $\pm$ 1.5
20:1(n-9)	37.1 $\pm$ 1.9	35.7 $\pm$ 8.8	45.4 $\pm$ 6.6	47.8 $\pm$ 4.1	31.4 $\pm$ 15.7	24.8 $\pm$ 6.3	27.5 $\pm$ 2.6	27.6 $\pm$ 3.3
20:1(n-11)	-	1.5 $\pm$ 7.0	-	-	-	0.5 $\pm$ 2.0	-	-
22:1(n-7)	-	0.4 $\pm$ 1.5	2.2 $\pm$ 2.5	0.6 $\pm$ 0.5	0.2 $\pm$ 0.3	3.6 $\pm$ 4.8	1.7 $\pm$ 1.2	0.8 $\pm$ 1.1
22:1(n-9)	2.8 $\pm$ 0.3	2.5 $\pm$ 0.7	3.5 $\pm$ 0.9	2.9 $\pm$ 1.0	5.8 $\pm$ 3.8	9.0 $\pm$ 9.2	8.7 $\pm$ 1.5	7.8 $\pm$ 1.7
22:1(n-11)	47.2 $\pm$ 1.8	41.9 $\pm$ 6.6	20.5 $\pm$ 4.1	21.9 $\pm$ 2.6	21.4 $\pm$ 13.8	36.0 $\pm$ 11.4	45.0 $\pm$ 5.0	50.2 $\pm$ 4.9
Stable Isotopes [‰]								
n	0	24	2	22	13	14	26	37
$\delta^{13}C'$	-	-24.1 $\pm$ 0.7	-26.1, -25.5	-24.2 $\pm$ 1.2	-23.7 $\pm$ 1.2	-24.9 $\pm$ 1.7	-25.0 $\pm$ 1.1	-23.6 $\pm$ 1.0
$\delta^{15}N$	-	6.3 $\pm$ 2.3	9.0, 8.7	7.5 $\pm$ 0.9	6.3 $\pm$ 1.3	7.4 $\pm$ 1.1	7.4 $\pm$ 1.2	5.1 $\pm$ 1.6

	Paraeuchaeta barbata		Paraeuchaeta glacialis			Paraeuchaeta norvegica	
	central	WS	EG	central	WS	central	WS
DM [mg ind^{-1}]	7.4 ± 3.5	6.2 ± 2.8	3.4 ± 2.1	3.4 ± 1.7	3.8 ± 1.5	5.1 ± 1.5	4.0 ± 1.6
TL [% DM]	44.1 ± 6.4	40.7 ± 6.5	40.4 ± 7.8	38.3 ± 13.9	35.5 ± 9.5	49.3 ± 17.7	48.8 ± 11.5
WE [% TL]	75.6 ± 6.3	77.3 ± 5.4	63.9 ± 12.5	60.8 ± 18.6	76.5 ± 2.7	57.9 ± 16.8	68.6 ± 8.4
n	11	14	20	10	3	6	14
Fatty acids [% TFA]							
14:0	0.6 ± 0.6	0.5 ± 0.5	0.8 ± 0.4	0.8 ± 0.4	0.5 ± 0.3	1.3 ± 1.0	1.4 ± 1.5
16:0	1.8 ± 1.0	1.9 ± 1.0	2.4 ± 1.1	3.2 ± 3.3	1.6 ± 0.5	3.2 ± 1.5	2.9 ± 1.5
iso 17:0	1.0 ± 0.2	1.0 ± 0.2	0.9 ± 0.2	1.0 ± 0.1	1.3 ± 0.1	1.1 ± 0.4	1.2 ± 0.3
18:0	0.5 ± 0.2	0.4 ± 0.3	0.3 ± 0.2	0.5 ± 0.6	0.2 ± 0.1	0.5 ± 0.2	0.5 ± 0.6
20:0	1.1 ± 0.2	1.1 ± 0.3	0.7 ± 0.2	0.7 ± 0.3	0.8 ± 0.4	0.6 ± 0.1	0.6 ± 0.1
16:1(n-7)	21.1 ± 3.0	22.5 ± 2.6	24.0 ± 8.6	20.4 ± 6.8	21.7 ± 0.6	15.5 ± 7.3	17.5 ± 8.9
16:3(n-4)	1.1 ± 0.2	1.3 ± 0.1	0.6 ± 0.3	0.6 ± 0.2	1.1 ± 0.1	0.7 ± 0.3	0.8 ± 0.3
16:4(n-1)	0.2 ± 0.2	0.2 ± 0.2	1.3 ± 0.8	0.8 ± 0.5	0.2 ± 0.3	0.2 ± 0.2	0.4 ± 0.2
18:1(n-5)	0.2 ± 0.2	0.2 ± 0.2	0.4 ± 0.1	0.7 ± 0.8	0.4 ± 0.3	0.2 ± 0.2	0.3 ± 0.2
18:1(n-7)	1.5 ± 0.4	1.2 ± 0.4	1.3 ± 0.3	1.1 ± 0.2	1.0 ± 0.2	1.1 ± 0.4	1.0 ± 0.2
18:1(n-9)	26.3 ± 3.4	30.6 ± 3.9	16.7 ± 6.6	16.4 ± 3.4	23.0 ± 4.3	20.4 ± 3.9	25.7 ± 7.5
18:2(n-6)	2.8 ± 0.3	2.7 ± 0.5	1.4 ± 0.3	1.6 ± 0.3	1.9 ± 0.7	1.4 ± 0.2	1.7 ± 0.3
18:3(n-3)	1.5 ± 0.3	1.4 ± 0.6	0.6 ± 0.4	0.9 ± 0.4	1.0 ± 0.4	0.7 ± 0.4	1.0 ± 0.5
18:4(n-3)	2.8 ± 1.4	1.9 ± 0.9	4.4 ± 2.3	3.1 ± 0.8	1.6 ± 0.7	1.9 ± 0.9	2.3 ± 1.6
20:1(n-7)	0.1 ± 0.2	0.1 ± 0.1	0.3 ± 0.1	0.3 ± 0.2	0.3 ± 0.0	0.1 ± 0.1	0.2 ± 0.2
20:1(n-9)	9.5 ± 2.1	9.7 ± 2.8	6.3 ± 2.7	9.2 ± 3.4	11.8 ± 4.8	8.6 ± 3.7	9.1 ± 2.5
20:1(n-11)	1.8 ± 0.3	2.2 ± 0.3	0.5 ± 0.2	0.7 ± 0.3	1.7 ± 0.1	1.0 ± 0.4	1.1 ± 0.3
20:4(n-3)	0.7 ± 0.4	0.4 ± 0.4	0.6 ± 0.3	0.5 ± 0.3	0.3 ± 0.4	0.6 ± 0.4	0.4 ± 0.2
20:5(n-3)	6.3 ± 2.6	5.0 ± 2.5	14.4 ± 5.4	11.2 ± 3.2	5.4 ± 3.3	7.8 ± 2.9	6.4 ± 2.0
22:1(n-9)	0.5 ± 0.4	0.2 ± 0.2	0.3 ± 0.3	0.3 ± 0.3	0.3 ± 0.2	0.6 ± 0.4	0.6 ± 0.3
22:1(n-11)	6.7 ± 2.9	6.3 ± 2.8	4.6 ± 3.1	7.7 ± 5.3	13.1 ± 6.8	13.3 ± 7.5	12.9 ± 4.3
24:1(n-9)	0.7 ± 0.3	0.8 ± 0.4	1.0 ± 0.4	1.3 ± 0.5	0.6 ± 0.4	1.1 ± 0.6	1.0 ± 0.6
22:6(n-3)	9.4 ± 3.6	7.1 ± 3.4	13.8 ± 5.8	12.9 ± 4.4	7.4 ± 2.2	15.0 ± 9.6	8.3 ± 2.9
Carnivory Index (CI)	0.51 ± 0.03	0.54 ± 0.03	0.35 ± 0.11	0.40 ± 0.09	0.46 ± 0.05	0.53 ± 0.10	0.59 ± 0.06
Fatty alcohols [% TFAlc]							
14:0	17.2 ± 3.4	17.3 ± 3.6	24.7 ± 16.5	18.2 ± 15.2	30.0 ± 9.3	22.5 ± 16.5	33.8 ± 9.7
16:0	16.7 ± 2.9	17.4 ± 4.0	25.3 ± 7.1	25.2 ± 16.1	14.7 ± 6.6	27.2 ± 11.7	23.0 ± 5.0
16:1	3.3 ± 0.6	3.2 ± 1.0	8.1 ± 3.8	5.2 ± 2.4	2.7 ± 1.1	3.0 ± 2.6	2.7 ± 2.4
18:0	0.2 ± 0.3	0.5 ± 0.3	1.1 ± 0.7	1.7 ± 1.2	0.9 ± 0.3	1.4 ± 0.5	1.4 ± 0.4
18:1(n-7)	5.7 ± 0.9	5.7 ± 1.6	4.3 ± 1.8	2.8 ± 1.8	2.9 ± 2.3	2.3 ± 1.4	2.2 ± 0.6
20:1(n-7)	1.5 ± 0.8	1.0 ± 0.6	1.4 ± 0.7	1.2 ± 1.0	0.6 ± 0.5	0.4 ± 0.6	0.2 ± 0.5
20:1(n-9)	15.3 ± 1.6	15.5 ± 1.8	15.1 ± 7.5	20.6 ± 6.3	17.4 ± 4.5	19.8 ± 7.2	17.3 ± 7.7
20:1(n-11)	-	-	1.9 ± 5.8	1.8 ± 5.4	-	-	-
22:1(n-7)	0.2 ± 0.7	0.1 ± 0.3	0.3 ± 0.5	0.2 ± 0.4	-	-	0.0 ± 0.2
22:1(n-9)	6.5 ± 2.6	4.5 ± 1.5	2.5 ± 1.4	2.8 ± 1.5	3.1 ± 1.1	1.8 ± 1.2	2.6 ± 3.7
22:1(n-11)	29.5 ± 3.8	30.5 ± 5.5	13.8 ± 6.8	18.5 ± 8.2	25.6 ± 2.5	20.4 ± 12.5	15.8 ± 5.4
Stable Isotopes [‰]							
n	4	10	4	9	6	1	15
$\delta^{13}C'$	-24.0 ± 1.0	-23.1 ± 0.6	-24.8 ± 1.0	-25.0 ± 0.8	-23.4 ± 0.3	-23.5	-23.2 ± 0.4
$\delta^{15}N$	10.5 ± 0.5	9.8 ± 0.8	11.2 ± 1.2	10.6 ± 1.4	7.0 ± 1.1	9.6	8.0 ± 0.9

	Themisto abyssorum			Themisto libellula		
	EG	**central**	**WS**	**EG**	**central**	**WS**
DM [mg ind⁻¹]	1.1 ± 0.7	9.8 ± 4.9	5.1 ± 3.5	4.32	11.2 ± 9.9	12.8 ± 8.1
TL [% DM]	37.8 ± 12.1	29.8 ± 7.5	29.2 ± 12.4	21.8	19.1 ± 9.1	23.3 ± 4.3
WE [% TL]	10.3 ± 3.5	34.9 ± 13.6	34.1 ± 11.8	10.2	32.5 ± 12.6	36.1 ± 4.7
n	4	15	19	1	10	7
Fatty acids [% TFA]						
14:0	2.7 ± 0.7	3.1 ± 1.0	3.4 ± 0.9	2.7	3.9 ± 2.0	4.4 ± 1.1
16:0	10.7 ± 0.7	9.4 ± 1.6	11.4 ± 2.0	9.2	13.1 ± 3.5	11.9 ± 2.0
iso 17:0	0.2 ± 0.3	0.0 ± 0.1	0.2 ± 0.2	0.2	0.1 ± 0.1	0.2 ± 0.1
18:0	1.3 ± 0.5	1.0 ± 0.2	1.4 ± 0.3	0.4	0.9 ± 0.2	1.0 ± 0.3
20:0	-	-	-	-	-	0.0 ± 0.1
16:1(n-7)	9.4 ± 4.5	8.5 ± 5.3	5.2 ± 1.0	10.7	5.0 ± 3.2	4.2 ± 1.4
16:3(n-4)	0.1 ± 0.1	0.3 ± 0.2	0.3 ± 0.2	0.5	0.2 ± 0.2	0.4 ± 0.2
16:4(n-1)	0.2 ± 0.4	0.2 ± 0.3	0.2 ± 0.3	0.8	0.1 ± 0.4	0.2 ± 0.3
18:1(n-5)	0.7 ± 0.1	0.8 ± 0.1	0.9 ± 0.2	0.8	0.7 ± 0.1	0.8 ± 0.1
18:1(n-7)	2.3 ± 0.8	2.1 ± 0.9	1.8 ± 0.8	2.4	2.0 ± 1.1	1.2 ± 0.5
18:1(n-9)	6.5 ± 1.6	11.2 ± 2.4	14.2 ± 3.3	4.4	9.9 ± 3.5	8.3 ± 1.3
18:2(n-6)	1.8 ± 0.5	1.5 ± 0.2	1.7 ± 0.3	0.9	1.9 ± 0.3	1.9 ± 0.3
18:3(n-3)	1.0 ± 0.1	1.1 ± 0.5	0.8 ± 0.4	0.7	0.9 ± 0.3	1.0 ± 0.5
18:4(n-3)	3.3 ± 1.0	5.2 ± 3.4	3.9 ± 2.0	4.5	5.0 ± 2.9	7.3 ± 1.6
20:1(n-7)	0.7 ± 0.4	1.2 ± 0.7	0.8 ± 0.4	0.5	0.5 ± 0.2	0.5 ± 0.2
20:1(n-9)	5.0 ± 2.2	12.3 ± 3.5	11.8 ± 2.7	3	8.4 ± 2.7	9.7 ± 2.5
20:1(n-11)	1.2 ± 0.2	4.0 ± 1.9	4.0 ± 1.6	1.2	2.7 ± 0.9	3.3 ± 0.9
20:4(n-3)	0.9 ± 0.1	0.8 ± 0.2	0.8 ± 0.2	1	1.0 ± 0.2	1.0 ± 0.1
20:5(n-3)	27.4 ± 3.8	11.5 ± 2.4	11.9 ± 1.8	27.9	14.6 ± 3.4	14.2 ± 1.5
22:1(n-9)	0.6 ± 0.4	1.5 ± 0.6	1.3 ± 0.6	0.4	0.7 ± 0.2	0.6 ± 0.1
22:1(n-11)	1.5 ± 0.3	7.5 ± 2.9	7.4 ± 2.2	1.5	4.6 ± 1.9	6.5 ± 1.3
24:1(n-9)	0.1 ± 0.1	0.3 ± 0.3	0.2 ± 0.3	0.5	0.2 ± 0.3	0.6 ± 0.2
22:6(n-3)	18.8 ± 4.7	12.7 ± 4.8	11.6 ± 3.8	21.7	20.4 ± 7.6	15.6 ± 4.6
Carnivory Index (CI)	0.32 ± 0.09	0.43 ± 0.10	0.56 ± 0.09	0.19	0.46 ± 0.13	0.40 ± 0.07
Fatty alcohols [% TFAlc]						
14:0	-	6.1 ± 4.3	8.1 ± 6.4	-	2.7 ± 1.3	1.7 ± 0.9
16:0	11.5 ± 2.3	8.6 ± 2.6	10.7 ± 6.0	16.6	7.7 ± 1.6	7.5 ± 0.9
16:1	3.6 ± 2.7	1.4 ± 1.8	0.7 ± 0.8	15.6	1.5 ± 1.3	1.7 ± 1.0
18:0	3.2 ± 2.1	0.4 ± 0.8	1.0 ± 0.7	2	0.3 ± 0.6	1.3 ± 0.8
18:1(n-7)	0.6 ± 1.0	0.8 ± 1.2	0.6 ± 0.7	2.7	0.3 ± 0.5	0.8 ± 0.5
20:1(n-7)	-	0.8 ± 1.1	0.1 ± 0.3	-	0.1 ± 0.4	-
20:1(n-9)	6.5 ± 11.3	28.0 ± 4.1	28.1 ± 5.2	22.2	33.4 ± 2.9	31.7 ± 1.5
20:1(n-11)	25.9 ± 16.2	-	-	-	-	-
22:1(n-7)	-	0.1 ± 0.5	1.3 ± 4.1	-	-	-
22:1(n-9)	5.2 ± 5.2	7.1 ± 2.4	5.4 ± 3.5	-	2.8 ± 1.7	9.4 ± 16.1
22:1(n-11)	43.0 ± 10.0	44.8 ± 6.6	42.3 ± 8.5	37.8	48.9 ± 4.9	42.7 ± 17.3
Stable Isotopes [‰]						
n	3	7	15	0	8	7
$\delta^{13}C'$	-23.9 ± 0.8	-22.5 ± 1.3	-21.6 ± 0.6	-	-23.4 ± 1.2	-21.0 ± 1.0
$\delta^{15}N$	7.5 ± 0.2	10.0 ± 0.9	7.7 ± 0.9	-	7.8 ± 1.2	6.9 ± 0.7

	Thysanoessa longicaudata			Eukrohnia sp.		
	EG	central	WS	EG	central	WS
DM [mg ind^{-1}]	7.5 ± 1.8	6.2 ± 1.8	5.5 ± 1.1	6.4 ± 1.8	6.4 ± 0.7	5.9 ± 1.6
TL [% DM]	46.5 ± 6.8	49.1 ± 7.3	51.4 ± 9.1	19.4 ± 5.5	19.3 ± 4.6	22.0 ± 3.7
WE [% TL]	-	-	-	51.8 ± 33.7	54.0 ± 25.8	72.4 ± 6.9
n	3	10	27	3	3	6
Fatty acids [% TFA]						
14:0	3.6 ± 0.6	3.4 ± 0.6	2.4 ± 0.6	1.7 ± 0.6	3.4 ± 1.9	3.7 ± 2.2
16:0	29.6 ± 4.1	30.9 ± 2.5	33.0 ± 3.9	6.7 ± 3.4	7.0 ± 2.4	5.3 ± 0.8
iso 17:0	0.1 ± 0.1	0.1 ± 0.1	0.2 ± 0.1	-	-	-
18:0	1.9 ± 0.4	1.9 ± 0.2	2.0 ± 0.3	1.0 ± 0.8	1.3 ± 0.7	0.9 ± 0.2
20:0	-	-	-	-	-	-
16:1(n-7)	12.8 ± 2.6	5.8 ± 1.4	4.7 ± 0.9	19.0 ± 2.8	7.8 ± 1.3	7.7 ± 1.1
16:3(n-4)	0.2 ± 0.1	0.3 ± 0.1	0.3 ± 0.1	0.7 ± 0.5	-	0.1 ± 0.2
16:4(n-1)	0.0 ± 0.1	0.0 ± 0.1	0.0 ± 0.1	2.0 ± 1.4	-	0.4 ± 0.3
18:1(n-5)	1.4 ± 1.6	0.3 ± 0.1	0.5 ± 0.2	1.0 ± 0.4	1.0 ± 0.3	1.0 ± 0.4
18:1(n-7)	6.1 ± 0.8	6.5 ± 0.5	6.7 ± 0.7	2.8 ± 2.4	0.7 ± 0.1	0.7 ± 0.1
18:1(n-9)	12.0 ± 0.9	16.5 ± 1.4	18.0 ± 2.0	6.3 ± 3.3	5.7 ± 0.5	5.6 ± 0.4
18:2(n-6)	1.2 ± 0.6	2.0 ± 0.7	1.5 ± 0.4	1.4 ± 0.9	1.5 ± 0.2	1.4 ± 0.3
18:3(n-3)	0.5 ± 0.4	1.0 ± 0.1	0.7 ± 0.4	0.4 ± 0.3	1.1 ± 0.2	1.2 ± 0.2
18:4(n-3)	1.2 ± 0.7	2.6 ± 1.1	1.2 ± 0.6	2.3 ± 0.3	5.5 ± 3.5	7.1 ± 2.0
20:1(n-7)	0.4 ± 0.1	0.6 ± 0.9	0.2 ± 0.1	1.3 ± 0.4	0.7 ± 0.1	0.8 ± 0.1
20:1(n-9)	2.8 ± 1.1	2.4 ± 0.5	3.3 ± 1.5	8.0 ± 1.5	11.6 ± 2.8	13.5 ± 1.9
20:1(n-11)	0.0 ± 0.1	0.0 ± 0.1	0.2 ± 0.4	0.5 ± 0.4	1.5 ± 0.4	1.5 ± 0.2
20:4(n-3)	0.2 ± 0.3	0.5 ± 0.2	0.5 ± 0.1	0.3 ± 0.2	0.6 ± 0.4	0.9 ± 0.1
20:5(n-3)	13.5 ± 2.7	11.6 ± 1.4	11.5 ± 2.1	17.9 ± 4.7	11.1 ± 0.4	10.9 ± 1.7
22:1(n-9)	1.0 ± 0.0	1.0 ± 0.2	1.1 ± 0.4	1.4 ± 0.3	1.6 ± 0.5	1.8 ± 0.6
22:1(n-11)	1.1 ± 0.6	0.3 ± 0.2	1.8 ± 2.1	7.3 ± 3.3	15.8 ± 2.0	17.3 ± 1.8
24:1(n-9)	0.4 ± 0.3	0.7 ± 0.1	0.8 ± 0.4	1.6 ± 0.6	1.6 ± 0.2	1.2 ± 0.3
22:6(n-3)	5.7 ± 3.2	9.2 ± 1.4	6.5 ± 1.9	13.2 ± 2.3	17.8 ± 2.9	14.0 ± 1.9
Carnivory Index (CI)	0.37 ± 0.03	0.53 ± 0.05	0.59 ± 0.04	0.19 ± 0.09	0.30 ± 0.04	0.26 ± 0.02
Fatty alcohols [% TFAlc]						
14:0	-	-	-	4.3 ± 3.1	1.6 ± 1.1	2.4 ± 0.6
16:0	-	-	-	12.9 ± 2.7	7.7 ± 1.6	7.7 ± 0.7
16:1	-	-	-	8.6 ± 3.5	0.9 ± 0.6	1.2 ± 0.3
18:0	-	-	-	0.7 ± 0.7	0.3 ± 0.4	1.0 ± 0.2
18:1(n-7)	-	-	-	6.0 ± 6.3	0.8 ± 0.5	0.8 ± 0.4
20:1(n-7)	-	-	-	2.0 ± 1.6	-	0.1 ± 0.3
20:1(n-9)	-	-	-	28.8 ± 2.3	34.7 ± 1.2	33.6 ± 1.6
20:1(n-11)	-	-	-	-	-	-
22:1(n-7)	-	-	-	0.5 ± 0.7	-	-
22:1(n-9)	-	-	-	2.8 ± 2.0	3.0 ± 0.4	4.2 ± 1.1
22:1(n-11)	-	-	-	31.8 ± 4.3	48.7 ± 7.0	46.1 ± 1.9
Stable Isotopes [‰]						
n	4	5	14	0	1	2
$\delta^{13}C'$	-23.2 ± 0.3	-22.8 ± 0.5	-23.3 ± 0.7	-	-24.8	-22.4, -23.4
$\delta^{15}N$	8.4 ± 1.1	7.2 ± 0.6	6.6 ± 0.9	-	3.4	4.1, 5.4

2.3.3 Fatty acids

Calanus

Lipid contents were generally comparable between the regions and the three *Calanus* species ranging from 41 to 47% DM (Table 2.1). Wax ester content showed a higher variability, ranging from 64 to 94% TL. Highest mean total lipid and WE contents were found in *C. hyperboreus*, except in the EG region, were *C. glacialis* showed higher values. In *C. glacialis*, mean WE contents were lower in the WS compared to the EG and central regions.

Principal component analysis (PCA) of *C. hyperboreus*, *C. glacialis* and *C. finmarchicus* C5 copepodids and C6 females with the dominant fatty acids (> 2% mean TFA) showed a clear separation between species as well as between the EG and WS regions (Figure 2.3). The first component of the PCA explained 30% of variation, the second component explained 28%. PC1 separated *C. finmarchicus* (negative values) from *C. hyperboreus* (positive values) in the WS region. Main fatty acid contributors in the WS were 18:4(n-3), 20:1(n-9), 22:1(n-9) and 22:1(n-11) for *C. hyperboreus*. PC2 distinguished between WS (positive PC1, negative PC2) and EG (negative PC1, positive PC2) areas for *C. hyperboreus* and *C. glacialis*. Important fatty acids for *C. glacialis* and *C. hyperboreus* in the EG were 16:1(n-7), 16:4(n-1) and 20:5(n-3).

Fuzzy clustering identified four clusters, which represent species and area distribution

Figure 2.3: Principal component analysis of fatty acid profiles of the three *Calanus* species. Color of symbols represent species and developmental stages; symbols represent regions. Numbers and text above symbols indicate stations. Colors of station labels represent cluster affiliation.

(Figure 2.3). Green: *C. finmarchicus* from the central and WS regions with two *C. glacialis*, one female and one C5, from WS; pink: *C. hyperboreus* from WS and central stations and one *C. glacialis* C5 from WS; blue: *C. hyperboreus* from EG and central stations and five *C. glacialis* from EG and central stations; red: *C. glacialis* from EG and central stations and one *C. hyperboreus* from WS.

Between species, *C. finmarchicus* and *C. hyperboreus* showed a clear separation in the WS and WS influenced Stns (46, HG5), which was also indicated by the results of the ANOSIM, i.e. large R-values and highly significant p-values. The three FA profiles of *C. glacialis* in the WS area clustered within the *C. finmarchicus* WS and the *C. hyperboreus* WS clusters, respectively. In the EG and at EG influenced central Stns (2°W, 0°, 21 and 48), clustering separated *C. hyperboreus* from *C. glacialis* females. The two *C. glacialis* C5 measurements were assigned to the *C. hyperboreus* EG cluster.

Between areas, *C. hyperboreus* and *C. glacialis* showed a clear separation between WS and EG influenced regions. This is supported by the ANOSIM, where the fatty acid composition from the EG was clearly different from the WS region for both species. Differences were smaller between the EG and central regions than between WS and the central regions.

SIMPER analysis identified the FAs that significantly contributed to the discrimination between the EG and WS regions. For *C. hyperboreus*, those FAs were the diatom markers 16:1(n-7) ($p = 0.03, 19\%$) and 20:5(n-3) ($p = 0.001, 18\%$), the (dino-)flagellate marker 18:4(n-3) ($p = 0.006, 14\%$) and the two *de novo* synthesized *Calanus* markers 20:1(n-9) ($p = 0.001, 10\%$) and 22:1(n-11) ($p = 0.001, 8\%$). For *C. glacialis*, the diatom marker 16:1(n-7) ($p = 0.03, 25\%$) and the carnivory marker 18:1(n-9) ($p = 0.004, 14\%$) significantly contributed to the discrimination. The (dino-)flagellate marker 18:4(n-3) was also important ($p = 0.051, 14\%$).

Based on the difference in contribution of diatom and (dino-)flagellate markers between areas revealed by PCA and SIMPER analysis for *C. hyperboreus* and *C. glacialis*, a west-east transect of those markers across all stations in Fram Strait was depicted in Figure 2.4. The diatom markers 16:1(n-7) and 20:5(n-3) had higher contributions to the total fatty content of *C. hyperboreus* and *C. glacialis* in EG influenced parts of Fram Strait. The contribution of those FA markers decreased towards the east. *Vice versa*, (dino-)flagellate markers 18:4(n-3) and 22:6(n-3) showed little contribution in the EG region and increasing importance towards the WS.

Paraeuchaeta

Lipid and WE contents of the three *Paraeuchaeta* species varied between 36 to 49% DM and 58 to 77% TL, respectively (Table 2.1). Highest lipid contents were observed for *P. norvegica*, followed by *P. barbata*, whereas *P. barbata* had highest WE contents, followed by *P. glacialis*. Between regions, values did not vary distinctly for each species.

PCA of *P. barbata*, *P. glacialis* and *P. norvegica* with the dominant fatty acids (> 2% mean TFA) showed a clear separation between species and regions (Figure 2.5). The first component of
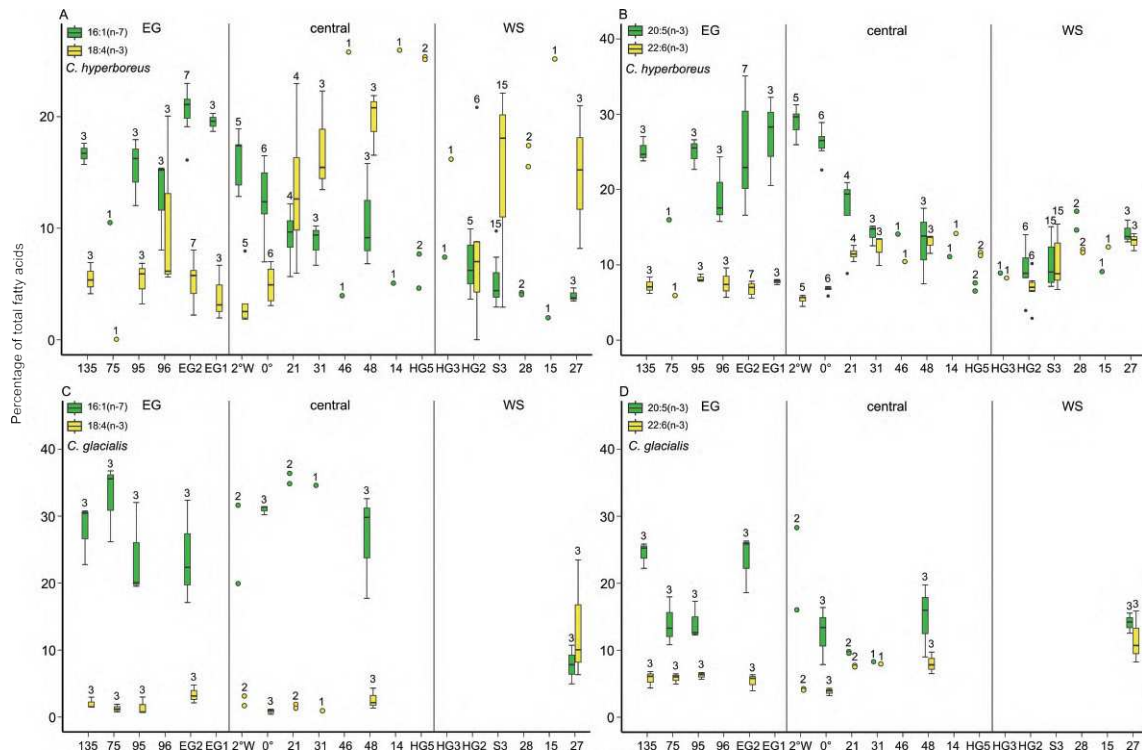
Figure 2.4: Contributions (% of total FAs) of the biomarker fatty acids 16:1(n-7) and 18:4(n-3) as well as 20:5(n-3) and 22:6(n-3) in *C. hyperboreus* (A and B) and *C. glacialis* (C and D) along a West (left) – East (right) transect across Fram Strait. Boxes represent the interquartile range (lower edge: 25th percentile, the upper edge: 75th percentile, central line: median, whiskers extend to minimum and maximum values within 1.5 times the interquartile range). Black dots represent potential outliers that are above or below 1.5 times the interquartile range, respectively. Values above the boxplots show number of measurements.

the PCA explained 37% of the variation, the second component explained an additional 22%. PC1 separated between species (*P. glacialis* positive, *P. barbata* and *P. norvegica* negative) and further discriminated between regions (WS negative, EG positive). The only three individuals of *P. glacialis*, which were sampled from the WS area, clustered together with *P. norvegica* and *P. barbata* in the WS cluster. PC2 separated *P. barbata* (positive PC2, negative PC1) from *P. norvegica* (negative PC2, negative PC1) in the WS and central regions. Important fatty acids for *P. glacialis* in EG were 18:4(n-3), 20:5(n-3) and 22:6(n-3). In the WS region, carnivory markers had a stronger influence, 20:1(n-9) and 22:1(n-1) in *P. norvegica* and 18:1(n-9) and 20:1(n-11) in *P. barbata*. Fuzzy clustering identified three clusters, with each cluster mainly representing one species (Figure 2.5).

ANOSIM supported the differentiation between species. Differences were highest between *P. barbata* and the other two species. *P. glacialis* and *P. norvegica* were more similar to each other. Between areas, the analysis revealed highly significant differences for *P. glacialis* from EG and WS areas and a small but significant difference between individuals of *P. norvegica* from central and WS. SIMPER analysis showed that for *P. glacialis* the *Calanus* markers 22:1(n-11) ($p = 0.017, 15\%$), 20:1(n-9) ($p = 0.004, 10\%$) and 20:1(n-11) ($p = 0.006, 1\%$) as well as the diatom marker 20:5(n-3) ($p = 0.012, 15\%$) and the (dino-)flagellate marker 18:4(n-3) ($p = 0.076, 5\%$)
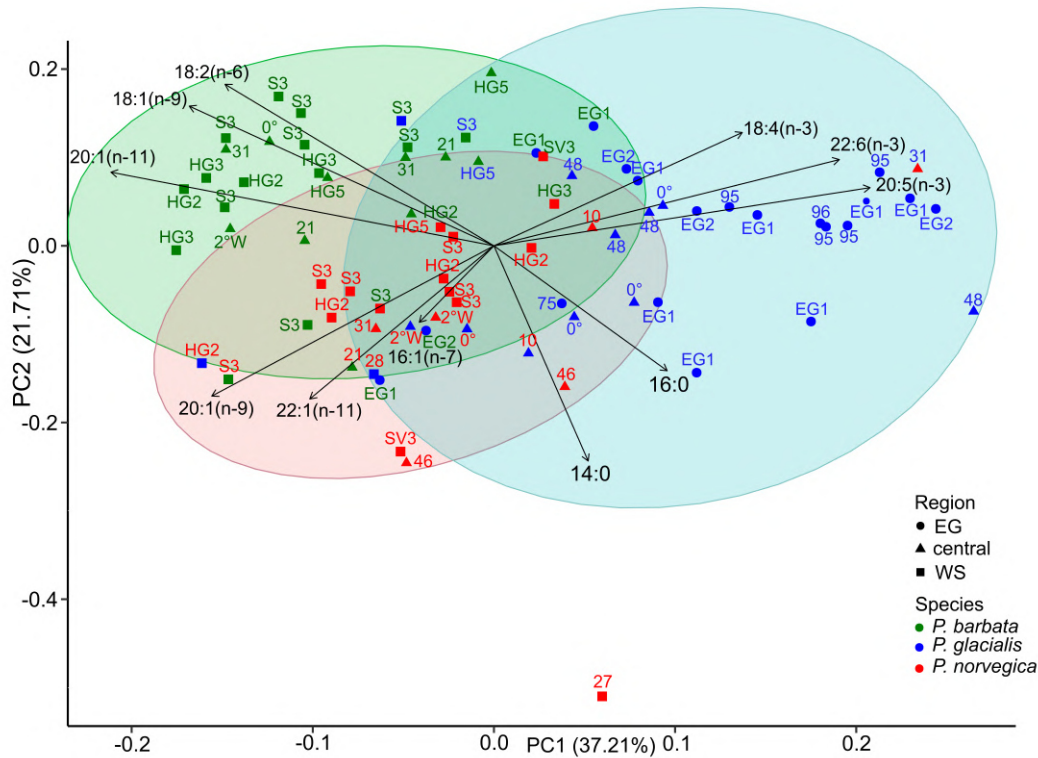
67

Figure 2.5: Principal component analysis of the fatty acid profiles of three *Paraeuchaeta* species. Colors of symbols represent species; symbols represent areas. Numbers and text above symbols indicate stations. Colors of station labels represent cluster affiliation.

significantly contributed to the differentiation between EG and WS.

Themisto

Lipid and WE contents were variable for the two *Themisto* species, ranging from 19 to 38% DM and from 10 to 36% TL, respectively (Table 2.1). *T. abyssorum* had slightly higher total lipid values in the EG compared to the central and WS region. Total lipid levels of *T. abyssorum* were higher than those of *T. libellula* in each region. WE contents were similar in both species, with lowest values in the EG and higher values in the central and WS regions.

The PCA of the fatty acid composition in *T. abyssorum* and *T. libellula* showed separation between species and regions (Figure 2.6). PC1 explained 37% of the variation, while PC2 explained an additional 22%. PC1 mainly separated the EG region (positive) from the WS (negative). Associated with the regions were different dietary markers, i.e. 20:5(n-3) and 22:6(n-3) with the EG (positive) and carnivory and *Calanus* FATMs with the WS (negative). Fuzzy clustering identified three clusters. The blue cluster mainly comprised individuals of both species from EG or EG influenced regions and depicted higher concentrations in algal FATMs. The red cluster almost exclusively included *T. abyssorum* (except for one *T. libellula* from the central region) from the WS and central regions and showed higher contents in *Calanus* FATMs and the carnivory marker

18:1(n-9). The green cluster comprised a mix of *T. libellula* and *T. abyssorum* from the WS and central regions.

ANOSIM showed a small, but significant difference between species in the WS and central regions. Between regions, the analysis depicted a significant and large difference between the EG and the WS for *T. abyssorum* ($R = 0.935$, $p = 0.001$). The difference between the WS and central region was smaller than between the EG and the central region.

SIMPER analysis identified 20:5(n-3) ($p = 0.001, 24\%$), 18:1(n-9) ($p = 0.001, 12\%$), 20:1(n-9) ($p = 0.002, 11\%$), 22:1(n-9) ($p = 0.001, 9\%$) and 20:1(n-11) ($p = 0.01, 4\%$) as significant contributors for the discrimination of *T. abyssorum* between EG and WS. For *T. libellula*, 20:5(n-3) significantly contributed to the differentiation between EG and WS ($p = 0.049, 23\%$).

Further taxa: *Thysanoessa longicaudata* and *Eukrohnia*

Total lipid contents did not show large variations across Fram Strait for the euphausiid *T. longicaudata* ($47 - 51\%$ DM) and the chaetognath *Eukrohnia* sp. ($19 - 22\%$ DM, Table 2.1). WE levels in *Eukrohnia* sp. ranged from 52 to 72% TL. *T. longicaudata* did not contain fatty alcohols and hence no WE.

ANOSIM detected large and significant differences between WS and EG for both *Eukrohnia* sp. and *T. longicaudata*. For *T. longicaudata*, differences between EG and the central region
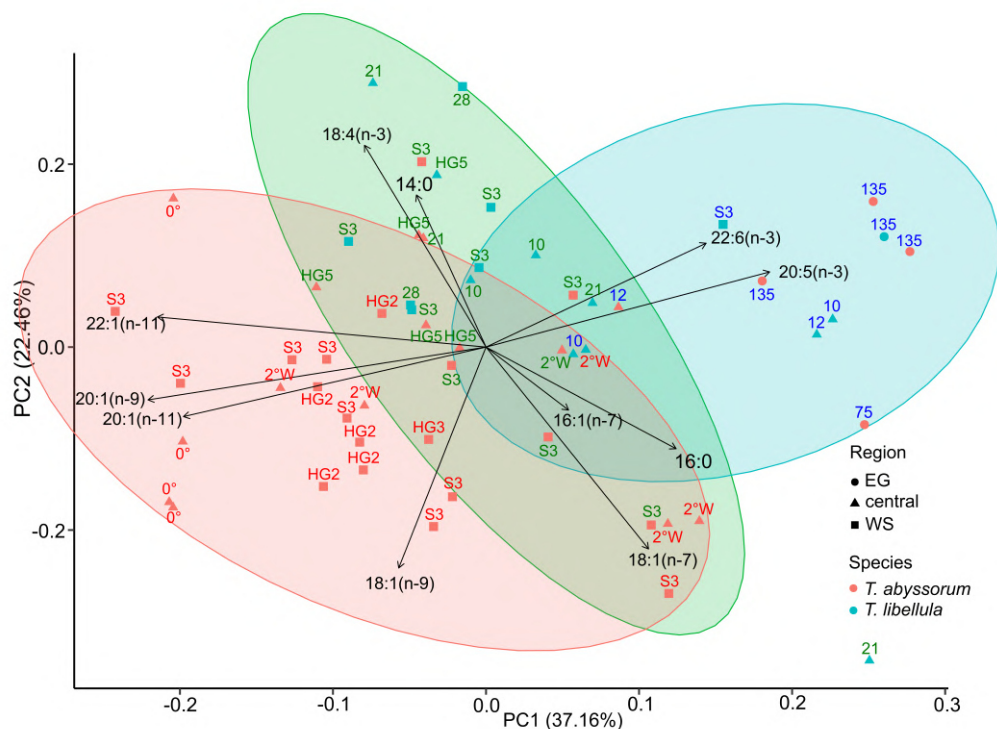
Figure 2.6: Principal component analysis of the fatty acid profiles of two *Themisto* species. Colors of symbols represent species; symbols represent areas. Numbers and text above symbols indicate stations. Colors of station labels represent cluster affiliation.

$(R = 0.783, p = 0.007)$ and between WS and the central region $(R = 0.241, p = 0.011)$ were also significant.

SIMPER analysis showed that for *Eukrohnia* sp. 16:1(n-7) ($p = 0.002, 18\%$), 22:1(n-11) ($p = 0.002, 16\%$), 20:5(n-3) ($p = 0.012, 11\%$), 20:1(n-9) ($p = 0.005, 9\%$), 18:4(n-3) ($p = 0.03, 8\%$) and 18:1(n-9) ($p = 0.006, 5\%$) significantly contributed to the differentiation between WS and EG. For *T. longicaudata*, 16:1(n-7) ($p = 0.001, 20\%$), 18:1(n-9) ($p = 0.001, 15\%$) and 20:1(n-5) ($p = 0.045, 4\%$) were significant fatty acids for the separation between regions.

2.3.4 Carnivory Index

The carnivory index (CI) demonstrated a consistent increase from the EG region to the WS region in all species outlined in Table 2.1. The largest increase was found in the amphipod *T. libellula*, from EG (0.10) to the central region (0.46), followed by the eupausiid *T. longicaudata* from EG (0.37) to WS (0.59) and the amphipod *T. abyssorum* from EG (0.32) to WS (0.56). The increase was less pronounced in the three *Calanus* species (Table 2.1).

Calanus spp. showed the lowest mean CIs of all species, ranging from 0.07 (*C. hyperboreus* in EG) to 0.21 (*C. finmarchicus* in WS). Within the genus, *C. finmarchicus* had the highest values in each region, followed by *C. glacialis*, while *C. hyperboreus* showed the lowest values. Mean CIs for *Paraeuchaeta* species ranged from 0.35 (*P. glacialis* in EG) to 0.59 (*P. norvegica* in WS) with maxima in each region detected for *P. norvegica*. *P. glacialis* showed lowest values in each region. CIs for *Themisto* species ranged from 0.19 (single value, *T. libellula* in EG) to 0.56 (*T. abyssorum* in WS). Between species, *T. abyssorum* generally had higher values, except for the central region, where *T. libelulla* showed a slightly higher mean CI.

2.3.5 Stable isotopes

For *Calanus* spp., *Paraeuchaeta* spp. and *T. libellula*, $\delta^{13}C'$ generally increased from EG to WS, whereas $\delta^{15}N$ decreased (Figure 2.7, Table 2.1). In *T. abyssorum* the trend was the same for $\delta^{13}C'$, but highest values of $\delta^{15}N$ were observed in the central region followed by values in the EG. For *T. longicaudata*, $\delta^{13}C'$ did not show the increasing trend from EG to WS, but values were comparable in both regions. Slightly higher isotope ratios were found in the central area (Figure 2.7, Table 2.1).

Between species, highest mean $\delta^{13}C'$ ratios were observed in *Themisto abyssorum* (-21.6‰ $\pm$ 0.6) and *T. libellula* (-21.0‰ $\pm$ 1.0) in the WS region (Table 2.1, Figure 2.6). Lowest values occurred in *C. glacialis* in the EG region (-26.1‰, -25.5‰). Highest mean $\delta^{15}N$ ratios were determined in *P. glacialis* in the EG area (11.2‰ $\pm$ 1.2) and lowest values occurred in *C. hyperboreus* in the WS (5.1‰ $\pm$ 1.6).

Calanus spp. showed similar mean $\delta^{13}C'$ values among species across Fram Strait, ranging from -26.1‰ (*C. glacialis*) in the EG to -23.6‰ $\pm$ 1.0 (*C. hyperboreus*) in the WS. *C. glacialis* had higher $\delta^{15}N$ than *C. hyperboreus* in EG and WS, values in the central region were similar.

Paraeuchaeta spp. depicted similar $\delta^{13}C'$ in WS and small differences in the central region,
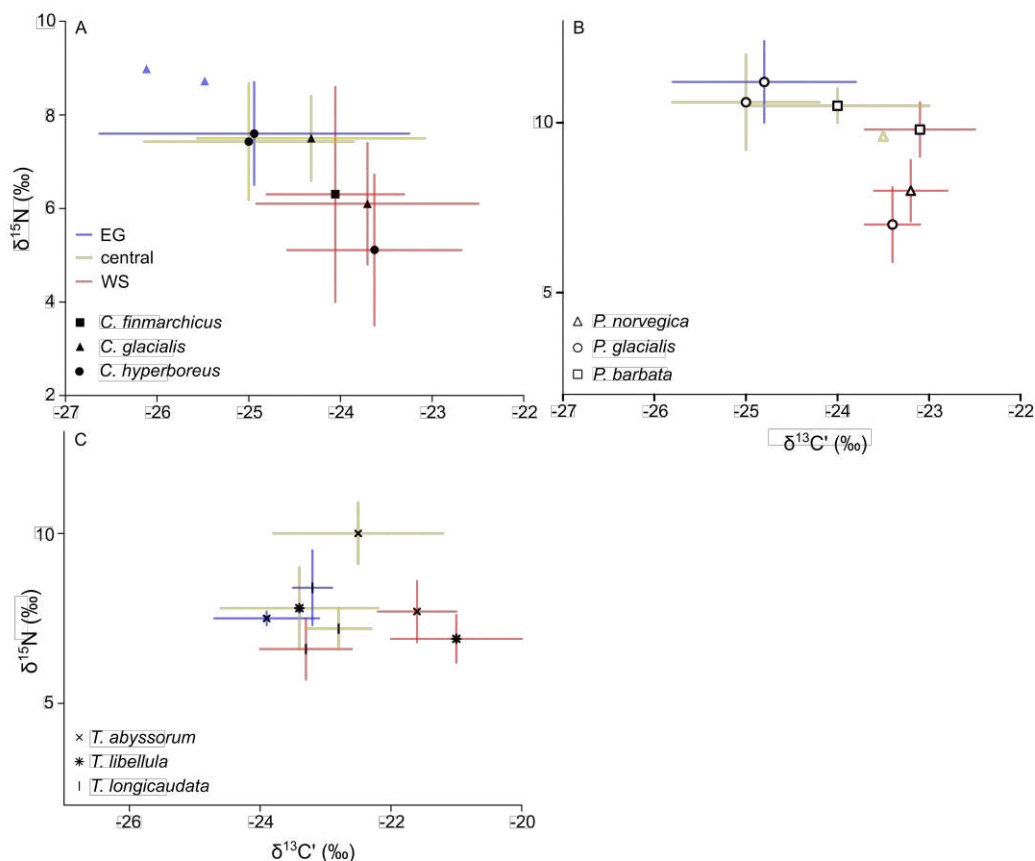
Figure 2.7: Isotope ratios $\delta^{13}C'$ and $\delta^{15}N$ of dominant zooplankton species across Fram Strait. (A) *Calanus* spp., (B) *Paraeuchaeta* spp., (C) *Themisto* spp. and *Thysanoessa longicaudata*. Symbols indicate species, colors represent regions. For n $\geq$ 3, mean and standard deviation are plotted.

where *P. glacialis* had lower values compared to the other two species. $\delta^{15}N$ values were similar between the species in the central region. In the WS, *P. barbata* had highest $\delta^{15}N$, *P. norvegica* showed intermediate and *P. glacialis* lowest values.

Both *Themisto* species had comparable $\delta^{13}C'$ in the WS region, while values were slightly lower in *T. libellula* in the central region. $\delta^{15}N$ values were always higher in *T. abyssorum* than in *T. libellula* (no measurements for *T. libelulla* in EG).

2.4 Discussion

In this study we combined several methodologies to present an integrated picture of differences in pelagic food web patterns across Arctic and Atlantic influenced regions in Fram Strait. Metabarcoding was applied to determine the different phytoplankton community compositions. This technique has demonstrated its value in the detection and identification even of rare and cryptic species, revealing a greater number of species compared to morphological analyses (Andersson et al. 2023). While the presence or absence of species is crucial for monitoring, quantitative data

become essential for assessments of species turnover in the course of climate change. The quantitative interpretation of metabarcoding results is still challenging and an area of ongoing research (Aylagas et al. 2018; Martin et al. 2022; Zimmermann et al. 2015). Despite potential accuracy limitations, quantitatively interpreting metabarcoding data can yield valuable insights (Lamb et al. 2019). In the current study, amplicon sequences variant (ASV) reads of different phytoplankton taxa were thus interpreted in a semi-quantitative way, i.e. depicting relative contributions and revealing differences between regions rather than treating reads as absolute numbers.

For the determination of zooplankton food web dynamics, trophic biomarkers were utilized. Fatty acid and stable isotope analyses have emerged as important tools in food web studies, providing detailed insights into trophic interactions and dietary preferences (Massing et al. 2022; Schukat et al. 2014; Søreide et al. 2013). While the FATM approach is comparably robust across different regions, variations in stable isotope ratios at the base of the food web occur even on small spatial scales (Massing et al. 2022). Therefore, it is essential to incorporate a regional baseline in isotopic research to effectively compare trophic positions across different systems (Grey 2006; Post 2002). Unfortunately, no such baseline is available for the three regions in the current study. Nevertheless, a consistent trend of isotope ratios of different zooplankton taxa was observed. Specifically, higher $\delta^{13}C'$ values were generally found in the WS area, while higher $\delta^{15}N$ values were observed in the EG region. These higher $\delta^{15}N$ ratios in zooplankton taxa from the EG region might be explained by source water originating from the Pacific (Jones et al. 2008), which is significantly enriched in $\delta^{15}N_{NO3}$ (Brown et al. 2015). Thus, algae incorporate higher quantities of heavier ^{15}N, which leads to an increased accumulation of ^{15}N up the food chain.

2.4.1 Regional differences in pelagic food webs across Fram Strait

The current study highlights considerable regional differences in phytoplankton communities and food web structures across Fram Strait from the Arctic influenced, cold and partly ice-covered western region to the Atlantic influenced, warm- and open-watered eastern region.

At the basis of the food web, differences in phytoplankton communities can be associated with different oceanographic regimes. The dominance of pelagic species of Chaetocerotanae (Bacillariophyta, diatoms) in the EG region is characteristic for polar algal communities in the presence of sea ice and could be an indicator of (facultative) ice algae (Søreide et al. 2006; Spies 1987). This is further supported by higher numbers of *Fragilariopsis cylindrus*, a common sea ice diatom, and *Micromonas polaris*, which is a dominant green algae in the Arctic (Bachy et al. 2022; Metfies et al. 2016). In the WS region, the diatom community changed to a dominance of Thalassiosirales (*Thalassiosira* spp. and *Skeletonema* spp.) and Bacillariales (mainly *Fragilariopsis sublineata*), while *Chloroparvula* spp. and Bathycoccaceae became more important among the Chlorophyta. Further, Haptophyta generally showed an increase in overall contribution towards the east, which is in accordance with studies reporting high abundances of *Phaeocystis* in the Atlantic influenced part of Fram Strait (Metfies et al. 2016; Nöthig et al. 2015).

Potential impacts of these regional differences in phytoplankton community composition were also detected by trophic biomarkers. In the polar region of the East Greenland Current, the food web was largely based on diatoms. This was especially evident of primarily herbivorous *Calanus* species, where diatom FATMs comprised up to 50% of TFA. The significance of diatoms in the diet of *Calanus* in the Arctic is in line with previous studies (Cleary et al. 2017; Falk-Petersen et al. 2009; Søreide et al. 2006). Those studies primarily highlighted the relevance of diatoms during early year spring blooms, whereas our findings extend this to later in the year.

The measured signals of FATMs are not necessarily representative of current conditions, but could also be an insight into feeding habits earlier in the season, due to a time lag from ingestion to incorporation (Graeve et al. 2005). Feeding experiments show that in *C. finmarchicus* fatty acid patterns could be replaced within six weeks (Graeve et al. 1994), while in *C. hyperboreus* lipids were exchanged within eleven days (Graeve et al. 2005). The high lipid contents do not suggest starvation of *Calanus* during the time of sampling. Thus, together with the observed rather quick incorporation times, we assume that the diatom signal is relatively recent and reflects active feeding conditions during the summer/autumn period.

Diatom FATMs also dominated in higher trophic levels in the EG region, such as *Eukrohnia* sp. (37% TFA), *Themisto* spp. (37 − 39% TFA), *Paraeuchaeta glacialis* (38% TFA) and *Thysanoessa longicaudata* (26% TFA), which could partly be a result of indirect assimilation through predation on herbivorous zooplankton. However, the comparably low levels of carnivory indices and *Calanus* FATMs of all species in the EG region might indicate limited ingestion of diatoms through prey and suggests, at least to some extent, direct feeding on diatoms. Direct assimilation of diatoms/phytoplankton has been indicated for Arctic *Eukrohnia hamata* (Grigor et al. 2020) and juvenile *Themisto* species (Havermans et al. 2019; Noyon et al. 2012). Individuals of *T. libellula* and *T. abyssorum* which were caught in EG were rather small (see low DM, Table 2.1), corresponding with DMs reported for juveniles (Auel and Werner 2003). The results highlight the importance of diatom-based production in the Arctic even for omnivorous species. For *Paraeuchaeta* direct feeding on algae is unlikely as they are strictly carnivorous, exclusively feeding on motile prey (Olsen et al. 2000).

In the region influenced by the West Spitsbergen Current, the food web was more diverse, involving a higher degree of flagellates and omni-/carnivory. In *Calanus* spp., an increase in the carnivory index coincided with low diatom signals in the Barents Sea (Kohlbach et al. 2021) and is in line with the higher CIs in *Calanus* species, when diatom FATMs are low in this study. *C. glacialis* is flexible in its diet, being able to switch to omnivory when phytoplankton production is low (Cleary et al. 2017; Søreide et al. 2008) and *C. finmarchicus* feeds extensively on heterotrophic protists during post-bloom conditions (Levinsen et al. 2000).

While elevated levels of carnivory markers could indicate feeding on mixo- or heterotrophic dinoflagellates (Graeve et al. 1994; Mansour et al. 1999), autotrophic *Phaeocystis* also contain high amounts of 18:1(n-9) (Dalsgaard et al. 2003; Hamm and Rousseau 2003), challenging the

applicability of this FA as a carnivory marker, when *Phaeocystis* production is high. Although its nutritional value is discussed, *Calanus* species can feed extensively on *Phaeocystis* (Estep et al. 1990; Søreide et al. 2008). Increased levels of 18:1(n-9) in *Calanus* in the WS region are thus possibly a combination of grazing on *Phaeocystis* and/or a more omnivorous diet. The ability of *Calanus* to efficiently feed on colonial or single cell *Phaeocystis* could be of importance in future Arctic scenarios, where an increase in frequency and expansion of *Phaeocystis* blooms with ongoing climate change and associated Atlantification/warming are predicted (Nöthig et al. 2015; Orkney et al. 2020).

Diatoms did not contribute considerably to the FATM patterns in higher trophic levels in the WS region, instead, carnivory and *Calanus* markers became of substantial relevance. The increased dietary importance of *Calanus* in the WS can be explained by the high abundances of *C. finmarchicus* in this region (Hirche et al. 1991; Nöthig et al. 2015; Svensen et al. 2011). High abundances of *C. finmarchicus* associated with Atlantic water could therefore become of greater importance to the diet of higher trophic levels in a warming Arctic. *C. finmarchicus* is smaller and less lipid-rich than its Arctic congeners, *C. hyperboreus* and *C. glacialis* and thus of less nutritional value for predators (Daase et al. 2021). However, high abundances and rapid population turnover of *C. finmarchicus* possibly result in high population lipid production, despite smaller size of individuals and could therefore be a valuable energy source for higher trophic levels (Renaud et al. 2018). Yet, this species shift may be disadvantageous for larger predators, such as the little auk (*Alle alle*), which are highly dependent on the larger *Calanus* species (Balazy et al. 2023; Kwaśniewski et al. 2010).

The dietary spectra of zooplankton in central Fram Strait, situated between the EG and WS regions, was variable between stations and within species. This variation is likely due to the dynamic and turbulent hydrographic conditions (Hattermann et al. 2016; Kawasaki and Hasumi 2016; von Appen et al. 2018), which in turn impact on zooplankton dynamics (Kaiser et al. 2021).

In summary, the regions across Fram Strait were characterized by distinct differences in their respective trophodynamics. The polar western side of Fram Strait showed a food web heavily reliant on diatom production. In contrast, the eastern Atlantic side exhibited more diverse trophic patterns, indicated by a higher proportion of flagellates and *Calanus* in the diet of zooplankton taxa. Consequently, our first hypothesis, which proposed that the Arctic and Atlantic influenced areas in Fram Strait would demonstrate significant differences in their food web structures, should be accepted. The results further emphasize the high nutritional flexibility of all analyzed zooplankton species in this region.

2.4.2 Role of ice algae

Ice algae play a crucial role in Arctic food webs and sympagic-pelagic-benthic coupling (Koch et al. 2023; Søreide et al. 2013). Especially during early spring, their blooms trigger and sustain reproduction and development of nauplii for many Arctic key species (Søreide et al. 2008; Søreide

et al. 2010). Fernández-Méndez et al. (2015) suggested that the warming-induced thinning of sea ice and the associated increase in light levels might extend the productive period of under-ice algae. During the time of sampling for the current study in July/August, $\delta^{13}C'$ values of all zooplankton taxa in the EG region were rather low, lower than in the WS and lower than values measured by Hobson et al. 1995 and Søreide et al. 2006 at stations located in this region. When the dietary input of ice algae is high, enriched $\delta^{13}C$ ratios are expected (Hobson et al. 2002). This apparent deviation from the expectation requires further research.

Yet, the applicability of $\delta^{13}C$ as an universal comprehensive pan-Arctic baseline for differentiation between pelagic and ice-based diets has been questioned (de la Vega et al. 2019; Leu et al. 2020; Søreide et al. 2006). Similar values of pelagic and ice-POM have been reported for the North Water Polynya and Canada Basin (Iken et al. 2005; Tremblay et al. 2006), emphasizing potential regional problems for this marker. Additionally, facultative ice algae, such as the diatom *Chaetoceros* spp., generally have isotopic values similar to those of pelagic algae (Søreide et al. 2006). These facultative ice algae can be dominant in snow-ice interface regimes (Fernández-Méndez et al. 2018). Consequently, the dominance of diatom FATMs across all zooplankton taxa in the EG region, along with the significant presence of Chaetocerotanae and sea ice diatoms (*Fragilariopsis cylindrus*), could indicate a more pronounced utilization of ice-associated diatom species, despite the low $\delta^{13}C$ ratios.

Our second hypothesis, stating that ice algae are increasingly grazed upon by zooplankton in the EG region, can neither be accepted, nor rejected. While the low $\delta^{13}C$ ratios may contradict an increased utilization of ice algae, high levels of diatom FATMs in zooplankton and the contribution of sea ice-associated algae to the community could suggest an increased importance of (facultative) ice algae for the food web in the Arctic influenced region of Fram Strait.

2.4.3 Ecological niches of congeners

The occupation of distinct niches plays a crucial role in facilitating the coexistence of ecologically and functionally similar species. Niche differentiation minimizes competition between species for essential resources such as food and habitat. As the Arctic environment continues to change, polar species may find themselves increasingly sharing their ecosystem with Atlantic invaders. It remains unclear, if a co-existence between Arctic and Atlantic congeners is possible, or whether the ecological niches are too similar, eventually leading to the exclusion of the less adapted species. In the current study, congeners of Arctic and boreal-Atlantic origin of *Calanus*, *Paraeuchatea* and *Themisto* were analyzed to assess similarities or differences in their dietary niches in regions of co-occurrence.

Between the Arctic congeners, *C. glacialis* showed a slightly higher trophic position than *C. hyperboreus* in each region. This in line with several studies, which suggest a more omnivorous diet for *C. glacialis*, at least during phases of low diatom availability (Cleary et al. 2017; Kunisch et al. 2023; Søreide et al. 2008). The opportunistic feeding of *C. glacialis* may prove

advantageous in a shifting Arctic system with an increased flagellate abundance (Ardyna et al. 2020; Nöthig et al. 2015). However, with an increasing Atlantification of the system, another competitor, the Atlantic congener *C. finmarchicus*, will become more abundant in Arctic systems. Of the three *Calanus* species, *C. finmarchicus* was the most omnivorous species in our study. This is in agreement with a high degree of omnivory reported for *C. finmarchicus* by Ohman and Runge (1994) and Yeh et al. (2020). When comparing the three species, *C. finmarchicus* and *C. glacialis* potentially occupy more similar trophic niches in the WS indicated by similar FA and SI profiles. In fact, environmental niches of *C. glacialis* and *C. finmarchicus* in two Svalbard fjords overlap almost completely (Weydmann-Zwolicka et al. 2022). Thus, competition pressure could be higher on *C. glacialis* in a future Arctic regime due to its pronounced ecological similarity to a potentially better adapted *C. finmarchicus* (Kaiser et al. 2022).

Vertical habitat partitioning is a significant factor in reducing inter-specific competition among species of *Themisto* and *Paraeuchaeta*. *T. abyssorum* and *P. barbata* both exhibit a deeper distribution ranges than their congeners (Auel and Hagen 2005; Dalpadado et al. 2001; Laakmann et al. 2009), which reflects in differences in diet and their higher trophic position. Such a distinct niche separation might allow boreal-Atlantic *T. abyssorum* and Arctic *T. libellula* to co-exist. Recent observations, however, indicate a decline in *T. libellula* populations in Fram Strait, while *T. abyssorum* is becoming more abundant (Havermans et al. 2019). However, this trend may be more related to the reduction of sea ice and the resulting loss of its associated food web, rather than due to competitive pressure by the boreal expatriate. *T. libellula* is more dependent on the cryo-pelagic pathways than *T. abyssorum*, which has a wider prey spectrum (Auel et al. 2002; Dalpadado 2002; Kohlbach et al. 2016; Noyon et al. 2009). Consequently, the shrinking sea ice habitat due to climate change could be a significant factor affecting the distribution range of *T. libellalu*.

Our study indicates that juveniles of both *Themisto* species exhibit a greater reliance on phytoplankton, particularly diatoms, as a nutritional source, compared to the adults. This suggests that in their early life stages the two species may occupy more similar ecological niches, which would mean increased competitive pressure among *Themisto* juveniles.

In contrast to the bathypelagic *P. barbata*, *P. norvegica* and *P. glacialis* are both epi- to mesopelagic species. Similar to the *Calanus* species, they are usually regionally separated in Fram Strait, with the boreal-Atlantic *P. norvegica* closely linked to the warmer WSC, while the polar *P. glacialis* is more commonly found in polar waters (Laakmann et al. 2009). With rising temperatures and ongoing Atlantification, the Arctic environment may become more habitable to boreal species, potentially leading to the more frequent co-occurrence of Arctic and boreal Atlantic species. In regions where *P. glacialis* and *P. norvegica* co-occur, our study indicated an overlap in dietary spectra, which may be attributed to their similar vertical distribution and hence access to the same prey. It is uncertain, whether this co-existence can be sustained, or if it will lead to the exclusion of one species.

Our third hypothesis, stating that sister species occupy distinct ecological niches, can only

partly be accepted, as it varies between different congener-pairs. Niches were distinctly different for the adult *Themisto* species, between *P. barbata* and its congeners, as well as between *C. hyperboreus* and its two sister species. A more pronounced overlap of dietary niches is indicated for *C. glacialis* and *C. finmarchicus* as well as for *P. glacialis* and *P. norvegica*.

2.5   Summary and conclusion

The current study provides an insight into Arctic and Atlantic influenced food webs across Fram Strait during late summer. It emphasizes the importance of diatoms in the Arctic ice-covered part of Fram Strait and shows a tendency towards a flagellate-based food web with a higher degree of omnivory in the Atlantic regime. The ability especially of Arctic species to rely on alternative food sources other than autotrophic diatoms becomes important with Atlantification and a corresponding potential increase in flagellate production in the future Arctic Ocean. Besides regional differences, the observed dietary variations were influenced by factors such as life stage and vertical distribution. We further provide a potential prospect of stronger inter-specific competition among polar and expanding boreal-Atlantic congeners in a future Arctic environment. We predict an increasing dietary overlap between *C. glacialis* and *C. finmarchicus* as well as between *P. glacialis* and *P. norvegica* in areas of co-occurrence.

Finally, the flexibility of zooplankton species to efficiently shift between diatom- and flagellate-dominated resources could be associated with seasonal requirements. In case of *Calanus*, during late summer/early autumn, reproductive processes had essentially ceased and large lipid depots (wax esters) had already been accumulated in preparation for diapause at depth. If a shift towards a flagellate-dominated diet during early-season production, coinciding with the onset of reproduction, can sustain dietary demands remains unclear and requires further investigation.

2.6   Funding

2.7 Acknowledgments

2.8 Supplementary material

Table S2.1: Overview of total lipids, mean fatty acid and wax ester percentages, stable isotope ratios and carnivory indices (± standard deviation) for zooplankton taxa across Fram Strait. EG: East Greenland Current region; WS: West Spitsbergen Current region; DM: dry mass; TL: total lipid; WE: wax ester; TFA: total fatty acids; TFAlc: total fatty alcohols. Measurements of different years (2016, 2017, 2019) and developmental stages (C5 and C6 females) are pooled.

| | *Aetideopsis rostrata* | | *Gaetanus brevispinus* | | *Apherusa glacialis* | | |
	central	WS	central	WS	EG	central	WS
DM [mg ind^{-1}]	1.0, 0.8	0.7	0.7 ± 0.3	1.1 ± 0.6	4.3 ± 1.5	7.1 ± 2.9	
TL [% DM]	23.5, 26.2	26.9	23.3 ± 6.7	28.3 ± 5.3	41.6 ± 2.7	34.9	
WE [% TL]	8.4, 12.3	12.6	53.0 ± 6.5	48.2 ± 3.9	-	-	
n	2	1	5	3	5	3	0
Fatty acids [% TFA]							
14:0	3.2, 3.0	2.1	1.9 ± 0.5	1.9 ± 0.4	3.2 ± 0.3	3.3 ± 0.8	
14:1(n-5)	0.1, 0.0	-	0.1 ± 0.1	0.2 ± 0.0	-	-	
iso 15:0	0.3, 0.3	0.3	0.1 ± 0.1	0.2 ± 0.0	-	-	
15:1(n-5)	-	-	-	-	-	-	
16:0	14.6, 11.4	10.2	6.9 ± 1.2	7.0 ± 0.8	13.9 ± 1.3	13.8 ± 0.2	
16:1(n-9)	0.3, 0.2	0.4	0.1 ± 0.1	0.2 ± 0.1	-	-	
16:1(n-7)	4.7, 6.3	6.5	14.2 ± 10.1	5.0 ± 1.7	45.6 ± 3.3	42.3 ± 4.6	
16:1(n-5)	0.5, 0.4	0.3	0.1 ± 0.1	0.2 ± 0.0	0.2 ± 0.0	0.2 ± 0.0	
iso 17:0	0.3, 0.2	-	0.6 ± 0.4	0.7 ± 0.4	0.2 ± 0.0	0.2 ± 0.0	
ante iso 17:0	0.1, 0.0	-	-	-	0.1 ± 0.1	0.0 ± 0.1	
16:2(n-4)	0.3, 0.3	-	0.3 ± 0.3	0.1 ± 0.2	0.7 ± 0.4	1.0 ± 0.0	
Phytanic acid	0.1, 0.1	-	0.3 ± 0.2	0.2 ± 0.2	-	-	
17:0	0.3, 0.2	-	0.1 ± 0.1	0.2 ± 0.1	-	-	
16:3(n-4)	0.9, 0.5	0.4	0.7 ± 0.2	0.8 ± 0.1	0.6 ± 0.2	0.7 ± 0.0	
17:1(n-7)	-	-	-	-	-	-	
branched 18:0	0.4, 0.4	0.3	0.1 ± 0.1	0.1 ± 0.1	-	-	
16:4(n-1)	.	-	0.1 ± 0.2	0.2 ± 0.0	1.5 ± 0.2	2.1 ± 0.3	
18:0	0.8, 0.6	0.7	0.5 ± 0.1	0.7 ± 0.1	0.8 ± 0.2	0.8 ± 0.1	
18:1(n-11)	-	0.4	-	-	-	-	
18:1(n-9)	12.6, 10.7	9.1	22.1 ± 5.7	30.7 ± 3.0	7.5 ± 0.9	7.4 ± 1.7	
18:1(n-7)	3.4, 3.9	3.0	4.8 ± 1.6	3.6 ± 0.4	2.6 ± 0.5	2.1 ± 0.4	
18:1(n-5)	1.3, 1.1	1.0	0.6 ± 0.2	0.7 ± 0.1	0.0 ± 0.1	-	
18:2(n-6)	1.5, 1.4	1.2	1.8 ± 0.4	1.9 ± 0.3	1.0 ± 0.3	0.9 ± 0.3	
18:2(n-4)	-	-	0.1 ± 0.1	-	-	-	
18:3(n-6)	-	-	0.2 ± 0.2	-	0.8 ± 0.2	0.8 ± 0.2	
18:3(n-3)	-	0.6	0.8 ± 0.2	0.7 ± 0.5	0.4 ± 0.3	0.4 ± 0.3	
18:4(n-3)	1.3, 1.4	1.1	1.9 ± 0.6	1.8 ± 0.2	1.7 ± 0.2	3.1 ± 0.5	
20:0	0.1, 0.0	-	0.9 ± 0.3	1.1 ± 0.2	-	-	
20:1(n-11)	0.7, 0.8	1.3	0.6 ± 0.2	0.7 ± 0.1	0.0 ± 0.1	-	
20:1(n-9)	6.2, 9.9	12.1	2.8 ± 0.8	2.6 ± 0.2	1.3 ± 0.9	1.3 ± 1.0	
20:1(n-7)	0.6, 1.2	1.0	0.3 ± 0.2	0.2 ± 0.1	0.8 ± 0.3	0.6 ± 0.1	
20:1(n-5)	0.2, 0.1	0.4	-	-	-	-	
20:4(n-6)	0.4, 0.4	0.4	0.3 ± 0.2	0.3 ± 0.0	0.4 ± 0.1	0.4 ± 0.1	
20:4(n-3)	0.8, 0.8	0.6	0.9 ± 0.3	0.9 ± 0.1	0.5 ± 0.0	0.7 ± 0.0	
20:5(n-3)	11.3, 10.1	9.6	13.9 ± 1.2	13.1 ± 0.4	13.4 ± 1.2	14.8 ± 0.9	
22:0	0.4, 0.2	-	0.0 ± 0.0	0.3 ± 0.2	-	-	
22:1(n-11)	6.0, 10.3	13.8	2.2 ± 0.8	1.5 ± 0.3	0.6 ± 0.6	0.5 ± 0.6	
22:1(n-9)	1.5, 2.6	3.0	0.3 ± 0.2	0.4 ± 0.1	0.3 ± 0.2	0.2 ± 0.2	
22:1(n-7)	0.2, 0.3	0.3	0.1 ± 0.1	-	0.1 ± 0.1	-	
22:1(n-5)	-	-	-	-	-	-	
22:2(n-6)	-	-	-	-	-	-	
22:5(n-3)	0.6, 0.8	0.8	0.4 ± 0.3	0.8 ± 0.1	0.0 ± 0.1	-	
24:1(n-11)	-	-	0.2 ± 0.4	-	-	-	
24:1(n-9)	3.5, 3.0	2.5	1.4 ± 0.8	1.8 ± 0.2	-	-	
22:6(n-3)	19.5, 16.0	16.5	17.0 ± 6.8	18.1 ± 2.1	1.5 ± 0.1	2.2 ± 0.5	

	Aetideopsis rostrata		Gaetanus brevispinus		Apherusa glacialis		
	central	WS	central	WS	EG	central	WS
Fatty alcohols [% TFAlc]							
14:0	5.4, 1.9	-	24.1 ± 7.0	23.1 ± 1.3	-	-	
16:0	14.0, 4.3	7.9	30.8 ± 3.2	34.6 ± 3.0	-	-	
16:1	-	-	0.8 ± 1.2	0.2 ± 0.2	-	-	
18:0	2.1, 0.0	-	0.9 ± 0.6	0.8 ± 0.6	-	-	
18:1(n-7)	2.6, 0.0	-	15.1 ± 6.2	11.4 ± 1.3	-	-	
20:1(n-11)	-	-	-	-	-	-	
20:1(n-9)	17.9, 24.9	26.4	10.3 ± 2.5	10.3 ± 0.6	-	-	
20:1(n-7)	-	-	2.5 ± 0.4	2.1 ± 0.7	-	-	
22:1(n-11)	46.0, 59.0	60.3	9.3 ± 4.7	6.5 ± 1.3	-	-	
22:1(n-9)	8.9, 9.9	5.5	4.8 ± 2.6	8.0 ± 3.1	-	-	
22:1(n-7)	-	-	0.4 ± 0.5	1.3 ± 0.9	-	-	
Stable Isotopes							
n	1	1	0	9	6	3	1
$\delta^{13}C'$	-22.7	-22.9	-	-23.2 ± 0.6	-22.6 ± 1.5	-22.8 ± 0.5	-21.8
$\delta^{15}N$	11.8	9.6	-	8.5 ± 1.0	7.5 ± 0.5	6.3 ±	

	Cyclocaris sp.		Thysanoessa inermis	Hymenodora glacialis	
	central	WS	EG	central	WS
DM [mg ind^{-1}]	3.5, 6.7	34.6, 13.7	44.2 ± 12.2	12.9 ± 6.0	4.6, 102.7
TL [% DM]	46.8, 42.9	43.9, 17.9	44.1 ± 3.2	36.3 ± 7.2	56.2, 41.7
WE [% TL]	60.5, 73.3	a34.1, 34.8	27.1 ± 3.2	70.3 ± 12.9	87.2, 89.8
n	2	2	7	4	2
Fatty acids [% TFA]					
14:0	2.4, 3.2	1.0, 3.1	2.5 ± 0.5	3.1 ± 1.7	2.3, 3.8
14:1(n-5)	0.0, 0.2	0.0, 0.2	0.1 ± 0.0	0.1 ± 0.1	0.0, 0.4
iso 15:0	-	0.0, 0.2	0.1 ± 0.1	0.2 ± 0.1	-
15:1(n-5)	-	-	-	-	-
16:0	6.7, 6.1	7.1, 11.2	17.4 ± 0.9	4.6 ± 0.9	3.5, 3.1
16:1(n-9)	-	0.2, 0.2	0.1 ± 0.1	0.5 ± 0.2	0.4, 0.0
16:1(n-7)	8.4, 6.7	9.9, 6.9	9.4 ± 5.9	12.1 ± 2.8	14.1, 11.9
16:1(n-5)	-	0.1, 0.4	0.2 ± 0.0	0.3 ± 0.1	0.3, 0.3
iso 17:0	-	-	0.2 ± 0.2	-	-
ante iso 17:0	-	-	0.1 ± 0.2	-	-
16:2(n-4)	0.0, 0.4	-	0.6 ± 0.1	0.2 ± 0.3	-
Phytanic acid	-	-	-	-	-
17:0	-	-	-	-	-
16:3(n-4)	-	0.4, 0.5	0.4 ± 0.2	0.5 ± 0.1	0.8, 0.8
17:1(n-7)	-	-	-	-	-
branched 18:0	-	0.2, 0.3	0.2 ± 0.1	0.1 ± 0.1	-
16:4(n-1)	-	0.3, 0.0	0.6 ± 0.2	-	-
18:0	0.6, 0.6	0.9, 0.9	1.7 ± 0.3	0.8 ± 0.3	0.4, 1.1
18:1(n-11)	0.9, 0.0	1.8, 0.5	0.1 ± 0.2	2.0 ± 2.6	6.8, 0.0
18:1(n-9)	12.4, 12.8	27.6, 18.5	13.9 ± 6.1	21.7 ± 8.0	36.2, 23.9
18:1(n-7)	1.6, 1.3	4.7, 1.9	8.9 ± 3.2	3.4 ±1.0	3.7, 3.3
18:1(n-5)	0.7, 0.7	0.9, 1.1	0.1 ± 0.1	1.0 ± 0.1	1.0, 0.8
18:2(n-6)	2.1, 1.9	1.5, 1.7	2.4 ± 1.0	1.9 ± 0.5	2.4, 1.7
18:2(n-4)	-	-	0.2 ± 0.1	-	-
18:3(n-6)	-	-	-	-	-
18:3(n-3)	0.9, 0.9	0.7, 0.8	1.4 ± 0.3	0.8 ± 0.2	1.0, 1.1
18:4(n-3)	12.3, 13.0	0.7, 2.2	7.1 ± 3.1	0.9 ± 0.7	0.0, 3.2
20:0	-	-	-	0.2 ± 0.2	0.5, 0.5
20:1(n-11)	3.4, 2.1	8.8, 2.8	0.1 ± 0.1	2.3 ± 1.0	3.8, 2.1
20:1(n-9)	11.6, 12.5	11.4, 8.6	1.7 ± 0.5	12.2 ± 3.4	6.8, 12.6
20:1(n-7)	1.3, 1.2	1.9, 0.7	0.2 ± 0.1	1.1 ± 0.5	0.6, 1.0
20:1(n-5)	-	0.2, 0.0	-	-	-
20:4(n-6)	0.6, 0.5	0.5, 0.9	0.6 ± 0.1	0.2 ± 0.2	-
20:4(n-3)	1.1, 1.6	0.4, 0.6	0.5 ± 0.2	0.8 ± 0.3	0.9, 0.9
20:5(n-3)	7.1, 8.7	4.7, 10.9	19.5 ± 2.0	5.5 ± 1.0	4.2, 6.3
22:0	-	-	-	-	-
22:1(n-11)	11.4, 10.5	7.4, 8.2	1.0 ± 0.5	12.6 ± 5.0	4.0, 12.4
22:1(n-9)	2.9, 4.2	2.0, 1.2	0.2 ± 0.1	2.1 ± 1.2	0.5, 1.9
22:1(n-7)	-	0.2, 0.0	-	0.1 ± 0.2	-
22:1(n-5)	-	-	-	-	-
22:2(n-6)	-	-	-	-	-
22:5(n-3)	1.0, 0.9	0.0, 0.6	0.1 ± 0.1	-	-

	Cyclocaris sp.		*Thysanoessa inermis*	*Hymenodora glacialis*	
	central	WS	EG	central	WS
Fatty acids [% TFA]					
24:1(n-11)	-	-	-	-	-
24:1(n-9)	0.0, 0.6	0.2, 0.7	0.1 ± 0.1	0.5 ± 0.3	-
22:6(n-3)	10.7, 8.4	3.8, 13.5	7.7 ± 1.3	8.0 ± 2.5	6.0, 6.8
Fatty alcohols [% TFAlc]					
14:0	4.4, 4.6	1.4, 6.8	35.6 ± 2.9	2.0 ± 1.3	1.2, 1.7
16:0	6.3, 6.1	6.2, 11.2	49.1 ± 4.1	9.8 ± 1.6	11.3, 8.5
16:1	0.7, 0.6	1.0, 0.9	8.5 ± 4.0	1.0 ± 0.4	1.6, 0.7
18:0	0.0, 0.7	1.5, 1.4	0.1 ± 0.2	1.5 ± 0.3	1.4, 1.5
18:1(n-7)	0.8, 1.2	2.6, 1.0	0.0 ± 0.1	2.3 ± 1.1	2.8, 1.7
20:1(n-11)	-	-	-	2.5 ± 2.9	6.9, 0.0
20:1(n-9)	25.0, 25.3	21.2, 29.4	3.0 ± 1.0	20.0 ± 3.4	15.0, 23.5
20:1(n-7)	1.6, 1.5	2.3, 0.0	-	1.5 ± 1.4	0.9, 1.1
22:1(n-11)	51.0, 49.9	45.6, 43.6	3.7 ± 2.5	33.4 ± 12.5	15.1, 47.4
22:1(n-9)	8.5, 10.3	8.3, 3.2	-	5.5 ± 2.5	2.0, 6.0
22:1(n-7)	-	2.3, 0.0	-	0.6 ± 1.0	-
Stable Isotopes					
n	1	0	6	3	2
$\delta^{13}C'$	-21.9	-	-22.7 ± 0.7	-22.2 ± 0.3	-22.4, -21.9
$\delta^{15}N$	11.9	-	7.7 ± 0.5	9.9 ± 0.3	10.0, 8.7

	Ostracoda		Atolla sp.	Clione limacina
	central	WS	central	central
DM [mg ind-1]	0.8 ± 0.2	1.0, 0.9	86.3, 76.3	24.2 ± 8.2
TL [% DM]	24.4 ± 3.3	26.0, 30.4	3.7, 2.3	17.6 ± 6.5
WE [% TL]	39.9 ± 4.9	32.4, 46.8	20.0, 31.9	-
n	4	2	2	5
Fatty acids [% TFA]				
14:0	1.7 ± 0.6	1.4, 1.9	1.0, 1.6	2.2 ± 0.2
14:1(n-5)	0.1 ± 0.1	-	-	0.1 ± 0.1
iso 15:0	0.2 ± 0.0	0.0, 0.2	0.3, 0.3	0.5 ± 0.1
15:1(n-5)	-	-	-	-
16:0	9.7 ± 1.1	11.0, 10.5	13.6, 12.6	10.3 ± 1.2
16:1(n-9)	0.0 ± 0.1	0.0, 0.2	0.0, 0.2	0.2 ± 0.1
16:1(n-7)	17.7 ± 3.0	16.0, 12.7	5.4, 5.4	7.6 ± 0.7
16:1(n-5)	0.5 ± 0.0	0.4, 0.4	0.0, 0.2	0.2 ± 0.1
iso 17:0	0.1 ± 0.2	-	0.7, 0.6	0.7 ± 0.2
ante iso 17:0	-	-	0.5, 0.0	0.5 ± 0.6
16:2(n-4)	0.2 ± 0.2	0.0, 0.3	0.0, 0.5	0.2 ± 0.1
Phytanic acid	-	-	-	-
17:0	0.0 ± 0.1	-	0.5, 0.4	3.0 ± 0.4
16:3(n-4)	0.3 ± 0.2	0.4, 0.3	0.0, 0.2	7.9 ± 4.3
17:1(n-7)	-	-	-	1.8 ± 3.5
branched 18:0	0.1 ± 0.1	0.2, 0.2	1.1, 1.1	0.8 ± 0.1
16:4(n-1)	0.1 ± 0.1	0.0, 0.3	-	-
18:0	1.8 ± 0.3	2.2, 2.0	4.3, 4.4	1.4 ± 0.2
18:1(n-11)	0.1 ± 0.2	0.4, 0.0	0.9, 0.2	0.1 ± 0.1
18:1(n-9)	15.5 ± 1.5	19.5, 16.0	6.6, 7.1	2.3 ± 0.3
18:1(n-7)	2.2 ± 0.2	2.1, 2.2	1.8, 1.6	2.6 ± 0.2
18:1(n-5)	0.5 ± 0.0	0.4, 0.4	2.1, 1.7	0.3 ± 0.1
18:2(n-6)	1.2 ± 0.1	0.9, 1.2	1.0, 0.9	0.8 ± 0.2
18:2(n-4)	-	-	-	-
18:3(n-6)	-	-	0.0, 0.3	0.1 ± 0.1
18:3(n-3)	0.8 ± 0.2	0.7, 0.7	0.0, 0.5	0.6 ± 0.5
18:4(n-3)	4.0 ± 0.9	2.7, 5.7	0.6, 2.4	2.6 ± 0.8
20:0	-	-	-	-
20:1(n-11)	2.1 ± 0.4	2.6, 2.3	0.4, 0.7	0.8 ± 0.1
20:1(n-9)	9.1 ± 1.3	8.5, 12.3	4.6, 3.8	1.7 ± 0.2
20:1(n-7)	0.4 ± 0.1	0.0, 0.4	7.2, 6.3	2.1 ± 0.3
20:1(n-5)	-	-	-	0.2 ± 0.1
20:4(n-6)	0.4 ± 0.0	0.0, 0.3	1.4, 1.5	1.1 ± 0.2
20:4(n-3)	0.7 ± 0.1	0.6, 0.8	0.5, 0.8	0.7 ± 0.1
20:5(n-3)	7.0 ± 0.9	5.9, 6.5	20.7, 20.7	12.8 ± 0.9

	Ostracoda		Atolla sp.	Clione limacina
	central	**WS**	**central**	**central**
Fatty acids [% TFA]				
22:6(n-3)	11.5 ± 2.3	12.3, 7.3	3.9, 6.1	27.8 ± 3.7
Fatty alcohols [% TFAlc]				
22:0	-	-	-	-
22:1(n-11)	9.6 ± 1.6	9.8, 11.2	4.5, 4.1	-
22:1(n-9)	1.0 ± 0.1	0.8, 1.3	1.4, 0.7	-
22:1(n-7)	-	-	-	-
22:1(n-5)	-	-	-	0.2 ± 0.1
22:2(n-6)	-	-	-	-
22:5(n-3)	-	0.0, 0.5	14.1, 12.4	0.4 ± 0.2
24:1(n-11)	-	-	-	-
24:1(n-9)	1.1 ± 0.1	1.1, 0.9	0.6, 0.5	-
14:0	8.8 ± 2.1	8.0, 3.7	8.7, 8.0	-
16:0	13.3 ± 1.9	13.7, 8.2	13.7, 15.4	-
16:1	1.3 ± 0.9	0.0, 0.8	0.0, 1.2	-
18:0	0.3 ± 0.6	0.0, 1.2	-	-
18:1(n-7)	1.2 ± 0.7	0.0, 0.9	16.8, 18.8	-
20:1(n-11)	-	-	-	-
20:1(n-9)	26.7 ± 1.6	29.0, 34.4	16.7, 17.4	-
20:1(n-7)	0.7 ± 1.2	-	2.3, 1.2	-
22:1(n-11)	42.0 ± 6.4	47.6, 44.9	23.6, 27.4	-
22:1(n-9)	3.9 ± 0.3	1.8, 4.6	11.2, 4.8	-
22:1(n-7)	-	-	-	-
Stable Isotopes [‰]				
n	3	1	1	1
$\delta^{13}C'$	-22.3 ± 0.6	-22.4	-23.4	-22.9
$\delta^{15}N$	9.8 ± 0.4	9.1	10.5	6.5
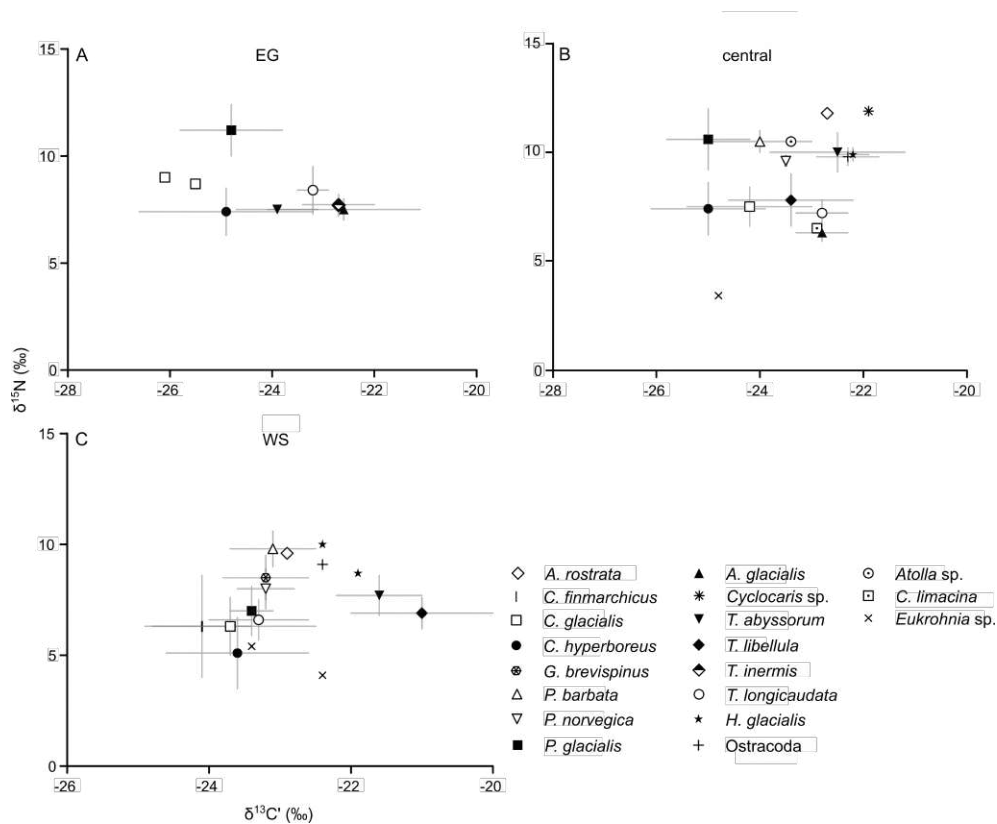
Figure S2.1: Isotope ratios $\delta^{13}C'$ and $\delta^{15}N$ of zooplankton species across Fram Strait. (A) EG (B) central and (C) WS. Symbols indicate species. For $n \geq 3$, mean and standard deviation are plotted.

References

Andersson, A, Zhao, L, Brugel, S, Figueroa, D, and Huseby, S (2023). Metabarcoding vs microscopy: comparison of methods to monitor phytoplankton communities. *Environ Sci Technol* 3, 2671–2680.

Ardyna, M, Mundy, CJ, Mills, MM, Oziel, L, Grondin, P-L, Lacour, L, Verin, G, Van Dijken, GL, Ras, J, Alou-Font, E, Babin, M, Gosselin, M, Tremblay, J-É., Raimbault, P, Assmy, P, Nicolaus, M, Claustre, H, and Arrigo, KR (2020). Environmental drivers of under-ice phytoplankton bloom dynamics in the Arctic Ocean. *Elem Sci Anth* 8. Edited by Deming, JW, 30.

Auel, H and Hagen, W (2005). Body mass and lipid dynamics of Arctic and Antarctic deep-sea copepods (Calanoida, *Paraeuchaeta*): ontogenetic and seasonal trends. *Deep-Sea Res I* 52, 1272–1283.

Auel, H, Harjes, M, Da Rocha, R, Stübing, D, and Hagen, W (2002). Lipid biomarkers indicate different ecological niches and trophic relationships of the Arctic hyperiid amphipods *Themisto abyssorum* and *T. libellula*. *Polar Biol* 25, 374–383.

Auel, H and Werner, I (2003). Feeding, respiration and life history of the hyperiid amphipod *Themisto libellula* in the Arctic marginal ice zone of the Greenland Sea. *J Exp Mar Bio Ecol* 296, 183–197.

Aylagas, E, Borja, Á., Muxika, I, and Rodríguez-Ezpeleta, N (2018). Adapting metabarcoding-based benthic biomonitoring into routine marine ecological status assessment networks. *Ecol Indic* 95, 194–202.

Bachy, C, Sudek, L, Choi, C, Eckmann, C, Nöthig, E-M, Metfies, K, and Worden, A (2022). Phytoplankton surveys in the Arctic Fram Strait demonstrate the tiny eukaryotic alga *Micromonas* and other picoprasinophytes contribute to deep sea export. *Microorganisms* 10, 961.

Balazy, K, Trudnowska, E, Wojczulanis-Jakubas, K, Jakubas, D, Præbel, K, Choquet, M, Brandner, MM, Schultz, M, Bitz-Thorsen, J, Boehnke, R, Szeligowska, M, Descamps, S, Strøm, H, and Błachowiak-Samołyk, K (2023). Molecular tools prove little auks from Svalbard are extremely selective for *Calanus glacialis* even when exposed to Atlantification. *Sci Rep* 13, 13647.

Beszczynska-Möller, A, Fahrbach, E, Schauer, U, and Hansen, E (2012). Variability in Atlantic water temperature and transport at the entrance to the Arctic Ocean, 1997–2010. *ICES Mar Sci Symp* 69, 852–863.

Bode, M, Hagen, W, Schukat, A, Teuber, L, Fonseca-Batista, D, Dehairs, F, and Auel, H (2015). Feeding strategies of tropical and subtropical calanoid copepods throughout the eastern Atlantic Ocean – latitudinal and bathymetric aspects. *Prog Oceanogr* 138, 268–282.

Brown, ZW, Casciotti, KL, Pickart, RS, Swift, JH, and Arrigo, KR (2015). Aspects of the marine nitrogen cycle of the Chukchi Sea shelf and Canada Basin. *Deep-Sea Res II* 118, 73–87.

Callahan, BJ, McMurdie, PJ, Rosen, MJ, Han, AW, Johnson, AJA, and Holmes, SP (2016). DADA2: High-resolution sample inference from Illumina amplicon data. *Nat Methods* 13, 581–583.

Clarke, KR and Gorley, RN (2006). *PRIMER v6: User Manual/Tutorial (Plymouth Routines in Multivariate Ecological Research). PRIMER-E, PlymoutH*. Version 6.

Cleary, AC, Søreide, JE, Freese, D, Niehoff, B, and Gabrielsen, TM (2017). Feeding by *Calanus glacialis* in a high arctic fjord: potential seasonal importance of alternative prey. *ICES Mar Sci Symp* 74, 1937–1946.

Daase, M, Berge, J, Søreide, JE, and Falk-Petersen, S (2021). Ecology of Arctic pelagic communities. *Arctic Ecology*. Edited by Thomas, DN, 231–259.

Dalpadado, P, Borkner, N, Bogstad, B, and Mehl, S (2001). Distribution of *Themisto* (Amphipoda) spp. in the Barents Sea and predator-prey interactions. *ICES Mar Sci Symp* 58, 876–895.

Dalpadado, Padmini (2002). Inter-specific variations in distribution, abundance and possible life-cycle patterns of *Themisto* spp. (Amphipoda) in the Barents Sea. *Polar Biol* 25, 656–666.

Dalsgaard, J, St. John, M, Kattner, G, Müller-Navarra, D, and Hagen, W (2003). Fatty acid trophic markers in the pelagic marine environment. *Advances in Mar Biol* 46, 225–340.

De la Vega, C, Jeffreys, RM, Tuerena, R, Ganeshram, R, and Mahaffey, C (2019). Temporal and spatial trends in marine carbon isotopes in the Arctic Ocean and implications for food web studies. *Glob Change Biol* 25, 4116–4130.

De Steur, L, Hansen, E, Gerdes, R, Karcher, M, Fahrbach, E, and Holfort, J (2009). Freshwater fluxes in the East Greenland Current: a decade of observations. *Geophys Res Lett* 36, 2009GL041278.

England, MR, Eisenman, I, Lutsko, NJ, and Wagner, TJW (2021). The recent emergence of Arctic amplification. *Geophys Res Lett* 48, e2021GL094086.

Estep, KW, Nejstgaard, JC, Skjoldal, HR, and Rey, F (1990). Predation by copepods upon natural populations of *Phaeocystis pouchetii* as a function of the physiological state of the prey. *Mar Ecol Prog Ser* 67, 235–249.

Falk-Petersen, S, Mayzaud, P, Kattner, G, and Sargent, JR (2009). Lipids and life strategy of Arctic *Calanus*. *Mar Biol Research* 5, 18–39.

Fernández-Méndez, M, Katlein, C, Rabe, B, Nicolaus, M, Peeken, I, Bakker, K, Flores, H, and Boetius, A (2015). Photosynthetic production in the central Arctic Ocean during the record sea-ice minimum in 2012. *Biogeosciences* 12, 3525–3549.

Fernández-Méndez, M, Olsen, LM, Kauko, HM, Meyer, A, Rösel, A, Merkouriadi, I, Mundy, CJ, Ehn, JK, Johansson, AM, Wagner, PM, Ervik, Å., Sorrell, BK, Duarte, P, Wold, A, Hop, H, and Assmy, P (2018). Algal hot spots in a changing Arctic Ocean: sea-ice ridges and the snow-ice interface. *Front Mar Sci* 5, 75.

Ferraro, M, Giordani, P, and Serafini, A (2019). fclust: An R package for fuzzy clusterinG. *RStudio, PBC* 11.

Folch, J, Lees, M, and Sloane Stanley, GH (1957). A simple method for the isolation and purification of total lipid from animal tissues. *Journal of Biological Chemistry* 226, 497–509.

Graeve, M, Albers, C, and Kattner, G (2005). Assimilation and biosynthesis of lipids in Arctic *Calanus* species based on feeding experiments with a ^{13}C labelled diatom. *J Exp Mar Bio Ecol* 317, 109–125.

Graeve, M, Kattner, G, and Hagen, W (1994). Diet-induced changes in the fatty acid composition of Arctic herbivorous copepods: experimental evidence of trophic markers. *J Exp Mar Bio Ecol* 182, 97–110.

Grey, J (2006). The use of stable isotope analyses Iin freshwater ecology: current awareness. *Pol J Ecol* 54, 563–584.

Grigor, JJ, Schmid, MS, Caouette, M, St.-Onge, V, Brown, TA, and Barthélémy, R-M (2020). Non-carnivorous feeding in Arctic chaetognaths. *Prog Oceanogr* 186, 102388.

Groisillier, A, Massana, R, Valentin, K, Vaulot, D, and Guillou, L (2006). Genetic diversity and habitats of two enigmatic marine alveolate lineages. *Aquat Microb Ecol* 42, 277–291.

Guillou, L, Bachar, D, Audic, S, Bass, D, Berney, C, Bittner, L, Boutte, C, Burgaud, G, De Vargas, C, Decelle, J, Del Campo, J, Dolan, JR, Dunthorn, M, Edvardsen, B, Holzmann, M, Kooistra, WHCF, Lara, E, Le Bescot, N, Logares, R, Mahé, F, Massana, R, Montresor, M, Morard, R, Not, F, Pawlowski, J, Probert, I, Sauvadet, A-L, Siano, R, Stoeck, T, Vaulot, D, Zimmermann, P, and Christen, R (2012). The Protist Ribosomal Reference database (PR2): a catalog of unicellular eukaryote small sub-unit rRNA sequences with curated taxonomy. *Nucleic Acids Res* 41, D597–D604.

Guillou, L, Viprey, M, Chambouvet, A, Welsh, RM, Kirkham, AR, Massana, R, Scanlan, DJ, and Worden, AZ (2008). Widespread occurrence and genetic diversity of marine parasitoids belonging to *Syndiniales* (Alveolata). *Environ Microbiol* 10, 3349–3365.

Hagen, W (2000). Lipids. *ICES Zooplankton Methodology Manual*. Edited by Harris, R, Wiebe, P, Lenz, J, Skjøldal, H, and Huntley, M. San Diego: Academic Press, 113–119.

Hagen, W and Auel, H (2001). Seasonal adaptations and the role of lipids in oceanic zooplankton. *Zoology* 104, 313–326.

Hamm, CE and Rousseau, V (2003). Composition, assimilation and degradation of *Phaeocystis globosa*-derived fatty acids in the North Sea. *J Sea Res* 50, 271–283.

Hattermann, TE, Isachsen, PE, Von Appen, W-J, Albretsen, J, and Sundfjord, A (2016). Eddy-driven recirculation of Atlantic Water in Fram Strait. *Geophys Res Lett* 43, 3406–3414.

Havermans, C, Auel, H, Hagen, W, Held, C, Ensor, NS, and Tarling, G (2019). Predatory zooplankton on the move: *Themisto* amphipods in high-latitude marine pelagic food webs. *Advances in Mar Biol* 82, 51–92.

Hirche, H-J, Baumann, MEM, Kattner, G, and Gradinger, R (1991). Plankton distribution and the impact of copepod grazing on primary production in Fram Strait, Greenland Sea. *J Mar Syst* 2, 477–494.

Hobson, KA, Ambrose Jr, WG, and Renaud, PE (1995). Sources of primary production, benthic-pelagic coupling, and trophic relationships within the Northeast Water Polynya: insights from $\delta^{13}C$ and $\delta^{15}N$ analysis. *Mar Ecol Prog Ser* 128, 1–10.

Hobson, KA, Fisk, A, Karnovsky, N, Holst, M, Gagnon, J-M, and Fortier, M (2002). A stable isotope ($\delta^{13}C$, $\delta^{15}N$) model for the North Water food web: implications for evaluating tropho-dynamics and the flow of energy and contaminants. *Deep-Sea Res II* 49, 5131–5150.

Iken, K, Bluhm, Ba, and Gradinger, R (2005). Food web structure in the high Arctic Canada Basin: evidence from $\delta^{13}C$ and $\delta^{15}N$ analysis. *Polar Biol* 28, 238–249.

Jones, EP, Anderson, LG, Jutterström, S, and Swift, JH (2008). Sources and distribution of fresh water in the East Greenland Current. *Prog Oceanogr* 78, 37–44.

Kaiser, P, Hagen, W, Bode-Dalby, M, and Auel, H (2022). Tolerant but facing increased competition: Arctic zooplankton versus Atlantic invaders in a warming ocean. *Front Mar Sci* 9, 908638.

Kaiser, P, Hagen, W, von Appen, W-J, Niehoff, N, Hildebrandt, N, and Auel, H (2021). Effects of a submesoscale oceanographic filament on zooplankton dynamics in the Arctic marginal ice zone. *Front Mar Sci* 8, 625395.

Kanzow, T (2017). The expedition PS100 of the research vessel *Polarstern* to the Fram Strait in 2016. *Reports on Polar and Marine Research, Alfred Wegener Institute for Polar and Marine Research* 705, 175 pp.

Kattner, G and Fricke, H SG (1986). Simple gas-liquid chromatographic method for the simultaneous determination of fatty acids and alcohols in wax esters of marine organisms. *J Chromatogr A* 361, 263–268.

Kattner, G and Hagen, W (1995). Polar herbivorous copepods — different pathways in lipid biosynthesis. *ICES Mar Sci Symp* 52, 329–335.

Kawasaki, T and Hasumi, H (2016). The inflow of Atlantic water at the Fram Strait and its inter-annual variability. *J Geophys Res Oceans* 121, 502–519.

Koch, CW, Brown, TA, Amiraux, R, Ruiz-Gonzalez, C, MacCorquodale, M, Yunda-Guarin, GA, Kohlbach, D, Loseto, LL, Rosenberg, B, Hussey, NE, Ferguson, SH, and Yurkowski, DJ (2023). Year-round utilization of sea ice-associated carbon in Arctic ecosystems. *Nat Commun* 14, 1964.

Kohlbach, D, Graeve, M, A Lange, B, David, C, Peeken, I, and Flores, H (2016). The importance of ice algae-produced carbon in the central Arctic Ocean ecosystem: food web relationships revealed by lipid and stable isotope analyses: ice algal carbon in Arctic food web. *Limnol Oceanogr* 61, 2027–2044.

Kohlbach, D, Hop, H, Wold, A, Schmidt, K, Smik, L, Belt, ST, Keck Al-Habahbeh, A, Woll, M, Graeve, M, Dąbrowska, AM, Tatarek, A, Atkinson, A, and Assmy, P (2021). Multiple trophic markers trace dietary carbon sources in Barents Sea zooplankton during late summer. *Front Mar Sci* 7, 610248.

Kortsch, S, Primicerio, R, Aschan, M, Lind, S, Dolgov, AV, and Planque, B (2019). Food-web structure varies along environmental gradients in a high-latitude marine ecosystem. *Ecography* 42, 295–308.

Kunisch, EH, Graeve, M, Gradinger, R, Flores, H, Varpe, Ø, and Bluhm, BA (2023). What we do in the dark: prevalence of omnivorous feeding activity in Arctic zooplankton during polar night. *Limnol Oceanogr*, 1853–1851.

Kwaśniewski, S, Gluchowska, M, Jakubas, D, Wojczulanis-Jakubas, K, Walkusz, W, and Karnovsky, N (2010). The impact of different hydrographic conditions and zooplankton communities on provisioning little auks along the west coast of Spitsbergen. *Prog Oceanogr* 87, 72–82.

Laakmann, S, Kochzius, M, and Auel, H (2009). Ecological niches of Arctic deep-sea copepods: vertical partitioning, dietary preferences and different trophic levels minimize inter-specific competition. *Deep-Sea Res I* 56, 741–756.

Lamb, PD, Hunter, E, Pinnegar, JK, Creer, S, Davies, RG, and Taylor, MI (2019). How quantitative is metabarcoding: a meta-analytical approach. *Mol Ecol* 28, 420–430.

Leu, E, Brown, TA, Graeve, M, Wiktor, J, Hoppe, CJM, Chierici, M, Fransson, A, Verbiest, S, Kvernvik, AC, and Greenacre, MJ (2020). Spatial and temporal variability of ice algal trophic markers - with recommendations about their application. *JMSE* 8, 676.

Levinsen, H, Turner, JT, Nielsen, TG, and Hansen, BW (2000). On the trophic coupling between protists and copepods in arctic marine ecosystems. *Mar Ecol Prog Ser* 204, 65–77.

Lim, SM, Payne, CM, Van Dijken, GL, and Arrigo, KR (2022). Increases in Arctic sea ice algal habitat, 1985–2018. *Elem Sci Anth* 10, 00008.

Mańko, MK, Gluchowska, M, and Weydmann-Zwolicka, A (2020). Footprints of Atlantification in the vertical distribution and diversity of gelatinous zooplankton in the Fram Strait (Arctic Ocean). *Prog Oceanogr* 189, 102414.

Mansour, MP, Volkman, JK, Jackson, AE, and Blackburn, SI (1999). The fatty acid and sterol composition of five marine dinoflagellates. *J Phycol* 35, 710–720.

Martin, JL, Santi, I, Pitta, P, John, U, and Gypens, N (2022). Towards quantitative metabarcoding of eukaryotic plankton: an approach to improve 18S rRNA gene copy number bias. *Metabarcoding Metagenomics* 6, e85794.

Martin, M (2011). Cutadapt removes adapter sequences from high-throughput sequencing reads. *EMBnet journal* 17, 10–12.

Massing, JC, Schukat, A, Auel, H, Auch, D, Kittu, L, Pinedo Arteaga, EL, Correa Acosta, J, and Hagen, W (2022). Toward a solution of the "Peruvian Puzzle": pelagic food-web structure and trophic interactions in the northern Humboldt Current upwelling system off Peru. *Front Mar Sci* 8, 759603.

Metfies, K (2020). The expedition PS121 of the research vessel *Polarstern* to the Fram Strait in 2019. *Reports on Polar and Marine Research, Alfred Wegener Institute for Polar and Marine Research* 738, 95 pp.

Metfies, K, Hessel, J, Klenk, R, Petersen, W, Wiltshire, KH, and Kraberg, A (2020). Uncovering the intricacies of microbial community dynamics at Helgoland Roads at the end of a spring bloom using automated sampling and 18S meta-barcoding. *PLoS ONE* 15, e0233921.

Metfies, K, von Appen, W-J, Kilias, E, Nicolaus, A, and Nöthig, E-M (2016). Biogeography and photosynthetic biomass of Arctic marine pico-eukaroytes during summer of the record sea ice minimum 2012. *PLoS ONE* 11, e0148512.

Mintenbeck, K, Brey, T, Jacob, U, Knust, R, and Struck, U (2008). How to account for the lipid effect on carbon stable-isotope ratio ($\delta^{13}C$): sample treatment effects and model bias. *J Fish Biol* 72, 815–830.

Nöthig, E-M, Bracher, A, Engel, A, Metfies, K, Niehoff, B, Peeken, I, Bauerfeind, E, Cherkasheva, Alexandra, Gäbler-Schwarz, Steffi, Hardge, Kristin, Kilias, Estelle, Kraft, A, Mebrahtom Kidane, Yohannes, Lalande, C, Piontek, J, Thomisch, K, and Wurst, M (2015). Summertime plankton ecology in Fram Strait—a compilation of long- and short-term observations. *Polar Res* 34, 23349.

Noyon, M, Gasparini, S, and Mayzaud, P (2009). Feeding of *Themisto libellula* (Amphipoda Crustacea) on natural copepods assemblages in an Arctic fjord (Kongsfjorden, Svalbard). *Polar Biol* 32, 1559–1570.

Noyon, M, Narcy, F, Gasparini, S, and Mayzaud, P (2012). Ontogenic variations in fatty acid and alcohol composition of the pelagic amphipod *Themisto libellula* in Kongsfjorden (Svalbard). *Mar Biol* 159, 805–816.

Ohman, MD and Runge, JA (1994). Sustained fecundity when phytoplankton resources are in short supply: omnivory by *Calanus finmarchicus* in the Gulf of St. Lawrence. *Limnol Oceanogr* 39, 21–36.

Oksanen, J, Simpson, GL, Guillaume Blanchet, F, Kindt, R, Legendre, P, Minchin, PR, O'Hara, RB, Solmyos, P, Stevens, MHH, Szoecs, E, Wagner, H, Barbour, M, Bedward, M, Bolker, B, Borcard, D, Carvalho, G, Chirico, M, De Caceres, M, Durand, S, Evangelista, HBA, FritzJohn, R, Friendly, M, Furneaux, B, Hannigan, G, Hill, MO, Lahti, L, McGlinn, D, Ouellette, MH, Cunha, ER, Smith, T, Stier, A, Ter Braak, CJF, and Weedon, J (2022). *vegan: Community Ecology PackagE R package version 2.6-4. https://CRAN.R-projecTorg/package=vegan*.

Olsen, EM, Jørstad, T, and Kaartvedt, S (2000). The feeding strategies of two large marine copepods. *J Plankton Res* 22, 1513–1528.

Orkney, A, Platt, T, Narayanaswamy, BE, Kostakis, I, and Bouman, HA (2020). Bio-optical evidence for increasing *Phaeocystis* dominance in the Barents Sea. *Phil Trans R Soc A* 378, 20190357.

Oziel, L, Baudena, A, Ardyna, M, Massicotte, P, Randelhoff, A, Sallée, J-B, Ingvaldsen, RB, Devred, E, and Babin, M (2020). Faster Atlantic currents drive poleward expansion of temperate phytoplankton in the Arctic Ocean. *Nat Commun* 11, 1705.

Pecuchet, L, Blanchet, M-A, Frainer, A, Husson, B, Jørgensen, LL, Kortsch, S, and Primicerio, R (2020). Novel feeding interactions amplify the impact of species redistribution on an Arctic food web. *Glob Change Biol* 26, 4894–4906.

Peters, J, Dutz, J, and Hagen, W (2007). Role of essential fatty acids on the reproductive success of the copepod *Temora longicornis* in the North Sea. *Mar Ecol Prog Ser* 341, 153–163.

Polyakov, IV, Pnyushkov, AV, Alkire, MB, Ashik, I M, Baumann, TM, Carmack, EC, Goszczko, Ilona, Guthrie, John, Ivanov, Vladimir V, Kanzow, T, Krishfield, R, Kwok, R, Sundfjord, A, Morison, J, Rember, R, and Yulin, A (2017). Greater role for Atlantic inflows on sea-ice loss in the Eurasian Basin of the Arctic Ocean. *Sci* 356, 285–291.

Post, DM (2002). Using stable isotopes to estimate trophic position: models, methods, and assumptions. *Ecology* 83, 703–718.

Previdi, M, Smith, KL, and Polvani, LM (2021). Arctic amplification of climate change: a review of underlying mechanisms. *Environ Res Lett* 16, 093003.

Priest, T, von Appen, W-J, Oldenburg, E, Popa, O, Torres-Valdés, S, Bienhold, C, Metfies, K, Boulton, W, Mock, T, Fuchs, BM, Amann, R, Boetius, A, and Wietz, M (2023). Atlantic water influx and sea-ice cover drive taxonomic and functional shifts in Arctic marine bacterial communities. *ISME J* 17, 1612–1625.

Rantanen, M, Karpechko, AY, Lipponen, A, Nordling, K, Hyvärinen, O, Ruosteenoja, K, Vihma, T, and Laaksonen, A (2022). The Arctic has warmed nearly four times faster than the globe since 1979. *Commun Earth Environ* 3, 168.

Renaud, PE, Daase, M, Banas, NS, Gabrielsen, TM, Søreide, JE, and Varpe, Ø (2018). Pelagic food-webs in a changing Arctic: a trait-based perspective suggests a mode of resilience. *ICES J Mar Sci* 75, 1871–1881.

Rey, F, Noji, TT, and Miller, LA (2000). Seasonal phytoplankton development and new production in the central Greenland Sea. *Sarsia* 85, 329–344.

Richardson, K, Markager, S, Buch, E, Lassen, MF, and Kristensen, AS (2005). Seasonal distribution of primary production, phytoplankton biomass and size distribution in the Greenland Sea. *Deep-Sea Res I* 52, 979–999.

Schewe, I (2018). The expedition PS107 of the research vessel *Polarstern* to the Fram Strait and the AWI-HAUSGARTEN in 2017. *Reports on Polar and Marine Research, Alfred Wegener Institute for Polar and Marine Research* 717, 120 pp.

Schukat, A, Auel, H, Teuber, L, Lahajnar, N, and Hagen, W (2014). Complex trophic interactions of calanoid copepods in the Benguela upwelling system. *J Sea Res* 85, 186–196.

Serreze, MC and Barry, RG (2011). Processes and impacts of Arctic amplification: a research synthesis. *Glob Planet Change* 77, 85–96.

Smith, WO, Codispoti, LA, Nelson, DM, Manley, T, Buskey, EJ, Niebauer, HJ, and Cota, GF (1991). Importance of *Phaeocystis* blooms in the high-latitude ocean carbon cycle. *Nat* 352, 514–516.

Smyntek, PM, Teece, MA, Schulz, KL, and Thackeray, SJ (2007). A standard protocol for stable isotope analysis of zooplankton in aquatic food web research using mass balance correction models. *Limnol Oceanogr* 52, 2135–2146.

Soltwedel, T, Bauerfeind, E, Bergmann, M, Bracher, A, Budaeva, N, Busch, K, Cherkasheva, A, Fahl, K, Grzelak, K, Hasemann, C, Jacob, M, Kraft, A, Lalande, C, Metfies, K, Nöthig, E-M, Meyer, K, Quéric, N-V, Schewe, I, Włodarska-Kowalczuk, M, and Klages, M (2016). Natural variability or anthropogenically-induced variation? Insights from 15 years of multidisciplinary observations at the arctic marine LTER site HAUSGARTEN. *Ecol Indic* 65, 89–102.

Søreide, JE, Carroll, ML, Hop, H, Ambrose, WG, Hegseth, EN, and Falk-Petersen, S (2013). Sympagic-pelagic-benthic coupling in Arctic and Atlantic waters around Svalbard revealed by stable isotopic and fatty acid tracers. *Mar Biol Research* 9, 831–850.

Søreide, JE, Falk-Petersen, S, Hegseth, EN, Hop, H, Carroll, ML, Hobson, KA, and Blachowiak-Samolyk, K (2008). Seasonal feeding strategies of *Calanus* in the high-Arctic Svalbard region. *Deep-Sea Res II* 55, 2225–2244.

Søreide, JE, Hop, H, Carroll, ML, Falk-Petersen, S, and Hegseth, EN (2006). Seasonal food web structures and sympagic–pelagic coupling in the European Arctic revealed by stable isotopes and a two-source food web model. *Prog Oceanogr* 71, 59–87.

Søreide, JE, Leu, E, Berge, J, Graeve, M, and Falk-Petersen, S (2010). Timing of blooms, algal food quality and *Calanus glacialis* reproduction and growth in a changing Arctic. *Glob Change Biol* 16, 3154–3163.

Spies, A (1987). Phytoplankton in the marginal ice zone of the Greenland Sea during summer, 1984. *Polar Biol* 7, 195–205.

Svensen, C, Seuthe, L, Vasilyeva, Y, Pasternak, A, and Hansen, E (2011). Zooplankton distribution across Fram Strait in autumn: Are small copepods and protozooplankton important? *Prog Oceanogr* 91, 534–544.

Tesi, T, Muschitiello, F, Mollenhauer, G, Miserocchi, S, Langone, L, Ceccarelli, C, Panieri, G, Chiggiato, J, Nogarotto, A, Hefter, J, Ingrosso, G, Giglio, F, Giordano, P, and Capotondi, L (2021). Rapid Atlantification along the Fram Strait at the beginning of the 20th century. *Sci Adv* 7, eabj2946.

Tremblay, J-É., Michel, C, Hobson, KA, Gosselin, M, and Price, NM (2006). Bloom dynamics in early opening waters of the Arctic Ocean. *Limnol Oceanogr* 51, 900–912.

Vihtakari, M, Welcker, J, Moe, B, Chastel, O, Tartu, S, and Hop, H (2018). Black-legged kittiwakes as messengers of Atlantification in the Arctic. *Sci Rep* 8, 1178.

Von Appen, W-J, Wekerle, C, Hehemann, L, Schourup-Kristensen, V, Konrad, C, and Iversen, MH (2018). Observations of a submesoscale cyclonic filament in the Marginal Ice Zone. *Geophys Res Lett* 45, 6141–6149.

Von Quillfeldt, CH (2000). Common diatom species in Arctic spring blooms: their distribution and abundance. *Bot Mar* 43, 499–516.

Wang, Q, Wekerle, C, Wang, X, Danilov, S, Koldunov, N, Sein, D, Sidorenko, D, von Appen, W-J, and Jung, T (2020). Intensification of the Atlantic water supply to the Arctic Ocean through Fram Strait induced by Arctic sea ice decline. *Geophys Res Lett* 47, e2019GL086682.

Weydmann, A, Carstensen, J, I, Goszczko, Dmoch, K, Olszewska, A, and Kwasniewski, S (2014). Shift towards the dominance of boreal species in the Arctic: inter-annual and spatial zooplankton variability in the West Spitsbergen Current. *Mar Ecol Prog Ser* 501, 41–52.

Weydmann-Zwolicka, A, Cottier, F, Berge, J, Majaneva, S, Kukliński, P, and Zwolicki, A (2022). Environmental niche overlap in sibling planktonic species *Calanus finmarchicus* and *C. glacialis* in Arctic fjords. *Ecol Evol* 12, e9569.

Yeh, HD, Questel, JM, Maas, KR, and Bucklin, A (2020). Metabarcoding analysis of regional variation in gut contents of the copepod *Calanus finmarchicus* in the North Atlantic Ocean. *Deep-Sea Res II* 180, 104738.

Zimmermann, J, Glöckner, G, Jahn, R, Enke, N, and Gemeinholzer, B (2015). Metabarcoding vs. morphological identification to assess diatom diversity in environmental studies. *Mol Ecol Resour* 15, 526–542.

References

3

Effects of a submesoscale oceanographic filament on zooplankton dynamics in the Arctic marginal ice zone

Patricia Kaiser[1], Wilhelm Hagen[1], Wilken-Jon von Appen[2], Barbara Niehoff[2], Nicole Hildebrandt[2], Holger Auel[1]

[1]Universität Bremen, BreMarE - Bremen Marine Ecology, Marine Zoology, P.O. Box 330440, 28334 Bremen, Germany

[2]Alfred Wegener Institute Helmholtz Center for Polar and Marine Research, Am Handelshafen 12, 27570 Bremerhaven, Germany

Abstract

Submesoscale structures, characterized by intense vertical and horizontal velocities, potentially play a crucial role in oceanographic dynamics and pelagic fluxes. Due to their small spatial scale and short temporal persistence, conditions for *in situ* measurements are challenging and thus the role of such structures for zooplankton distribution is still unclear. During RV *Polarstern* expedition PS107 to Arctic Fram Strait in July/August 2017, a submesoscale filament was detected, which initiated an *ad hoc* oceanographic and biological sampling campaign. To determine zooplankton taxonomic composition, horizontal and vertical distribution, abundance and biomass, vertical MultiNet hauls (depth intervals: 300-200-100-50-10-0 m) were taken at four stations across the filament. Zooplankton data were evaluated in context with the physical-oceanographic observations of the filament to assess submesoscale physical-biological interactions. Our data show that submesoscale features considerably impact zooplankton dynamics. While structuring the pelagial with distinct zooplankton communities in a vertical as well as horizontal dimension, they accumulate abundance and biomass of epipelagic species at the site of convergence. Further, high-velocity jets associated with such dynamics are possibly of major importance for species allocation and biological connectivity, accelerating for instance processes such as the 'Atlantification' of the Arctic. Thus, submesoscale features affect the surrounding ecosystem in multiple ways with consequences for higher trophic levels and biogeochemical cycles.

3.1   Introduction

Mesoscale dynamics (horizontal scale of 10 to 100 km), including fronts and eddies, have been studied extensively and, even though still not fully understood, significant knowledge about underlying oceanographic mechanisms as well as their influence on biological and biogeochemical processes has been gained (McGillicuddy 2016; McWilliams 2008). Impacts can vary widely, including the support of new production by inducing vertical mixing and thus modulating the supply of nutrients into the euphotic layer (e.g., Lee and Williams 2000; Mahadevan and Archer 2000; McGillicuddy Jr et al. 2003). Numerical studies investigating the mesoscale injection of nutrients found that estimated primary production increased by up to 30%, better matching empirical observations (Lévy et al. 2001). esides enhancing vertical velocities, mesoscale dynamics can also act as vectors of transport for organisms in a horizontal direction. Fronts have been shown to concentrate organisms at the site of convergence, creating foraging areas, which are actively sought by top predators such as birds, whales and tunas (Acha et al. 2015). Several studies further demonstrate that mesoscale eddies can serve as a vector of transport, dispersing zooplankton and larvae to oceanic regions (Batten and Crawford 2005; Mackas and Galbraith 2002), or as a retention mechanism, keeping offspring close to their spawning site (Singh et al. 2018). However, while mesoscale dynamics play a vital role for such processes, the resolution of empirical studies still

seems to be too coarse.

Finer, so-called submesoscale, dynamics have thus recently gained increasing interest among physical and biological oceanographers (Lévy et al. 2018). In contrast to mesoscale fronts and dynamics, submesoscale structures are rapidly evolving features with horizontal scales of 0.1-10 km. They are defined by a high Rossby number $\sim \geq 1$ (mesoscale: ≤ 0.1), resulting in ageostrophic circulation and associated significant vertical velocities (D'Asaro et al. 2018; Zhabin and Andreev 2019; Rossby number: horizontal velocity gradients divided by Coriolis frequency). Thus, meso- and submesoscale dynamics are different regimes and cannot be summarized as one process.

Although the existence of submesoscale motions has been acknowledged since the 1980s (McWilliams 1985), their impact was considered as weak, and computational abilities were too limited to include them in numerical simulations (Marsac et al. 2014). However, expanding computational capacities during the last decade allowed the modeling of oceanographic structures on a higher resolution. Such models highlighted the intense vertical and horizontal velocities within submesoscale dynamics and hence indicated their underestimated potential in affecting pelagic fluxes and processes (Klein et al. 2008; Klein and Lapeyre 2009).

Submesoscale structures are ubiquitous throughout the oceans and often appear between mesoscale eddies (Lévy et al. 2018; Lévy et al. 2001) or in the presence of strong horizontal gradients, for instance in the marginal ice zone (MIZ) (von Appen et al. 2018). Due to their small spatial (0.1 to 10 km) and short temporal (hours to weeks) scales, *in situ* measurements, especially the assessment of their impact on biological processes, are difficult. Recent studies utilizing satellite data to analyze the effect of submesoscale fronts on phytoplankton revealed increased chlorophyll concentrations in such regions (Guo et al. 2019; Liu and Levine 2016; Shulman et al. 2015a). The main underlying cause is presumably due to the intense vertical velocities associated with small-scale dynamics, which lead to an enhanced upward transport of nutrients (Mahadevan 2016; Mahadevan and Archer 2000). Although submesoscale processes are limited in space and time, this nutrient injection has major implications for phytoplankton productivity, as the relevant time scales are similar to those of phytoplankton growth (Mahadevan 2016). These studies emphasize the impact of submesoscale structures on phytoplankton, yet little is known about interactions between such small-scale dynamics and zooplankton ecology. Zooplankton research is still largely dependent on point sampling by net hauls from research vessels, with the distance between stations usually too coarse to resolve submesoscale features. Few studies reported elevated mesozooplankton abundances at submesoscale fronts (Ohman et al. 2012; Powell and Ohman 2015; Trudnowska et al. 2016), yet the biological and physical mechanisms supporting such accumulations are still far from understood.

During the expedition PS107 of the German research icebreaker RV *Polarstern* to the Arctic marginal ice zone in Fram Strait in July/August 2017, a submesoscale filament was detected by *in situ* observation and satellite imagery (Schewe 2018). A high-resolution *ad hoc* sampling campaign was designed, combining physical oceanographic measurements (published by von

von Appen et al. 2018) with depth stratified zooplankton sampling. The objective of the present study is to link community structure, vertical distribution and dynamics of zooplankton to physical oceanographic properties of the submesoscale filament. Specifically, we demonstrate that (1) despite the short temporal and spatial scale of submesoscale feature, the convergence of surface water results in the accumulation of epipelagic zooplankton close to the filament center; (2) distinct water masses at different depths and/or on different sides of the filament are characterized by different zooplankton communities despite the small vertical and horizontal distances; (3) mesopelagic species emerge and occur at shallower depths close to the filament center due to doming of the isopycnals in the mesopelagic layer; and (4) the along-frontal jets on both sides of the filament have the potential to act as high-speed vectors for the transport of zooplankton organisms.

3.2 Materials and methods

3.2.1 Study area and physical oceanographic characterization of the submesoscale filament

Fram Strait, between Greenland and the Svalbard Archipelago, is the only deep-water connection between the North Atlantic and the Arctic Ocean. On the eastern side, the West Spitsbergen Current (WSC) transports warm, saline water masses from the Atlantic ('Atlantic Water' – AW) northwards (von Appen et al. 2016). On the western side, the East Greenland Current (EGC) exports cold and rather fresh Polar Surface Water (PSW) and sea ice from the Arctic Ocean into the Atlantic (de Steur et al. 2009). Part of the AW flows northward into the Arctic Ocean, while the rest turns westward to 'recirculate' and subduct below the PSW (Hattermann et al. 2016). The zone in between the WSC and EGC is thus characterized by a highly dynamic and turbulent regime of mesoscale features (Kawasaki and Hasumi 2016; von Appen et al. 2018). This highly dynamic regime, together with the semi-permanent sea-ice edge (von Appen et al. 2016) and the large horizontal density gradients observed in the MIZ, may be beneficial for and contribute to the development of submesoscale features (von Appen et al. 2018).

During the expedition PS107 with the German research icebreaker RV *Polarstern*, a submesoscale filament was detected via satellite data (Figure 3.1), due to the presence of a nearly straight sea ice streak of 500 m width and 50 km length extending in northeast-southwest direction in the MIZ of Fram Strait. Extensive *in situ* oceanographic as well as biological sampling of the filament was conducted in cross-frontal direction (Schewe 2018, Figure 3.1A). The physical oceanographic structure of the filament was described in detail by von von Appen et al. (2018). The observed 'cyclonic filament' is comparable to the theoretical description of a 'dense filament' by McWilliams et al. (2009). It can be regarded as two parallel fronts between light-dense and dense-light surface waters. The flow field is characterized by geostrophically balanced cyclonic along-frontal jets and an ageostrophic secondary circulation in cross-frontal direction. Specifically, cold polar

water ($\leq 0\,^\circ$C) prevailed at the surface at distances of 6 to 8 km on both sides of the filament, while in between warmer Atlantic water ($\geq 1\,^\circ$C) dominated the uppermost layer (Figure 3.1B present study; Figs. 2a, 3b in von Appen et al. (2018)). The ageostrophic circulation resulted in convergence towards the center of the filament, accumulating and stabilizing the narrow streak of sea ice (Figure 3.1A+C). The convergence led to downwelling, subducting dense water which was evident in a depression of the 27 isopycnal at the center of the filament (Figure 3.1C). Vice versa, below 100 m depth, a doming, i.e. an upward deflection, of isopycnals was apparent, resulting in a characteristic hourglass shape of isopycnals at the filament center (with depressed isopycnals at the surface and doming ones below 100 m). Associated with this structure, strong geostrophic along-frontal jets with a maximum speed of $\geq 0.5\,\mathrm{ms^{-1}}$ in 50 to 100 m m at around 3 km distance from the center occurred on both sides of the filament (Fig. 1B+C). On the eastern side, the along-filament flow was directed northward, whereas the jet on the western side flowed southward. The temporal persistence and frequency of such filaments in the MIZ is unknown. Our best guess for the time period over which the sampled submesoscale filament persisted is one to a few weeks.
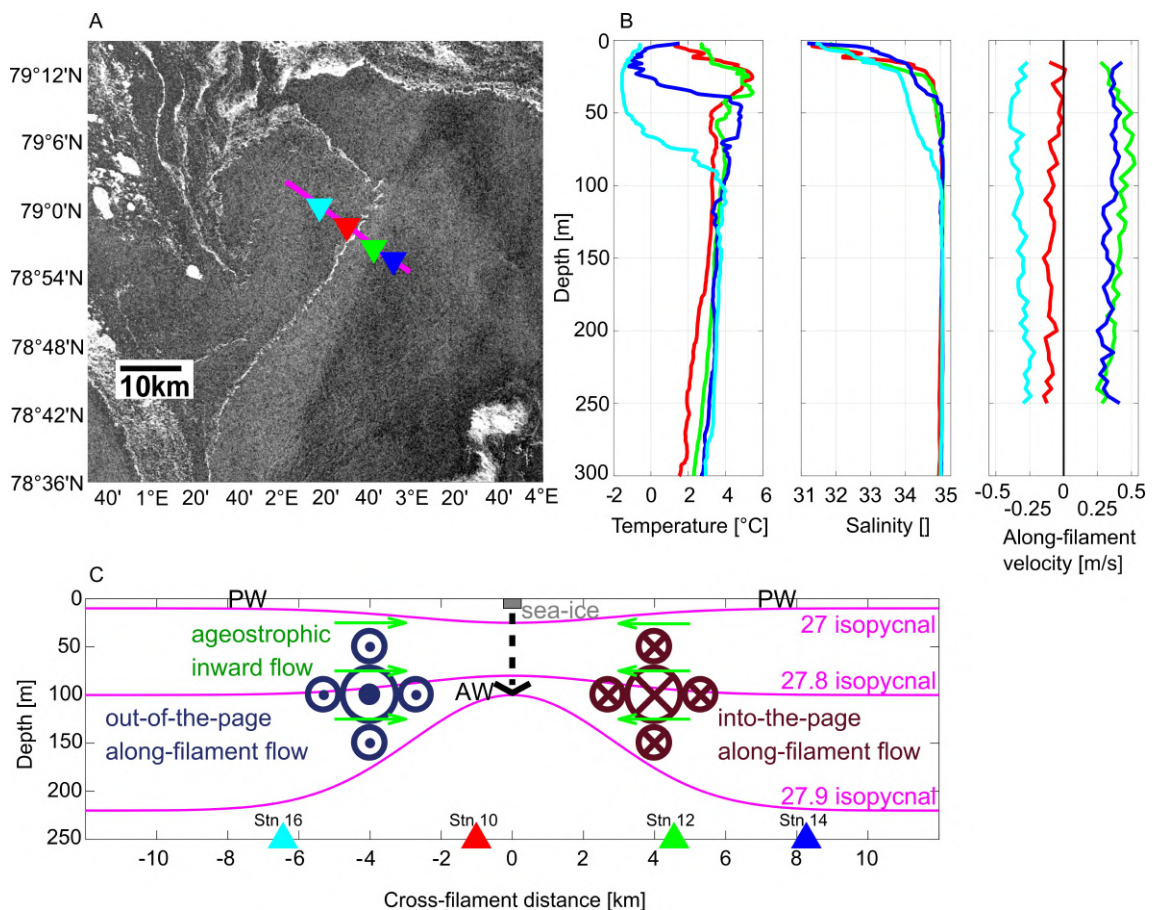
Figure 3.1: (A) Sentinel 1A (©European Space Agency) radar reflectivity on 26 July 2017 including the position of the cross frontal transect with the four MultiNet stations. (B) CTD profiles of temperature and salinity as well as along-filament velocities at the four MultiNet stations. (C) Schematic illustration of the submesoscale filament in the Arctic marginal ice zone in cross-frontal direction (modified after von Appen et al. 2018). PW: Polar Water. Colored triangles indicate locations of MultiNet stations.

97

3.2.2 Zooplankton sampling, abundance and biomass analysis

Four stations (stns) across the submesoscale filament were analyzed for zooplankton abundance, biomass and taxonomic composition. Stns 10 and 12 were located near the center, stns 14 and 16 further away from the center (Figure 3.1A). Two stations were situated on either side of the central convergence zone, i.e. stns 16 and 10 on the western side and stns 12 and 14 on the eastern side (Table 3.1, Figure 3.1A+C). Sampling was conducted within 30 h (Table 3.1) with a multiple opening and closing net equipped with five nets for stratified vertical hauls (Hydrobios MultiNet Midi, mouth opening 0.25 m^2, mesh size 150 μm, sampling speed 0.5 m^{-1}). Oceanographic observations indicated an extent of the filament to $\geq$ 250 m depth, thus, zooplankton sampling depths were adjusted accordingly, with five vertical sampling intervals covering 300-200-100-50-10-0 m. Immediately after the haul the samples were preserved in a 4% borax-buffered formaldehyde seawater solution. Prior to each MultiNet station, oceanographic data were obtained by a CTD attached to a rosette water sampler at the same stations.

Table 3.1: Geographic position, sampling date and time as well as the distance to the center of the filament (w: to the western side of the center, e: to the eastern side) of the four MultiNet Stations sampled across a submesoscale filament in Fram Strait.

Station	Latitude	Longitude	Sampling date	Sampling time (UTC)	Distance to center (km)
10	78° 58' 21" N	2° 29' 35" E	29.07.17	19:12	0.9
12	78° 56' 45" N	2° 42' 3" E	30.07.17	03:28	4.6
14	78° 55' 42" N	2° 51' 12" E	30.07.17	15:14	8.4
16	79° 0' 5" N	2° 16' 48" E	30.07.17	23:58	6.5

For the microscopic analysis, zooplankton samples were split into subsamples (1/2 to 1/128, depending on the total abundance of the sample) using a Motoda plankton splitter (Motoda 1959). Identification was performed to the lowest possible taxonomic level using a dissecting microscope Leica MZ12.5. Copepoda (calanoid, cyclopoid, harpacticoid), Amphipoda, Euphausiacea and Pteropoda were generally identified to genus or, if possible, to species level, including developmental stages for Copepoda. Individuals were counted until at least 80 specimens were reached within a complete subsample. Biomass values were calculated for abundant species by multiplying the abundance data with published individual dry mass values for the Greenland Sea (Richter 1994 and references therein).

In the Arctic, three *Calanus* species co-occur and usually dominate zooplankton communities in terms of biomass and ecological importance (Auel and Hagen 2002; Kosobokova and Hirche 2009; Mumm et al. 1998). While *Calanus hyperboreus* is easily identified based on morphological characteristics and its larger body size, *Calanus finmarchicus* and *Calanus glacialis* are two sister species, which are morphologically not distinguishable. A differentiation between both species

based on prosome length has been proposed and widely used, considering copepodite stages CV larger than 2.9 to 3.0 mm and adult females larger than 3.2 mm to be *C. glacialis*, whereas smaller individuals are assigned to *C. finmarchicus* (e.g., Kwasniewski et al. 2003; Unstad and Tande 1991). However, several recent studies question the applicability of prosome length as a valid characteristic for *Calanus* species identification as the size ranges of both species can considerably overlap (e.g., Choquet et al. 2017; Choquet et al. 2018; Nielsen et al. 2014). Thus, fixed size thresholds are not applicable for species identification. In this study, we measured the prosome lengths of all 2661 *C. finmarchicus* and *C. glacialis* specimens to check the applicability of length-frequency distributions for species identification. Depth-specific size distributions generally revealed distinct, non-overlapping bimodal size distributions, based on which adult females and copepodids CV of these two species were distinguished from each other. *Calanus* copepodids CI-III were pooled as *Calanus* spp. CI-III. *Calanus* copepodids CIV were separated between *C. hyperboreus* CIV and *C. finmarchicus/glacialis* CIV.

3.2.3 Community analysis and impact of environmental factors

Statistical analyses were conducted with PRIMER6 (version 6.1.6; Clarke and Gorley 2006) and R (version 3.5.3, Team 2019). To investigate if and how the stations differed in terms of species composition, averaged Bray-Curtis dissimilarities were calculated based on $log(x+1)$ transformed total abundances of all species and on depth-specific abundances at each station. A non-metric multidimensional scaling (nMDS) plot and dendrogram were generated with PRIMER6 to visualize the differences, respectively.

To further evaluate how environmental factors affected the distribution of zooplankton species across the filament, we applied canonical correspondence analysis (CCA) using the vegan package in R (version 2.5-6, Oksanen et al. 2019). CCA is a multivariate method to help explain the relationships between species assemblages and their environment (Greenacre and Primicerio 2013; ter Braak and Verdonschot 1995) and has found widespread use in aquatic science (e.g., Herman and Dahms 1992; Pinto-Coelho et al. 2005; Sell and Kröncke 2013). For the analysis, species abundances (ind m^{-3}) for each of the five depth intervals were used with the mean depth and mean temperature of the respective depth interval as well as the distance of the four stns to the filament center as the abiotic factors. Distance was used as positive values. Thus, the analysis does not differentiate between east and west of the filament center, but rather indicates the distribution of species close to and far away from the center of the filament. Permutation tests were further performed in R with the vegan package using the anova.cca function (version 2.5-6, Oksanen et al. 2019).

3.3 Results

3.3.1 Zooplankton abundance and biomass

Total zooplankton abundance was by far the highest in the upper 50 m of stn 10 (0 to 10 m 18 257 ind m^{-3}, 10 to 50 m 10 912 ind m^{-3}), close to the center of the filament (Figure 3.2). Below 50 m numbers dropped to 1152 ind m^{-3} (50 to 100 m) and less than 250 ind m^{-3} (100 to 300 m). Surface abundance at stn 12 was also high but approximately half the values of stn 10. The elevated numbers at both stns were largely due to *Oithona* spp. and copepod nauplii. Stns 14 and 16 had lowest total abundances in surface waters (<1,800 ind m^{-3}), values in the upper 50 m comprised less than 16% of the numbers at stn 10. Between 100 and 300 m *Microcalanus* spp., *Oithona* spp. and *Oncaea* spp. became important components in terms of contribution to abundance. Total abundance below 100 m was similar at all stns.
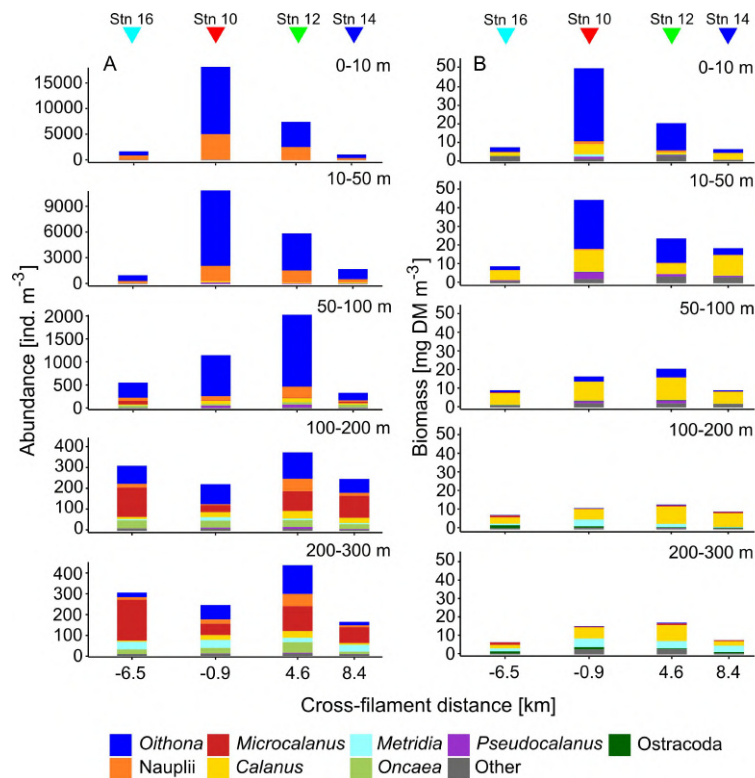
Figure 3.2: Vertical distribution of total zooplankton abundance (ind m^{-3}, A) and biomass (mg dry mass m^{-3}, B) across the submesoscale filament. Colors indicate the contributions of different taxa. Colored triangles indicate the location of the four stations (16, 10, 12, 14) across the filament.

Similar to abundance, total biomass was highest in surface waters at the center of the filament (stn 10), followed by stn 12 (Figure 3.2). At the outer stations, biomass in the upper 50 m was 27% (stn 14) or even below 20% (stn 16) of the value at stn 10. This difference was again mainly due to the dominance of *Oithona* spp. at stns 10 and 12, but higher numbers of copepod nauplii, *Pseudocalanus* spp., *Calanus* CI-III, *C. finmarchicus/glacialis* CIV also contributed to the increased biomass. Due to their small size, *Oithona* spp. are usually not the main contributors to biomass.

However, at stn 10, and partly also at stn 12, *Oithona* spp. appeared in such high densities (13 126 ind m^{-3} at stn 10), that it comprised up to 78% of total biomass in the upper 10 m, compared to only 30% at stns 14 and 16. *Calanus* spp. were main contributors to total biomass throughout the sampled water column, while *Metridia longa* contributed significantly below 100 m. Similar to abundance, the variability of total biomass between the stns decreased with depth.

In total, 35 different taxonomic categories were identified at the four stns (Table 3.2). With at least 27 species, copepods were the most diverse and abundant taxon, comprising about 80% of total abundance at all stns. While Calanoida were the most species-rich order, Cyclopoida (mainly *Oithona* spp.) dominated in terms of abundance with 59% to 93% of all copepods at all stns.

Table 3.2: Abundance (ind m^{-3}) of zooplankton taxa at the four stations across the submesoscale filament in Fram Strait, July/August 2017. The stations are arranged from left to right in cross-frontal direction to reflect their geographic position in relation to the filament.

	Depth interval [m]	Stn 16 0-10	10-50	50-100	100-200	200-300	Stn 10 0-10	10-50	50-100	100-200	200-300	Stn 12 0-10	10-50	50-100	100-200	200-300	Stn 14 0-10	10-50	50-100	100-200	200-300
Crustacea																					
Copepoda	Nauplii	853.3	236.0	67.3	18.4	12.5	4928.0	1768.7	89.4	4.5	20.7	2528.0	1433.6	237.3	60.8	60.2	389.3	357.8	27.1	14.5	9.4
Cyclopoida	*Oithona* cf. *similis* CI-CV	741.3	556.0	170.7	34.2	7.1	12960.0	8273.5	779.3	80.5	48.5	4864.0	4134.4	1205.3	75.5	102.4	613.3	928.0	88.0	31.2	9.6
	Oithona cf. *similis* CVI	57.3	117.1	153.0	44.7	12.4	166.0	511.0	110.2	14.4	20.6	55.0	211.6	358.0	45.6	33.8	61.0	259.6	69.3	29.3	6.8
	Oithona atlantica f	0.3	0.1	4.7	7.6	3.9	-	1.9	0.7	1.2	1.6	-	0.5	1.9	6.1	4.7	0.3	0.6	5.9	6.0	1.1
	Oncaea spp. CI-CVI	6.7	13.6	40.9	39.4	23.5	10.5	6.2	35.9	34.2	26.6	7.0	1.5	50.4	33.4	51.1	12.7	42.6	59.7	22.5	12.1
Calanoida	*Pseudocalanus* spp. CI-CVI	10.0	20.0	2.6	1.4	0.3	51.0	161.8	48.4	5.9	2.1	19.5	57.0	63.4	10.0	4.0	3.7	30.2	6.1	1.5	0.5
	Calanus spp. CI-CIII	2.0	21.9	2.5	0.4	0.1	22.5	105.3	16.0	1.2	0.4	6.0	39.9	24.2	1.6	0.6	5.7	62.5	3.7	0.4	0.4
	C. finmarchicus/glacialis CIV	0.7	9.1	4.3	1.4	0.3	16.0	42.9	38.1	8.3	1.8	3.0	23.2	49.3	9.8	4.0	2.0	24.0	9.5	1.7	0.9
	C. finmarchicus CV	0.7	7.0	10.2	5.2	3.6	4.0	0.8	8.4	7.2	18.6	1.5	1.3	7.8	11.2	22.7	2.0	7.2	15.4	11.0	6.1
	C. finmarchicus f	0.3	1.6	5.8	3.2	1.7	2.0	0.6	4.5	7.2	1.6	0.5	1.0	5.7	13.2	4.4	1.0	0.4	2.2	10.8	1.4
	C. finmarchicus m	-	-	-	-	-	-	0.1	0.1	<0.05	-	-	-	-	0.2	-	-	-	-	-	-
	C. glacialis CV	1.0	0.3	0.1	<0.05	0.2	0.5	-	-	0.1	-	-	-	0.1	0.3	0.3	-	0.4	-	-	-
	C. glacialis f	0.7	0.3	0.6	0.2	0.1	-	-	-	-	<0.05	-	-	-	-	-	0.3	0.6	-	0.1	0.1
	C. hyperboreus CIV	0.3	0.9	1.0	0.5	0.1	1.5	5.1	2.9	0.4	0.5	0.5	0.8	1.8	0.9	1.1	1.3	1.7	0.3	0.4	0.1
	C. hyperboreus CV	-	-	0.1	<0.05	-	-	-	-	-	-	-	-	0.1	-	0.1	-	0.9	-	-	<0.05
	C. hyperboreus f	-	-	-	0.1	<0.05	-	-	0.1	-	0.1	-	-	-	<0.05	-	0.7	0.4	-	0.1	<0.05
	Microcalanus spp. CI-CVI	16.7	17.4	78.6	141.1	199.7	8.5	5.4	8.8	33.6	55.9	15.0	1.9	9.8	93.7	121.9	10.3	7.8	34.9	106.4	78.3
	Oithona spp. CI-CV	1.3	0.1	3.8	1.8	35.6	-	0.2	0.1	4.2	25.5	-	0.1	0.1	0.9	9.5	0.3	-	0.2	5.0	24.0
	Metridia longa CVIf	-	-	-	3.0	1.3	4.0	0.4	0.2	12.1	11.9	0.1	0.1	0.3	6.2	12.5	-	0.2	-	0.9	8.6
	Metridia longa CVIm	-	-	0.1	-	-	0.5	-	0.1	0.1	2.5	-	-	-	-	0.4	-	-	0.1	<0.05	0.7
	Metridia lucens CVI	-	-	-	-	-	-	-	-	<0.05	-	-	-	-	-	0.1	-	-	-	-	<0.05
	Scolecithricella minor CI-CVI	-	0.1	1.0	0.6	0.5	-	-	0.5	0.2	0.5	-	-	0.4	0.6	0.4	0.3	0.3	0.4	0.4	0.4
	Paraeuchaeta spp. CI-CIV	-	-	1.3	0.8	0.9	-	-	0.3	0.3	0.7	-	-	0.4	0.6	0.6	-	0.2	0.6	1.0	1.1
	P. norvegica CV-CVI	-	-	1.3	0.9	0.9	-	-	0.3	0.5	0.7	-	-	0.4	0.7	0.7	-	0.2	0.6	1.1	1.1
	P. glacialis CV-CVI	-	0.1	-	<0.05	-	-	-	-	0.1	<0.05	-	-	-	-	-	-	0.1	-	-	-
	Heterorhabdus spp. CI-CVI	-	-	0.1	0.1	0.5	-	-	0.1	0.1	0.5	-	-	-	0.1	0.2	-	-	-	-	0.2
	Spinocalanus spp. CI-CVI	-	-	-	-	-	-	-	-	0.6	<0.05	-	-	-	0.1	-	-	-	-	-	0.2
	Gaetanus tenuispinus f	-	-	-	-	0.1	-	-	-	-	0.1	-	-	-	-	<0.05	-	-	-	-	<0.05
	Chiridius obstusifrons CV-CVI	-	-	-	-	<0.05	-	-	-	-	<0.05	-	-	-	-	<0.05	-	-	-	-	<0.05
	Scaphocalanus magnus CV	-	-	-	-	-	-	-	-	-	<0.05	-	-	-	-	0.1	-	-	-	-	<0.05
	Jaschnovia brevis CIV-CVI	-	-	-	-	0.1	-	-	-	-	-	-	-	-	-	-	-	-	-	-	0.1
Harpacticoida	*Microsetella norvegica*	3.0	0.6	0.2	<0.05	<0.05	15.5	5.3	0.2	<0.05	<0.05	2.0	2.0	0.3	0.1	0.1	2.3	0.9	0.1	0.1	<0.05
	Other harpacticoids	0.7	0.1	-	0.1	<0.05	-	0.3	0.1	-	-	-	0.2	-	0.2	0.1	0.3	0.6	0.1	0.1	0.1
Isopoda		-	-	-	0.1	<0.05	0.5	-	-	<0.05	0.2	-	-	-	0.1	<0.05	-	-	0.1	0.1	0.1
Amphipoda	*Themisto libellula*	-	-	-	-	-	-	0.1	0.7	0.1	0.6	0.5	0.4	0.2	-	0.1	-	0.1	0.3	0.1	<0.05
	Themisto abyssorum	-	-	0.5	0.2	0.2	-	-	0.1	0.1	0.2	-	-	-	0.2	0.5	-	-	-	-	0.5
Ostracoda		0.7	-	0.6	3.6	2.7	-	0.5	0.7	1.8	2.6	0.5	-	0.6	1.0	1.1	-	0.2	0.4	1.0	1.7
Euphausiacea	*Thysanoessa longicaudata*	-	-	-	-	<0.05	-	0.1	0.1	<0.05	0.3	-	0.1	-	-	0.3	-	0.1	-	-	<0.05

Mysidacea		-	-	0.3	0.1	-	-	-	-	-	-	-	0.3	-	-	-	0.3	0.4	1.0	0.1	-
Cnidaria																					
Hydrozoa		0.3	-	-	-	-	-	-	-	-	<0.05	-	-	-	<0.05	<0.05	-	-	-	-	0.1
Mollusca																					
Bivalvia	Bivalvia larvae	1.3	1.5	-	-	-	-	0.6	0.2	<0.05	-	-	3.1	2.3	<0.05	-	0.3	2.9	0.3	<0.05	-
Gastropoda	*Limacina helicina*	6.3	3.6	0.4	<0.05	<0.05	2.5	3.5	0.2	<0.05	0.1	3.5	3.7	2.3	0.1	<0.05	2.0	7.0	0.4	-	<0.05
	Clione limacina	-	-	-	-	-	-	-	-	0.2	-	-	-	-	0.2	0.2	-	-	-	-	-
Annelida																					
Polychaeta		-	-	0.1	0.2	0.8	-	-	-	<0.05	0.2	-	-	-	0.1	0.3	-	-	0.1	-	-
Echinodermata																					
Ophiuroidea	Ophiopluteus larvae	1.7	19.9	1.8	<0.05	-	-	-	0.1	-	-	1.0	0.2	0.7	-	-	-	5.9	0.5	-	-
Chaetognatha																					
Sagittoidea		-	-	5.8	4.0	1.9	5.0	7.4	6.9	4.7	5.7	-	1.2	11.3	4.0	6.7	0.7	3.4	7.6	3.4	2.3
Chordata																					
Appendicularia		74.0	7.3	1.0	0.7	0.7	58.5	9.1	-	-	<0.05	11.5	0.9	0.3	<0.05	0.1	26.3	6.5	1.3	0.3	0.2

3.3.2 Zooplankton distribution across the filament

Visualization of Bray-Curtis dissimilarities between the four stations as a nMDS plot indicate that stns 14 and 16, even though they were the furthest apart from each other, were the most similar with regard to species composition (Figure 3.3A). Stn 10 deviated most from the other stations. Stn 12 was somewhere in between the central stn 10 and the outer stns 14 and 16. The hierarchical cluster analysis of depth-specific species composition at each station revealed that depth had a strong influence on differences between and within stations (Figure 3.3B). Two main clusters were formed, with surface waters (0 to 100 m, D1-3) in one and lower epipelagic to mesopelagic depths in the other cluster (100 to 300 m, D4-5), except for 50 to 100 m (D3) of stn 10 and 12 which was included in the cluster of surface samples. Similar to the nMDS plot, the hierarchical cluster analysis also indicated that stn 14 and 16 were more similar, as all five depth intervals clustered together. Stn 10 and 12 also had lower distances to each other, except 0 to 10 metre (D1) at stn 12, which grouped to stns 14 and 16.
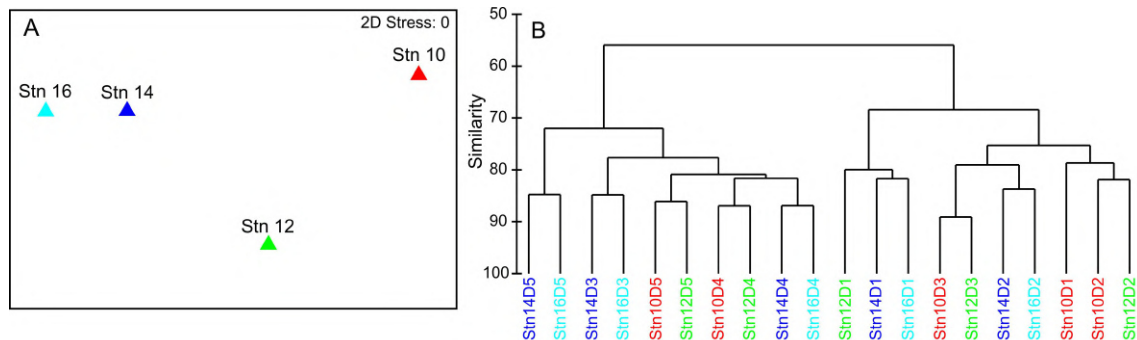
Figure 3.3: (A) nMDS plot of the four stations across the filament based on a Bray-Curtis dissimilarity matrix of $log(x+1)$ transformed total abundances of all species at each station. (B) Hierarchical cluster analysis based on a Bray-Curtis dissimilarity matrix of $log(x+1)$ transformed depth-specific species abundances at each station. D1: 0 to 10m, D2: 10 to 50m, D3: 50 to 100m, D4: 100 to 200m, D5: 200 to 300m.

To evaluate distribution patterns across the filament, a canonical correspondence analysis (CCA) was performed, using depth, temperature and the absolute distance to the filament center as environmental variables. The two axes with highest explanatory factors were used to generate the ordination plot (Figure 3.4). The first axis explained 60% of total variance, the second axis added another 4%. Thus, 64% of total variance was explained. Depth was mainly correlated to CCA1, i.e. increasing towards the right. Temperature and distance to the filament center were associated with the second axis, but in opposite directions, i.e. lower temperatures with increasing distance to the center.

Based on the arrangement of the taxa in the CCA triplot, the following four distinct distribution patterns across the filament were identified:
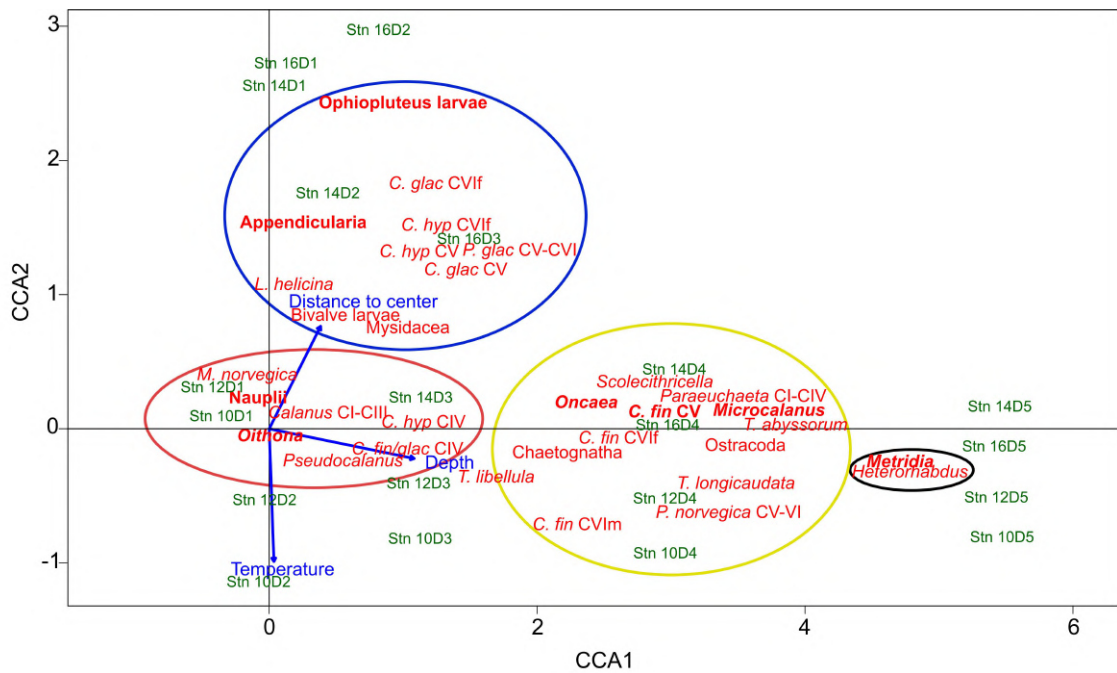
Figure 3.4: Canonical correspondence analysis (CCA) triplot of the most common zooplankton taxa, environmental variables (depth, temperature and distance to the filament center) and individual depth stratified samples across the submesoscale filament. Stn: Station. D1 to D5 indicate depth intervals, D1: 0 to 10m, D2: 10 to 50m, D3: 50 to 100m, D4: 100 to 200m, D5: 200 to 300m. The first axis (CCA1) explains 60%, the second axis (CCA2) explains 4% of the total variance. Colored circles indicate the association of taxa with the four distribution types, red: convergence and concentration of surface inhabitants close to the filament center, blue: polar taxa at outer stations, black: emergence of mesopelagic taxa beneath the filament, yellow: mesopelagic taxa, including travelers with along-frontal jets. Indicated in bold are the main contributors of respective distribution types. Species abbreviations: *C. glac*: *Calanus glacialis*, *C. hyp*: *Calanus hyperboreus*, *C. fin*: *Calanus finmarchicus*, *P. glac*: *Paraeuchaeta glacialis*, *P. norvegica*: *Paraeuchaeta norvegica*, *M. norvegica*: *Microsetella norvegica*, *T. libellula*: *Themisto libellula*, *T. abyssorum*: *Themisto abyssorum*, *T. longicaudata*: *Thysanoessa longicaudata*, *L. helicina*: *Limacina helicina*. CI to CVI: copepodite stage; f: female, m: male.

(A) Convergence and concentration of surface inhabitants close to the filament center

Taxa of this group showed an accumulation in the surface layer (upper 50 m) close to the center of the filament, while occurring at much lower concentrations at the outer stations. This group includes *Oithona* spp., copepod nauplii, *Pseudocalanus* spp., *Calanus* copepodids CI-III, *C. finmarchicus/glacialis* CIV, *Microsetella norvegica* and *C. hyperboreus* CIV (Figure 3.4, red circle). The distributions of the two most abundant representatives of this group (*Oithona* and nauplii) are visualized in Figure 3.5, Group A.

(B) Polar taxa at the outer stations

In contrast to taxa of Group A with high abundances in surface waters close to the filament center, *C. glacialis* CV and adult females, *C. hyperboreus* CV and adult females, *Paraeuchaeta glacialis* CV-CVI, ophiopluteus larvae, the pteropod *Limacina helicina*, Bivalvia larvae, Mysidacea and Appendicularia were generally more abundant in the polar surface waters of the outer

Group A: Convergence and concentration at filament center

Depth [m]

Oithona

	Stn 16	Stn 10	Stn 12	Stn 14
0–10	799	13126	4919	675
10–50	673	8786	4347	1188
50–100	328	890	1565	163
100–200	87	96	127	66
200–300	23	71	141	17

Nauplii

	Stn 16	Stn 10	Stn 12	Stn 14
0–10	853	4928	2528	389
10–50	236	1769	1434	358
50–100	67	89	237	27
100–200	18	4	61	14
200–300	13	21	60	9

Group B: Polar species at outer stations

Ophiopluteus larvae

	Stn 16	Stn 10	Stn 12	Stn 14
	1.7	0	1.0	0
	19.9	0	0.2	5.9
	1.8	0	0.7	0.5
	<0.05	0	0	0
	0	0	0	0

Appendicularia

	Stn 16	Stn 10	Stn 12	Stn 14
	74	58.5	11.5	26.3
	7.3	9.1	0.9	6.5
	1.0	0	0.3	1.3
	0.7	0	<0.05	0.3
	0.7	<0.05	0.1	0.2

C. glacialis CV-CVI

	Stn 16	Stn 10	Stn 12	Stn 14
	1.7	0.5	0	0.3
	0.5	0	0	0.9
	0.7	0	0.1	0
	0.3	0.1	0.3	0.1
	0.2	<0.05	0.3	0.1

C. hyperboreus CV-CVI

	Stn 16	Stn 10	Stn 12	Stn 14
	0	0	0	0.7
	0	0	0	1.3
	0.1	0.1	0.1	0
	0.2	0	<0.05	0.1
	<0.05	0.1	0.1	0.1

Group C: Isopycnal upwelling

Metridia

	Stn 16	Stn 10	Stn 12	Stn 14
	1.3	4.5	0.1	0.3
	0.1	0.5	0.2	0.2
	3.9	0.4	0.3	0.3
	4.8	16.4	7.1	5.9
	36.9	40.0	22.5	33.3

Group D: Travellers with along-frontal jets

Microcalanus

	Stn 16	Stn 10	Stn 12	Stn 14
	16.7	8.5	13.0	10.3
	17.4	5.4	1.9	7.8
	78.6	8.8	9.8	34.9
	141.1	33.6	93.7	106.4
	199.7	55.9	121.9	78.4

C. finmarchicus CVIf

	Stn 16	Stn 10	Stn 12	Stn 14
	0.3	2.0	0.5	1.0
	1.6	0.6	1.0	0.4
	5.8	4.5	5.7	2.2
	3.2	7.2	13.2	10.8
	1.7	1.6	4.4	1.4

Figure 3.5: Distribution heatmaps of most abundant and/or ecologically important zooplankton taxa sorted according to the four distribution types (Group A to D) across the submesoscale filament. Numbers inside the heatmaps show abundances (ind m^{-3}). Darker shading indicates higher abundances.

stns 14 and 16 (Figure 3.4, blue circle).

This distribution pattern was most prominent for ophiopluteus larvae (Figure 3.5, Group B), which were completely absent at stn 10 and only appeared in low numbers in the upper 100 m at stn 12 (51 ind m^{-2}), while exhibiting much higher densities at stn 14 (261 ind m^{-2}) and stn 16 (903 ind m^{-2}). Appendicularians were the most abundant representative of Group B (Figure 3.5), with high numbers in the upper 100 m at the outer stns (631 ind m^{-2} at stn 14; 1,222 ind m^{-2} at stn 16), but also exhibiting high abundances at stn 10 (952 ind m^{-2}). *C. glacialis* and *C. hyperboreus* copepodids

CV and adults were most abundant in the Polar Surface Water at the outer stns (Figure 3.5, Group B). While *C. glacialis* occurred at both sides of the filament, *C. hyperboreus* was only present on the eastern side.

(C) Emergence of mesopelagic taxa beneath the filament / isopycnal upwelling

Occurrences of *Oithona* spp., comprising mainly *M. longa* and only few *M. lucens*, and *Heterorhabdus* spp. (mainly *H. norvegicus*) were both highly correlated with depth (Figure 3.4, black circle). In contrast to the surface-inhabiting taxa of Groups A and B, their distribution was less influenced by the distance to the filament center.

The distribution pattern is depicted for *Oithona* spp. in Figure 3.5, Group C. *Metridia* was rare in the epipelagic at all stns and showed highest abundances below 200 m. At stn 10, *Oithona* spp. showed an elevated abundance between 100-200 m compared to the other stns, linked to the characteristic doming of the isopycnals at that depth close to the center of the filament.

(D) Travelers with the along-frontal jets

Group D includes *Microcalanus* spp., *C. finmarchicus* adult females (presented in Figure 3.5) and Ostracoda. While these taxa were rather abundant throughout the sampled water column below 50 m, patches of higher concentrations occurred at the shoulders of the filament in the areas of the frontal jets. This pattern was most distinct for *Microcalanus* spp. (Figure 3.5, Group D), with minimum abundances at stn 10, but maxima between 100 to 300m at stns 12, 14 and 16. Adult females of *C. finmarchicus* showed a similar pattern, but in contrast to *Microcalanus* spp., they were more abundant on the eastern side of the filament at stns 12 and 14 between 50 to 200m (Figure 3.5, Group D). In contrast, ostracods were most abundant on the western side of the filament at stn 16 between 100 to 300m (Table 3.2).

C. finmarchicus copepodids CV occurred in the lower epipelagic to mesopelagic layers, but without emergence at the filament center. Similar to females, they were also found in the northward flowing along-front jet on the eastern side. Highest densities were determined between 200 and 300 mat stns 10 and 12 and between 50 and 200 m at stn 16 (Table 3.2).

Permutation tests to analyze the importance of the environmental variables revealed that depth was highly significant in explaining the variance of zooplankton distribution across the filament ($p = 0.001$), whereas temperature ($p = 0.112$) and distance to the filament center ($p = 0.449$) were not significant. However, when only surface species (red and blue clusters; Group A and B) were included in the analysis, temperature became a significant variable ($p = 0.031$), i.e. temperature significantly impacted epipelagic zooplankton distribution. The p-value of distance to the filament center also improved, but remained non-significant ($p = 0.082$).

3.3.3 Depth-dependent size-frequency distributions of *C. finmarchicus* and *C. glacialis*

Prosome lengths of *C. finmarchicus* and *C. glacialis* copepodids CV and adult females increased with depth at all stns (Figure 3.6). This trend was most pronounced in copepodids CV (Figure 3.6A), but was also observed in adult females (Figure 3.6B). Thus, fixed size thresholds are not applicable for the discrimination of the two co-occurring *Calanus* species. As individual size increases with depth, the threshold to differentiate between *C. finmarchicus* and *C. glacialis* has to increase as well, otherwise deeper occurring larger specimens of *C. finmarchicus* would be incorrectly identified as *C. glacialis*.
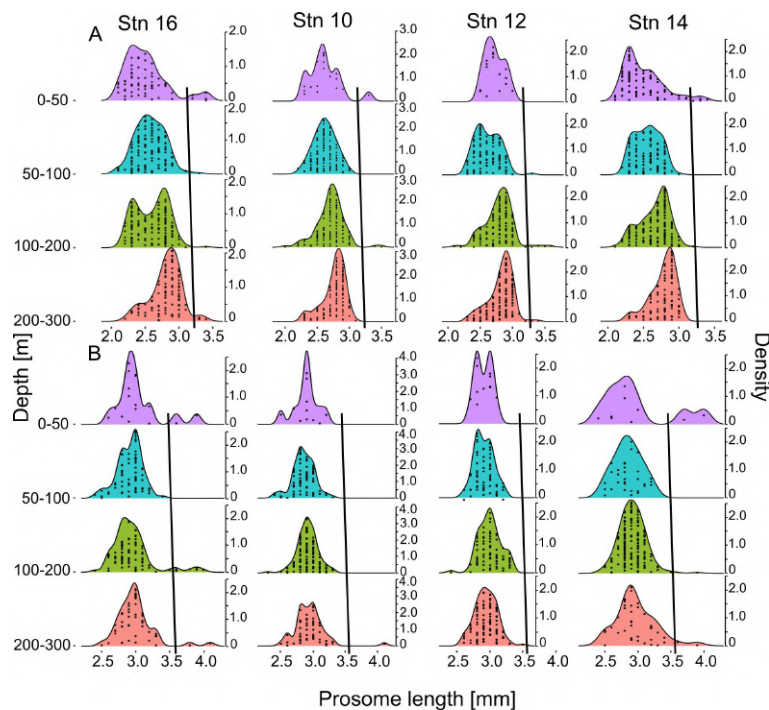
Figure 3.6: Density plot of size distributions of *C. finmarchicus/glacialis* CV (A) and adult females (B) prosome lengths for four distinct depth intervals at stations 10, 12, 14 and 16. Sampling intervals 0 to 10 m and 10 to 0 m were pooled due to low numbers of individuals. Second y-axes indicate kernel density estimations. Stations are arranged in cross-frontal direction. Each dot within the size-frequency distribution indicates one individual per respective size. Black lines show the thresholds for species separation of *C. finmarchicus* and *C. glacialis*, i.e. smaller individuals to the left of the respective line were identified as *C. finmarchicus*, larger specimens to the right as *C. glacialis*.

Several samples, in particular those from the outer stns dominated by Polar Surface Water, showed bimodal length-frequency distributions of *Calanus* with smaller secondary maxima at 3.2 to 3.5 mm in copepodids CV and ≥3.5 mm in adult females, respectively (Figure 3.6). For the present study, individuals from those secondary peaks were considered *C. glacialis* with a depth-dependent increase in the length threshold for species identification (black lines in Figure 3.6A and B).

3.4 Discussion

3.4.1 *Calanus* depth-dependent size distribution

Body size of *C. finmarchicus* and *C. glacialis* copepodids CV and adult females increased with increasing depth even on the relatively small vertical scale from 0 to 300 m (epipelagic to upper mesopelagic). Such a body size-dependent habitat partitioning within developmental stages of *Calanus* has to our knowledge not been published before. *Calanus* species are capable of diel vertical migrations (DVM), seeking shelter from predators in deeper layers during day and migrating to the surface to feed under the cover of darkness at night. However, several studies demonstrate that in polar regions DVM is only weakly pronounced during periods of midnight sun due to only little fluctuations in the light regime (Blachowiak-Samolyk et al. 2006; Cottier et al. 2006). The sampling campaign of the submesoscale filament was within the timespan of constant daylight. Further, local time of samplings varied over the day between the stations (9 pm, 5:30 am, 5 pm and 2 am). Although sampling times differed, the size-depth distribution pattern stayed the same at the four stations. Hence, it is highly unlikely that DVM was responsible for the size-depth distribution of *Calanus*. Among other explanations of depth-dependent increases in body size or vertical segregation by size in zooplankton are predator avoidance with size-specific differences in predation risk (de Robertis et al. 2000; Hunt and Harrison 1990) and niche selection (e.g., Laakmann et al. 2009, for vertical partitioning to avoid inter-specific competition; Kaiser et al. 2018, for cryptic species). In addition, variations in lipid content may affect buoyancy and the start of the ontogenetic descent to overwintering depths (Hirche 1997; Melle et al. 2014). However, those mechanisms usually act on larger scales and between ontogenetic stages. Vertical sampling with high spatial resolution by optical methods (e.g., LOKI, Hirche et al. 2014) will be required to elucidate the reasons for the fine-scale vertical zonation by body size within ontogenetic stages of *Calanus*.

3.4.2 Ecological roles of submesoscale filaments

The present study reveals several key effects of submesoscale structures on zooplankton distribution, ecology and dynamics.

Accumulation of zooplankton biomass

Convergence of surface water has the potential to increase abundance and biomass of planktonic organisms in frontal zones (Epstein and Beardsley 2001; Ohman et al. 2012; Strass et al. 2002). Empirical studies often focus on phytoplankton, as the applicability of methods like remote sensing allows an investigation of the influence of small-scale structures in much easier and feasible ways compared to zooplankton research. With the aid of satellite data those studies identified increased chlorophyll concentrations associated with submesoscale fronts (Guo et al. 2019; Liu and Levine 2016; Shulman et al. 2015b).

Across the filament, extreme differences in densities of epipelagic zooplankton species were observed, with maximum abundance and biomass values in the upper 50 m at the stns closest to the center of the filament (stns 10 and 12). The concentration of epipelagic zooplankton in the center of the filament is likely the result of physical-biological interactions (Folt and Burns 1999). Physically, the convergence of surface water associated with the submesoscale filament, which also led to the accumulation of sea ice (von Appen et al. 2018), concentrates epipelagic organisms at the site of downwelling. Among the zooplankton taxa which occurred across the filament, different swimming capabilities are found. Species of euphausiids and hyperiid amphipod *Themisto* are usually considered good and active swimmers (Kraft et al. 2012; Richerson et al. 2015) and thus may resist accumulation processes. Generally, however, planktonic organisms are said to passively drift with horizontal ocean currents, but they can, to some extent, swim against vertical velocities (Genin et al. 2005). Several studies demonstrated a strong fidelity of zooplankton species to particular depth layers and associated environmental conditions (Ashjian et al. 1994; Ashjian and Wishner 1993).

Active vertical counter-swimming leads to zooplankton accumulation at downwelling sites (Olson et al. 1994). In our case, an over 10- and 16-fold increase in abundance of epipelagic zooplankton close to the center of the filament in comparison to the outer stations supports our first objective.

Ohman et al. (2012) detected elevated mesozooplankton abundances at a submesoscale front in the California Current, including local maxima of calanoid copepods and *Oithona*. A higher ratio of nauplii to copepodids at the front suggested enhanced secondary production. In our study, the nauplii to copepodids ratio remained constant across the filament. However, the presence of *Calanus* males and eggs at stn 10 and 12 (Table 1, H. Auel, pers. obs.) indicated reproductive activities. The generation times of zooplankton usually exceed the persistence of small-scale dynamics. Nevertheless, the enhanced availability of phytoplankton at convergence zones creates beneficial feeding conditions and may stimulate secondary production. In turn, elevated concentrations of zooplankton at small-scale frontal zones represent foraging hotspots for top predators, as indicated by increased foraging success or time spend at such fronts for tunas (Snyder et al. 2017), seabirds (de Monte et al. 2012; Hyrenbach et al. 2006), elephant seals (Rivière et al. 2019; Siegelman et al. 2019) and whales (Davis et al. 2002).

Structuring the pelagic realm

Depth is usually the main factor structuring zooplankton communities, as demonstrated for the Arctic by Auel and Hagen (2002) and Kosobokova et al. (2010). However, the present study shows that submesoscale filaments can alter the vertical distribution of certain zooplankton species on very small horizontal and vertical scales. The doming of isopycnals in the upper mesopelagic at the filament center leads to an emergence of the mesopelagic copepods *Oithona* spp. and *Heterorhabdus* spp. Most likely, they passively followed the upwelling of the surrounding water body

in order to stay in their preferred environmental conditions in terms of temperature and salinity (Ashjian et al. 1994; Ashjian and Wishner 1993). In addition, enhanced food availability (phytoplankton and small copepods) caused by the accumulation through convergence in the center of the filament could have attracted these omnivorous copepods closer to the surface.

The center and intermediate depths of the filament were characterized by Atlantic Water and its associated species, such as *C. finmarchicus* and *Paraeuchaeta norvegica*, but also carried more widespread taxa such as *Microcalanus*. In contrast, surface waters at the outer stations 14 and 16 were of polar origin and contained clearly different communities. Polar species, such as the copepods *C. glacialis*, *C. hyperboreus* and *Paraeuchaeta glacialis*, the pteropod *L. helicina* and Ophiopluteus larvae, were considerably more abundant in those waters. The high spatial heterogeneity of zooplankton communities on small spatial scales matches physical oceanographic observations, which show that distinct unmixed water masses can occur close to each other in submesoscale filaments (von Appen et al. 2018).

The results support our second and third objective: different water masses associated with the filament are characterized by distinct zooplankton communities even on short spatial scales and the doming isopycnals at the filament center cause the emergence of mesopelagic species.

Vector for biological connectivity

Associated with the submesoscale filament, along-frontal jets with enhanced velocities at intermediate depths on both sides of the convergence zone were observed. Hancke et al. (2014) suggested that such fast-flowing along-frontal currents could act as vectors of biological connectivity. They demonstrated that drifters traveling within frontal jets crossed the Mozambique Channel significantly faster compared to drifters trapped in much slower propagating eddies. The transport in those jets represents a suitable time frame for the survival of planktonic larvae and thus may explain the biological connectivity between regions across the Mozambique Channel (Hancke et al. 2014; Marsac et al. 2014).

In the current study, patches of higher abundances of certain species were detected within the along-frontal jets. It is important to note that abundances of those species were different on both sides of the filament. Thus, the northward and southward jets should not be seen as compensating each other with zero net transport. For instance, abundance of *C. finmarchicus* was higher in the northward jet, indicating a northward net transport. The along-frontal jets exhibited a maximum speed exceeding $0.5\,\text{ms}^{-1}$ (von Appen et al. 2018), which is equivalent to 43 km per day. In comparison, the mean current velocity of the core of the West Spitsbergen Current is around $0.15\,\text{ms}^{-1}$ with a maximum of $\geq 0.2\,\text{ms}^{-1}$. Velocities of the offshore West Spitsbergen Current branch range between 0 and $0.15\,\text{ms}^{-1}$ (Beszczynska-Möller et al. 2012). Similar and even higher values for along-frontal jets, up to $1\,\text{ms}^{-1}$, were reported by Hernández-Hernández et al. (2020) for a submesoscale frontal zone south of the Canary Islands. A drifting sediment trap, which was deployed during our filament survey close to the northward frontal jet, traversed 26 km in 21 h,

further emphasizing the impact of such filament-associated flows (von Appen et al. 2018).

The length of the sea-ice streak suggests a horizontal extension of the filament of at least 50 km. Thus, zooplankton traveling within the fast-flowing jets may only have a short residence time of one to a few days in the filament. However, Hancke et al. (2014) demonstrated the connectivity between fronts by drifters moving from one frontal zone to another, enabling the coverage of large distances in a short time. Especially in highly dynamic systems like the MIZ, submesoscale dynamics may be omnipresent and could thus (involuntarily) be utilized by zooplankton as 'transportation highways'. Hence, submesoscale dynamics could not only play a role in plankton patchiness and structuring the pelagic realm, but the associated along-frontal jets may also be relevant for biological connectivity and species distribution, supporting our fourth objective.

The elevated abundance of CV and females of *C. finmarchicus*, an expatriate species from the boreal-Atlantic, in the northward flowing eastern jet could particularly be of importance for the Arctic marine ecosystem. Due to ongoing climate change and associated rising of pelagic species can be observed, with Atlantic species extending their ranges northward (Beaugrand et al. 2009). Further, due to rising temperatures, the width of the MIZ is constantly increasing during summer (Strong et al. 2013), possibly providing an extending area for submesoscale dynamics and associated fast-flowing jets, which may accelerate 'Atlantification' processes in the Arctic, although further supportive evidence is needed.

Atlantic zooplankton species tend to be smaller, less lipid-rich, i.e. less nutritious, and have different life-cycle strategies than their Arctic counterparts (Auel et al. 2009; Hagen 1999; Scott et al. 2000). Shifts in species distribution can have major implications for polar ecosystems (Wesławski et al. 2009). For instance, several studies demonstrate the strong dependency of the Arctic planktivorous little auk (*Alle alle*) on the larger Arctic *Calanus* species (Kwasniewski et al. 2010). The advection of different water masses can rapidly change the composition of zooplankton communities in Arctic fjords (Willis et al. 2006). When Atlantic water carrying *C. finmarchicus* intrudes, little auks accept longer foraging trips in order to find Arctic water masses with their preferred prey (Karnovsky et al. 2010; Kwasniewski et al. 2010).

Figure 3.7 summarizes the different effects of the submesoscale filament on zooplankton dynamics, integrating underlying oceanographic mechanisms with biological implications: (A) convergence and associated accumulation of epipelagic zooplankton at the filament center; (B) distinct water masses in close proximity leading to changes in zooplankton community structure over short distances; (C) emergence of mesopelagic species at the filament center coinciding with the doming of isopycnals below 100 m depth; (D) along-frontal jets as high-speed transport vectors for certain zooplankton species.
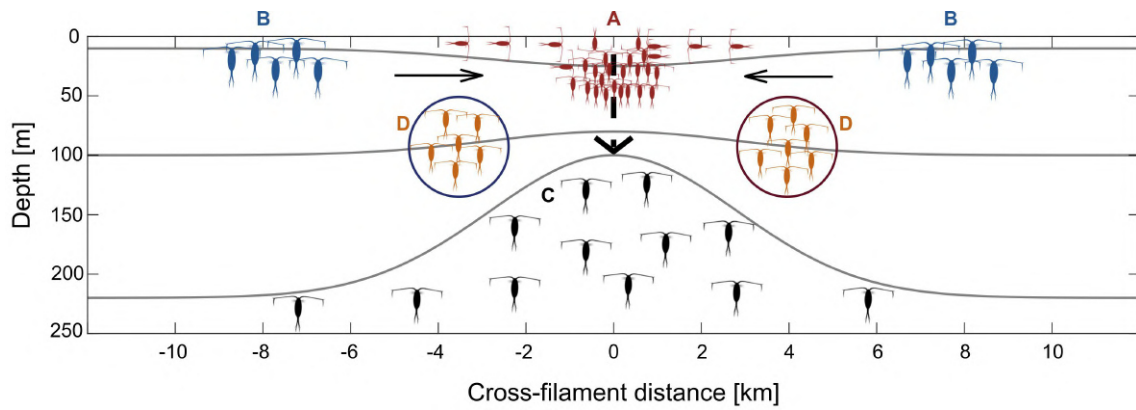
Figure 3.7: Schematic illustration of the effects of a submesoscale filament on zooplankton dynamics in the Arctic marginal ice zone. Colors of copepods represent different distribution patterns, i.e. red: convergence of surface species at the filament center (Group A), blue: concentration of Arctic species in Polar Surface Water at the outer stations (Group B), black: emergence of mesopelagic species by isopycnal doming / upwelling (Group C), orange: species in along-frontal jets (Group D).

3.5 Funding

3.6 Acknowledgements

References

Acha, M, Piola, A, Iribarne, O, and Mianzan, H (2015). Ecological Processes at Marine Fronts: oases in the Ocean. Berlin: Springer, 68 pp.

Ashjian, CJ, Smith, SL, Flagg, CN, Mariano, AJ, Behrens, WJ, and Lane, PVZ (1994). The influence of Gulf Stream meander on the distribution of zooplankton biomass in the slope water, the Gulf Stream, and the Sargasso Sea, described using shipboard acoustic doppler current profiler. *Deep-Sea Res I* 41, 23–50.

Ashjian, CJ and Wishner, KF (1993). Temporal persistence of copepod species groups in the Gulf Stream. *Deep-Sea Res I* 40, 483–516.

Auel, H and Hagen, W (2002). Mesozooplankton community structure, abundance and biomass in the central Arctic Ocean. *Mar Biol* 140, 1013–1021.

Auel, H, Hagen, W, and Schiel, S (2009). Size does matter – in the sea of giants and dwarfs. *Biological Studies in Polar Oceans. Exploration of Life in Icy Waters*. Edited by Hempel, I and Hempel, G. Bremerhaven: NW Verlag, 93–98.

Batten, SD and Crawford, WR (2005). The influence of coastal origin eddies on oceanic plankton distribution in the eastern Gulf of Alaska. *Deep-Sea Res II* 52, 991–1009.

Beaugrand, G, Luczak, C, and Edwards, M (2009). Rapid biogeographic plankton shifts in the North Atlantic Ocean. *Glob Change Biol* 15, 1790–1803.

Beszczynska-Möller, A, Fahrbach, E, Schauer, U, and Hansen, E (2012). Variability in Atlantic water temperature and transport at the entrance to the Arctic Ocean, 1997–2010. *ICES J Mar Sci* 69, 852–863.

Blachowiak-Samolyk, K, Kwasniewski, S, Richardson, K, Dmoch, K, Hansen, E, and Hop, H (2006). Arctic zooplankton do not perform diel vertical migration (DVM) during Periods of midnight sun. *Mar Ecol Prog Ser* 308, 101–116.

Choquet, M, Hatlebakk, M, Dhanasiri, AKS, Kosobokova, K, Smolina, I, and Søreide, JE (2017). Genetics redraws pelagic biogeography of *Calanus*. *Biol Lett* 13, 20170588.

Choquet, M, Kosobokova, K, Kwaśniewski, S, Hatlebakk, M, Dhanasiri, AKS, Melle, W, Daase, M, Svensen, C, Søreide, JE, and Hoarau, G (2018). Can morphology reliably distinguish between the copepods *Calanus finmarchicus* and *C. glacialis*, or is DNA the only way? *Limnol Oceanogr: Methods* 16, 237–252.

Clarke, KR and Gorley, RN (2006). *PRIMER v6: User Manual/Tutorial (Plymouth Routines in Multivariate Ecological Research*. PRIMER-E, Plymouth.

Cottier, FR, Tarling, GA, Wold, A, and Falk-Petersen, S (2006). Unsynchronised and synchronised vertical migration of zooplankton in a high Arctic Fjord. *Limnol Oceanogr* 51, 2586–2599.

D'Asaro, EA, Shcherbina, AY, Klymak, JM, Molemaker, J, Novelli, G, and Guigand, CM (2018). Ocean convergence and the dispersion of flotsam. *Proc Natl Acad Sci USA* 115, 1162–1167.

Davis, RW, Ortega-Ortiz, JG, Ribic, CA, Evans, WE, Biggs, DC, and Ressler, PH (2002). Cetacean habitat in the northern oceanic Gulf of Mexico. *Deep-sea Res I* 49, 121–142.

De Monte, S, Cotté, C, d'Ovidio, F, Lévy, M, Le Corre, M, and Weimerskirch, H (2012). Frigate-bird behaviour at the ocean-atmosphere interface: integrating animal behaviour with multi-satellite data. *Journal of The Royal Society Interface* 9, 3351–3358.

De Robertis, A, Jaffe, JS, and Ohman, MD (2000). Size-dependent visual predation risk and the timing of vertical migration in zooplankton. *Limnol Oceanogr* 45, 1838–1844.

De Steur, L, Hansen, E, Gerdes, R, Karcher, M, Fahrbach, E, and Holfort, J (2009). Freshwater fluxes in the East Greenland Current: a decade of observations. *Geophys Res Lett* 36, 23611.

Epstein, AW and Beardsley, RC (2001). Flow-induced aggregation of plankton at a front: a 2-D Eulerian model study. *Deep-Sea Res* II 48, 395–418.

Folt, CL and Burns, CW (1999). Biological drivers of zooplankton patchiness. *Trends Ecol Evol* 14, 300–305.

Genin, A, Jaffe, JS, Reef, R, Richter, C, and Franks, PJS (2005). Swimming against the flow: a mechanism of zooplankton aggregation. *Science* 308, 860–862.

Greenacre, M and Primicerio, R (2013). *Multivariate Analysis of Ecological Data*. Bilboa: Fundación BBVA, 331 pp.

Guo, M, Xiu, P, Chai, F, and Xue, H (2019). Mesoscale and submesoscale contributions to high sea surface chlorophyll in subtropical gyres. *Geophys Res Lett* 46, 13217–13226.

Hagen, W (1999). Reproductive strategies and energetic adaptations of polar zooplankton. *Invertebr Repr Dev* 36, 25–34.

Hancke, L, Roberts, MJ, and Ternon, JF (2014). Surface drifter trajectories highlight flow pathways in the Mozambique Channel. *Deep-Sea Res II* 100, 27–37.

Hattermann, T, Isachsen, PE, von Appen, W-J, Albretsen, J, and Sundfjord, A (2016). Eddy-driven recirculation of Atlantic Water in Fram Strait. *Geophys Res Lett* 43, 3406–3414.

Herman, RL and Dahms, HU (1992). Meiofauna communities along a depth transect off Halley Bay (Weddell Sea-Antarctica. *Polar Biol* 12, 313–320.

Hernández-Hernández, N, Arístegui, J, Montero, MF, Velasco-Senovilla, E, Blatbar, F, and Marrero-Díaz, Á. (2020). Drivers of plankton distribution across mesoscale eddies at submesoscale range. *Front Mar Sci* 7, 667.

Hirche, H-J (1997). Life cycle of the copepod *Calanus hyperboreus* in the Greenland Sea. *Mar Biol* 128, 607–618.

Hirche, H-J, Barz, K, Ayon, P, and Schulz, J (2014). High resolution vertical distribution of the copepod *Calanus chilensis* in relation to the shallow oxygen minimum zone off northern Peru using LOKI, a new plankton imaging system. *Deep-Sea Res I* 88, 63–73.

Hunt, G L JR and Harrison, N M (1990). Foraging habitat and prey taken by least auklets at King Island, Alaska. *Mar Ecol Prog Ser* 65, 141–150.

Hyrenbach, KD, Veit, RR, Weimerskirch, H, and Hunt Jr, GL (2006). Seabird associations with mesoscale eddies: the subtropical Indian Ocean. *Mar Ecol Prog Ser* 324, 271–279.

Kaiser, P, Bode, M, Cornils, A, Hagen, W, Arbizu, PM, and Auel, H (2018). High-resolution community analysis of deep-sea copepods using MALDI-TOF protein fingerprinting. *Deep-Sea Res I* 138, 122–130.

Karnovsky, N, Harding, A, Walkusz, W, Kwasniewski, S, Goszczko, I, and Wiktor, J (2010). Foraging distributions of little auks *Alle alle* across the Greenland Sea: implications of present and future Arctic climate change. *Mar Ecol Prog Ser* 415, 283–293.

Kawasaki, T and Hasumi, H (2016). The inflow of Atlantic water at the Fram Strait and its inter-annual variability. *J Geophys Res: Oceans* 121, 502–519.

Klein, P, Hua, BL, Lapeyre, G, Capet, X, Le Gentil, S, and Sasaki, H (2008). Upper ocean turbulence from high-resolution 3D simulations. *J Phys Oceanogr* 38, 1748–1763.

Klein, P and Lapeyre, G (2009). The oceanic vertical pump induced by mesoscale and submesoscale turbulence. *Annu Rev Mar Sci* 1, 351–375.

Kosobokova, KN and Hirche, H-J (2009). Biomass of zooplankton in the eastern Arctic Ocean – a base line study. *Prog Oceanogr* 82, 265–280.

Kosobokova, KN, Hopcroft, RR, and Hirche, H-J (2010). Patterns of zooplankton diversity through the depths of the Arctic's central basins. *Mar Biodiv* 41, 29–50.

Kraft, A, Bauerfeind, E, Nöting, EA, and Bathmann, UV (2012). Size structure and life cycle patterns of dominant pelagic amphipods collected as swimmers in sediment traps in the eastern Fram Strait. *J Mar Syst* 95, 1–15.

Kwasniewski, S, Gluchowska, M, Jakubas, D, Wojczulanis-Jakubas, K, Walkusz, W, and Karnovsky, N (2010). The impact of different hydrographic conditions and zooplankton communities on provisioning little auks along the west coast of Spitsbergen. *Prog Oceanogr* 87, 72–82.

Kwasniewski, S, Hop, H, Falk-Petersen, S, and Pedersen, G (2003). Distribution of *Calanus* species in Kongsfjorden, a glacial fjord in Svalbard. *J Plankton Res* 25, 1–20.

Laakmann, S, Kochzius, M, and Auel, H (2009). Ecological niches of Arctic deep-sea copepods: vertical partitioning, dietary preferences and different trophic levels minimize inter-specific competition. *Deep-Sea Res I* 56, 741–756.

Lee, MM and Williams, RG (2000). The role of eddies in the isopycnic transfer of nutrients and their impact on biological production. *J Mar Res* 58, 895–917.

Lévy, M, Franks, PJS, and Shafer Smith, K (2018). The role of submesoscale currents in structuring marine ecosystems. *Nat Commun* 9, 4758.

Lévy, M, Klein, P, and Treguier, AM (2001). Impact of sub-mesoscale physics on production and subduction of phytoplankton in an oligotrophic regime. *J Mar Res* 59, 535–565.

Liu, X and Levine, NM (2016). Enhancement of phytoplankton chlorophyll by submesoscale frontal dynamics in the North Pacific Subtropical Gyre. *Geophys Res Lett* 43, 1651–1659.

Chapter III - Role of submesoscale processes

Mackas, DL and Galbraith, MD (2002). Zooplankton distribution and dynamics in a North Pacific eddy of coastal origin: I. Transport and loss of continental margin species. *Oceanography* 58, 725–738.

Mahadevan, A (2016). The impact of submesoscale physics on primary productivity of plankton. *Annu Rev Mar Sci* 8, 161–184.

Mahadevan, A and Archer, D (2000). Modeling the Impact of Fronts and Mesoscale Circulation on the Nutrient Supply and Biogeochemistry of the Upper Ocean. *J Geophys Res* 105, 1209–1225.

Marsac, F, Barlow, R, Ternon, JF, Ménard, F, and Roberts, M (2014). Ecosystem functioning in the Mozambique Channel: synthesis and future research. *Deep-Sea Res II* 100, 212–220.

McGillicuddy Jr, DJ (2016). Mechanisms of physical-biological-biogeochemical interaction at the oceanic mesoscale. *Annu Rev Mar Sci* 8, 125–159.

McGillicuddy Jr, D J, Anderson, L A, Doney, S C, and Maltrud, M E (2003). Eddy-driven sources and sinks of nutrients in the upper ocean: results from a 0.1° resolution model of the North Atlantic. *Global Biogeochem Cycles* 17.

McWilliams, JC (1985). Submesoscale, coherent vortices in the ocean. *Rev Geophys* 23, 165–182.

McWilliams, JC (2008). The nature and consequences of oceanic eddies. *Ocean Modeling in an Eddying Regime*. Edited by Hecht, M W and Hasumi, H. Volume 177. Washington D.C.: Wiley, 5–15.

McWilliams, JC, Colas, F, and Molemaker, M (2009). Cold filamentary intensification and oceanic surface convergence lines. *Geophys Res Lett* 36, 18602.

Melle, W, Runge, J, Head, E, Plourde, S, Castellani, C, and Licandro, P (2014). The North Atlantic Ocean as habitat for *Calanus finmarchicus*: evironmental factors and life history traits. *Prog Oceanogr* 129, 244–284.

Motoda, S (1959). Devices of simple plankton apparatus. *Mem Fac Fish Hokkaido Univ* 7, 73–94.

Mumm, N, Auel, H, Hanssen, H, Hagen, W, Richter, C, and Hirche, H-J (1998). Breaking the ice: large-scale distribution of mesozooplankton after a decade of Arctic and transpolar cruises. *Polar Biol* 20, 189–197.

Nielsen, TG, Kjellerup, S, Smolina, I, Hoarau, G, and Lindeque, P (2014). Live discrimination of *Calanus glacialis* and *C. finmarchicus*: can we trust phenological differences? *Mar Biol* 161, 1299–1306.

Ohman, MD, Powell, JR, Picheral, M, and Jensen, DW (2012). Mesozooplankton and particulate matter response to a deep-water frontal system in the southern California Current System. *J Plankton Res* 34, 815–827.

Oksanen, J, Guillaume Blanchet, F, Friendly, M, Kindt, R, Legendre, P, and McGlinn, D (2019). *Vegan: Community Ecology Package. R package version 2.56*.

Olson, DB, Hitchcock, GL, Mariano, AJ, Ashjian, CJ, Peng, G, and Nero, RW (1994). Life on the edge: marine life and fronts. *Oceanography* 7, 52–60.

Pinto-Coelho, R, Pinel-Alloul, B, Méthot, G, and Havens, KE (2005). Crustacean zooplankton in lakes and reservoirs of temperate and tropical regions: variation with trophic status. *Can J Fish Aquat Sci* 62, 348–361.

Powell, JR and Ohman, MD (2015). Covariability of zooplankton gradients with glider-detected density fronts in the southern California Current system. *Deep-Sea Res II* 112, 79–90.

Richerson, K, Watters, GM, Santora, JA, Schroeder, ID, and Mangel, M (2015). More than passive drifters: a stochastic dynamic model for the movement of Antarctic krill. *Mar Ecol Prog Ser* 529, 35–48.

Richter, C (1994). Regional and seasonal variability in the vertical distribution of mesozooplankton in the Greenland Sea. *Rep Polar Res* 154, 1–96.

Rivière, P, Jaud, T, Siegelman, L, Klein, P, Cotté, C, and Le Sommer, J (2019). Sub-mesoscale fronts modify elephant seals foraging behavior. *Limnol Oceanogr Lett* 4, 193–204.

Schewe, I (2018). The Expedition PS107 of the research vessel *Polarstern* to the Fram Strait and the AWI-HAUSGARTEN in 2017. *Rep Polar Mar Res* 717, 120 pp.

Scott, CL, Kwasniewski, S, Falk-Petersen, S, and Sargent, JR (2000). Lipids and life strategies of *Calanus finmarchicus*, *Calanus glacialis* and *Calanus hyperboreus* in late autumn, Kongsfjorden, Svalbard. *Polar Biol* 23, 510–516.

Sell, AF and Kröncke, I (2013). Correlations between benthic habitats and demersal fish assemblages – a case study on the Dogger Bank (North Sea). *J Sea Res* 80, 12–24.

Shulman, I, Penta, B, Richman, J, Jacobs, G, Anderson, S, and Sakalaukus, P (2015a). Impact of submesoscale processes on dynamics of phytoplankton filaments. *J Geophys Res Oceans* 120, 2050–2062.

Shulman, I, Penta, B, Richman, J, Jacobs, G, Anderson, S, and Sakalaukus, P (2015b). Impact of submesoscale processes on dynamics of phytoplankton filaments. *J Geophys Res Oceans* 120, 2050–2062.

Siegelman, L, O'Toole, M, Flexas, M, Rivière, P, Klein, P, Singh, SP, Groeneveld, JC, Hart-Davis, MG, Backeberg, BC, and WillowsMunro, S (2019). Submesoscale ocean fronts act as biological hotspots for southern elephant seal. *Sci Rep* 9, 5588.

Singh, SP, Groeneveld, JC, Hart-Davis, MG, Backeberg, BC, and Willows-Munro, S (2018). Seascape genetics of the spiny lobster *Panulirus homarus* in the western Indian Ocean: understanding how oceanographic features shape the genetic structure of species with high larval dispersal potential. *Ecol Evol* 8, 12221–12237.

Snyder, S, Franks, PJS, Talley, LD, Xu, Y, and Kohin, S (2017). Crossing the line: tunas actively exploit submesoscale fronts to enhance foraging success. *Limnol Oceanogr Lett* 2, 187–194.

Strass, VH, Naveira Garabato, AC, Pollard, RT, Fischer, HI, Hense, I, and Allen, JT (2002). Mesoscale frontal dynamics: shaping the environment of primary production in the Antarctic Circumpolar Current. *Deep-Sea Res II* 49, 3735–3769.

Strong, C, Rigor, IG, Braak, CJF, and Verdonschot, PFM (2013). Arctic marginal ice zone wider in summer and narrower in winter. *Geophys Res Lett* 40, 4864–4868.

Team, RCore (2019). *R: A Language and Environment for Statistical Computing*. Vienna: R Foundation for Statistical Computing.

Ter Braak, Cajo J F and Verdonschot, Piet F M (1995). Canonical correspondence analysis and related multivariate methods in aquatic ecology. *Aquatic Science* 57, 255–289.

Trudnowska, E, Gluchowska, M, Beszczynska-Möller, A, Blachowiak-Samolyk, K, and Kwasniewski, S (2016). Plankton patchiness in the Polar Front region of the West Spitsbergen Shelf. *Mar Ecol Prog Ser* 560, 1–18.

Unstad, KH and Tande, KS (1991). Depth distribution of *Calanus finmarchicus* and *C. glacialis* in relation to environment conditions in the Barents Sea. *Polar Res* 10, 409–420.

Von Appen, W-J, Schauer, U, Hattermann, T, and Beszczynska-Möller, A (2016). Seasonal cycle of mesoscale instability of the West Spitsbergen Current. *J Phys Oceanogr* 46, 1231–1254.

Von Appen, W-J, Wekerle, C, Hehemann, L, Schourup-Kristensen, V, Konrad, C, and Iversen, MH (2018). Observations of a submesoscale cyclonic filament in the Marginal Ice Zone. *Geophys Res Lett* 45, 6141–6149.

Wesławski, JM, Kwasniewski, S, and Stempniewicz, L (2009). Warming in the Arctic may result in the negative effects of increased biodiversity. *Polarforsch 78*, 105–108.

Willis, K, Cottier, F, Kwasniewski, S, Wold, A, and Falk-Petersen, S (2006). The influence of advection on zooplankton community composition in an Arctic fjord (Kongsfjorden), Svalbard. *J Marine Syst* 61, 39–54.

Zhabin, IA and Andreev, AG (2019). Interaction of mesoscale and submesoscale eddies in the Sea of Okhotsk on satellite data. *Izv Atmos Ocean Phys 55*, 1114–1124.

4

PROTEOMIC FINGERPRINTING ENABLES QUANTITATIVE BIODIVERSITY ASSESSMENTS OF SPECIES AND ONTOGENETIC STAGES IN *Calanus* CONGENERS (COPEPODA, CRUSTACEA) FROM THE ARCTIC OCEAN

Sven Rossel[1], Patricia Kaiser[2], Maya Bode-Dalby[2], Jasmin Renz[3], Silke Laakmann[4,5], Holger Auel[2], Wilhelm Hagen[2], Pedro Martínez Arbizu[1], Janna Peters[3]

[1]German Centre for Marine Biodiversity Research (DZMB), Senckenberg Research Institute, 26382 Wilhelmshaven, Germany

[2]Universität Bremen, BreMarE - Bremen Marine Ecology, Marine Zoology, 28334 Bremen, Germany

[3]German Centre for Marine Biodiversity Research (DZMB), Senckenberg Research Institute, 20146 Hamburg, Germany

[4]Helmholtz Institute for Functional Marine Biodiversity at the University of Oldenburg (HIFMB), 26129 Oldenburg, Germany

[5]Alfred Wegener Institute, Helmholtz-Centre for Polar and Marine Research (AWI), 27570 Bremerhaven, Germany

Abstract

Species identification is pivotal in biodiversity assessments and proteomic fingerprinting by MALDI-TOF mass spectrometry has already been shown to reliably identify calanoid copepods to species level. However, MALDI-TOF data may contain more information beyond mere species identification. In this study, we investigated different ontogenetic stages (copepodids C1-C6 females) of three co-occurring *Calanus* species from the Arctic Fram Strait, which cannot be identified to species level based on morphological characters alone. Differentiation of the three species based on mass spectrometry data was without any error. In addition, a clear stage-specific signal was detected in all species, supported by clustering approaches as well as machine learning using Random Forest. More complex mass spectra in later ontogenetic stages as well as relative intensities of certain mass peaks were found as the main drivers of stage distinction in these species. Through a dilution series, we were able to show that this did not result from the higher amount of biomass that was used in tissue processing of the larger stages. Finally, the data were tested in a simulation for application in a real biodiversity assessment by using Random Forest for stage classification of specimens absent from the training data. This resulted in a successful stage-identification rate of almost 90%, making proteomic fingerprinting a promising tool to investigate polewards shifts of Atlantic *Calanus* species and, in general, to assess stage compositions in biodiversity assessments of Calanoida, which can be notoriously difficult using conventional identification methods.

4.1   Introduction

Species identification is crucial for biodiversity assessments. Traditionally, these have been carried out by morphological identification of single specimens. However, taxonomical work requires expert knowledge and is time-consuming when e.g. dissection of body parts is required for species identification. Especially in groups with enormous abundances such as planktonic calanoid copepods, species identification can consume many working hours. Usually identification keys are based on adult characters only. As an alternative to this taxonomic work, methods such as COI barcoding have been introduced for species identification (Hebert et al. 2003). Using self-assessed or public reference libraries like BOLD (Ratnasingham and Hebert 2007) or GenBank (Benson et al. 2012), genetic data can be used for identification without a comprehensive, taxonomic knowledge. However, quantitative genetic applications are costly. Moreover, it may be of interest to receive information beyond the level of mere species identification, e.g. to investigate population dynamics and cohort analysis of natural communities (Laakmann et al. 2020). Genetic barcodes like COI are invariant through the life of the organism, thus having the advantage of allowing species identification from the egg to adult stage. A caveat is that no differentiation between ontogenetic stages can be done.

Proteomic fingerprinting using matrix-assisted laser desorption/ionization time-of-flight (MALDI-TOF) mass spectrometry facilitates species identification based mainly on peptide- and protein compositions of specimens (Singhal et al. 2015). Molecules are embedded in a matrix solution to protect these from destruction by radiation through a laser during analyte ionization (Singhal et al. 2015). Molecule mass is measured by time-of-flight through a TOF tube towards a detector, resulting in species-specific proteome fingerprints. The method originates from microbiology where it is applied for pathogen identification (Chen et al. 2021; Papagiannopoulou et al. 2020; van Driessche et al. 2019). However, in metazoan identification it is still in its infancy. Nevertheless, successful species identification of specimens has been achieved from a large variety of taxonomic groups such as different crustaceans (Bode et al. 2017; Hynek et al. 2018; Kaiser et al. 2018; Kürzel et al. 2022; Laakmann et al. 2013; Paulus et al. 2022; Rossel and Martínez Arbizu 2018b; Rossel and Martínez Arbizu 2019), fish (Maász et al. 2017; Mazzeo et al. 2008; Rossel et al. 2020; Volta et al. 2012), cnidarians (Holst et al. 2019; Korfhage et al. 2022), mollusks (Hamlili et al. 2021; Wilke et al. 2020) and a large variety of insects, preferentially those, which are potential disease vectors (Dieme et al. 2014; Hasnaoui et al. 2022; Loaiza et al. 2019; Mathis et al. 2015; Nabet et al. 2021; Nebbak et al. 2017; Yssouf et al. 2014).

Calanus species belong to the most important copepods with regard to biomass and food-web dynamics in many parts of the North Atlantic basins. However, identification to species level remains challenging despite its relevance. In Arctic Fram Strait, three species of *Calanus* co-occur, two 'true-Arctic' species, *C. hyperboreus* Krøyer, 1838 and *C. glacialis* Jaschnov, 1955, and the boreal-Atlantic expatriate, *C. finmarchicus* (Gunnerus, 1770) (Choquet et al. 2017).

While in *C. hyperboreus* copepodids of stage C4 and older are easily identified by morphology and size (Brodskii et al. 1983), the morphological identification of the congeneric species *C. finmarchicus* and *C. glacialis* is problematic due to the absence of consistent differences. A common method to distinguish *C. finmarchicus* from *C. glacialis* is based on differences in prosome length. However, this approach is inaccurate because the species overlap in body size in areas, where they co-occur (Gabrielsen et al. 2012; Lindeque et al. 2006; Trudnowska et al. 2020; Weydmann and Kwasniewski 2008). They also show high size plasticity depending on environmental conditions (Trudnowska et al. 2020). Recent comparisons of genetic and morphological identification indicate that no morphological criterion can reliably distinguish between *C. glacialis* and *C. finmarchicus* (Choquet et al. 2018). Yet, accurate species identification is crucial considering the increasing northward shift of boreal species due to climate change (Beaugrand et al. 2009; Weydmann et al. 2014a), with a recent study indicating the successful recruitment of *C. finmarchicus* in Fram Strait (Tarling et al. 2022). A shift from generally larger and lipid-richer Arctic *C. hyperboreus* and *C. glacialis* to boreal-Atlantic, smaller and less lipid-rich *C. finmarchicus* has consequences for Arctic food-webs. For instance, little auks (*Alle alle* ([Linnaeus, 1758]) actively select larger Arctic *Calanus* and even perform longer foraging trips to find their preferred prey (Kwasniewski et al. 2010). Thus, accurate, reliable and efficient species identification in order to

monitor distribution developments is essential.

In spite of pronounced morphological similarities, genetic identification of *Calanus* congeners is possible at any of the six naupliar and six copepodid developmental stages with the use of a variety of different molecular tools (Choquet et al. 2018; Gabrielsen et al. 2012; Hill et al. 2001; Lindeque et al. 2006; Weydmann et al. 2014b; Weydmann et al. 2017). Taking the above into account, the best current method for the effective species and developmental stage identification of this genus seems to be using conventional microscopy together with molecular markers, although it remains laborious.

Previously, studies have been carried out on species identification of Calanoida using MALDI-TOF MS and some authors mentioned specific clustering of different ontogenetic stages (Kaiser et al. 2018; Laakmann et al. 2013; Riccardi et al. 2012). However, these studies were carried out either as pilot studies to test the application of proteomic fingerprinting for identification or in actual biodiversity assessments. Thus, the existence of a stage-specific signal in calanoid identification has not been investigated in more detail. Because stage-level identification would add a further dimension of community composition in rapid biodiversity assessments, in this study on Arctic *Calanus* species we aim at i) testing for the existence of a stage-specific signal and ii) investigating the cause of this signal.

4.2 Material and Methods

4.2.1 Sampling

Specimens of *Calanus finmarchicus*, *Calanus glacialis* and *Calanus hyperboreus* were obtained from two sampling sites during the expedition PS121 in August/September 2019 with the research vessel *Polarstern* to Arctic Fram Strait. Station SV3 was located on the eastern side of Fram Strait close to Svalbard under strong Atlantic influence of the West Spitsbergen Current (78° 59.898 N; 8° 14.930 E). By contrast, station EG1 was on the western side of Fram Strait close to the East Greenland shelf and influenced by the polar East Greenland Current (78° 58.854 N; 5° 21.639 W). Both stations were sampled from the sea surface down to bottom depth (900 and 1000 m) using a multiple opening and closing net equipped with five nets (Hydrobios Multinet Midi, mouth opening 0.25 m^2, mesh size $150 \mu\text{m}$). Immediately after the haul, the samples were preserved in undenatured ethanol (96%). Samples were stored for 2 years at $0\,^\circ\text{C}$ before measurements.

Specimens of the three *Calanus* species were sorted from the ethanol-preserved samples by morphology using a dissecting microscope (Leica MZ12.5). For each sorted specimen, stage as well as prosome and urosome length were noted and, based on its size and sampling location, assigned to a species to allow a double check with MALDI-TOF identification results (see Table 4.1 for species- and stage-specific prosome lengths of sorted individuals). For *C. hyperboreus*, besides its much larger size, a protrusion at the prosome end from copepodite stage 4 on was

used for morphological discrimination. Copepodite stages were determined based on number of swimming legs (P) and number of urosome (U) segments, i.e. C1 has two P, U with two segments; C2 with three P, U with two segments; C3 with four P, U with two segments; C4 with five P, U with three segments; C5 with five P, U with four segments; adult female with five P, U with four segments, first segment of U with well-developed genital somite. Each specimen was cut in half, i.e. in an anterior prosome and a posterior prosome including the urosome. Each half was stored separately in an Eppendorf tube with absolute ethanol for subsequent genetic and proteomic analyses.

Table 4.1: Prosome lengths [mm] of *Calanus* copepodid stages C1 to females (C6f) from Fram Strait included in this study.

Species	Prosome length [mm]					
	C1	C2	C3	C4	C5	C6f
C. finmarchicus	0.5-0.7	0.9-1.0	1.1-1.4	1.6-1.9	2.1-2.8	2.4-3.0
C. glacialis	0.8-1.0	1.2-1.6	1.8-2.1	2.3-3.0	3.3-3.6	3.4-4.1
C. hyperboreus	-	1.5-1.7	2.3-2.8	3.5-3.9	4.4-5.4	5.9-6.7

DNA barcoding

The posterior thoracic segments 2-5 in stages C4 to C6 females (C6f) including the urosome, for the younger stages C1-3 approximately the posterior body half, were used for DNA extraction and subsequent amplification of the COI barcode fragment of three randomly chosen specimens from each developmental stage (C1-C6f) and suspected species.

Samples were incubated in 30 μL chelex (InstaGene Matrix, Bio-Rad) for 50 min at 56 °C, followed by a denaturation of the enzymes for 10 min at 96 °C. Of the DNA extract, 2 μL were used as template for the PCR in a volume of 20 μL with 10 μL Accu Start (2x PCR master mix, Quantabio), 7.6 μL molecular grade water and 0.2 μL of each primer (20 pmol μL^{-1}). For amplification of the COI barcoding region, Folmer primers LCO1490 and HCO2198 (Folmer et al. 1994) were used for *C. hyperboreus*. Amplification was carried out with the following settings: initial step at 94 °C for 5 min, denaturation step at 94 °C for 45 s, annealing at 42 °C for 45 s, elongation at 72 °C for 80 s and a final elongation for 7 min. Denaturation, annealing and elongation were carried out in 38 cycles. Amplification of the COI fragment for *C. finmarchicus* and *C. glacialis* was done using Coxf and CoxR2 primers (Cheng et al. 2013). Cycler settings were: initial denaturation at 94 °C for 5 min, denaturation at 94 °C, annealing at 44 °C for 75 s, elongation at 72 °C for 60 s and final elongation at 72 °C for 3 min. Denaturation, annealing and elongation were repeated 42 times. Purification and sequencing of the resulting PCR products was carried out at Macrogen Europe, Amsterdam, Netherlands.

Resulting sequencing reads were assembled in Geneious R7 v. 7.0.6. and checked for contamination (e.g. bacteria, fungi, non-crustacean taxa) as well as for correct species-level identification using the basic local alignment search tool (BLAST) (Altschul et al. 1997) against GenBank.

4.2.2 MALDI-TOF MS measurements

The anterior prosome body parts of 179 specimens were used for MALDI-TOF MS measurements. Depending on size, these were incubated in 3 to 30 µL (in adults: 5 µL for *C. finmarchicus*, *C. glacialis* in 10 µL and *C. hyperboreus* in 30 µL) of a matrix solution covering the entire specimen with some supernatant. The matrix contained $\alpha-Cyano-4-hydroxycinnamic$ acid (HCCA) as a saturated solution in 50% acetonitrile, 47.5% molecular grade water, and 2.5% trifluoroacetic acid. After 5 min of incubation, 1.5 µL was transferred to a target plate for co-crystallization of matrix and molecules. Subsequently, measurements were carried out using a Microflex LT/SH System (Bruker Daltonics). Employing the flexControl 3.4. (Bruker Daltonics) software, molecule masses were measured from 2 to 20k Dalton (kDA). A centroid peak detection algorithm was carried out for peak evaluation by analyzing the mass peak range from 2 to 20kDa. Furthermore, peak evaluation was carried out by a signal-to-noise threshold of two and a minimum intensity threshold of 600 with a peak resolution higher than 400. To validate fuzzy control, the proteins/oligonucleotide method was employed by maximal resolution of ten times above the threshold. To create a sum spectrum, a total of 160 laser shots were applied to a spot. Each spot was measured three times.

4.2.3 MALDI-TOF data processing

MALDI-TOF raw data were imported to R, Version 4.1.0 (R-Core-Team 2022) and processed using R packages MALDIquantForeign, Version 0.12 (Gibb 2015) and MALDIquant, Version 1.20 (Gibb and Strimmer 2012). Spectra were square-root transformed, smoothed using the Savitzky Golay method (Savitzky and Golay 1964), baseline corrected using the SNIP method (Ryan et al. 1988) and spectra normalized using the TIC method. Repeated measurements were averaged by using mean intensities. Peak picking was carried out using a signal to noise ratio (SNR) of 12 and a half window size of 13. Mass peaks smaller than a SNR of 12 were however retained, if they occurred in other mass spectra as long as these were larger than a SNR value of 1.75, which is assumed as a lower detection limit. Repeated peak binning was carried out to align homologous mass peaks. Resulting data was Hellinger transformed (Legendre and Gallagher 2001) and used for further analyses.

Hierarchical clustering was carried out in R using Ward's D and Euclidean distances. Random Forest (RF) (Breimann 2001) was carried out using the R package randomForest, Version 4.6.14 (Liaw and Wiener 2002). Settings were used according to Rossel and Martínez Arbizu (2018b) (ntree=2,000, mtry=35, sampsize= number of specimens in the smallest class). Classifications were tested using the RF *post-hoc* test (Rossel and Martínez Arbizu 2018a), function rf.post.hoc in package RFtools Version 0.0.3 (https://github.com/pmartinezarbizu/RFtools). Classifications were tested for correct class assignment based on empirical assignment probabilities of the RF model. Specimens with correct RF classification and assignment probabilities not deviating significantly (p < 0.05) from the empirical distribution were considered true positive (tp) assignments. Specimens with correct RF classification and significantly different assignment probability

were recorded as false positives (fp). If RF classification was incorrect and the assignment probability for the class a specimen was assigned to did not differ significantly, the classification was recorded as true negative (tn). Considered as false negatives (fn) were specimens assigned to the incorrect class by RF but the assignment probability differed significantly from the empirical distribution of the respective class. To test for significant differences between stages, pairwise adonis of all species-stage combinations was carried out using the R-package pairwiseAdonis, Version 0.4 (Martínez Arbizu 2022) (https://github.com/pmartinezarbizu /pairwiseAdonis).

The respective RF models, using either species or species and stage as classes, were also used to find the most important variables for differentiation of the groups using the Gini index, which shows the degree of dissimilarity of the respective variables (Han et al. 2016). T-distributed Stochastic Neighbor Embedding (t-SNE) plots were created using R package Rtsne Version 0.15 (Krijthe 2015) with the following settings: perplexity=15, max_iter=4,000 and theta=0.

4.2.4 Dilution series

To test the effect of decreasing amounts of biomass on the stage-specific signal, a dilution series was carried out. The cephalosomes of five adult specimens per species were prepared and measured as described above. The amount of matrix used for the source specimens depended on the size of the respective species. *C. finmarchicus* cephalosome was incubated in 5 μL, *C. glacialis* in 10 μL and *C. hyperboreus* in 30 μL matrix solution. The remaining matrix solution was then used to set up a dilution series with dilutions of 1:1, 1:2, 1:4, 1:8, 1:16, 1:32, 1:64 and 1:128 with further HCCA matrix.

4.3 Results

From all 179 specimens a mass spectrum was obtained. Based on hierarchical clustering (Figure 4.1) and prior morphological staging of copepodites, specimens were randomly chosen for DNA barcoding to support species level identifications. In total, from 49 specimens a DNA barcode with up to 792 bp was obtained, supporting the identifications as *C. glacialis*, *C. hyperboreus* and *C. finmarchicus*. This is further supported by an RF classification model on species level without any misclassifications within the model.

C. finmarchicus was collected mainly from station SV3 at depths ranging from 0 to 50 m (C1 and C2) and 50 to 100 m (C3 to C6f). However, a single adult female was found between 200 to 500 m at station EG1. The identification of this specimen was supported based on proteomic fingerprinting and DNA barcoding. All *C. glacialis* specimens were obtained from station EG1. In depths from 0 to 50 m, all stages were found. From 50 to 200 m stages C2 and C3 and from 200 to 500 m only C6 females were identified. For *C. hyperboreus,* only stages from C2 to adult females were identified, which were all found in 0 to 50 m depth. Copepodids C2, C3 and C6 females were also retrieved from 50 to 200 m. The latter two were also collected at depths from 200 to 500 m.

Hierarchical clustering including all specimens resulted in distinct clusters for the three species (Figure 4.1) supporting the species-specificity of the proteomic fingerprint. Using an RF model on species level, none of the analyzed specimens was misclassified. However, five classifications were recognized by the *post-hoc* test as false positives (Table 4.2A). In addition, all species show a more or less pronounced clustering by stages. In *C. finmarchicus* C1, C2 and C6f specimens show strong stage-specific clustering with only two C1 specimens clustering with C2 specimens (Figure 4.1). Copepodids C3 to C5 also cluster stage-specifically, but clustering of single specimens with specimens from other stages happens more frequently. The same is true for the different stages of *C. hyperboreus* and *C. glacialis*. In both species, stages tend to cluster into stage-specific clusters. However, variability is more pronounced compared to C1, C2 and C6f in *C. finmarchicus* (Figure 4.1). Species and stage differentiation is also emphasized by a t-SNE analysis, showing distinct groups for the species and, within these, clear separations for the respective copepodite stages (Figure 4.2A). This also depicts the more pronounced differentiation of *C. finmarchicus* C1 and C2 specimens compared to the remaining stages. Pairwise adonis between all species-stage combinations shows significant differences (p-value < 0.01) for all pairs, supporting differentiation of ontogenetic stages based on protein mass spectra.
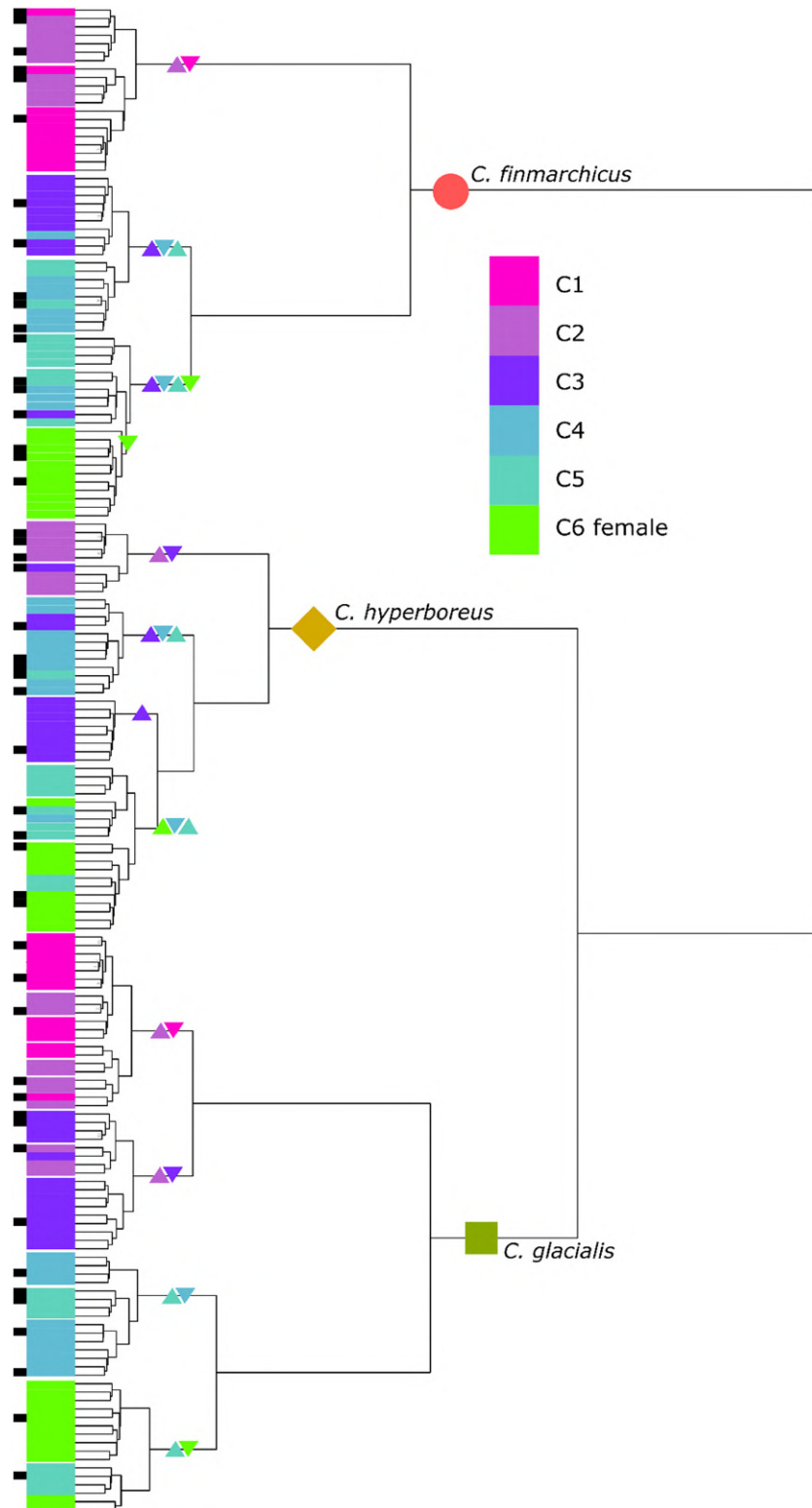
Figure 4.1: Hierarchical clustering of copepodite stages C1-C6f of the three *Calanus* species included in this study. Species names indicate branches including only specimens of the respective species. Triangles indicate copepodite stages included in a certain branch. Colored tips indicate the stage of the respective specimen. The analysis supports a clear species-specific signal and illustrates similarity of certain copepodite stages within a species. Black bars indicate specimens analyzed using DNA barcoding.

Table 4.2: Classification errors within Random Forest (RF) models generated in this study and classification error of classification tests. In classification tests, one specimen was taken out of the model and classified using the remaining specimens. (a) Species level model without stages assigned within the classification test. (b) Species-stage level model and classification test. (c) Model containing only adult specimens and test of classification of juvenile specimens. (d) Model containing only juvenile specimens and test of classification of adult specimens

Species	Stage	Within RF model			RF classification		post hoc test			
		n specimens	n misassigned	Class error	n correct	n incorrect	n tp	n fp	n fn	n tn
C. finmarchicus	not assigned	61	0	0	61	0	57	4	0	0
C. glacialis	not assigned	69	0	0	69	0	67	2	0	0
C. hyperboreus	not assigned	49	0	0	49	0	45	4	0	0
Total		179	0		179	0	169	10	0	0

Species	Stage	Within RF model			RF classification		post hoc test			
		n specimens	n misassigned	Class error	n correct	n incorrect	n tp	n fp	n fn	n tn
C. finmarchicus	C1	10	1	0.10	9	1	9	0	0	1
C. finmarchicus	C2	10	1	0.10	9	1	8	1	1	0
C. finmarchicus	C3	10	1	0.10	9	1	9	0	1	0
C. finmarchicus	C4	10	2	0.20	8	2	7	1	1	1
C. finmarchicus	C5	10	3	0.30	7	3	6	1	0	3
C. finmarchicus	C6f	11	0	0.00	11	0	10	1	0	0
C. glacialis	C1	13	0	0.00	13	0	13	0	0	0
C. glacialis	C2	11	1	0.09	10	1	9	1	0	1
C. glacialis	C3	14	1	0.01	13	1	12	1	0	1
C. glacialis	C4	11	0	0.00	11	0	11	0	0	0
C. glacialis	C5	8	1	0.13	7	1	6	1	1	0
C. glacialis	C6f	12	0	0.00	12	0	10	2	0	0
C. hyperboreus	C2	8	0	0.00	8	0	8	0	0	0
C. hyperboreus	C3	11	3	0.27	8	3	7	1	1	2
C. hyperboreus	C4	10	1	0.10	8	2	7	1	1	1
C. hyperboreus	C5	10	2	0.20	8	2	8	0	1	1
C. hyperboreus	C6f	10	2	0.20	9	1	8	1	0	1
Total		179	19		160	19	148	12	7	12

Model containing only adult specimens		Within RF model			Classification of juvenile specimens		*post hoc* test			
Species	Stage	n specimens	n misassigned	Class error	n correct	n incorrect	n tp	n fp	n fn	n tn
C. finmarchicus	adult	11	0	0	50	0	30	20	0	0
C. glacialis	adult	12	0	0	56	1	5	51	3	0
C. hyperboreus	adult	10	0	0	36	3	21	15	0	0
Total		33	0		142	4	56	86	3	0
Model containing only juvenile specimens		**Within RF model**			**Classification of adult specimens**		*post hoc* **test**			
Species	Stage	n specimens	n misassigned	Class error	n correct	n incorrect	n tp	n fp	n fn	n tn
C. finmarchicus	juvenile	50	0	0	11	0	10	1	0	0
C. glacialis	juvenile	57	0	0	12	0	8	4	0	0
C. hyperboreus	juvenile	39	0	0	10	0	10	0	0	0
Total		146	0		33	0	33	0	0	0
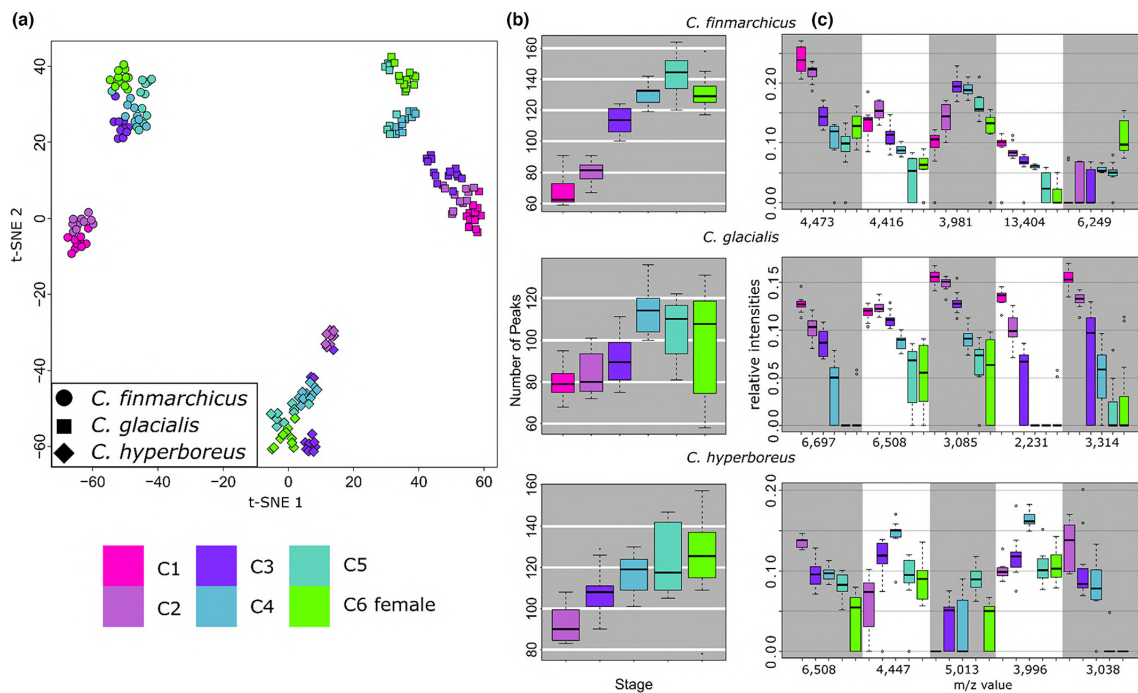
Figure 4.2: A t-SNE plot of the *Calanus* specimens included in this study, shape-coded by species and color-coded by stage. **B** Number of peaks per species and stage. **C** Relative intensities of the five most important mass peaks for classification using Random Forest displayed by species and stage. Color coding in all images according to the legend in the bottom left side.

A RF classification model using stages by species as classes results in model-class errors ranging from 0 to 0.3 (Table 4.2B). In *C. glacialis* all specimens were classified as the correct copepodite stage within the model except for one individual of stages C2, C3 and C5 each. In *C. finmarchicus*, no misclassification was found for the adult specimens; in C1 to C3 one specimen each was misclassified. Moreover, two specimens in C4 and three in C5 show ambiguous signals. In *C. hyperboreus,* no misclassifications were found for C2 specimens. However, for the remaining stages between one to three specimens each showed ambiguous classifications within the model.

In a classification test, single specimens were removed from the RF training data set and subsequently classified using the classification model. On stage level, the classification test resulted in correct stage classifications for the vast majority. In total, of 179 specimens, 160 (89.4%) were staged correctly. Of the 19 misclassified specimens, seven are considered false negatives. Thus, their misclassification would have been recognized. The classifications of the remaining 12 specimens were considered correct by the *post-hoc* test, making these unrecognized misclassifications (Table 4.2B). Twelve correctly classified specimens were considered false positives by the *post-hoc* test. None of the specimens were assigned to a different species but only to a different stage. The majority of these stage misclassifications occurred for neighboring classes. Only one *C. finmarchicus* C3 was classified as a C5 specimen. Of 61 *C. finmarchicus* specimens eight (13.1%) were misassigned, of 49 *C. hyperboreus* eight (16.3%) were misassigned and for *C. glacialis,* of 69 specimens only two (2.9%) were misclassified. It must be noted that the training dataset was

smallest for *C. hyperboreus.*

The classification approach mentioned above with a complete reference library showed high correct classification rates. However, comprehensive libraries are not always available. Thus, we tested the classification success in the absence of either adult or juvenile specimens.

Using a reference library including only adult specimens, the success rate was still very high. Of 145 classified specimens, four (2.8%) were classified as another species. However, only 56 were recognized by the *post-hoc* test as true positives (Table 4.2C). The smaller the developmental stage of the classified specimen, the more likely it was to be recognized as false positive by the *post-hoc* test with lower p-values. Conversely, including only C1-C5 specimens in the RF model resulted in successful classification of all adult specimens in the data set. Of these, five specimens were assigned by the *post-hoc* test as false positives with $p < 0.01$ (Table 4.2D).

First differences among mass spectra of the different copepodite stages are apparent, when looking at the raw spectra of the different stages (Figure 4.3). With increasing ontogenetic stages, dominant mass peaks of sizes larger than $m/z 10000$ are becoming smaller in relation to the remaining signal (Figure 4.3 arrowed). This remains true for all three investigated species. However, regarding the most important mass peaks for stage differentiation (Figure 4.2C), as retained from RF analyses, among the five most important peaks for stage classification almost no peak larger than m/z 10000 was found. Only in *C. finmarchicus* the 13404 peak was identified as the decisive peak, which showed decreasing relative intensity with increasing developmental stages (Figure 4.2C). From the RF model, important peaks for stage classification were present in most stages rather than being present in a single stage. Older stages of all species generally showed more peaks but at the same time decreasing intensities of the classification peaks (Figure 4.2B). Thus, relative intensities seem to be important for discrimination and the differences among copepodite stages may be attributable to increasing mass spectra complexity with the ontogenetic stage and partly to the relative intensities of some larger molecules.

Even though the results rather point at relative intensities being responsible for stage discrimination in RF classification, still an effect of less biomass resulting in less overall mass peaks and subsequently in stage distinction needs to be excluded. Thus, using a dilution series of material taken from additional adult specimens, the influence of the amount of biomass on mass spectra was tested. However, dilutions of up to 1:128 of the original concentration did not result in patterns, as they were found in mass spectra from smaller ontogenetic stages (Figure 4.4). Also in clustering approaches, t-SNE plots (Figure 4.5A) or RF models and classification tests, these were not more likely to be assigned to smaller stages. At least for *C. finmarchicus* and *C. hyperboreus*, dilution of matrix:tissue ratio resulted in a decreasing number of peaks (Figure 4.5B) making the amount of peaks comparable to smaller ontogenetic stages. Still, this did not result in making C6f mass spectra more similar to those obtained from smaller ontogenetic stages. This is also emphasized by Euclidean distances of the different stages and dilutions to C1 (C2 in *C. hyperboreus*) (Figure 4.5C). In all species, Euclidean
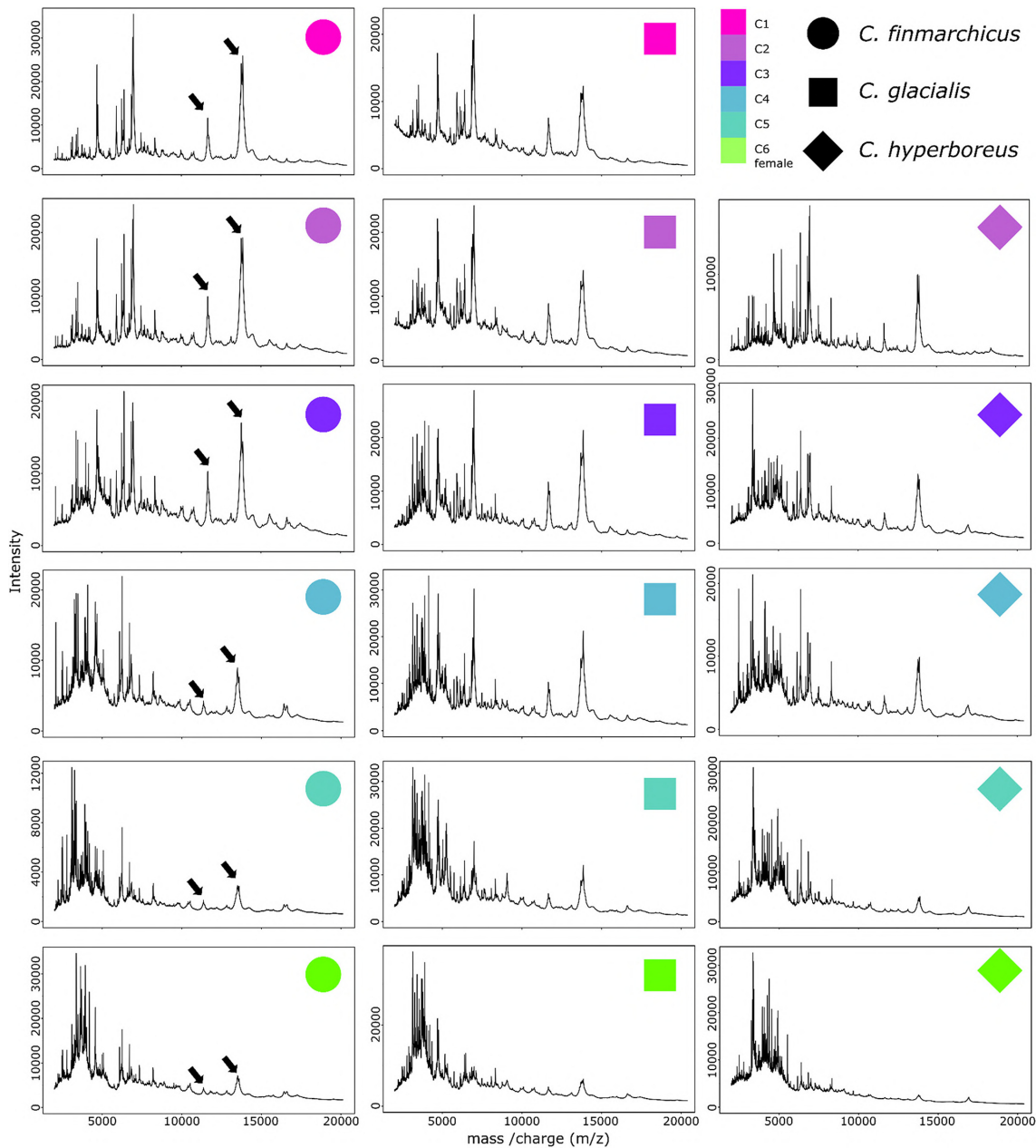
Figure 4.3: Raw mass spectra from all copepodite stages of the investigated three *Calanus* species. Displayed mass spectra are averaged from all specimens of the respective species and stage. In all species dominant peaks of larger molecules (>m/z 10 000) show decreasing relative intensities with increasing ontogenetic stages (arrowed in *C. finmarchicus*).

distances of mass spectra from different stages increased with each stage. The distances further increased to mass spectra obtained from diluted samples, even though the number of peaks became more similar to mass spectra obtained from smaller stages (compare Figure 4.2B and Figure 4.5B).
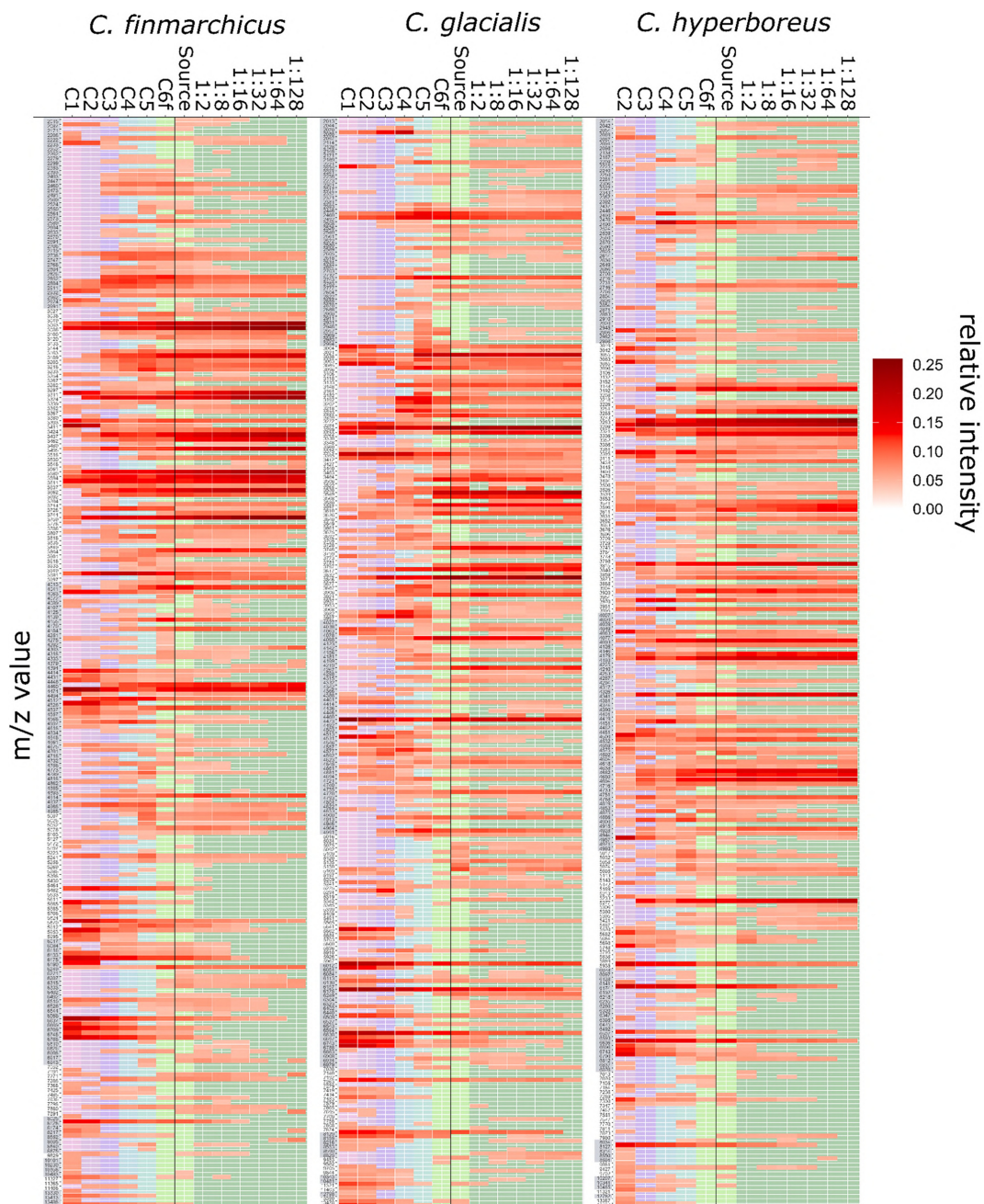
Figure 4.4: Peaks and the respective relative intensities shown for the three *Calanus* species separately by stage and dilution. Sources are mass spectra from protein extracts that have not been diluted. From these, dilutions were produced. In all species, the number of peaks is increasing from younger to older stages. In diluted measurements, the number of peaks is reduced, but the spectra do not resemble the younger stages. As evidenced in Figure 4.5 A spectra derived from dilution of C6f are still clearly separated from other stages in ordination space.

4.4 Discussion

Applying three *Calanus* congeners as model cases, we showed that species identification by proteomic fingerprinting is stable in Calanoida over all ontogenetic stages despite increasing complexity of proteomic profiles during development. Species identification accuracy was 100%, sim-

135
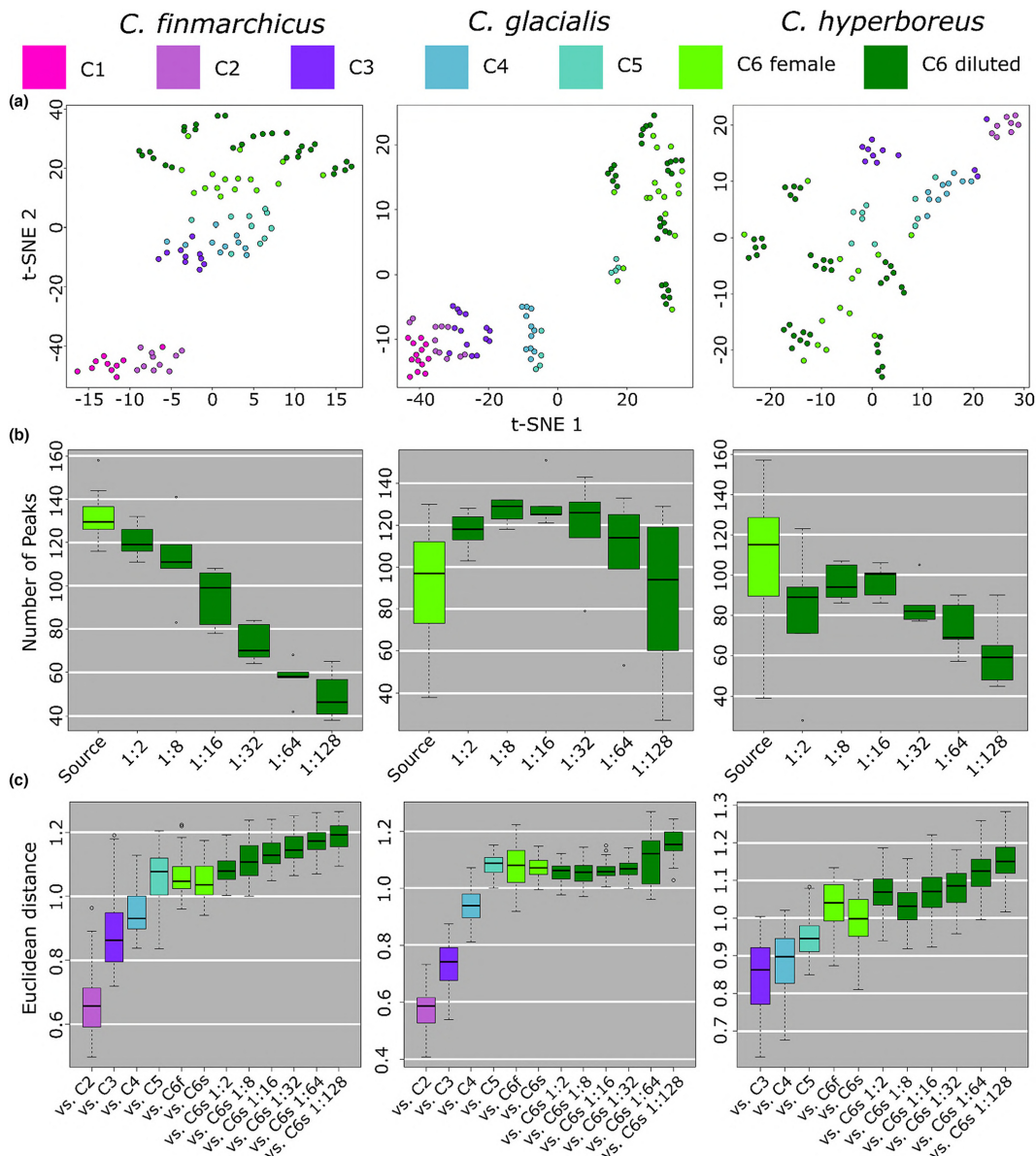
Figure 4.5: A tSNE-plots of the dilution experiments with the three *Calanus* species. Displayed in dark green are mass spectra retained from different dilutions of material taken from C6 female specimens. These mass spectra still are more similar to other adult specimens rather than to juvenile stages. **B** Number of peaks of mass spectra from diluted samples. Undiluted samples are displayed in light green. Diluted samples are represented in dark green. **C** Euclidean distances of the mass spectra from different stages and dilutions to mass spectra from C1 specimens for *C. finmarchicus* and *C. glacialis* and from C2 individuals for *C. hyperboreus*.

ilar to high success rates shown by other studies on Calanoida (Bode et al. 2017; Kaiser et al. 2018; Laakmann et al. 2013). With a success rate of almost 90%, the RF model assigned specimens even to their ontogenetic stages with misassignments mainly occurring between neighboring ontogenetic stages. In an actual application, based on *post-hoc* test results, classifications of 148 specimens (82.68%) would be accepted (tp); for 19 specimens (fp and fn) the test would recommend a (morphological) re-investigation of the specimens. Correct morphological staging of these

specimens would then add up the total correct stage classification of 167 specimens (93.30%). Only 12 (6.70%) misclassifications would remain undiscovered.

Reliable morphological species identification is, specifically in zooplankton, often restricted to adult stages. For application of proteomic fingerprinting in monitoring or field studies it would be highly beneficial, if species identification of juveniles could be done based on an adult reference library only. For all three *Calanus* species it was possible to identify most juvenile specimens using the adult reference library, however, with lower success regarding the *post-hoc* test for the RF classification. Conversely, adult specimens were reliably identified using a juvenile-based library. This, as well as the increasing number of peaks in later developmental stages, implies that major components of the proteomic fingerprint are acquired already in early stages, but some peaks are only found in later developmental stages. Observed differences in the proteome among ontogenetic stages in other calanoid copepod species were, similar to our findings, always smaller than interspecific differences (Kaiser et al. 2018; Laakmann et al. 2013).

Differences among stages were found in proteomic spectra of different arthropod species, albeit to varying degrees. While nymphal and adult stages of the insect Heteroptera *Cimex hirundinis* (Lamarck, 1816) differed distinctly, still several major homologous peaks were detected in both stages with more complexity in adult patterns (Hamlili et al. 2021). Similar differences between nymphal and adult stages were observed for the acarid *Ixodes ricinus* (Linnaeus, 1758) (Karger et al. 2019). Proteomic spectra of phlebotomine sand fly larvae were distinguishable at the species level and quite stable (Halada et al. 2018), contrasting the distinct differences we observed among copepodite stages in *Calanus*. However, after metamorphosis, spectra of adult sand flies strongly changed with more peaks being expressed. This fundamental change has also been observed for other holometabolous insects, e.g. ceratopogonid and culicid larvae, which showed only a small number of identical peaks between adult and larvae (Steinmann et al. 2013). Therefore, larvae were not identified in their approach as the respective adults of the species from the reference library. Overall changes in the proteomic fingerprint observed in *Calanus* species were less pronounced than in these insects. Because juvenile and adult pelagic copepods share the same habitat and do not undergo such drastic morphological changes, a more uniform proteome composition can be expected. Although nauplii stages of *Calanus* were not considered in the present study, Laakmann et al. (2013) demonstrated the stability of species identification based on proteomic spectra even when nauplii were included.

In contrast to genetic markers, proteomic spectra are more variable and influenced by the environment, reflecting physiological responses (Karger et al. 2019). We observed several well-expressed peaks in the later copepodite stages (which remained abundant also in diluted samples) that are completely missing in younger stages, e.g. in copepodids C1 and C2. This is most likely a consequence of severe physiological changes with a certain stage. Drastic changes in the expression of genes with changing copepodite stages have been observed for several processes such as lipid biosynthesis (Lenz et al. 2014). This may be also the reason for the observed misclassifica-

tion between stages. These misclassified specimens may have been in an intermoult condition, in which the specimens would be physiologically advanced, but still showing the exoskeleton of a previous stage. Based on the m/z values only, it remains, however, pure speculation, which processes are behind the observed patterns. It cannot be ruled out with certainty that external factors could also have caused changes in the composition and patterns of proteomic spectra. To date, there is no information about mass spectra variability of marine species based on their distribution range and environmental conditions. Mass-spectra variability due to different ontogenetic stages may also be affected by abiotic or ecological differences such as varying temperatures, salinities or feeding regimes. This may not only be relevant for stage separation but also for the general composition of the library. Caution needs to be taken when applying proteomic fingerprinting for the identification of widely distributed species. Reference libraries may need updates from different investigated regions of the species´ distribution range. Otherwise, similar to the identification of juveniles based on an adult-specimen reference library, problems may occur either with classification or at least with classification supported by a *post-hoc* test, because the reference library may not cover the full mass spectra variability of a widely distributed species.

However, if stage specificity of proteomic profiles as observed here is confirmed to be universal also e.g. in controlled experiments, this would be an extreme advantage of MALDI-TOF analyses in monitoring applications. While in a morphological assessment, staging of *Calanus* specimens would be possible, species identification would hardly be possible due to the lack of taxonomic features throughout the younger developmental stages (Laakmann et al., 2020). Thus, a rapid biodiversity assessment using proteome fingerprinting would be superior to a mere morphological or molecular-genetic approach, since the identification of the developmental stage as well as the species could be performed in only one analytical step and provide supplementary information on the recruitment processes and generations of investigated copepod populations. Compared to the MALDI-TOF MS, the alternative approach on morphological staging and genetic barcoding is less cost-effective and more time consuming (Kaiser et al. 2018; Rossel et al. 2019).

Costs of consumables for proteomic fingerprinting range between €0.02 to €0.75 per specimen (depending on amount of matrix used), compared to at least €5.65 for DNA barcoding (Rossel et al. 2019, see the supplementary material of the study for a detailed list of the costs). Those calculations did not include labor costs and general lab equipment such as thermocyclers for barcoding or the mass spectrometer for proteomic fingerprinting. In a study on expenses for microbiological identifications including labor, costs were summed up to $61.39 for molecular sequencing and $6.44 for MALDI-TOF MS identifications (Tran et al. 2015). The major bottleneck of MALDI-TOF MS is instrument accessibility. Prices are high and therefore instruments are not acquirable for everyone. Still, due to its low costs for consumables it is said that instrument costs offset after a few years of usage (Tran et al. 2015). Costs for application of MALDI-TOF MS are mainly influenced by the amount of HCCA matrix for specimen preparation. Specimens in the present study were rather large, and thus a comparably higher volume of matrix was used,

increasing costs. These could be lowered by using smaller body parts and less HCCA matrix. In the present study, conditions for all species were kept as similar as possible by using the complete prosome body part for measurements. This may not be necessary as smaller parts can be suitable as well. For instance, using only legs of analyzed specimens for instance was shown to work well in other species such as deep-sea isopods to differentiate between specimens of a cryptic-species complex (Kürzel et al. 2022; Paulus et al. 2022).

In a further approach it could be investigated, if even more power lies in proteomic fingerprinting for community assessments. Rossel and Martínez Arbizu (Rossel et al. 2019) reported about the discrimination of adult harpacticoid copepods between sexes in some species. Including this in future assessments would increase the resolution accomplished using mass spectrometry even more.

4.5   Acknowledgment

4.6   Data availability statement

MALDI-TOF MS raw data and respective meta data are stored at Dryad data repository (10.5061/dryad.3r2280gkc . Additionally, R-scripts for processing of data on species and stage level are stored here. This includes a script for parallel computing for classification approaches. COI data can be found in the BOLD project *Calanus* stage identification using proteome fingerprinting (CSIPF) and on GenBank (Accession numbers ON480204-ON48025).

References

Altschul, SF, Madden, TL, Schäffer, AA, Zhang, J, Zhang, Z, Miller, W, and Lipman, DJ (1997). Gapped BLAST and PSI-BLAST: a new generation of protein database search programs. *Nucleic Acids Res* 25, 3389–3402.

Beaugrand, G, Luczak, C, and Edwards, M (2009). Rapid biogeographical plankton shifts in the North Atlantic Ocean. *Glob Change Biol* 15, 1790–1803.

Benson, DA, Cavanaugh, M, Clark, K, Karsch-Mizrachi, I, Lipman, DJ, Ostell, J, and Sayers, EW (2012). GenBank. *Nucleic Acids Res* 41, 36–42.

Bode, M, Laakmann, S, Kaiser, P, Hagen, W, Auel, H, and Cornils, A (2017). Unravelling diversity of deep-sea copepods using integrated morphological and molecular techniques. *J Plankton Res* 39, 600–617.

Breimann, L (2001). Random Forests. *Mach learn* 45, 5–32.

Brodskii, K, Vyshkvartseva, N, Kos, M, and Markhatseva, E (1983). Copepods (Copepoda: Calanoida) of the seas of the USSR and adjacent waters. *Keys to the fauna of the USSR* 1, 358.

Chen, X-F, Hou, X, Xiao, M, Zhang, L, Cheng, J-W, Zhou, M-L, Huang, J-J, Zhang, J-J, Xu, Y-C, and Hsueh, P-R (2021). Matrix-assisted laser desorption/ionization time of flight mass spectrometry (MALDI-TOF MS) analysis for the identification of pathogenic microorganisms: a review. *Microorganisms* 9, 1536.

Cheng, F, Wang, M, Sun, S, Li, C, and Zhang, Y (2013). DNA barcoding of Antarctic marine zooplankton for species identification and recognition. *Adv Polar Sci* 24, 119–127.

Choquet, M, Hatlebakk, M, Dhanasiri, AKS, Kosobokova, K, Smolina, I, and Søreide, JE (2017). Genetics redraws pelagic biogeography of *Calanus*. *Biol Lett* 13, 20170588.

Choquet, M, Kosobokova, K, Kwasniewski, S, Hatlebakk, M, Dhanasiri, AKS, and Melle, W (2018). Can morphology reliably distinguish between the copepods *Calanus finmarchicus* and *C. glacialis*, or is DNA the only way? *Limnol Oceanogr Methods* 16, 237–252.

Dieme, C, Yssouf, A, Vega-Rúa, A, Berenger, J-M, Failloux, A-B, Raoult, D, Parola, P, and Almeras, L (2014). Accurate identification of Culicidae at aquatic developmental stages by MALDI-TOF MS profiling. *Parasit Vectors* 7, 544.

Folmer, O, Black, MB, and C, VR (1994). DNA primers for amplification of mitochondrial cytochrome c oxidase subunit I from diverse metazoan invertebrates. *Mar Biol Biotechnol* 3, 294–299.

Gabrielsen, TM, Merkel, B, Søreide, JE, Johansson-Karlsson, E, Bailey, A, Vogedes, D, Nygård, H, Varpe, Ø, and Berge, J (2012). Potential misidentifications of two climate indicator species of the marine arctic ecosystem: *Calanus glacialis* and *C. finmarchicus*. *Polar Biol* 35, 1621–1628.

Gibb, S (2015). *MALDIquantForeign: Import/Export routines for MALDIquan. A package for R*.

Gibb, S and Strimmer, K (2012). MALDIquant: a versatile R package for the analysis of mass spectrometry data. *Bioinform* 28, 2270–2271.

Halada, P, Hlavackova, K, Dvorak, V, and Volf, P (2018). Identification of immature stages of phlebotomine sand flies using MALDI-TOF MS and mapping of mass spectra during sand fly life cycle. *Insect Biochem Mol Biol* 93, 47–56.

Hamlili, FZ, Bérenger, J-M, Diarra, AZ, and Parola, P (2021). Molecular and MALDI-TOF MS identification of swallow bugs *Cimex hirundinis* (Heteroptera: Cimicidae) and endosymbionts in France. *Parasit Vectors* 14, 587.

Han, H, Guo, X, and Yu, H (2016). Variable selection using mean decrease accuracy and mean decrease gini based on random forest. *2016 7th IEEE International Conference on Software Engineering and Service Science (ICSESS)*, 219–224.

Hasnaoui, B, Diarra, AZ, Berenger, J-M, Medkour, H, Benakhla, A, Mediannikov, O, and Parola, P (2022). Use of the proteomic tool MALDI-TOF MS in termite identification. *Sci Rep* 12, 718.

Hebert, PDN, Cywinska, A, Ball, SL, and deWaard, JR (2003). Biological identifications through DNA barcodes. *Proc R Soc B* 270, 313–321.

Hill, R, Allen, L, and Bucklin, A (2001). Multiplexed species-specific PCR protocol to discriminate four N. Atlantic *Calanus* species, with an mtCOI gene tree for ten *Calanus* species. *Mar Biol* 139, 279–287.

Holst, S, Heins, A, and Laakmann, S (2019). Morphological and molecular diagnostic species characters of Staurozoa (Cnidaria) collected on the coast of Helgoland. *Mar Biol* 49, 1775–1797.

Hynek, R, Kuckova, S, Cejnar, P, Junková, P, Přikryl, I, and Říhová Ambrožová, J (2018). Identification of freshwater zooplankton species using protein profiling and principal component analysis. *Limnol Oceanogr: Methods* 16, 199–204.

Kaiser, P, Bode, M, Cornils, A, Hagen, W, Arbizu, PM, and Auel, H (2018). High-resolution community analysis of deep-sea copepods using MALDI-TOF protein fingerprinting. *Deep-Sea Res I* 138, 122–130.

Karger, A, Bettin, B, Gethmann, JM, and Klaus, C (2019). Whole animal matrix-assisted laser desorption/ionization time-of-flight (MALDI-TOF) mass spectrometry of ticks – are spectra of *Ixodes ricinus* nymphs influenced by environmental, spatial, and temporal factors? *PLOS ONE* 14, 0210590.

Korfhage, SA, Rossel, S, Brix, S, McFadden, CS, Ólafsdóttir, SH, and Martínez Arbizu, P (2022). Species delimitation of Hexacorallia and Octocorallia around Iceland using nuclear and mitochondrial DNA and proteome fingerprinting. *Front Mar Sci* 9, 838201.

Krijthe, J (2015). *R wrapper for van der Maaten's Barnes-Hut implementation of t-distributed stochastic neighbor embedding.*

Kürzel, K, Kaiser, S, Lörz, A-N, Rossel, S, Paulus, E, Peters, J, Schwentner, M, Martínez Arbizu, P, Coleman, CO, Svavarsson, J, and Brix, S (2022). Correct species identification and its implications for conservation using Haploniscidae (Crustacea, Isopoda) in Icelandic waters as a proxy. *Front Mar Sci* 8.

Kwasniewski, S, Gluchowska, M, Jakubas, D, Wojczulanis-Jakubas, K, Walkusz, W, and Karnovsky, N (2010). The impact of different hydrographic conditions and zooplankton communities on provisioning little auks along the west coast of Spitsbergen. *Prog Oceanogr* 87, 72–82.

Laakmann, S, Blanco-Bercial, L, and Cornils, A (2020). The crossover from microscopy to genes in marine diversity: from species to assemblages in marine pelagic copepods. *Philos Trans R Soc Lond B Biol Sci* 375, 20190446.

Laakmann, S, Gerdts, G, Erler, R, Knebelsberger, T, Martínez Arbizu, P, and Raupach, MJ (2013). Comparison of molecular species identification for North Sea calanoid copepods (Crustacea) using proteome fingerprints and DNA sequences. *Mol Ecol Resour* 13, 862–876.

Legendre, P and Gallagher, ED (2001). Ecologically meaningful transformations for ordination of species data. *Oecologia* 129, 271–280.

Lenz, PH, Roncalli, V, Hassett, RP, Wu, L-S, Cieslak, MC, Hartline, DK, and Christie, AE (2014). De novo assembly of a transcriptome for *Calanus finmarchicus* (Crustacea, Copepoda) – the dominant Zooplankter of the North Atlantic Ocean. *PLOS ONE* 9, 88589.

Liaw, A and Wiener, M (2002). Classification and regression by randomForest. *R news* 2, 18–22.

Lindeque, PK, Hay, SJ, Heath, MR, Ingvarsdottir, A, Rasmussen, J, Smerdon, GR, and Waniek, JJ (2006). Integrating conventional microscopy and molecular analysis to analyse the abundance and distribution of four *Calanus* congeners in the North Atlantic. *J Plankton Res* 28, 221–238.

Loaiza, JR, Almanza, A, Rojas, JC, Mejia, L, Cervantes, ND, Sanchez-Galan, JE, Merchán, F, Grillet, A, Miller, MJ, and León, LF (2019). Application of matrix-assisted laser desorption/ionization mass spectrometry to identify species of Neotropical *Anopheles* vectors of malaria. *Malar J* 18, 95.

Maász, G, Takács, P, Boda, P, Várbiró, G, and Pirger, Z (2017). Mayfly and fish species identification and sex determination in bleak (*Alburnus alburnus*) by MALDI-TOF mass spectrometry. *Sci Total Environ* 601, 317–325.

Martínez Arbizu, P (2022). PairwiseAdonis [R].

Mathis, A, Depaquit, J, Dvovrák, V, Tuten, H, Bañuls, A-L, Halada, P, Zapata, S, Lehrter, V, Hlavavcková, K, and Prudhomme, J (2015). Identification of phlebotomine sand flies using one MALDI-TOF MS reference database and two mass spectrometer systems. *Parasit Vectors* 8, 266.

Mazzeo, MF, Giulio, BD, Guerriero, G, Ciarcia, G, Malorni, A, Russo, GL, and Siciliano, RA (2008). Fish authentication by MALDI-TOF mass spectrometry. *J Agric Food Chem* 56, 11071–11076.

Nabet, C, Kone, AK, Dia, AK, Sylla, M, Gautier, M, Yattara, M, Thera, MA, Faye, O, Braack, L, and Manguin, S (2021). New assessment of *Anopheles* vector species identification using MALDI-TOF MS. *Malar J* 20, 1–16.

Nebbak, A, El Hamzaoui, B, Berenger, J-M, Bitam, I, Raoult, D, Almeras, L, and Parola, P (2017). Comparative analysis of storage conditions and homogenization methods for tick and flea species for identification by MALDI-TOF MS. *Med Vet Eentomol* 31, 438–448.

Papagiannopoulou, C, Parchen, R, Rubbens, P, and Waegeman, W (2020). Fast pathogen identification using single-cell matrix-assisted laser desorption/ionization-aerosol time-of-flight mass spectrometry data and deep learning methods. *Anal Chem* 92, 7523–7531.

Paulus, E, Brix, S, Siebert, A, Martínez Arbizu, P, Rossel, S, Peters, J, Svavarsson, J, and Schwentner, M (2022). Recent speciation and hybridization in Icelandic deep-sea isopods: an integrative approach using genomics and proteomics. *Mol Ecol* 31, 313–330.

R-Core-Team (2022). *R: A language and environment for statistical computing (4.1.0)*. R Foundation for Statistical Computing.

Ratnasingham, S and Hebert, PD (2007). BOLD: The barcode of life data system (http://www.barcodinglife.org). *Mol Ecol Resour* 7, 355–364.

Riccardi, N, Lucini, L, Benagli, C, Welker, M, Wicht, B, and Tonolla, M (2012). Potential of matrix-assisted laser desorption/ionization time-of-flight mass spectrometry (MALDI-TOF MS) for the identification of freshwater zooplankton: a pilot study with three *Eudiaptomus* (Copepoda: Diaptomidae) species. *J Plankton Res* 34, 484–492.

Rossel, S, Barco, A, Kloppmann, M, Martínez Arbizu, P, Huwer, B, and Knebelsberger, T (2020). Rapid species level identification of fish eggs by proteome fingerprinting using MALDI-TOF MS. *J Proteomics* 103993.

Rossel, S, Khodami, S, and Martínez Arbizu, P (2019). Comparison of rapid biodiversity assessment of meiobenthos using MALDI-TOF MS and metabarcoding. *Front Mar Sci* 6, 659.

Rossel, S and Martínez Arbizu, P (2018a). Automatic specimen identification of Harpacticoids (Crustacea:Copepoda) using Random Forest and MALDI-TOF mass spectra, including a post hoc test for false positive discovery. *Methods in Ecol Evol* 9, 1421–1434.

Rossel, S and Martínez Arbizu, P (2018b). Effects of sample fixation on specimen identification in biodiversity assemblies based on proteomic data (MALDI-TOF). *Front Mar Sci* 5, 149.

Rossel, S and Martínez Arbizu, P (2019). Revealing higher than expected diversity of Harpacticoida (Crustacea: Copepoda) in the North Sea using MALDI-TOF MS and molecular barcoding. *Sci Rep* 9, 9182.

Ryan, C, Clayton, E, Griffin, W, Sie, S, and Cousens, D (1988). SNIP, a statistics-sensitive background treatment for the quantitative analysis of PIXE spectra in geoscience applications. *Nucl Instrum Meth B* 34, 396–402.

Savitzky, A and Golay, MJ (1964). Smoothing and differentiation of data by simplified least squares procedures. *Anal Chem* 36, 1627–1639.

Singhal, N, Kumar, M, Kanaujia, PK, and Virdi, JS (2015). MALDI-TOF mass spectrometry: an emerging technology for microbial identification and diagnosis. *Front Microbiol* 6.

Steinmann, IC, Pflüger, V, Schaffner, F, Mathis, A, and Kaufmann, C (2013). Evaluation of matrix-assisted laser desorption/ionization time of flight mass spectrometry for the identification of ceratopogonid and culicid larvae. *Parasitol* 140, 318–327.

Tarling, GA, Freer, JJ, Banas, NS, Belcher, A, Blackwell, M, Castellani, C, Cook, KB, Cottier, FR, Daase, M, Johnson, ML, Last, KS, Lindeque, PK, Mayor, DJ, Mitchell, E, Parry, HE, Speirs, DC, Stowasser, G, and Wootton, M (2022). Can a key boreal *Calanus* copepod species now complete its life-cycle in the Arctic? Evidence and implications for Arctic food-webs. *Ambio* 51, 333–344.

Tran, A, Alby, K, Kerr, A, Jones, M, and Gilligan, PH (2015). Cost savings realized by implementation of routine microbiological identification by matrix-assisted laser desorption ionization–time of flight mass spectrometry. *J Clin Microbiol* 53, 2473–2479.

Trudnowska, E, Balazy, K, Stoń-Egiert, J, Smolina, I, Brown, T, and Gluchowska, M (2020). In a comfort zone and beyond—ecological plasticity of key marine mediators. *Ecol Evol* 10, 14067–14081.

Van Driessche, L, Bokma, J, Deprez, P, Haesebrouck, F, Boyen, F, and Pardon, B (2019). Rapid identification of respiratory bacterial pathogens from bronchoalveolar lavage fluid in cattle by MALDI-TOF MS. *Sci Rep* 9, 18381.

Volta, P, Riccardi, N, Lauceri, R, and Tonolla, M (2012). Discrimination of freshwater fish species by matrix-assisted laser desorption/ionization-time of flight mass spectrometry (MALDI-TOF MS): a pilot study. *J Limnol* 71, 17.

Weydmann, A, Carstensen, J, Goszczko, I, Dmoch, K, Olszewska, A, and Kwasniewski, S (2014a). Shift towards the dominance of boreal species in the Arctic: inter-annual and spatial zooplankton variability in the West Spitsbergen Current. *Mar Ecol Prog Ser* 501, 41–52.

Weydmann, A, Coelho, NC, Ramos, AA, Serrão, EA, and Pearson, GA (2014b). Microsatellite markers for the Arctic copepod *Calanus glacialis* and cross-amplification with *C. finmarchicus*. *Conserv Genet Resour* 6, 1003–1005.

Weydmann, A and Kwasniewski, S (2008). Distribution of *Calanus* populations in a glaciated fjord in the Arctic (Hornsund, Spitsbergen)—the interplay between biological and physical factors. *Polar Biol* 31, 1023–1035.

Weydmann, A, Przyłucka, A, Lubośny, M, Walczyńska, KS, Serrão, EA, Pearson, GA, and Burzyński, A (2017). Mitochondrial genomes of the key zooplankton copepods Arctic *Calanus glacialis* and North Atlantic *Calanus finmarchicus* with the longest crustacean non-coding regions. *Sci Rep* 7, 13702.

Wilke, T, Renz, J, Hauffe, T, Delicado, D, and Peters, J (2020). Proteomic fingerprinting discriminates cryptic gastropod species. *Malacologia* 63, 131–137.

Yssouf, A, Parola, P, Lindström, A, Lilja, T, L'Ambert, G, Bondesson, U, Berenger, J-M, Raoult, D, and Almeras, L (2014). Identification of European mosquito species by MALDI-TOF MS. *Parasitol Research* 113, 2375–2378.

SYNOPTIC DISCUSSION

The current changes in the Arctic, mainly due to anthropogenic impacts, are occurring over mere decades. This rapid pace offers limited time for Arctic organisms to adapt, potentially leading to significant ecological consequences. Therefore, a better understanding of climate change effects on species and potential mechanisms driving shifts in community structures is crucial.

This thesis aims to enhance our understanding of how aspects of climate change affect the ecology and dynamics of zooplankton in the Arctic ecosystem. It integrates biological, ecological, oceanographic and new technical approaches to provide a comprehensive perspective. Chapter I and II focus on the physiological responses, trophic structures and ecological interactions of zooplankton species. The findings emphasize that Arctic zooplankton species are rather resilient to rising temperatures and changes in food web structures, indicated by a lack of metabolic stress response, a relatively wide thermal tolerance window and considerable dietary flexibility. More importantly, increasing importance of ecological interactions of Arctic species with invading boreal congeners might lead to increasing competitive pressure as a major driver for regime shifts (Kaiser et al. 2022).

Chapter III examines the impact of submesoscale hydrographic features on species distribution and advection processes. This chapter highlights the crucial role that these dynamics play in structuring the pelagic realm and potentially facilitating Atlantification processes through high-velocity jets (Kaiser et al. 2021).

Finally, proteomic fingerprinting was introduced as a reliable, efficient and cost-effective alternative to traditional morphological or genetic approaches for species identification in Chapter IV. The technique's ability to discriminate not only between species, but also between developmental stages heralds a new era in rapid monitoring and biodiversity assessments (Rossel et al. 2023).

The following discussion concentrates on key representatives of the polar Arctic zooplankton community: the primarily herbivorous copepods *Calanus hyperboreus* and *Calanus glacialis*, the carnivorous copepod *Paraueuchaeta glacialis* and the amphipod *Themisto libellula*. *Calanus finmarchicus*, *Paraeuchaeta norvegica* and *Themisto abyssorum* are further considered as boreal-Atlantic expatriates. The section focuses on evaluating the impacts of climate change on these species, specifically investigating how rising temperatures influence their physiology and analyzing the consequences of reduced ice algal productivity, linked to a decrease in sea ice, on the food web dynamics. Additionally, ecological implications of the northward range shift of boreal species

are examined. It is important to note, that the mechanisms described for these species may not be generally applicable to other Arctic zooplankton taxa. Yet, based on the physiological response, trophic dynamics and potential ecological interactions of these species, this study aims to establish a framework for understanding how changes in the Arctic ecosystem could impact pelagic species and dynamics.

Physiological and ecological implications of rising temperatures

Temperature plays a crucial role in biological processes. Organisms exhibit distinct thermal tolerance windows, determining their rate of metabolic performance and ultimately defining their biogeographic distribution (Schulte et al. 2011). Arctic species live at the lower end of temperatures observed in the marine environment, leaving them limited scope to adjust their distribution with ongoing global warming. Consequently, determining their thermal tolerance range and assessing their response to warming is essential in evaluating their ability to cope with rising temperatures. In addition, this assessment is vital to understand potential drivers of regime shifts.

Arctic zooplankton in a warming ocean

Arctic zooplankton species are more resilient to warming than expected, indicated by a rather eurytherm metabolic response and relatively broad thermal tolerance windows of all species investigated (Chapter I). The slow increase in metabolic rates (low Q_{10} values) contradicts a stenothermic response, which is typically characterized by a sharp increase in metabolism, a narrow optimum and a steep decline at elevated temperatures (high Q_{10} values, Pörtner et al. 2017).

At its lower and upper end, the thermal window is restricted by absolute physiological temperature limits, which are defined as temperatures at which 50% mortality occurs (Pörtner et al. 2017). Lower critical or lethal temperatures are generally not relevant for Arctic zooplankton species, as they are adapted to and able to cope with lowest *in situ* temperatures down to the freezing point of seawater (Pörtner 2012). Upper lethal limits were observed at 12 °C for Arctic *Calanus hyperboreus* and *C. glacialis* (Chapter I), although the small number of replicates at this temperature may not be representative. Even higher temperatures (> 15 °C) have been reported for these *Calanus* species by Hirche (1987). For *Paraeuchaeta glacialis* no comparable literature data are available, whereas for *Themisto libellula* earlier studies reported lethal temperatures at 9 °C (Percy 1993) or 14 °C (Wing 1976). The high survival rates at 8 °C and missing metabolic stress response of both species (Chapter I) suggest that the lethal limit of *P. glacialis* has not yet been reached and supports the higher lethal temperatures observed by Wing (1976) for *T. libellula*. Very high lethal temperatures (20 °C) are reported for Arctic krill *Thysanoessa inermis* (Huenerlage et al. 2016), emphasizing the ability of Arctic zooplankton species to tolerate temperatures distinctly above those within their natural distribution range. This tolerance could be particularly important considering marine heat waves (MHW). MHW are defined as anomalously warm water events, lasting from days to months (Mohamed et al. 2022), and expected to increase in frequency and intensity (Frölicher and Laufkötter 2018).

The observed wider thermal tolerance is supported by studies on the performance of *Calanus* (Henriksen et al. 2012; Hirche and Kosobokova 2007; Kjellerup et al. 2012), supporting that Arctic zooplankton species are rather resilient to warming. They maintain or even enhance their metabolism (Aarflot et al. 2023; Hatlebakk et al. 2022), potentially resulting in accelerated development and shortened life cycles. Above a certain temperature threshold, however, performance losses may occur (Grote et al. 2015; Hildebrandt et al. 2014). Defining this threshold is still an area of investigation and potentially differs across taxa, between populations (phenotypic plasticity) and developmental stages, and may also be affected by external factors such as food availability. Performance losses were reported in some studies for Arctic *Calanus* species between temperatures of 5 to 10 °C, suggesting that these temperatures could be approaching such a threshold (Alcaraz et al. 2014; Hildebrandt et al. 2014; Pasternak et al. 2013).

Competitive scope of Arctic and boreal species

Boreal species are expatriates in high-latitude environments, and Arctic *in situ* temperatures are typically at the lower end of their thermal windows. Although boreal species such as *C. finmarchicus* can somewhat cope with the low *in situ* temperatures, they experience limitations in reproduction and/or development. With ongoing warming, however, temperatures in the Arctic pelagic environment are changing towards conditions, which support optimal performance for boreal species (Chapter I).

In contrast to their Arctic congeners, boreal species show a more rapid and steeper increase in metabolic rates with rising temperatures, as indicated by higher Q_{10} values (Chapter I), suggesting higher activity and thus a more active lifestyle. The high metabolic demand is reflected in increased performances at higher temperatures (Hirche et al. 1997; Pasternak et al. 2013), with *C. finmarchicus* surpassing for instance egg production rates of *C. glacialis* at temperatures above 5 to 7.5 °C (Kjellerup et al. 2012).

While Arctic species are physiologically more tolerant to ocean warming than expected, this implies that they might face increased competition by their better adapted Atlantic congeners beyond a certain temperature threshold in areas of strong distribution overlap (Chapter I). Figure 1 presents a conceptual sketch illustrating the impact of rising temperatures on the performance of investigated Arctic versus boreal-Atlantic species. At low temperatures, Arctic zooplankton species are more effectively adapted and exhibit superior performance compared to their boreal counterparts, thereby having a competitive advantage. The enhanced performance of Arctic species in colder conditions may indicate a metabolic cold adaptation. This concept suggests that polar ectotherms possess higher metabolic rates to overcome the effects of low temperature (Peck 2018 and references therein). The inferior performance of boreal species at low temperatures may also be related to physiological limitation due to an increased stress response (Smolina et al. 2015). With increasing temperature, the performance of both Arctic and boreal species increases. However, while the performance of Arctic species shows only slow and weak responses,

149

the performance of boreal species rapidly increases. Around a proposed threshold of 5 to 6 °C, the performance of boreal species surpasses that of Arctic species, which is stagnating and/or starting to decline around these temperatures. While the overall absolute tolerance range of Arctic species might only be slightly narrower than that of their boreal relatives, their performance is adversely affected at temperatures above 7 to 10 °C, a range in which boreal species continue to thrive. It is important to note that these specific temperature windows are based on studies on Arctic and boreal-Atlantic *Calanus* species. For other Arctic and boreal congeneric pairs, the exact temperature thresholds potentially differ, but the overarching concept may still be applicable. Similar lethal (> 14 °C) and physiologically (7 to 8 °C) limiting temperatures were proposed for *T. libellula* in an earlier study (Wing 1976), which is in agreement with the concept.

Thus, from an ecological perspective, the temperatures at which expatriate species might surpass the performance of native Arctic ones, may significantly influence species distributions, rather than merely reaching species-specific critical physiological temperatures.
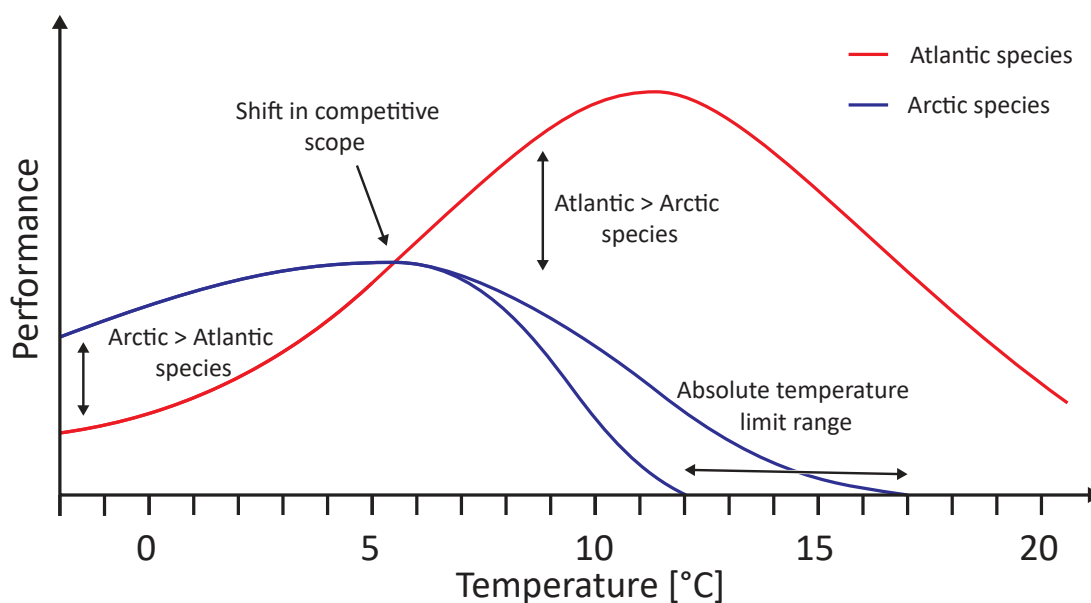
Figure 1: Conceptual figure of temperature effects on the performance of Arctic and boreal-Atlantic species. Based on references for: lethal temperature (Chapter I; Hirche 1987), 5 − 6 °C threshold (Chapter I; Jung-Madsen and Nielsen 2015; Kjellerup et al. 2012), performance (Chapter I; Grote et al. 2015; Henriksen et al. 2012; Hildebrandt et al. 2014; Hirche and Kosobokova 2007; Hirche et al. 1997; Kjellerup et al. 2012; Makri et al. 2024; Møller et al. 2012; Pasternak et al. 2013).

Borealization of Arctic food webs: loss of ice algae and lipid-rich zooplankton

Climate change is distinctly altering both the phenology and community composition of primary production in the Arctic. The melting of sea ice extends the seasonally ice-free period, resulting in a shorter duration of ice algal blooms while simultaneously expanding the area and time available for phytoplankton growth (Arrigo et al. 2008; Kahru et al. 2011; Selz et al. 2018; Tedesco and Vichi 2014). This is accompanied by a shift in species composition, marked by an in-

creasing influence of flagellates (Nöthig et al. 2015; Orkney et al. 2020), with an unknown impact on pelagic food web dynamics.

Arctic food web 'status quo' – big and lipid-rich

The Arctic pelagic food web is strongly coupled with and dictated by sea ice and associated primary production. Especially diatoms play a crucial role, contributing a large part to the algal biomass, generally dominating (under) ice and hytoplankton blooms (Arrigo 2014; Fernández-Méndez et al. 2018; von Quillfeldt 2000).

The importance of (sea ice) diatoms is reflected in food web dynamics in the partially ice-covered Fram Strait in summer (Chapter II). The diet of primarily herbivorous species *Calanus glacialis* and *C. hyperboreus* is largely dominated by diatoms. Additionally, high contributions of diatom trophic marker signals are evident in higher trophic levels such as *Eukrohnia* sp. (Chaetognatha), *Themisto libellula*, *T. abyssorum* (Amphipoda), *Thysanoessa longicaudata* (Euphausiacea) and *Paraeuchaeta glacialis*. The results emphasize that the presence of sea ice and its associated sympagic and pelagic algal communities largely define the nutrition in ice-covered regions of the Arctic during the productive season.

Diatoms are generally considered to be of high nutritional value for herbivorous grazers due to their rich content of eicosapentaenoic acid (EPA, 20:5(n-3)) and 16C polyunsaturated fatty acids (Dalsgaard et al. 2003; Falk-Petersen et al. 1998). The omega-3 fatty acid EPA is essential for zooplankton recruitment and development (Becker and Boersma 2003; Jónasdóttir et al. 2002; Jónasdóttir et al. 2009), making diatoms a key factor in supporting secondary production in the Arctic environment. Primary consumers, particularly *Calanus* spp., efficiently incorporate these fatty acids, accumulating and biosynthesizing large amounts of lipids, which are stored as wax esters (Chapter II). The high energy content of these Arctic zooplankton species make them a highly valuable food source not only for carnivorous zooplankton such as *Paraeuchaeta* spp. and *Themisto* spp. (Chapter II) but also for larger predators such as polar cods (Bouchard and Fortier 2020; McNicholl et al. 2016) and the little auks (Kwaśniewski et al. 2010). The Arctic pelagic food web is thus generally short, lipid-rich and highly efficient.

Ice associated diatoms are not only an important carbon source for sympagic and pelagic, but also for benthic organisms. High amounts of large, rapidly sinking diatom aggregates in ice-covered regions of the Arctic lead to a high carbon export efficiency (Fadeev et al. 2021) and, therefore, to a strong coupling between the sympagic/pelagic and the benthic food web (Boetius et al. 2013; Koch et al. 2023; Søreide et al. 2013).

Boreal, ice-free food web – role of flagellates

In the Atlantic-influenced regions of the Arctic, such as eastern Fram Strait and the Barents Sea, flagellates, especially *Phaeocystis* spp., are becoming increasingly dominant (Ardyna and Arrigo 2020; Nöthig et al. 2015; Orkney et al. 2020), and may regionally even replace diatom blooms in summer (Assmy et al. 2023; Hegseth and Tverberg 2013). The ability of zooplankton

to efficiently feed on *Phaeocystis* spp. and other small flagellates could thus be of importance for secondary production in future Arctic scenarios.

The stronger influence of flagellates is reflected in pelagic food web structures in the West Spitsbergen Current region, which was predominantly based on by flagellates, possibly on *Phaeocystis* spp. and/or mixo-/heterotrophic dinoflagellates as a food source for *Calanus* spp. (Chapter II, Søreide et al. 2013; Søreide et al. 2008). Diatoms also played a role in the diet, but to a lesser extent than in the polar region, which is in agreement with an observed decreasing importance of diatoms in eastern Fram Strait in summer (Nöthig et al. 2015).

The ability of zooplankton species to graze on *Phaeocystis* spp. is largely affected by its size (Nejstgaard et al. 2007). In the Arctic, the prevalent *Phaeocystis pouchetii* occurs either as small single cells ($< 7\,\mu m$) or in form of colonies of up to 2 mm in diameter (Schoemann et al. 2005). Both Arctic *Calanus* species efficiently graze on the colonial form, but cannot or do not feed on small single cells (Huntley et al. 1987; Levinsen et al. 2000). In contrast, their smaller boreal congener *C. finmarchicus* is able to graze on the small, single cells (Hansen et al. 1994; Levinsen et al. 2000). In case of a shift towards smaller algal cells (Li et al. 2009), *C. finmarchicus* could have a competitive advantage, due to its ability to exploit this size range, whereas *C. glacialis* and *C. hyperboreus* rely on larger algal cells and/or *Phaeocystis* colonial forms.

The findings show that older stages of *Calanus* spp. can and do feed on colonial *Phaeocystis* spp. (Chapter II; Søreide et al. 2013; Søreide et al. 2008). However, it is unclear, if a shift towards a flagellate-dominated phytoplankton production can meet their energy demands during the period of reproduction, growth and development, or if it is a suitable food source for juvenile stages. *Calanus glacialis* and *C. finmarchicus* showed much higher recruitment following a diatom-dominated bloom, in contrast to a bloom dominated by *Phaeocystis* spp. in an Arctic fjord (Assmy et al. 2023). Flagellates are generally deficient in the omega-3 fatty acid EPA, but enriched in docosahexaenoic acid (DHA, 22:6(n-3)) and C18 polyunsaturated fatty acids (Dalsgaard et al. 2003; Schmidt et al. 2024). The discrepancy in recruitment success might thus not be related to variable nutritional value of the different algae, but rather to the unsuitability of *Phaeocystis* spp. as a food source for nauplii and/or young copepodite stages. Indeed, younger stages of *C. finmarchicus* show absent (nauplii) or distinctly lower (C1-3 copepodids) ingestion rates of *Phaeocystis* spp. colonies ($> 50\,\mu m$), compared to the diatom *Thalassiosira nordenskioeldii* ($20\,\mu m$). This difference is not apparent for the older, larger stages C4-5 (Hansen et al. 1990; Irigoien et al. 2003). Thus, if primary production shifts towards one mainly dominated by *Phaeocystis* spp. colonies, nauplii and juvenile stages of *Calanus* spp. might not find sufficient adequate food. This emphasizes the importance to consider not only algal species but also their size ranges in food web studies.

Similar to young *Calanus* stages, smaller copepod species, such as *Pseudocalanus* spp., may not be able to effectively graze on *Phaeocystis* spp. (Nejstgaard et al. 2007). It is suggested, that under *Phaeocystis* spp. bloom conditions, the food web is elongated by at least one step, with microzooplankton such as heterotrophic dinoflagellates feeding on *Phaeocystis* spp. (Grattepanche

et al. 2011). In turn, mesozooplankton increasingly switch to omnivorous feeding on microzooplankton (Vernet et al. 2017). *Phaeocystis*-dominated blooms further have consequences for the pelagic-benthic coupling, due to slower sinking rates and higher pelagic recycling, resulting in lower carbon export (Fadeev et al. 2021).

Calanus finmarchicus as prey – quantity over quality?

Over recent decades *C. finmarchicus* has increased in biomass in the Atlantic sector of the Arctic (Carstensen et al. 2019; Skjoldal et al. 2021), which could significantly influence food web dynamics and energy flux. *C. finmarchicus* is generally smaller (Chapter IV) and less lipid-rich than its Arctic congeners and thus potentially of less nutritional value. Yet, the high abundances and rapid population turnover rates, including observations of a second generation in one year (Skjoldal et al. 2021), suggest a substantial overall lipid production by the population over the year (Renaud et al. 2018). Indeed, the relevance of *Calanus* fatty acid trophic markers to the diet of higher trophic levels in the eastern Atlantic-influenced region of Fram Strait was two to three times greater than in western, Arctic Fram Strait (Chapter II). It is not possible to determine the specific contributions of each *Calanus* species using these markers alone. However, the high levels are likely attributed to *C. finmarchicus* given its high biomass associated with Atlantic waters (Chapter III; Hirche and Kosobokova 2007; Nöthig et al. 2015; Svensen et al. 2011). This may indicate that the higher abundance and secondary production of *C. finmarchicus* can compensate for its lower individual lipid content, which may still support many Arctic and boreal pelagic predators. However, not all predators may benefit from this abundance. For larger predators like the little auk, which actively select larger *Calanus* species, the numerous but smaller individuals may not represent an adequate food source (Balazy et al. 2023; Kwaśniewski et al. 2010).
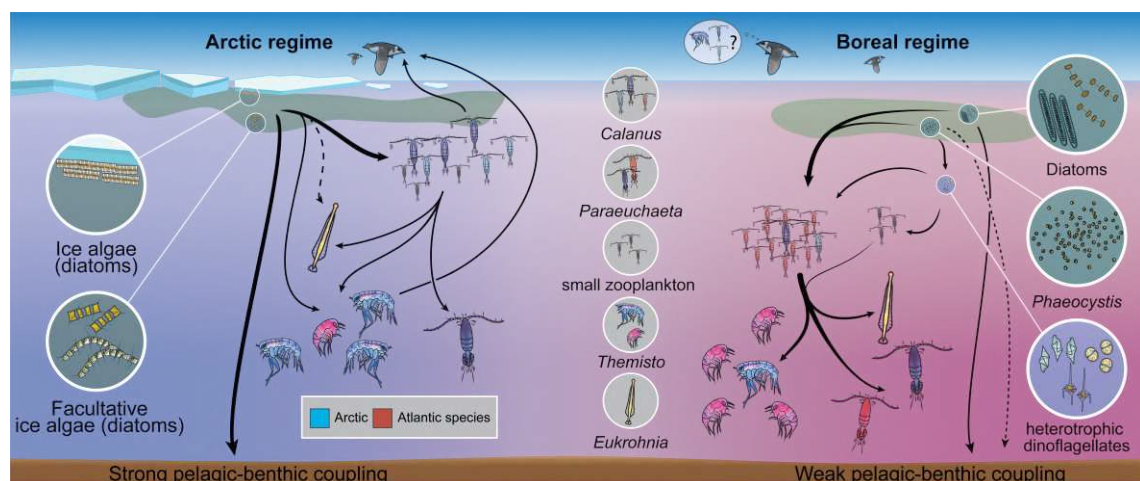

Figure 2: Overview of Arctic (left) and boreal (right) influenced pelagic food webs in Fram Strait.

Figure 2 illustrates and summarizes the key differences between Arctic and Atlantic influenced/boreal food webs. It highlights (1) the high proportion of (sea ice) diatoms in the Arctic regime, resulting in a strong pelagic-benthic coupling; (2) the importance of diatoms to the diet of

herbivorous and omnivorous zooplankton species in the Arctic region; (3) an increasing relevance of *Phaeocystis* spp. in the Atlantic regime, which weakens the pelagic-benthic coupling; (4) a more diverse diet of zooplankton in the Atlantic region, dominated by flagellates for primarily herbivorous *Calanus* species; (5) the longer food chains especially for smaller zooplankton species, when *Phaeocystis* spp. dominates; (6) an increased importance of *Calanus*, likely *C. finmarchicus*, in the diets of many carnivorous zooplankton species; and (7) the unsuitability of *C. finmarchicus* as prey for larger predators such as the little auk.

Zooplankton in a future Arctic

In the previous two sections, consequences of changing temperatures and food web dynamics for Arctic and boreal expatriate zooplankton species were considered individually and their ecological implications were briefly introduced. The following section integrates these aspects, with a greater focus on the expatriation of boreal species and potential consequences for ecological interactions.

Flexibility of Arctic zooplankton species

Arctic zooplankton species exhibit a considerable resilience to rising temperatures and changes in food web dynamics (Chapter I and II). This adaptability is further emphasized by a plasticity in their life history. Generally, the long lifespans of Arctic zooplankton are an adaptation to the cold environment with a short productive season (Falk-Petersen et al. 2009). However, under warmer conditions and/or a prolonged productive season, Arctic species such as *Calanus glacialis*, *C. hyperboreus* and *Themisto libellula* are able to benefit from these conditions by accelerating their development and completing their life cycles in a shorter time (Aarflot et al. 2022; Arnkværn et al. 2005; Dunbar 1957; Feng et al. 2018; Hirche et al. 1997; Smith and Schnack-Schiel 1990).

Recent observations of active *C. glacialis* in surface waters during polar night further challenge the traditional understanding of diapause and indicate a more flexible overwintering strategy for this species (Błachowiak-Samołyk et al. 2015; Kunisch et al. 2023). Ascending early may be a strategic response in a highly variable environment, where the onset of the phytoplankton bloom is difficult to predict due to high interannual variability in the timing of sea-ice breakup (Berge et al. 2020). During this period, *C. glacialis* shifts to an omnivorous diet, consuming a range of organisms for including protists and metazoan prey such as smaller copepods and chaetognath eggs (Berge et al. 2020; Cleary et al. 2017; Kunisch et al. 2023), showing its high adaptability in dietary habits (Chapter II). Apparently, the fitness of individuals that ascend earlier is not negatively affected, as long as alternative food sources are available (Hobbs et al. 2020). Remaining active during winter could also be a fallback strategy, when diapause is not feasible either due to inadequate lipid accumulation during summer or an environment, which is too shallow for overwintering (Hobbs et al. 2020).

Many studies investigating the impact of environmental change focus on *Calanus*, thus comparable studies on *Themisto libellula* and *Paraeuchaeta glacialis* are scarce. To my knowledge,

154

this study provides first information on the effects of increasing temperatures on the metabolism of *Paraeuchaeta glacialis* (and *P. norvegica*) (Chapter I). Based on the resilience of *T. libellula* and *P. glacialis* to rising temperatures (Chapter I) and their dietary flexibility (Chapter II), these species demonstrate a considerable adaptability to changing conditions.

In conclusion, the investigated Arctic zooplankton species can buffer a certain degree of environmental change due to their high plasticity not only in coping with variable conditions, but also in adjusting their life history. They may even benefit from and partially thrive under more boreal regimes (Aarflot et al. 2023; Hatlebakk et al. 2022; Kosobokova and Pertsova 2018). This resilience is crucial in the face of ongoing climate change.

Mechanisms of the biological Atlantification of the Arctic

The import of Atlantic species into the Eurasian Arctic via Fram Strait and the Barents Sea has been documented since the early Arctic expeditions (Sars 1900). It is thus not a new phenomenon related to climate change, but can be explained by the connectivity of the systems via major currents, such as the Norwegian Atlantic Slope Current and the West Spitsbergen Current (Schauer et al. 2008; Schauer et al. 2002), and the passive drifting nature of zooplankton. The advection of Atlantic zooplankton contributes substantially to the diversity and biomass in the Eurasian Basin of the central Arctic Ocean (Kosobokova 2009). While many species die shortly after entering the Arctic Ocean, unable to cope with the harsh Arctic conditions, some species like *C. finmarchicus* have a broad thermal tolerance range (Chapter I) that enables them to intrude into the Basin (Kosobokova et al. 2011; Wassmann et al. 2015). However, *C. finmarchicus* is generally assumed to be infertile in this environment (Hirche and Kosobokova 2007). Consequently, the presence of boreal species in the Arctic Ocean is (still) dependent on replenishment from southerly populations (Wassmann et al. 2015).

The range of the intrusion is ultimately determined by the origin of the population, the transit time via currents and the lifespan of advected species (Kosobokova et al. 2011). For instance, *C. finmarchicus* would reach the southern tip of Svalbard within approximately two months, assuming an advection from its main center of distribution in the Norwegian Sea (Conover 1988), an average current velocity of 30 km day^{-1} for the Norwegian Atlantic Slope Current (Hansen et al. 2011) and 13 km day^{-1} for the West Spitsbergen Current (Beszczynska-Möller et al. 2012), respectively. Within this time, *C. finmarchicus* can develop from egg to copepodite stage C5 (at 4 °C and excess of food, Campbell et al. 2001). Under favorable conditions, advected C5s may progress to females and produce a second generation (Dalpadado et al. 2012; Gluchowska et al. 2017). However, this second generation is unlikely to develop to overwintering stages C4 or C5 (Hirche 1996) within the limited span of the productive season. Alternatively, C5s may descend to deeper layers and enter diapause. From here, they could either be carried back southward by the recirculation of Atlantic water in central Fram Strait (Espinasse et al. 2022; Hattermann et al. 2016) or get dispersed further into the Arctic Basin, reaching as far east as the Kara Sea in high abundances and the Laptev Sea

155

in low numbers (Wassmann et al. 2015).

Largely underestimated submesoscale oceanographic processes can play an essential role in such advection processes. Associated with such dynamics are high velocity horizontal jets, which can be three to six times faster than the average speed of the West Spitsbergen Current (Hernández-Hernández et al. 2020; von Appen et al. 2018), and thus may act as 'transportation highways' (Chapter III), resulting in an accelerated and enhanced transport of organisms.

As climate change and Atlantification progress, Arctic regions are beginning to exhibit characteristics more resembling boreal ecosystems, i.e. elevated temperatures, reduced sea ice and associated altered phenology of primary production (Kahru et al. 2011; Selz et al. 2018; Waga and Hirawake 2020). The extended season of phytoplankton primary production may facilitate improved local recruitment of boreal species. Concurrently, as ambient temperatures approach the thermal optimum of these species, their overall performance is enhanced (Chapter I). An increase in performance includes an acceleration in development, which increases the likelihood of offspring to reach the overwintering stage within the limited timeframe of the productive season. Indeed, there are growing indications of local populations of boreal species such as *C. finmarchicus* and *Pseudocalanus moultoni* in Arctic regions including eastern Fram Strait (Tarling et al. 2022), Kongsfjorden (Hop et al. 2019; Kwaśniewski et al. 2003) and Adventfjorden (Ershova et al. 2021b). Although a large part of boreal species abundance in these regions still remains linked to advection with Atlantic waters (Basedow et al. 2004), their ability to sustain local populations underscores the increasingly favorable conditions for these species in Arctic environments. The northward expansion of boreal source populations has several implications. Combining advected with local abundances increases the biomass of boreal species in these regions. Concurrently, the presence of boreal species will become less dependent on advection processes. Additionally, shifting source populations northward might extend their advective range further into the Arctic Basin. Such changes have consequences for local ecological dynamics, particularly for interactions with endemic species.

Arctic-boreal coexistence or competition?

The distribution of Arctic and boreal-Atlantic species will increasingly overlap due to the resilience of Arctic species to environmental changes and the northward range shift of boreal species. In warmer, more stable Arctic scenarios, the efficient adaptation of Arctic species to the cold and highly pulsed system might not be a competitive advantage anymore (Figure 1, Kjellerup et al. 2012), raising the question if a coexistence of Arctic and boreal species is possible.

In Kongsfjorden and the West Spitsbergen Current, the increasing abundance of *C. finmarchicus* has so far not been accompanied by a decrease in both Arctic *Calanus* species (Carstensen et al. 2019; Hop et al. 2019). Contrary to this 'coexistence', recent trends in the Barents Sea point to a decline in the biomass of the Arctic *C. glacialis*, while there has been an increase in the biomass of its boreal congener (Aarflot et al. 2018). Similarly, abundances of *T. libellula* are declining in

Fram Strait and the Barents Sea, whereas boreal *T. abyssorum* is becoming more abundant (CAFF 2017).

During the last two decades, the Barents Sea has experienced an increasing inflow of Atlantic waters, accompanied by a decrease in the extent of Arctic water masses (Dalpadado et al. 2012; Matishov et al. 2009; Polyakov et al. 2023). Consequently, variations in species abundances in the Barents Sea, i.e. an increase in boreal species and a decrease in Arctic species, rather reflects a shift in the dominance of the respective water masses than ecological interactions among congeners. Similarly, a shift from *C. hyperboreus* to *C. finmarchicus* in the Norwegian Sea was due to westward retraction of the cold and low saline East Icelandic Water tongue (Kristiansen et al. 2016). This mechanism seems particularly relevant in regions, where both Arctic and boreal species are expatriates rather than sustain local populations. *C. finmarchicus* is known to be advected into the Barents Sea from the Norwegian Sea (Torgersen and Huse 2005), whereas the source of *C. glacialis* in the Barents Sea is less clear (Aarflot et al. 2023). A recent study suggests that *C. glacialis* is advected into the Barents Sea from populations of adjacent Nordic Seas (Langbehn et al. 2023), supporting the strong correlation of species abundances with the proportions of the respective water masses. In this context, the concept of continuous re-colonization could regionally explain a coexistence of ecologically similar Arctic and boreal congeners (Auel 1999). In regions where considerable proportions of their respective population are attributed to advection processes rather than local recruitment, the permanent resupply of new individuals potentially sustains both despite nterspecific competition.

Vertical habitat portioning can substantially contribute to the avoidance of competition and thus facilitate the coexistence of species. Among the investigated species, differences in vertical distribution occur between the congeners of *Themisto*. Boreal *T. abyssorum* exhibits a deeper distribution range than Arctic *T. libellula* (Dalpadado et al. 2001), which reflects in differences in diet and the higher trophic position of *T. abyssorum* (Chapter II; Auel and Hagen 2002. Carnivorous *Paraeuchaeta glacialis* and *P. norvegica* are both epi- to mesopelagic species (Auel 2004). In regions where these species co-occur, they exhibit an overlap in dietary spectra (Chapter II), which may be attributed to their similar vertical distribution and hence access to the same prey.

Primarily herbivorous zooplankton species, such as *Calanus* spp., are restricted to epipelagic layers for feeding. Fine-scale vertical habitat selection may serve as a strategy to reduce competition among species with similar dietary demands (Chapter III; Trudnowska et al. 2015; Schmid and Fortier 2019). Vertical sampling of zooplankton often lacks the resolution to accurately depict vertical distribution of species. Few studies with high-resolution vertical sampling showed distinct differences in vertical distribution of the three *Calanus* species relative to the chlorophyll maximum (Herman 1983; Schmid and Fortier 2019). Specifically, *C. hyperboreus* is predominantly found within the core of the chlorophyll maximum, whereas *C. glacialis* and *C. finmarchicus* are typically concentrated above and/or below this layer. Different algae inhabit distinct vertical niches (Latasa et al. 2017), thus *Calanus* species possibly select their vertical position based on the avail-

ability of the preferred phytoplankton groups and/or cell sizes (Schmid and Fortier 2019) and, thereby, avoid competition for food. Among the three congeners, *C. finmarchicus* and *C. glacialis* occupy more similar trophic niches in regions of co-occurrence (Chapter II), which in line with the observation of more similar vertical niches (Herman 1983).

Fine-scale differences in vertical distribution patterns might also result from competitive exclusion, with one species displacing the others from the optimal zone within the chlorophyll maximum (Schmid and Fortier 2019). Alternatively, they might represent a tradeoff with exposure to visual predation, with larger specimens generally preferring deeper layers to reduce visibility (Chapter III).

The top-down control by pelagic predators is a factor which can largely influence species distribution and biomass and, thus, local success, but is often neglected in zooplankton studies. The borealization of Arctic regimes also increases the abundance of mesopelagic boreal planktivore fishes (Fossheim et al. 2015; Vihtakari et al. 2018). Further, the shift from perennial to seasonal ice cover or open water increases the light availability, and hence, supports visual predators (Langbehn et al. 2023; Langbehn and Varpe 2017). Especially larger species such as *Calanus hyperboreus*, *C. glacialis* and *Themisto libellula* are more susceptible to visual predation, as they are more easily spotted (O'Brien 1979). Decreasing abundances could thus regionally be a result of increasing predation pressure, rather than competition between congeners.

Differences in phenology among congeners may further facilitate coexistence. Arctic and boreal species of *Calanus* and *Themisto* show distinct differences in timing and strategy of reproduction. Both Arctic *Calanus* species can spawn fueled by internal lipid reserves prior to the onset of the algal bloom (capital breeding), whereas boreal *C. finmarchicus* is depended on direct food intake for reproduction (income breeding) (Hirche and Niehoff 1996). However, recent studies indicate population structures appear to be more similar in region of co-occurrence among *C. glacialis* and *C. finmarchicus* (Trudnowska et al. 2020; Weydmann-Zwolicka et al. 2022), suggesting similar spawning of these two species times under more boreal like conditions. Females of *T. libellula* generally release their juveniles earlier (March to May) compared to *T. abyssorum* (May to June) in regions of co-occurrence (Dalpadado et al. 1994; Dalpadado 2002). The ability of *T. libellula* to spawn earlier may be facilitated by their higher wax ester content compared to *T. abyssorum* (Noyon et al. 2011).

To conclude, there is a high degree of ecological niches differentiation between *Themisto* congeners and between *C. hyperboreus* and its two sister species, as indicated by temporal separation in their recruitment, greater variance in diet (Chapter II) and, in case of *Themisto* spp., distinct vertical separation. The observed decline in *T. libellula* abundances in Fram Strait and the Barents Sea seems unlikely due to competition with *T. abyssorum*, but rather due to the association with respective water masses, increased top-down control and/or higher degree of dependence on the cryo-pelagic food web (Dalpadado et al. 2001; Kohlbach et al. 2016).

However, given the high ecological similarity between *C. glacialis* and *C. finmarchicus* as well

158

as between *P. glacialis* and *P. norvegica*, including recruitment timing and diet in regions of co-occurrence, the differentiation of niches appears insufficient to fully explain a coexistence (Chapter II; Auel 1999; Hatlebakk et al. 2022; Weydmann-Zwolicka et al. 2022). With ongoing climate change *C. finmarchicus* and *P. norvegica* will increasingly be able to sustain local populations and thus enhance their local biomass in Arctic regimes. In such a scenario, results of this thesis show that these boreal species may outcompete their Arctic congeners due to superior performance at elevated temperatures (Chapter I).

Understanding species distribution, fluctuations in their biomass and potential regime shifts is complex and depends on many intrinsic and external factors. The interplay of physiological responses to environmental changes, ecological interactions like competition with congeners and top-down control by predators, and hydrographic processes, plays a significant role in affecting zooplankton distribution. A comprehensive understanding thus requires a holistic approach that recognizes the combined influence of these factors.

Conclusions

This thesis demonstrates that Arctic zooplankton species show high flexibility to cope with variable conditions, including rising temperatures and the ability to switch between different food sources. Their astonishing ability to adjust their life-cycle strategies depending on changing conditions gives them an essential advantage over boreal species in an interannually and seasonally variable high-latitude regime. While Arctic species can function in warmer and more boreal-like conditions, they cannot enhance their performance to the same extent as boreal species. Boreal species, however, need stable conditions in order to be competitive and sustain local populations. As long as there is considerable variability in environmental conditions such as the timing of the sea-ice break up and the onset of the phytoplankton bloom, boreal species may struggle to sustain local populations on a year-to-year basis. Consequently, their occurrence in Arctic ecosystems will be rather dependent on the constant replenishment of specimens from southerly source populations. However, with ongoing Atlantification of the Arctic and the associated increasing potential of boreal species to establish local populations, their distribution will become less dependent on advection processes and increasingly overlap with Arctic counterparts. In regions of strong overlap, it is unclear, if coexistence is possible or if one species will eventually outcompete the other. Results of this thesis suggest that for the congener pairs with a distinct overlap in ecological niches, boreal congeners will eventually outperform their Arctic sister species due to much higher fitness at elevated temperatures.

Outlook

This thesis emphasizes, that while Arctic zooplankton is rather resilient to environmental change, they are increasing confronted with competition from their boreal congeners. This competition may lead to the regional extinction of Arctic zooplankton species. However, high-latitude regions will continue to experience significant seasonality in the light regime, a factor which will not be affected by climate change. A recent study indicates a northward shift of polar species such as *C. hyperboreus* and *C. glacialis* further into the Arctic Basin (Ershova et al. 2021a). As both species need a period of reduced sea ice to complete their life cycle, the retreating sea ice potentially makes the Arctic Ocean more accessible for these species. The efficient adaptations of Arctic species to the highly pulsed system may facilitate their potential to shift further into the Arctic Basin. This region will likely remain inaccessible to their boreal congeners and thus may serve as a 'refuge' for Arctic species.

Additionally, reliable monitoring methods are essential to fully understand regime shifts. In Arctic fjords of Svalbard, recent warming had led to smaller body sizes of *C. glacialis*, possibly due to accelerated development (Balazy et al. 2023). Size ranges of Arctic *C. glacialis* and boreal *C. finmarchicus* are now regionally completely overlapping, leading to a distinct overestimation of *C. finmarchicus* when size is the only differentiation feature used. Although the consequence for the ecosystem may be the similar, i.e. shift to smaller individuals with lower individual lipid content, it emphasizes that precise species identification is critical for correctly understanding the impacts of climate change on the physiology and ecology of species.

References

Aarflot, JM, Eriksen, E, Prokopchuk, IP, Svensen, C, Søreide, JE, Wold, A, and Skogen, MD (2023). New insights into the Barents Sea *Calanus glacialis* population dynamics and distribution. *Prog Oceanogr* 217, 103106.

Aarflot, JM, Hjøllo, SS, Strand, E, and Skogen, MD (2022). Transportation and predation control structures the distribution of a key calanoid in the Nordic Seas. *Prog Oceanogr* 202, 102761.

Aarflot, JM, Skjoldal, HR, Dalpadado, P, and Skern-Mauritzen, M (2018). Contribution of *Calanus* species to the mesozooplankton biomass in the Barents Sea. *ICES Mar Sci Symp* 75, 2342–2354.

Alcaraz, M, Felipe, J, Grote, U, Arashkevich, E, and Nikishina, A (2014). Life in a warming ocean: thermal thresholds and metabolic balance of arctic zooplankton. *J Plankton Res* 36, 3–10.

Ardyna, M and Arrigo, KR (2020). Phytoplankton dynamics in a changing Arctic Ocean. *Nat Clim Chang* 10, 892–903.

Arnkværn, G, Daase, M, and Eiane, K (2005). Dynamics of coexisting *Calanus finmarchicus*, *Calanus glacialis* and *Calanus hyperboreus* populations in a high-Arctic fjord. *Polar Biol* 28, 528–538.

Arrigo, KR (2014). Sea ice ecosystems. *Annu Rev Mar Sci* 6, 439–467.

Arrigo, KR, Van Dijken, G, and Pabi, S (2008). Impact of a shrinking Arctic ice cover on marine primary production. *Geophys Res Lett* 35, 2008GL035028.

Assmy, P, Cecilie Kvernvik, A, Hop, H, Hoppe, CJM, Chierici, M, David, TD, Duarte, P, Fransson, A, García, LM, Patuła, W, Kwaśniewski, S, Maturilli, M, Pavlova, O, Tatarek, A, Wiktor, JM, Wold, A, Wolf, KKE, and Bailey, A (2023). Seasonal plankton dynamics in Kongsfjorden during two years of contrasting environmental conditions. *Prog Oceanogr* 213, 102996.

Auel, H (1999). The ecology of Arctic deep-sea copepods (Euchaetidae and Aetideidae): aspects of their distribution, trophodynamics and effect on the carbon flux. *Rep Polar Res* 319, 1–97.

Auel, H (2004). Egg size and reproductive adaptations among Arctic deep-sea copepods (Calanoida, *Paraeuchaeta*). *Helgol Mar Res* 58, 147–153.

Auel, H and Hagen, W (2002). Mesozooplankton community structure, abundance and biomass in the central Arctic Ocean. *Mar Biol* 140, 1013–1021.

Balazy, K, Trudnowska, E, Wojczulanis-Jakubas, K, Jakubas, D, Præbel, K, Choquet, M, Brandner, MM, Schultz, M, Bitz-Thorsen, J, Boehnke, R, Szeligowska, M, Descamps, S, Strøm, H, and Błachowiak-Samołyk, K (2023). Molecular tools prove little auks from Svalbard are extremely selective for *Calanus glacialis* even when exposed to Atlantification. *Sci Rep* 13, 13647.

Basedow, SL, Eiane, K, Tverberg, V, and Spindler, M (2004). Advection of zooplankton in an Arctic fjord (Kongsfjorden, Svalbard). *Estuar Coast Shelf Sci* 60, 113–124.

Becker, Claes and Boersma, Maarten (2003). Resource quality effects on life histories of *Daphnia*. *Limnol Oceanogr* 48, 700–706.

Berge, J, Daase, M, Hobbs, L, Falk-Petersen, S, Darnis, G, and Søreide, JE (2020). Zooplankton in the polar night. *Polar Night Marine Ecology*. Edited by Berge, J, Johnsen, G, and Cohen, JH. Volume 4. Series Title: Advances in Polar Ecology. Cham: Springer International Publishing, 113–159.

Beszczynska-Möller, A, Fahrbach, E, Schauer, U, and Hansen, E (2012). Variability in Atlantic water temperature and transport at the entrance to the Arctic Ocean, 1997–2010. *ICES Mar Sci Symp* 69, 852–863.

Błachowiak-Samołyk, K, Wiktor, JM, Hegseth, EN, Wold, A, Falk-Petersen, S, and Kubiszyn, AM (2015). Winter tales: the dark side of planktonic life. *Polar Biol* 38, 23–36.

Boetius, A, Albrecht, S, Bakker, K, Bienhold, C, Felden, J, Fernández-Méndez, M, Hendricks, S, Katlein, C, Lalande, C, Krumpen, T, Nicolaus, M, Peeken, I, Rabe, B, Rogacheva, A, Rybakova, E, Somavilla, R, Wenzhöfer, F, and RV *Polarstern* ARK27-3-Shipboard Science Party (2013). Export of algal biomass from the melting Arctic sea ice. *Sci* 339, 1430–1432.

Bouchard, C and Fortier, L (2020). The importance of *Calanus glacialis* for the feeding success of young polar cod: a circumpolar synthesis. *Polar Biol* 43, 1095–1107.

CAFF (2017). *State of the Arctic marine biodiversity report*. Akureyri, Iceland: Convention of Arctic Flora and Fauna International Secretariat, 200 pp.

Campbell, RG, Wagner, MM, Teegarden, GJ, Boudreau, CA, and Durbin, EG (2001). Growth and development rates of the copepod *Calanus finmarchicus* reared in the laboratory. *Mar Ecol Prog Ser* 221, 161–183.

Carstensen, J, Olszewska, A, and Kwasniewski, S (2019). Summer mesozooplankton biomass distribution in the West Spitsbergen Current (2001–2014). *Front Mar Sci* 6, 202.

Cleary, AC, Søreide, JE, Freese, D, Niehoff, B, and Gabrielsen, TM (2017). Feeding by *Calanus glacialis* in a high arctic fjord: potential seasonal importance of alternative prey. *ICES Mar Sci Symp* 74, 1937–1946.

Conover, RJ (1988). Comparative life histories in the genera *Calanus* and *Neocalanus* in high latitudes of the northern hemisphere. *Hydrobiologia* 167, 127–142.

Dalpadado, P, Borkner, N, Bogstad, B, and Mehl, S (2001). Distribution of *Themisto* (Amphipoda) spp. in the Barents Sea and predator-prey interactions. *ICES Mar Sci Symp* 58, 876–895.

Dalpadado, P, Borkner, N, and Skjoldal, HR (1994). Distribution and life history of *Themisto* (Amphipoda) spp., north of 73° N in the Barents Sea. *Fisk Havet* 12, 1–42.

Dalpadado, P, Ingvaldsen, RB, Stige, LC, Bogstad, B, Knutsen, T, Ottersen, G, and Ellertsen, B (2012). Climate effects on Barents Sea ecosystem dynamics. *ICES Mar Sci Symp* 69, 1303–1316.

Dalpadado, Padmini (2002). Inter-specific variations in distribution, abundance and possible life-cycle patterns of *Themisto* spp. (Amphipoda) in the Barents Sea. *Polar Biol* 25, 656–666.

Dalsgaard, J, St. John, M, Kattner, G, Müller-Navarra, D, and Hagen, W (2003). Fatty acid trophic markers in the pelagic marine environment. *Advances in Mar Biol* 46, 225–340.

Dunbar, MJ (1957). The determinants of production in northerns seas: a study of the biology of *Themisto libellula* Mandt. *Can J Zool* 35, 797–819.

Ershova, EA, Kosobokova, KN, Banas, NS, Ellingsen, I, Niehoff, B, Hildebrandt, N, and Hirche, H-J (2021a). Sea ice decline drives biogeographical shifts of key *Calanus* species in the central Arctic Ocean. *Glob Change Biol* 27, 2128–2143.

Ershova, EA, Nyeggen, MU, Yurikova, DA, and Søreide, JE (2021b). Seasonal dynamics and life histories of three sympatric species of *Pseudocalanus* in two Svalbard fjords. *J Plankton Res* 43, 209–223.

Espinasse, B, Daase, M, Halvorsen, E, Reigstad, M, Berge, J, and Basedow, SL (2022). Surface aggregations of *Calanus finmarchicus* during the polar night. *ICES Mar Sci Symp* 79, 803–814.

Fadeev, E, Rogge, Andreas, Ramondenc, Simon, Nöthig, E-M, Wekerle, C, Bienhold, C, Salter, Ian, Waite, Anya M, Hehemann, L, Boetius, A, and Iversen, MH (2021). Sea ice presence is linked to higher carbon export and vertical microbial connectivity in the Eurasian Arctic Ocean. *Commun Biol* 4, 1255.

Falk-Petersen, S, Mayzaud, P, Kattner, G, and Sargent, JR (2009). Lipids and life strategy of Arctic *Calanus*. *Mar Biol Research* 5, 18–39.

Falk-Petersen, S, Sargent, JR, Henderson, J, Hegseth, EN, Hop, H, and Okolodkov, YB (1998). Lipids and fatty acids in ice algae and phytoplankton from the Marginal Ice Zone in the Barents Sea. *Polar Biol* 20, 41–47.

Feng, Z, Ji, R, Ashjian, C, Campbell, R, and Zhang, J (2018). Biogeographic responses of the copepod *Calanus glacialis* to a changing Arctic marine environment. *Glob Change Biol* 24, e159–e170.

Fernández-Méndez, M, Olsen, LM, Kauko, HM, Meyer, A, Rösel, A, Merkouriadi, I, Mundy, CJ, Ehn, JK, Johansson, AM, Wagner, PM, Ervik, Å., Sorrell, BK, Duarte, P, Wold, A, Hop, H, and Assmy, P (2018). Algal hot spots in a changing Arctic Ocean: sea-ice ridges and the snow-ice interface. *Front Mar Sci* 5, 75.

Fossheim, M, Primicerio, R, Johannesen, E, Ingvaldsen, RB, Aschan, MM, and Dolgov, V (2015). Recent warming leads to rapid borealization of fish communities in the Arctic. *Nat Clim Change* 5, 673–677.

Frölicher, TL and Laufkötter, C (2018). Emerging risks from marine heat waves. *Nat Commun* 9, 650.

Gluchowska, M, Dalpadado, P, Beszczynska-Möller, A, Olszewska, A, Ingvaldsen, R B, and Kwasniewski, Slawomir (2017). Interannual zooplankton variability in the main pathways of the Atlantic water flow into the Arctic Ocean (Fram Strait and Barents Sea branches). *ICES Mar Sci Symp* 74, 1921–1936.

Grote, U, Pasternak, A, Arashkevich, E, Halvorsen, E, and Nikishina, A (2015). Thermal response of ingestion and egestion rates in the Arctic copepod *Calanus glacialis* and possible metabolic consequences in a warming ocean. *Polar Biol* 38, 1025–1033.

Hansen, B, Tande, KS, and Berggreen, UC (1990). On the trophic fate of *Phaeocystis pouchetii* (Hariot). III. Functional responses in grazing demonstrated on juvenile stages of *Calanus finmarchicus* (Copepoda) fed diatoms and *Phaeocystis*. *J Plankton Res* 12, 1173–1187.

Hansen, B, Verity, P, Falkenhaug, T, Tande, KS, and Norrbin, F (1994). On the trophic fate of *Phaeocystis pouchetti* (Harriot). V Trophic relationships between *Phaeocystis* and zooplankton: an assessment of methods and size dependence. *J Plankton Res* 16, 487–511.

Hansen, MW, Johannessen, JA, Dagestad, KF, Collard, F, and Chapron, B (2011). Monitoring the surface inflow of Atlantic Water to the Norwegian Sea using Envisat ASAR. *J Geophys Res* 116 (C12), C12008.

Hatlebakk, M, Kosobokova, K, Daase, M, and Søreide, JE (2022). Contrasting life traits of sympatric *Calanus glacialis* and *C finmarchicus* in a warming Arctic revealed by a year-round study in Isfjorden, Svalbard. *Front Mar Sci* 9, 877910.

Hattermann, TE, Isachsen, PE, Von Appen, W-J, Albretsen, J, and Sundfjord, A (2016). Eddy-driven recirculation of Atlantic Water in Fram Strait. *Geophys Res Lett* 43, 3406–3414.

Hegseth, Else Nøst and Tverberg, Vigdis (2013). Effect of Atlantic water inflow on timing of the phytoplankton spring bloom in a aigh Arctic fjord (Kongsfjorden, Svalbard). *J Mar Syst* 113–114, 94–105.

Henriksen, MV, Jung-Madsen, S, Nielsen, TG, Møller, EF, Henriksen, KV, Markager, S, and Hansen, BW (2012). Effects of temperature and food availability on feeding and egg production of *Calanus hyperboreus* from Disko Bay, western Greenland. *Mar Ecol Prog Ser* 447, 109–126.

Herman, AW (1983). Vertical distribution patterns of copepods, chlorophyll, and production in northeastern Baffin Bay. *Limnol Oceanogr* 28, 709–719.

Hernández-Hernández, N, Arístegui, J, Montero, MF, Velasco-Senovilla, E, Baltar, F, Marrero-Díaz, Á., Martínez-Marrero, A, and Rodríguez-Santana, Á. (2020). Drivers of plankton distribution across mesoscale eddies at submesoscale range. *Front Mar Sci* 7, 667.

Hildebrandt, N, Niehoff, B, and Sartoris, FJ (2014). Long-term effects of elevated CO_2 and temperature on the Arctic calanoid copepods *Calanus glacialis* and *C. hyperboreus*. *Mar Pollut Bull* 80, 59–70.

Hirche, H-J (1987). Temperature and plankton: II. Effect on respiration and swimming activity in copepods from the Greenland Sea. *Mar Biol* 94, 347–356.

Hirche, H-J (1996). Diapause in the marine copepod, *Calanus finmarchicus* — a review. *Ophelia* 44, 129–143.

Hirche, H-J and Kosobokova, K (2007). Distribution of *Calanus finmarchicus* in the northern North Atlantic and Arctic Ocean—expatriation and potential colonization. *Deep-Sea Res II* 54, 2729–2747.

Hirche, H-J, Meyer, U, and Niehoff, B (1997). Egg production of *Calanus finmarchicus*: effect of temperature, food and season. *Mar Biol* 127, 609–620.

Hirche, H-J and Niehoff, B (1996). Reproduction of the Arctic copepod *Calanus hyperboreus* in the Greenland Sea - field and laboratory observations. *Polar Biol* 16, 209–219.

Hobbs, L, Banas, Neil S, Cottier, FR, Berge, J, and Daase, M (2020). Eat or sleep: availability of winter prey explains mid-winter and spring activity in an Arctic *Calanus* population. *Front Mar Sci* 7, 541564.

Hop, H, Wold, A, Vihtakari, M, Daase, M, Kwasniewski, S, Gluchowska, M, Lischka, S, Buchholz, F, and Falk-Petersen, S (2019). Zooplankton in Kongsfjorden (1996–2016) in relation to climate change. *The Ecosystem of Kongsfjorden, Svalbard*. Edited by Hop, H and Wiencke, C. Volume 2. Cham: Springer International Publishing, 229–300.

Huenerlage, K, Cascella, K, Corre, E, Toomey, L, Lee, CY, Buchholz, F, and Toullec, JY (2016). Responses of the arcto-boreal krill species *Thysanoessa inermis* to variations in water temperature: coupling Hsp70 isoform expressions with metabolism. *Cell Stress Chaperon* 21, 969–981.

Huntley, M, Tande, K, and Eilertsen, HC (1987). On the trophic fate of *Phaeocystis pouchetii* (Hariot). II. Grazing rates of *Calanus hyperboreus* (Kraryer) on diatoms and different size categories of *Phaeocystis pouchetii*. *J Exp Mar Bio Ecol* 110, 197–212.

Irigoien, X, Titelman, J, Harris, RP, Harbour, D, and Castellani, C (2003). Feeding of *Calanus finmarchicus* nauplii in the Irminger Sea. *Mar Ecol Prog Ser* 262, 193–200.

Jónasdóttir, S, Gudfinnsson, H, Gislason, A, and Astthorsson, O (2002). Diet composition and quality for *Calanus finmarchicus* egg production and hatching success off south-west Iceland. 140, 1195–1206.

Jónasdóttir, SH, Visser, AW, and Jespersen, C (2009). Assessing the role of food quality in the production and hatching of *Temora longicornis* eggs. *Mar Ecol Prog Ser* 382, 139–150.

Jung-Madsen, S and Nielsen, TG (2015). Early development of *Calanus glacialis* and *C. finmarchicus*. *Limnol Oceanogr* 60, 934–946.

Kahru, M, Brotas, V, Manzano-Sarabia, M, and Mitchell, BG (2011). Are phytoplankton blooms occurring earlier in the Arctic? *Glob Change Biol* 17, 1733–1739.

Kaiser, P, Hagen, W, Bode-Dalby, M, and Auel, H (2022). Tolerant but facing increased competition: Arctic zooplankton versus Atlantic invaders in a warming ocean. *Front Mar Sci* 9, 908638.

Kaiser, P, Hagen, W, von Appen, W-J, Niehoff, N, Hildebrandt, N, and Auel, H (2021). Effects of a submesoscale oceanographic filament on zooplankton dynamics in the Arctic marginal ice zone. *Front Mar Sci* 8, 625395.

References

Kjellerup, S, Dünweber, M, Swalethorp, R, Nielsen, TG, Møller, EF, Markager, S, and Hansen, BW (2012). Effects of a future warmer ocean on the coexisting copepods *Calanus finmarchicus* and *C. glacialis* in Disko Bay, western Greenland. *Mar Ecol Prog Ser* 447, 87–108.

Koch, CW, Brown, TA, Amiraux, R, Ruiz-Gonzalez, C, MacCorquodale, M, Yunda-Guarin, GA, Kohlbach, D, Loseto, LL, Rosenberg, B, Hussey, NE, Ferguson, SH, and Yurkowski, DJ (2023). Year-round utilization of sea ice-associated carbon in Arctic ecosystems. *Nat Commun* 14, 1964.

Kohlbach, D, Graeve, M, A Lange, B, David, C, Peeken, I, and Flores, H (2016). The importance of ice algae-produced carbon in the central Arctic Ocean ecosystem: food web relationships revealed by lipid and stable isotope analyses: ice algal carbon in Arctic food web. *Limnol Oceanogr* 61, 2027–2044.

Kosobokova Kand Hirche, H-J (2009). Biomass of zooplankton in the eastern Arctic Ocean – a base line study. *Prog Oceanogr* 82, 265–280.

Kosobokova, KN, Hopcroft, RR, and Hirche, H-J (2011). Patterns of zooplankton diversity through the depths of the Arctic's central basins. *Mar Biodiv* 41, 29–50.

Kosobokova, KN and Pertsova, NM (2018). Zooplankton of the White Sea: communities' structure, seasonal dynamics, spatial distribution, and ecology. *Biogeochemistry of the Atmosphere, Ice and Water of the White Sea*. Edited by Lisitsyn, A P and Gordeev, Viacheslav V. Volume 81. Cham: Springer International Publishing, 223–266.

Kristiansen, I, Gaard, E, Hátún, H, Jónasdóttir, S, and Ferreira, ASA (2016). Persistent shift of *Calanus* spp. in the southwestern Norwegian Sea since 2003, linked to ocean climate. *ICES Mar Sci Symp* 73, 1319–1329.

Kunisch, EH, Graeve, M, Gradinger, R, Flores, H, Varpe, Ø, and Bluhm, BA (2023). What we do in the dark: prevalence of omnivorous feeding activity in Arctic zooplankton during polar night. *Limnol Oceanogr*, 1853–1851.

Kwaśniewski, S, Gluchowska, M, Jakubas, D, Wojczulanis-Jakubas, K, Walkusz, W, and Karnovsky, N (2010). The impact of different hydrographic conditions and zooplankton communities on provisioning little auks along the west coast of Spitsbergen. *Prog Oceanogr* 87, 72–82.

Kwaśniewski, S, Hop, H, Falk-Petersen, S, and Pedersen, G (2003). Distribution of *Calanus* species in Kongsfjorden, a glacial fjord in Svalbard. *J Plankton Res* 25, 1–20.

Langbehn, TJ, Aarflot, JM, Freer, JJ, and Varpe, Ø (2023). Visual predation risk and spatial distributions of large Arctic copepods along gradients of sea ice and bottom depth. *Limnol Oceanogr* 68, 1388–1405.

Langbehn, TJ and Varpe, Ø (2017). Sea-ice loss boosts visual search: fish foraging and changing pelagic interactions in polar oceans. *Glob Change Biol* 23, 5318–5330.

Levinsen, H, Turner, JT, Nielsen, TG, and Hansen, BW (2000). On the trophic coupling between protists and copepods in arctic marine ecosystems. *Mar Ecol Prog Ser* 204, 65–77.

Li, WKW, McLaughlin, FA, Lovejoy, C, and Carmack, EC (2009). Smallest algae thrive as the Arctic Ocean freshens. *Sci* 326, 539–539.

Makri, M, Hansen, PJ, and Nielsen, TG (2024). Impact of salinity and temperature on the vital rates of co-occurring *Calanus glacialis* and *C. finmarchicus* from West Greenland. *Mar Ecol Prog Ser* 729, 47–62.

Matishov, GG, Matishov, DG, and Moiseev, DV (2009). Inflow of Atlantic-origin waters to the Barents Sea along glacial troughs. *Oceanologia* 51, 321–340.

McNicholl, DG, Walkusz, W, Davoren, GK, Majewski, AR, and Reist, JD (2016). Dietary characteristics of co-occurring polar cod (*Boreogadus saida*) and capelin (*Mallotus villosus*) in the Canadian Arctic, Darnley Bay. *Polar Biol* 39, 1099–1108.

Mohamed, B, Nilsen, F, and Skogseth, R (2022). Marine heatwaves characteristics in the Barents Sea based on high resolution satellite data (1982–2020). *Front Mar Sci* 9, 821646.

Møller, EF, Maar, M, Jónasdóttir, SH, Nielsen, TG, and Tönnesson, K (2012). The effect of changes in temperature and food on the development of *Calanus finmarchicus* and *Calanus helgolandicus* populations. *Limnol Oceanogr* 57, 211–220.

Nejstgaard, JC, Tang, KW, Steinke, M, Dutz, J, Koski, M, Antajan, E, and Long, JD (2007). Zooplankton grazing on *Phaeocystis*: a quantitative review and future challenges. *Biogeochemistry* 83, 147–172.

Nöthig, E-M, Bracher, A, Engel, A, Metfies, K, Niehoff, B, Peeken, I, Bauerfeind, E, Cherkasheva, Alexandra, Gäbler-Schwarz, Steffi, Hardge, Kristin, Kilias, Estelle, Kraft, A, Mebrahtom Kidane, Yohannes, Lalande, C, Piontek, J, Thomisch, K, and Wurst, M (2015). Summertime plankton ecology in Fram Strait—a compilation of long- and short-term observations. *Polar Res* 34, 23349.

Noyon, M, Narcy, F, Gasparini, Stéphane, and Mayzaud, P (2011). Growth and lipid class composition of the Arctic pelagic amphipod *Themisto libellula*. *Mar Biol* 158, 883–892.

O'Brien, WJ (1979). The predator-prey interaction of planktivorous fish and zooplankton: Recent research with planktivorous fish and their zooplankton prey shows the evolutionary thrust and parry of the predator-prey relationship. *Am Sci* 67, 572–581.

Orkney, A, Platt, T, Narayanaswamy, BE, Kostakis, I, and Bouman, HA (2020). Bio-optical evidence for increasing *Phaeocystis* dominance in the Barents Sea. *Phil Trans R Soc A* 378, 20190357.

Pasternak, AF, Arashkevich, EG, Grothe, U, Nikishina, AB, and Solovyev, KA (2013). Different effects of increased water temperature on egg production of *Calanus finmarchicus* and *C. glacialis*. *Oceanol* 53, 547–553.

Peck, Lloyd S (2018). Antarctic marine biodiversity: adaptations, environments and responses to change. *Oceanogr Mar Biol*. Edited by Hawkins, SJ, Evans, AJ, Dale, AC, Firth, LB, and Smith, IP. 1st edition. CRC Press, 105–236.

Percy, JA (1993). Energy consumption and metabolism during starvation in the Arctic hyperiid amphipod *Themisto libellula* Mandt. *Polar Biol* 13, 549–555.

Polyakov, IV, Ingvaldsen, RB, Pnyushkov, AV, Bhatt, US, Francis, JA, Janout, M, Kwok, R, and Skagseth, Ø (2023). Fluctuating Atlantic inflows modulate Arctic atlantification. *Sci* 381, 972–979.

Pörtner, H (2012). Integrating climate-related stressor effects on marine organisms: unifying principles linking molecule to ecosystem-level changes. *Mar Ecol Prog Ser* 470, 273–290.

Pörtner, H-O, Bock, C, and Mark, FC (2017). Oxygen- and capacity-limited thermal tolerance: bridging ecology and physiology. *J Exp Biol* 220, 2685–2696.

Renaud, PE, Daase, M, Banas, NS, Gabrielsen, TM, Søreide, JE, and Varpe, Ø (2018). Pelagic food-webs in a changing Arctic: a trait-based perspective suggests a mode of resilience. *ICES J Mar Sci* 75, 1871–1881.

Rossel, S, Kaiser, P, Bode-Dalby, M, Renz, J, Laakmann, S, Auel, H, Hagen, W, Arbizu, PM, and Peters, J (2023). Proteomic fingerprinting enables quantitative biodiversity assessments of species and ontogenetic stages in *Calanus* congeners (Copepoda, Crustacea) from the Arctic Ocean. *Mol Ecol Res* 23, 382–395.

Sars, GO (1900). V Crustacea. *The Norwegian north polar expedition 1893-1896. Scientific results*. Edited by Nansen, F, 137 pp.

Schauer, U, Beszczynska-Möller, A, Walczowski, W, Fahrbach, E, Piechura, J, and Hansen, E (2008). Variation of measured heat flow through the Fram Strait between 1997 and 2006. *Arctic–Subarctic Ocean Fluxes*. Edited by Dickson, R R, Meincke, J, and Rhines, P. Dordrecht: Springer Netherlands, 65–85.

Schauer, U, Loeng, H, Rudels, B, Ozhigin, VK, and Dieck, W (2002). Atlantic water flow through the Barents and Kara Seas. *Deep-Sea Res I* 49, 2281–2298.

Schmid, Moritz S and Fortier, L (2019). The intriguing co-distribution of the copepods *Calanus hyperboreus* and *Calanus glacialis* in the subsurface chlorophyll maximum of Arctic seas. *Elem Sci Anth* 7, 50.

Schmidt, K, Graeve, M, Hoppe, CJM, Torres-Valdes, S, Welteke, N, Whitmore, LM, Anhaus, P, Atkinson, A, Belt, ST, Brenneis, T, Campbell, RG, Castellani, G, Copeman, LEA, Flores, H, Fong, AA, Hildebrandt, N, Kohlbach, D, Nielsen, JM, Parrish, CC, Rad-Menéndez, C, Rokitta, SD, Tippenhauer, S, and Zhuang, Y (2024). Essential omega-3 fatty acids are depleted in sea ice and pelagic algae of the Central Arctic Ocean. *Glob Change Biol* 30, e17090.

Schoemann, V, Becquevort, S, Stefels, J, Rousseau, V, and Lancelot, C (2005). *Phaeocystis* blooms in the global ocean and their controlling mechanisms: a review. *J Sea Res* 53, 43–66.

Schulte, PM, Healy, TM, and Fangue, NA (2011). Thermal performance curves, phenotypic plasticity, and the time scales of temperature exposure. *Integr Comp Biol* 51, 691–702.

Selz, Virginia, Saenz, BT, Van Dijken, G L, and Arrigo, KR (2018). Drivers of ice algal bloom variability between 1980 and 2015 in the Chukchi Sea. *J Geophys Res Oceans* 123, 7037–7052.

Skjoldal, HR, Aarflot, JM, Bagøien, E, Skagseth, Ø, Rønning, J, and Lien, VS (2021). Seasonal and interannual variability in abundance and population development of *Calanus finmarchicus* at the western entrance to the Barents Sea, 1995–2019. *Prog Oceanogr* 195, 102574.

Smith, SL and Schnack-Schiel, SB (1990). Polar zooplankton. *Polar Oceanography, Part B: Chemistry, Biology and Geology*. Edited by Smith, WO. San Diego: Academic Press, 527–598.

Smolina, I, Kollias, S, Møller, EF, Lindeque, P, AYM, Sundaram, JMO, Fernandes, and Hoarau, G (2015). Contrasting transcriptome response to thermal stress in two key zooplankton species, *Calanus finmarchicus* and *C. glacialis*. *Mar Ecol Prog Ser* 534, 79–93.

Søreide, JE, Carroll, ML, Hop, H, Ambrose, WG, Hegseth, EN, and Falk-Petersen, S (2013). Sympagic-pelagic-benthic coupling in Arctic and Atlantic waters around Svalbard revealed by stable isotopic and fatty acid tracers. *Mar Biol Research* 9, 831–850.

Søreide, JE, Falk-Petersen, S, Hegseth, EN, Hop, H, Carroll, ML, Hobson, KA, and Blachowiak-Samolyk, K (2008). Seasonal feeding strategies of *Calanus* in the high-Arctic Svalbard region. *Deep-Sea Res II* 55, 2225–2244.

Svensen, C, Seuthe, L, Vasilyeva, Y, Pasternak, A, and Hansen, E (2011). Zooplankton distribution across Fram Strait in autumn: Are small copepods and protozooplankton important? *Prog Oceanogr* 91, 534–544.

Tarling, GA, Freer, JJ, Banas, NS, Belcher, A, Blackwell, M, Castellani, C, Cook, KB, Cottier, Finlo R, Daase, M, Johnson, ML, Last, KS, Lindeque, PK, Mayor, DJ, Mitchell, E, Parry, HE, Speirs, DC, Stowasser, G, and Wootton, M (2022). Can a key boreal *Calanus* copepod species now complete its life-cycle in the Arctic? Evidence and implications for Arctic food-webs. *Ambio* 51, 333–344.

Tedesco, L and Vichi, M (2014). Sea ice biogeochemistry: a guide for modellers. *PLoS ONE* 9, e89217.

Torgersen, T and Huse, G (2005). Variability in retention of *Calanus finmarchicus* in the Nordic Seas. *ICES J Mar Sci* 62, 1301–1309.

Trudnowska, E, Balazy, K, Stoń-Egiert, J, Smolina, I, Brown, T, and Gluchowska, M (2020). In a comfort zone and beyond—ecological plasticity of key marine mediators. *Ecol Evol* 10, 14067–14081.

Vernet, M, Richardson, TL, Metfies, K, Nöthig, E-M, and Peeken, I (2017). Models of plankton community changes during a warm water anomaly in Arctic waters show altered trophic pathways with minimal changes in carbon export. *Front Mar Sci* 4, 160.

Vihtakari, M, Welcker, J, Moe, B, Chastel, O, Tartu, S, and Hop, H (2018). Black-legged kittiwakes as messengers of Atlantification in the Arctic. *Sci Rep* 8, 1178.

References

Von Appen, W-J, Wekerle, C, Hehemann, L, Schourup-Kristensen, V, Konrad, C, and Iversen, MH (2018). Observations of a submesoscale cyclonic filament in the Marginal Ice Zone. *Geophys Res Lett* 45, 6141–6149.

Von Quillfeldt, CH (2000). Common diatom species in Arctic spring blooms: their distribution and abundance. *Bot Mar* 43, 499–516.

Waga, H and Hirawake, T (2020). Changing occurrences of fall blooms associated with variations in phytoplankton size structure in the Pacific Arctic. *Front Mar Sci* 7, 209.

Wassmann, P, Kosobokova, KN, Slagstad, D, Drinkwater, KF, Hopcroft, RR, Moore, SE, Ellingsen, I, Nelson, RJ, Carmack, E, Popova, E, and Berge, J (2015). The contiguous domains of Arctic Ocean advection: trails of life and death. *Prog Oceanogr* 139, 42–65.

Weydmann-Zwolicka, A, Cottier, F, Berge, J, Majaneva, S, Kukliński, P, and Zwolicki, A (2022). Environmental niche overlap in sibling planktonic species *Calanus finmarchicus* and *C. glacialis* in Arctic fjords. *Ecol Evol* 12, e9569.

Wing, BL (1976). Ecology of *Parathemisto libellula* and *P. pacifica* (Amphipoda: Hyperiidea) in Alaskan coastal waters. *Open Access Dissertations* 1409, 1–266.

ACKNOWLEDGEMENTS

First, I would like to express my deepest gratitude to Prof. Dr. Wilhelm Hagen and PD. Dr. Holger Auel for providing me with the opportunity to conduct this thesis. Thank you for your continuous support, your scientific guidance and many discussions during the last years. Your assistance was essential for the accomplishment of this thesis.

I would like to thank PD Dr. Barbara Niehoff for taking the time and evaluating this thesis.

Thanks to the members of my GLOMAR thesis committee, Prof. Dr. Wilhelm Hagen, PD Dr. Holger Auel, PD Dr. Barbara Niehoff, Dr. Maya Bode-Dalby and Dr. Silke Laakmann for their guidance and assistance.

Special thanks to the Marine Zoology working group: Dr. Anna Schukat, Dr. Maya Bode-Dalby and Sabrina Dorschner. Thank you for providing scientific and mental support during the years. Thank you, Sabrina, for your excellent technical support.

I would like to thank Dr. Tobias Mildenberger and Jan Brüwer for providing the LaTeX script used to format this thesis. Thanks to Lennart Stock for his endless help with formatting, and Anna Schukat, Mirco Wölfelschneider and Jan Brüwer for proof-reading.

Thank you, Anna, for being the best roommate during most of this thesis. From the initial days as the 'Arbeitslosen WG' up to today, you have been a great friend and steady source of support.

Thank you, Mirco, for being the best co-brewer.

I am very grateful for all the friends which have been part of my life. Thank you Monika, Julian, and Max for your constant support and friendship since the beginning of our Bachelor studies. Thanks to my PS121 Mädels, Anabel, Swantje, Theresa and Véro for the unforgettable expedition, conference (including the roadtrip) and countless fun moments. Thanks to the INES

Universität Bremen
Fachbereich 2
Prüfungsamt Chemie
z. Hd. Frau Frauke Ernst
Leobener Straße

28359 Bremen
Deutschland

Prüfungsamt
Chemie

Frauke Ernst
Geschäftsstelle
Fachbereich 02
Leobener Str. / NW2
D-28359 Bremen

Verwaltungspavillon 06
Tel. 0421 218-62802
Fax 0421 218-9862802
frauke.ernst@uni-bremen.de
www.fb2.uni-bremen.de

<u>Versicherung an Eides Statt</u>

Name, Vorname	Kaiser, Patricia
Straße	James-Watt-Str. 1
Ort, PLZ	Bremen, 28359

Ich, Patricia Kaiser,

versichere an Eides Statt durch meine Unterschrift, dass ich die vorstehende Arbeit selbständig und ohne fremde Hilfe angefertigt und alle Stellen, die ich wörtlich dem Sinne nach aus Veröffentlichungen entnommen habe, als solche kenntlich gemacht habe, mich auch keiner anderen als der angegebenen Literatur oder sonstiger Hilfsmittel bedient habe.
Ich versichere an Eides Statt, dass ich die vorgenannten Angaben nach bestem Wissen und Gewissen gemacht habe und dass die Angaben der Wahrheit entsprechen und ich nichts verschwiegen habe.
Die Strafbarkeit einer falschen eidesstattlichen Versicherung ist mir bekannt, namentlich die Strafandrohung gemäß § 156 StGB bis zu drei Jahren Freiheitsstrafe oder Geldstrafe bei vorsätzlicher Begehung der Tat bzw. gemäß § 161 Abs. 1 StGB bis zu einem Jahr Freiheitsstrafe oder Geldstrafe bei fahrlässiger Begehung.

_____
Ort, Datum / Unterschrift